

This item was submitted to [Loughborough's Research Repository](#) by the author.
Items in Figshare are protected by copyright, with all rights reserved, unless otherwise indicated.

Modelling of colour appearance

PLEASE CITE THE PUBLISHED VERSION

PUBLISHER

© Xiaohong Wang

LICENCE

CC BY-NC-ND 4.0

REPOSITORY RECORD

Wang, Xiaohong. 2019. "Modelling of Colour Appearance". figshare. <https://hdl.handle.net/2134/13687>.

This item was submitted to Loughborough University as a PhD thesis by the author and is made available in the Institutional Repository (<https://dspace.lboro.ac.uk/>) under the following Creative Commons Licence conditions.



For the full text of this licence, please go to:
<http://creativecommons.org/licenses/by-nc-nd/2.5/>

**LOUGHBOROUGH
UNIVERSITY OF TECHNOLOGY
LIBRARY**

AUTHOR/FILING TITLE

WANG, X

ACCESSION/COPY NO.

040.101490

VOL. NO.

CLASS MARK

30 JUN 1995

28 JUN 1996

LOAN COPY
date due
for return:-

17 FEB 1998

**LOAN 3 WKS. + 3
UNLESS RECALLED**

0401014908



MODELLING OF COLOUR APPEARANCE

By

Xiaohong Wang

A Doctoral Thesis

Submitted in partial fulfilment of the requirement

for the award of

Doctor of Philosophy

of the Loughborough University of Technology

July 1994

© *Xiaohong Wang 1994*

Loughborough University of Technology	
Date	Jan 95
Class	
Acc. No.	040101490

V8909632

ABSTRACT

A colour may have a different appearance under different viewing conditions. This causes many problems in the colour reproduction industry. Thus the importance of prediction of colour appearance has arisen. In this study, a mathematical model to predict colour appearance was developed based on the investigation of the changes of colour appearance under a wide range of media and viewing conditions.

The media studied included large cut-sheet transparency films, 35mm projected slides, reflection samples and monitor colours. The viewing conditions varied were light source, luminance level and viewing background. Colour appearance was studied using the magnitude estimation technique.

In general, colours appeared more colourful, lighter and brighter with an increase in luminance level. Background and flare light had considerable influence on colour appearance for cut-sheet transparency media. Simultaneous contrast effects occurred when a monitor colour was displayed against a chromatic surround. The monitor colour appeared lighter with a darker induction field. When a coloured area was enlarged, lightness tended to increase while colourfulness tended to decrease. Colour appearance was also affected by the closest neighbouring colour. In this case, the hue of the colour largely shifted towards the direction of the opponent hue of the induction colour.

The data obtained were applied to test three colour spaces and two colour appearance models. For reflection media, the Hunt91 model performed the best. However it was not satisfactory when applied to transmissive media. Based on these results, the Hunt93 model was developed by modification of the Hunt91 model. The new model widens the application range of the Hunt91 and is reversible.

ACKNOWLEDGEMENTS

I am grateful to my supervisor Dr. R.P. Knott for his work on administration and ex-supervisor Professor S.A.R. Scrivener for his guidance and encouragement in this study.

I am greatly indebted to my external supervisor Dr. M. R. Luo for his guidance in this project and constructive criticism in the writing of this thesis.

Dr. C.J. Hinde read my thesis and gave a lot of useful advice in the final stage of my study. His contributions are gratefully acknowledged.

My thanks go to Mrs. H.L. Luo, Mss. S. Siripoksup, S.P. Heggie, and M. C. Lo, Miss. R.M. Jones, Drs. M. R. Luo and J. H. Xin, W.S. Yousif and Mr. S. M. Clark for their assistance as observers, also Mr. A. A. Clarke and Mr. A. S Schappo who gave a lot of support in this work. Without them, completion of this project is impossible.

I offer my gratitude and sincerely thanks to my husband, Dr. Fengge Gao for his enduring encouragement throughout this study. Thanks also go to my baby daughter, Alice who made so many efforts to keep her "quiet" during my writing.

This work was financially supported by DTI, SERC, Crosfield Electronics Ltd. and Coats Viyella Plc. and received technical supervision from Dr. R.W.G. Hunt. Their support is gratefully acknowledged.

CONTENTS

	Page
1. INTRODUCTION	1
2. LITERATURE REVIEW	3
2.1 THE SCOPE OF COLOUR SCIENCE	3
2.1.1 Light	3
2.1.2 Coloured Objects	5
2.1.2.1 Transmission	5
2.1.2.2 Reflection	5
2.1.2.3 Spectral Characterisation of Materials	5
2.1.3 Colour Vision	6
2.1.3.1 Structure of the Eye	6
2.1.3.2 Colour Vision Theory	6
2.1.4 Colour Specification	8
2.1.4.1 Colorimetry	8
2.1.4.2 Subjective Estimation	9
2.2 COLOUR SPECIFICATION SYSTEM	11
2.2.1 CIE System	11
2.2.1.1 CIE Standard Sources and Illuminants	11
2.2.1.2 CIE Standard Observers	12
2.2.1.3 Standard White, Standard Illuminating / Viewing Conditions	13
2.2.1.4 Calculating the CIE Tristimulus Values	14
2.2.1.5 Chromaticity Coordinates and Chromaticity Diagram	15
2.2.1.6 Uniform Chromatic Scales (UCS)	15
2.2.1.7 Uniform Colour Space	16
2.2.2 Colour Order Systems	19
2.2.2.1 Munsell Colour System	20
2.2.2.2 The Natural Colour System (NCS)	21
2.2.2.3 The OSA UCS Colour System	21
2.3 COLOUR APPEARANCE	23

2.3.1 Light Adaptation and Dark Adaptation	23
2.3.2 Chromatic Adaptation	24
2.3.3 Some Common Types of Transformation for Chromatic Adaptation	26
2.3.3.1 Von Kries Transformation	27
2.3.3.2 Nayatani's Transformation	28
2.3.4 Some Phenomena on Colour Appearance	28
2.3.4.1 Hunt Effect	28
2.3.4.2 Helmholtz-Kohlrausch Effect	29
2.3.4.3 Helson-Judd Effect	29
2.3.4.4 Effect of Colour Temperature	29
2.3.4.5 Stevens Effect	30
2.3.4.6 Simultaneous Contrast Effect	30
2.3.2 Experimental Methods to Determine Colour Appearance	32
2.3.5.1 Haploscopic Matching	33
2.3.5.2 Differential Retinal Conditioning	33
2.3.5.3 Memory Matching	33
2.3.5.4 Direct Scaling and Magnitude Estimation	34
2.3.6 Prediction of Colour Appearance	36
2.3.6.1 Hunt Colour Appearance Models	37
2.3.6.2 Nayatani Colour Appearance Models	39
2.4 THE IMPLICATION OF COLOUR APPEARANCE MODELS	41
2.4.1 Application Area	41
2.4.2 Field Trials of Models	41
2.5 OUTLINE OF RESEARCH	43
3. EXPERIMENTAL METHODS	44
3.1 TEST OF DEFECTIVE COLOUR VISION	44
3.2 MAGNITUDE ESTIMATION OF COLOUR ATTRIBUTES	46
3.2.1 Lightness Scaling	46
3.2.2 Brightness Scaling	46
3.2.3 Hue Scaling	47
3.2.4 Colourfulness Scaling	47

3.3 MAGNITUDE ESTIMATION EXPERIMENTS	48
3.3.1 Experiment 1: Training Experiment	48
3.3.1.1 The Apparatus	48
3.3.1.2 Experimental Procedure	50
3.3.2 Experiment 2: Cut-Sheet Transparency Medium	51
3.3.2.1 The Apparatus	51
3.3.2.2 Sample Preparation	53
3.3.2.3 Experimental Procedure	54
3.3.3 Experiment 3: 35 mm Projected Slide Medium	55
3.3.3.1 The Apparatus	55
3.3.3.2 Experimental Procedure	57
3.3.4 Experiment 4: Reflection Print Medium	58
3.3.4.1 The Apparatus	58
3.3.4.2 Experimental Procedure	59
3.3.5 Experiment 5: Luminous Colour Experiment	60
 4. EXPERIMENTAL RESULTS AND DISCUSSION	 63
4.1 DATA ANALYSIS	63
4.1.1 Methods for calculating Mean Visual Results	63
4.1.1.1 Lightness	63
4.1.1.2 Hue	63
4.1.1.3 Colourfulness	63
4.1.1.4 Brightness	64
4.1.2 Investigation of Changes of Colour Appearance Between Different Viewing Parameters	64
4.1.3 Evaluation of Performance of Colour Spaces and Models	65
 4.2 EXPERIMENT 1: STUDIES ON THE PERFORMANCE OF OBSERVERS	 67
4.2.1 Observers' Repeatability and Accuracy Performance	67
4.2.2 Observers' Consistency	68
 4.3 EXPERIMENTS 2 AND 3: TRANSMISSIVE MEDIA	 70
4.3.1 Introduction	70
4.3.2 Observers' Performance	71
4.3.3 Effect of Different Viewing Parameters	71

4.3.3.1 Effect of Luminance Levels	72
4.3.3.2 Effect of Extra Flare Light	72
4.3.3.3 Effect of Luminance Factors of Backgrounds	73
4.3.3.4 Effect of Borders	73
4.3.3.5 Helmholtz-Kohlrausch Effect	74
4.3.3.6 Effect of Colour Temperature	74
4.3.4 Testing Performance of Colour Spaces and Models	75
4.3.4.1 Lightness Predictions	75
4.3.4.2 Chroma and Colourfulness Predictions	77
4.3.4.3 Hue Predictions	78
4.3.5 Modifying Hunt91 Colour Appearance Model	78
4.3.5.1 Modification of Hunt Model's Lightness Scale	78
4.3.5.2 Modification of Hunt Model's Chroma and Hue Scales	80
 4.4 EXPERIMENT 4 : REFLECTION PRINT MEDIUM	 82
4.4.1 Introduction	82
4.4.2 Observers' Performance	82
4.4.3 Effect of Various Adapting Luminance Levels	83
4.4.4 Testing of Performance of Colour Spaces and Models	84
4.4.4.1 Lightness Predictions	85
4.4.4.2 Brightness Predictions	85
4.4.4.3 Chroma and Colourfulness Predictions	86
4.4.4.4 Hue Predictions	86
 4.5 EXPERIMENT 5: SIMULTANEOUS CONTRAST EXPERIMENT	 88
4.5.1 Introduction	88
4.5.2 Observers' Performance	88
4.5.3 Simultaneous Contrast Effect	88
4.5.3.1 Effect on Lightness	89
<i>A. Lightness on lightness</i>	89
<i>B. Hue on lightness</i>	90
<i>C. The size of test patch on lightness</i>	90
4.5.3.2 Effect on Colourfulness	91
<i>A. Lightness and Hue on colourfulness</i>	91
<i>B. The size of the test patch on colourfulness</i>	92
4.5.3.3 Effect on Hue	92
4.5.4 Testing Hunt Colour Vision Model for Predicting	

the Simultaneous Contrast Effect	93
4.6 SUMMARY	96
4.6.1 Summary Results of All the Experiments	96
4.6.1.1 Summary of Observer Performance	96
4.6.1.2 Summary of the Performance of Colour Spaces and Models	96
4.6.2 Further Modifying Hunt Chroma and Colourfulness Scales	97
4.7. REVISED HUNT MODEL AND THE REVERSING MODEL	99
4.7.1 Comparison of Revised Hunt91 Model with NCS and Munsell Data	99
4.7.1.1 Constant-Hue Loci	99
4.7.1.2 Constant-Chroma Loci	100
4.7.2 The Formulae of Forward Revised Hunt91 Model	101
4.7.2.1 Input Data	101
4.7.2.2 Computing Procedures of The Hunt93 Model	102
4.7.3 Reversing Hunt93 Model	110
4.7.3.1 Input Data	110
4.7.3.2 Calculating Procedures for Reversing Hunt93 Model	111
4.7.3.3 Testing A Reverse Hunt93 Model	119
5. CONCLUSIONS	121
6. RECOMMENDATION FOR FUTURE WORK	123
7. REFERENCES	124
8. APPENDICES	139
TABLES	
FIGURES	

1. INTRODUCTION

The colour of an object appears different when viewed under different conditions^[1]. A green dress is chosen from a catalogue; a yellow paint is picked out for the kitchen; or a jacket and trousers from different suppliers are carefully matched in a shop ---- the appearance of each may change when they are taken home. This frequently causes customers to complain. Hence the prediction of colour appearance is important for the colour industry.

Colour appearance is essentially determined by a light source, an object and an observer^[2]. Of these factors, the contribution of a light source and an object to colour appearance can be scanned by measuring the physical quality of the illumination and the interaction of this radiation with the object. However, the response of an observer to a colour may be influenced by the state of adaptation as well as the viewing conditions^[3-5]. Thus a basic consideration of the prediction of colour appearance is to gain an understanding of relationships between a human being's response and the other factors. Colour appearance can then be predicted by the application of modelled relationships to transform the physical stimuli into a human being's subjective colour attributes.

The study of colour was begun as early as the 19th century. It was first recognised in Young-Helmholtz theory that only three colour receptors existed in the human eye: red, green, and blue^[6,7]. Thus a colour can be quantified by adjusting the amount of three primary colours^[8]. However, a human being's response to a colour is affected not only by the colour itself, but also by the state of the eye's adaptation, as well as the viewing conditions. In recent years, many researchers, (Bartleson^[9,10], Pointer et al.^[11,12], Troscianko^[13,14] etc.) have studied colour appearance in terms of lightness, colourfulness, and hue attributes and the relationships between the eye's response and viewing conditions.

Progress in the modelling of colour appearance has been made by Hunt^[15-21] and Nayatani et al.^[22-26]. These models are based on a simplified theory of colour vision for

chromatic adaptation together with a uniform colour space. They can predict colour appearance to a high degree within a certain range of viewing environments.

In order to widen the range of application and improve the accuracy of predictions, extensive study of the human response under a wide range of viewing conditions is required to modify the models further. With this in mind, the colour appearance of various media under a wide range of viewing conditions was studied in this project; further modification of Hunt91 model was attempted.

This thesis includes six sections. The relevant literatures are reviewed in Section 2. The following section gives experimental methods. Experimental results are described in Section 4. This section includes observers' performance, cut-sheet transparency, 35mm slide, reflection print, and luminous colour experiments together with modification of the Hunt91 model and development of its reversing form. Conclusions and recommendations for future work are given in Sections 5 and 6.

2. LITERATURE REVIEW

2.1 THE SCOPE OF COLOUR SCIENCE

Colour is an attribute of visual experience and closely related to the other science^[27-29]. Physics defines light as the electromagnetic radiation in the visible spectrum. Physiologists study the colour receptor mechanisms in the human eye and brain. Colour psychology studies the response of an observer to colour sensations, e.g. whether he or she calls it red or green. Psychophysics is involved in understanding relationships between physical stimulus and subjective response. Mathematics attempts to describe these relationships by numbers and equations. Chemistry is related in two ways: the mechanisms by which light is absorbed in the eye, and the use of dyes and pigments to produce coloured objects^[30,31].

The perception of a coloured object ordinarily requires three components: a light source, an object and an observer.

2.1.1 Light

Colour is a property of light rather than of bodies^[29,32]. Without light, colour can not be sensed. White light, such as sunlight, is not a simple energy, but consists of different colour light travelling at thousands of trillion frequencies each second between the short-wave ultra-violet with high frequency and the long-wave infrared with low frequency. Light can be described by its wavelength for which the nanometre (nm) is a convenient unit of length^[33] (One nanometre is 1/1,000,000 millimetre). The light source emits radiant energy well distributed in the spectrum between 380 and 780 nm. When these rays strike the eye simultaneously, the sensation of "white light" is perceived. This remarkable fact was first proved by Sir Isaac Newton at Cambridge in 1666 by means of a triangular glass prism and a beam of sunlight in a darkened room^[34]. In this experiment, sunlight was passed through from a small round hole in the window shutter

of a darkened room. The beam was directed on to the side of a prism, emerged onto a white surface and altered to a long band consisting of bars of seven different colours. These colours were described as violet, indigo, blue, green, yellow, orange, and red from short to long wavelengths. This coloured band of light is named 'spectrum', the basis of colour science. Figure 2.1 schematically shows the process used by Newton to produce a spectrum^[32].

If the seven coloured lights in the spectrum are projected onto a spot on a screen in a darkened room simultaneously, the result will be a patch of "white" or colourless light. Thus light similar to daylight can be artificially produced. If only three of the seven colours, red, green, and blue, are projected on to the same spot on a screen, a white light patch will also be produced. This implies that the three colours are sufficient to form the others. This type of mixture is called additive mixing and is schematically illustrated in Figure 2.2. The three (independently variable) chromatic lights or colorant substances necessary to match all colours in a given group are called primaries^[28]. The action of making a colour appear the same as a given colour by adjusting three primaries of an additive colour mixture is called trichromatic matching or colour matching^[16].

In his experiments, Newton attempted to relate the wavelength of light to the appearance of colour. The colour we recognise as blue lies below about 480 nm; green, roughly between 480 and 560 nm; yellow, between 560 and 590 nm; orange, between 590 and 630 nm; and red at wavelength longer than 630 nm^[2].

A light from any source can be described in terms of the relative power emitted at each wavelength. Plotting this power as a function of wavelength gives the spectral power distribution curve of the light source. The spectral power distribution of a given light source can be measured by a spectroradiometer. Colour temperature is another term for specifying light sources. One group of light sources are called blackbodies. When heated, they glow like metals, first a dull red like a hot electric stove, then progressively brighter and whiter like the filaments of incandescent light bulbs. Real blackbodies are hollow heated chambers. Their spectral power distribution and their colour appearance only

depend on their temperature rather than their composition. The temperature of the blackbody is defined as colour temperature with the unit of Kelvin (K)^[2,35]. If the colour of a real light source (e.g. a fluorescent lamp) does not visually match any of these colours in a blackbody, a correlate of colour temperature can be found. This is defined as the temperature of the blackbody whose perceived colour gives the closest match to that of a given stimulus seen at the same brightness under a set of specified viewing conditions^[16].

2.1.2 Coloured Objects

When light strikes an object, one or more things pertinent to colour can happen^[2,28,32]. Most objects owe their colour to substances that absorb radiant energy within the visible spectrum. These substances are called colorants: if insoluble, pigments; if soluble, dyes.

2.1.2.1 Transmission

Transmission is the passage of radiation through a medium without change of frequency (that is, without fluorescence)^[16]. When light can go through essentially unchanged, it is said to be transmitted through the material. The material is described as transparent.

2.1.2.2 Reflection

Light may be scattered when it interacts with a material. Reflection is the return of radiation by a medium without change of frequency (that is, without fluorescence)^[16]. When the reflection is so intense that no light passes through the material (some absorption must be present, too), it is said to be opaque.

2.1.2.3 Spectral Characterisation of Materials

From the standpoint of colour, the light received and evaluated from an object can be described by its spectral transmittance or reflectance curve, depending upon whether the object is transparent or opaque. These curves show the fraction of light transmitted through an object to that transmitted through a suitable standard (often air) at each wavelength, or reflected from a material compared to that reflected from a perfect white diffuser at each wavelength. The spectral transmittance or reflectance of an object is commonly measured by a spectrophotometer.

2.1.3 Colour Vision

2.1.3.1 Structure of the Eye

A schematic illustration of a cross-section of human eye is given in Figure 2.3^[16]. Most of the optical power is provided by the curved surface of the cornea (shown in the figure). The main function of the lens is to alter that power by changing its shape; thinner for viewing far objects and thicker for near object. The cornea and lens acting together form a small inverted image of the outside world on the retina, the light-sensitive surface of the eye. The retina lines most of the interior of the approximately spherically-shaped eye. This provides the eye with a very wide field of view.

There are two types of receptor in the retina, one is called the cone and the other is the rod named according to their shapes. The function of the rods in the retina is to give monochromatic vision under low levels of illumination. This scotopic form of vision operates when the stimulus has luminance of less than several hundredths of a candela per square meter (cd/m^2). The function of the cones in retina is to give chromatic vision at normal levels of illumination. This photopic form of vision operates when the stimulus has a luminance of several cd/m^2 or more.

2.1.3.2 Colour Vision Theory

Colour vision is the result of a system comprising the eye, the nervous system, and the brain. Thomas Young^[6] first propounded the trichromatic theory of colour vision including three types of cone receptors (or colour receptors) in the eye, red, green, and violet, following Newton's earlier investigation. In 1852 it was revised and elaborated by Helmholtz. The modified theory is known as the Young-Helmholtz theory of colour vision^[7]. This assumed that the eye contained only three spectrally unique cone receptors, primarily red, green, and blue. In 1878 Edwald Hering provided additional insight, proposing six independent colours, red, green, yellow, blue, white, and black^[36]. These colours are registered by three opponent colour systems, black-white, red-green, and yellow-blue. Thus an observer sees colour in terms of redness or greenness, and yellowness or blueness. In 1930 Müller^[37] found that the Young-Helmholtz concept on three types of colour receptor in the retina of the eye was correct, but that responses from these three receptors were converted in the elaborate nerve-signal switching areas within the eye and optic nerve to opponent-colours such as Hering postulated. He described the visual process in three stages, an initial photochemical stage, an intermediate chemical stage relating to the chromatic aspect, and a final stage of excitations of the optic-nerve fibres. Both the Young-Helmholtz theory and Hering theory paved the road for subsequent research.

Since three types of independent variation in the eye are required to match all possible colours, normal colour vision is called trichromatic^[28]. The spectral response curves are used to describe the response of the eye at different wavelengths. Curves plotting the amounts of R (red), G (green) and B (blue) required to match a constant amount of power per small constant-width wavelength interval at each wavelength of the spectrum for an observer are called colour-matching functions and designated by symbols $r(\lambda)$, $g(\lambda)$, and $b(\lambda)$ ^[16]. The λ is the visible wavelength. These colour-matching functions were determined independently by Guild^[38] and Wright^[39]. Figure 2.4 schematically shows the basic experimental arrangement^[2]. The test colour produced by the test lamp is to be matched and displayed in the bottom of the field of view. In the top, an observer sees an additive mixture of beams of red, green, and blue lights. The composition of the lights are then adjusted to match the test colour.

In Guild's investigation^[38], 7 observers made colour matches throughout the visible spectrum. The amounts of red, green, and blue were obtained and were expressed in terms of Guild's instrumental stimuli (heterochromatic primaries obtained with coloured filters) after the units has been adjusted to give equal amounts of the primaries to match the National Physical Laboratory standard white at the National Physical Laboratory (NPL) at Teddington, U.K..

Wright^[39] utilised monochromatic primaries at 650, 530, and 460 nm. Their units (the quantity of each primary) were adjusted so that equal amount of red and green stimuli were required in a match of a monochromatic yellow (582.5 nm), and equal amount of green and blue were required in a match of a monochromatic cyan (494 nm). Using 10 observers, Wright carried out the experiment at Imperial College, London, U.K..

Although remarkably different techniques were applied by the two researchers, their results could be converted to the same set of primaries due to the algebraic nature of colour. The primaries chosen were R (700 nm), G (546.1nm) and B (435.8 nm). The units of R, G, and B were adjusted to be equal in a match on an 'equal-energy' white (a white in which the energy per unit wavelength was constant through the visual spectrum). The amounts of each primary used to obtain a match are known as tristimulus values, R, G, and B. Tristimulus values can be converted into chromaticity coordinates by Eq.(2.1):

$$r = \frac{R}{R+G+B} \quad g = \frac{G}{R+G+B} \quad b = \frac{B}{R+G+B} \quad (2.1)$$

2.1.4 Colour Specification

2.1.4.1 Colorimetry

As mentioned earlier, colour perception requires three factors: a source of light, an

object, and a detector, usually the eye and brain. Each of these can be described by an appropriate curve across the visible wavelength. The combination of these comprises a colour or colour stimulus. A quantitative method to describe a colour stimulus is shown in Figure 2.5^[2].

In 1931, the International Commission on Illumination (CIE) adopted a system of colour specification which has lasted to the present time, known as the CIE system of colorimetry (see Section 2.2). In this system, a colour is defined by a set of X, Y, Z values, called tristimulus values. Two samples with identical material should be judged as an exact match when their tristimulus values are the same.

2.1.4.2 Subjective Estimation

Colour can also be subjectively specified by means of visual percepts. In the OSA Colour Committee terminology the word 'colour' is clearly defined as follows^[40], "*Color consists of the characteristics of light other than spatial and temporal inhomogeneities; light being the aspect of radiant energy of which a human being is aware through the visual sensations which arise from the stimulation of the retina of the eye*". Colour appearance is defined by Judd as "*the color perceived to belong to the visual object to which attention is directed*"^[3]. The hue, colourfulness and lightness, abstracted from complete visual experiences, are used to represent dimensions along which colour may vary independently. *Hue* is defined as the attribute of a visual sensation according to which an area appears to be similar to one, or to proportions of two, of the perceived colours, red, yellow, green, and blue. *Colourfulness* is the attribute of a visual sensation according to which an area appears to exhibit more or less of its hue. *Chroma* is the colourfulness of an area judged in proportion to the brightness of a similarly illuminated area that appears to be white or highly transmitting. *Saturation* refers to the colourfulness of an area judged in proportion to its brightness. *Brightness* implies the attribute of a visual sensation according to which an area appears to exhibit more or less light. *Lightness* is the brightness of an area judged relative to the brightness of a similarly illuminated area that appears to be white or highly transmitting^[41,42].

There are two colour modes depending upon the colour being perceived. One is 'object mode' and another is 'aperture' (or 'light-source mode'). Object mode is when a visual object appears as being illuminated by an external emitting light. This may be observed when the object is viewed under the surrounding of the other objects. Aperture colours imply that the visual object is emitting light by itself. A colour is perceived as a hole filled with a colour light when the surrounding field of the visual object is completely dark. Colours seen in these special circumstances are often referred as 'unrelated colours'. An aperture colour may also be observed in its background to other visual objects which, however, are usually of a low luminance. The above two modes of colour can not be perceived simultaneously^[43].

2.2 COLOUR SPECIFICATION SYSTEMS

2.2.1 CIE System

In colorimetry, a system of colour specification has been developed to relate certain stimulus characteristics to the calculated response of a standardised average observer. In any given set of viewing conditions, a colour stimulus may be matched by a unique mixture of three appropriately different colour stimuli.

A system was adopted in 1931 by the CIE, which stands for French "Commission Internationale de l'Eclairage", as the international authority for standardising colorimetric specification^[44]. This system introduced elements of standardisation of light source, observer, and the methodology to derive values to provide a measure of a colour observed under a standard illuminant by a standard observer. A standard set of colour-matching functions, primarily based upon extensive experimental investigations by Wright^[38] and Guild^[39] (see section 2.1.3.2) was adopted. The idea was to reduce any spectral radiance distribution to only three variables (X , Y , Z), and to state that, for colour vision, any two stimuli described by the same values of each of these variables, no matter how physically different, would be defined as colorimetrically matched.

The CIE system is a numerical method of specification which is independent of the existence of physical colour standards. This has been made possible by the development of standard viewing conditions including sources, observers and optical geometry. These are introduced in the following sections:

2.2.1.1 CIE Standard Sources and Illuminants

A light source is a real physical light, whose spectral power distribution can be experimentally measured. Some standard light sources have been recommended by CIE for colour description^[45].

One of these, CIE Source A, is a tungsten-filament lamp operating at a colour temperature of 2854 K, while CIE Sources B and C are derived from Source A by passing its light through special liquid filters (the Davis-Gibson filters). Source B, with a colour temperature of about 4870 K, is an approximation of noon sunlight. Source C, about 6770 K, is the light of average daylight. Other light sources widely used in colour matching are the xenon arc and Macbeth 7500 K Daylight, the latter obtained by modifying light from a tungsten-filament lamp with glass filters. The spectral power distribution curves for some of these sources are shown in Figure 2.6^[46].

When the spectral power distributions were measured, the standard sources A, B, and C were soon defined as standard illuminants A, B, and C by CIE in 1931. An illuminant is defined by a spectral power distribution. It may or may not be possible to make a source to represent it. In 1965 the CIE recommended a series of illuminants to supplement illuminants A, B and C based on the experimental results from the spectral power distribution of natural daylight^[35]. They represent average daylight over the spectral range of 300 to 830 nm and have correlated colour temperatures between 4000 and 25,000 K. The most important ones are illuminants D65 and D50, having a correlated colour temperature of 6500 K and 5000 K respectively. Table 2.1 shows the 1931 chromaticity coordinates of the standard illuminants A, B, C, D65 and D50^[47].

2.2.1.2 CIE Standard Observers

The scientific basis for measuring a colour is the existence of three different colour-response mechanisms in the human eye. These three responses come from the colour-receptors functions of visual wavelengths and were standardised and incorporated into the CIE standard observers. These functions were derived using the experimental results obtained by 10 and 7 observers in Wright's and Guild's investigations respectively (see Section 2.1.3.2). Their experimental set-up is shown in Figure 2.4. Wright's and Guild's results were in such a good agreement that the CIE (1931) was able to take the mean results as defining the response of an average observer. The experiments leading to the 1931 CIE standard observer were performed using only the fovea of human eye,

which covers only about a 2° angle of vision. Hence the CIE 1931 standard colorimetric observers are also referred to as 2° CIE standard observer^[7] which should be applied when an object subtends a viewing angle of less than 4° .

However, in some industry applications, colour matching functions for viewing large fields are required. (The structure of the eye is different in the central region of the retina, the fovea, and in the surrounding regions^[37,48]. The retinal images of large and small fields cover different areas and may evoke different colour responses.) In 1964 the CIE recommended a new standard observer to supplement the use of the 1931 observer in an effort to obtain better correlation with visual perception for large samples, covering an angle of viewing field of more than 4° . This is called the 1964 CIE supplementary standard observer or 10° CIE standard observer which was based on the experimental work conducted by Stiles and Burch^[49] and Speranskaya^[50] in 1959. Their experiment employed a total of 67 observers using mixtures of monochromatic lights, matched fields of 10° angular subtense. Figure 2.7 shows the actual sample size of a 2° field and a 10° field seen at a normal viewing distance of 45 cm (18 in)^[2].

2.2.1.3 Standard White, Standard Illuminating/Viewing Geometry

The CIE recommended the perfect reflecting diffuser as a reference for making measurements of reflectance factor. In recent years, disks pressed from magnesium oxide (MgO) powder or barium sulphate (BaSO₄) powder have been used as a suitable working standard or white standard. The spectral reflectance of such working standards lies around 0.970 to 0.985 in the visible spectrum.

Illuminating and viewing geometry also play a significant part in affecting colour appearance^[16]. In the case of an object with a glossy reflecting surface, its appearance is greatly affected by the angle of view relative to the angles at which the illuminating light falls on the surface. When an object has completely matte surfaces, the angles of viewing/illuminating have little effect. For the instrument measurements, the CIE recommended four sets of illuminating and viewing conditions. These include the sample

which is illuminated at 45° from the normal to its surface, and viewed along the normal, known as 45/0 geometry. Also, the diffuse illumination and near normal viewing geometry d/0, and the reverse conditions of these two (0/45 and 0/d) were recommended. For 45/0 geometry, the angle between the direction of viewing and the normal to the specimen should not exceed 10°. In the condition of d/0, the specimen is illuminated diffusely by an integrating sphere, the angle between the normal to the specimen and the axis of the viewing beam should be less than 10°.

2.2.1.4 CIE Tristimulus Values

Different sets of red, green, and blue primaries (expressed using wavelengths) were used by Wright and Guild in their experiments to obtain colour matching functions^[46]. Their results were linearly transformed to a new set of functions with no negative values. This resulted in a change from the original red, green, and blue primaries to a new set, which cannot be produced by any real lights, called X, Y, and Z primaries. The calculations are given below:

$$\begin{aligned} X &= 100 \frac{\int P_{\lambda} R_{\lambda} \bar{x}_{\lambda} d\lambda}{\int P_{\lambda} \bar{y}_{\lambda} d\lambda} \\ Y &= 100 \frac{\int P_{\lambda} R_{\lambda} \bar{y}_{\lambda} d\lambda}{\int P_{\lambda} \bar{y}_{\lambda} d\lambda} \\ Z &= 100 \frac{\int P_{\lambda} R_{\lambda} \bar{z}_{\lambda} d\lambda}{\int P_{\lambda} \bar{y}_{\lambda} d\lambda} \end{aligned} \quad (2.2)$$

where

$\bar{x}_{\lambda}, \bar{y}_{\lambda}, \bar{z}_{\lambda}$: The three standard observer colour matching functions. These specify the response of the CIE standard observer at a wavelength λ .

R_{λ} : Reflectance or transmittance of the object at the wavelength λ .

P_{λ} : Spectral power from a light source at the wavelength λ .

Y is known as the luminance factor. This function is directly related to the perceived lightness of a sample. If P is in watts per steradian and per square metre (a irradiance unit), and $\int P_{\lambda} \bar{y}_{\lambda} d\lambda$ is set to 0.146, then Y is the luminance in candela per square metre (cd/m^2) that is frequently used in photometry^[46]. In definition, the Y for the perfect diffuser is always 100, because R_{λ} is equal to unity at any wavelength λ for the perfect white.

2.2.1.5 Chromaticity Coordinates and Chromaticity Diagram

Each colour is frequently specified in terms of chromaticity coordinates, which describe the quantities of a colour in addition to its luminance factor, i.e., its chromaticity should be related to a certain extent to its hue and chroma. In the CIE system, the chromaticity coordinates x, y and z are thus obtained as:

$$x = \frac{X}{X+Y+Z} \quad y = \frac{Y}{X+Y+Z} \quad z = \frac{Z}{X+Y+Z} \quad (2.3)$$

Since $x + y + z = 1$, only two of the three coordinates are independent variables. One of three tristimulus values, usually Y, must be specified for describing lightness. Colour as described in the CIE system can be plotted in a chromaticity diagram, usually in the form of y vs x. Figure 2.8 gives the CIE 1931 chromaticity diagram. The figure shows the horseshoe-shaped spectrum locus (the line connecting the points representing the chromaticities of the spectrum colours identified by their wavelength), the purple line joining the ends of the spectrum locus, as well as the chromaticities of blackbody illuminants and the CIE standard illuminants A, B, C, and D65^[2].

2.2.1.6 Uniform Chromaticity Scales (UCS)

A uniform colour scale is a colour space or colour solid in which the difference between points correspond to the perceptual (visual) difference between the colours represented by these points^[46]. In 1976, the CIE recommended a 1976 CIE u' , v' uniform chromaticity scale diagram which was the linear transformation of the 1931 CIE system

and was an approximation to uniform visual perception^[51,52]. The equations were:

$$\begin{aligned} u' &= \frac{4X}{X+15Y+3Z} = \frac{4x}{-2x+12y+3} \\ v' &= \frac{9Y}{X+15Y+3Z} = \frac{9y}{-2x+12y+3} \end{aligned} \quad (2.4)$$

The reverse transformation was:

$$\begin{aligned} x &= \frac{9u'}{6u' - 16v' + 12} \\ y &= \frac{4v'}{6u' - 16v' + 12} \end{aligned} \quad (2.5)$$

2.2.1.7 Uniform Colour Space

Colour specifications often involve, not only nominal values, but also the definition of tolerances for colour differences from them. To meet these requirements, the CIE has recommended the use of two alternative colour spaces, CIE 1976 ($L^*u^*v^*$) colour space (or CIELUV) and CIE 1976 ($L^*a^*b^*$) colour space (or CIELAB). These CIE Colour Spaces have been used for evaluating colour differences in connection with the colour rendering of light sources and colour difference control for surface colour industries such as textiles, painting, printing etc.. The two stimuli under question should be presented using identical media and be viewed under the same viewing conditions defined by the CIE. The spaces are provided by plotting three quantities, along three axes at right angles to each other. The formulae of these quantities are given below:

CIE $L^*u^*v^*$ colour space:

$$\begin{aligned} L^* &= 116 \left(\frac{Y}{Y_n} \right)^{\frac{1}{3}} - 16 & \text{for } \frac{Y}{Y_n} > 0.008856 \\ L^* &= 903.3 \left(\frac{Y}{Y_n} \right) & \text{for } \frac{Y}{Y_n} \leq 0.008856 \end{aligned} \quad (2.6)$$

Where Y is the luminance factor of the sample and Y_n is the luminance factor for

reference white. L^* is equal to 100 for a reference white and zero for black.

$$\begin{aligned} u^* &= 13L^* (u' - u'_n) \\ v^* &= 13L^* (v' - v'_n) \end{aligned} \quad (2.7)$$

Where u'_n, v'_n are the u', v' values of a suitable reference white.

CIEL^{*}a^{*}b^{*} colour space:

$$\begin{aligned} L^* & \text{ (defined by Eq. (2.6))} \\ a^* &= 500 \left[f\left(\frac{X}{X_n}\right) - f\left(\frac{Y}{Y_n}\right) \right] \\ b^* &= 200 \left[f\left(\frac{Y}{Y_n}\right) - f\left(\frac{Z}{Z_n}\right) \right] \end{aligned} \quad (2.8)$$

Where X_n, Y_n , and Z_n are the tristimulus values of the reference white and

$$\begin{aligned} f(F) &= F^{\frac{1}{3}} & \text{for } F > 0.008856 \\ f(F) &= 0.787F + \frac{16}{116} & \text{for } F \leq 0.008856 \end{aligned}$$

The reverse transformation (for $Y/Y_n, X/X_n$, and $Z/Z_n > 0.008856$) are:

$$\begin{aligned} X &= X_n \left(\frac{L^* + 16}{116} + \frac{a^*}{500} \right)^3 \\ Y &= Y_n \left(\frac{L^* + 16}{116} \right)^3 \\ Z &= Z_n \left(\frac{L^* + 16}{116} - \frac{b^*}{200} \right)^3 \end{aligned} \quad (2.9)$$

For $Y/Y_n, X/X_n$, and $Z/Z_n \leq 0.008856$, the reverse transformation are:

$$\begin{aligned}
 X &= X_n \frac{\frac{0.787}{903.3} L^* + \frac{a^*}{500}}{0.787} \\
 Y &= Y_n \frac{L^*}{903.3} \\
 Z &= Z_n \frac{\frac{0.787}{903.3} L^* - \frac{b^*}{200}}{0.787}
 \end{aligned} \tag{2.10}$$

As a part of its 1976 recommendation, the CIE also defined the following colour terms: metric hue angle, metric chroma, and metric saturation. Because saturation is related to and derived from chromaticity, it is defined only for a linear transformation of the CIE x, y system, i.e. CIEL $^*u^*v^*$. These formulae are given below:

CIEL $^*u^*v^*$ and CIEL $^*a^*b^*$ hue angle:

$$\begin{aligned}
 h_{uv} &= \arctan\left(\frac{v^*}{u^*}\right) \\
 h_{ab} &= \arctan\left(\frac{b^*}{a^*}\right)
 \end{aligned} \tag{2.11}$$

Where $h_{uv} (h_{ab}) = 0$ ($+u^*$ or $+a^*$) represents red, $h_{uv} (h_{ab}) = 90$ ($+v^*$ or $+b^*$) yellow, $h_{uv} (h_{ab}) = 180$ ($-u^*$ or $-a^*$) green, and $h_{uv} (h_{ab}) = 270$ ($-v^*$ or $-b^*$) blue.

CIEL $^*u^*v^*$ and CIEL $^*a^*b^*$ chroma:

$$\begin{aligned}
 C_{uv}^* &= \sqrt{u^{*2} + v^{*2}} \\
 C_{ab}^* &= \sqrt{a^{*2} + b^{*2}}
 \end{aligned} \tag{2.12}$$

CIEL $^*u^*v^*$ saturation:

$$S_{uv} = 13 \sqrt{(u' - u'_n)^2 + (v' - v'_n)^2} \tag{2.13}$$

Where u'_n and v'_n are the values of u' , v' for a reference white.

Figure 2.9 gives a three dimensional representation of the CIEL*u*v* space^[16]. Hue angle in the diagram is measured in degrees starting with $h_{uv} = 0$ in the direction of +u* (red) and increasing in counterclockwise. Chroma is measured as the length of line from the neutral point ($u^* = v^* = 0$) to the sample point. The CIEL*a*b* space is similar but without representation of saturation.

Another uniform colour space is based on the CMC(*l:c*) colour difference formula^[53]. It has been confirmed that the CMC(*l:c*) formula correlates with visual colour difference judgments better than other published formulae^[54,55]. The uniform colour space based on this formula is calculated as followed:

$$L_{ucs} = (1/l) [21.75 \ln L^* + 0.3838L^* - 38.54] \quad (2.14)$$

unless $L^* < 16$ when $L_{ucs} = 1.744 L^*/l$.

$$C_{ucs} = (l/c) \{0.162C + 10.92[\ln(0.638 + 0.07216C^*)] + 4.907\} \quad (2.15)$$

$$h_{ucs} = h + Df \quad (2.16)$$

where $D = k_4 + k_5 P |P|k_6$

$$P = \cos(k_7h + k_8) \quad (2.17)$$

$$f = \{ (C1^*)^4 / [(C1^*)^4 + 1900]^{1/2} \} \quad (2.18)$$

and the values of the k_4 to k_8 for different ranges of h are given in Table 2.2. L^* , C^* , and h are calculated from CIE $L^*a^*b^*$ uniform colour scale.

2.2.2 Colour Order Systems

A colour order system is a rational method or a plan for ordering and specifying all object colours within a limited domain. It includes a set of material standards presented using physical chips^[29]. All colour order systems fall mainly into 3 major groups. Those in the first group are based primarily on the principles of additive colour

mixtures. Colours produced by systematic variations of the settings of a Maxwell disk or tristimulus colorimeter are duplicated by material samples. The second group is based on the regular adjustment of a limited number of dyes or pigments. Its purpose is to identify the gamut and other properties of a particular set of colorants. The third group is based on the perception of colours by an observer with normal colour vision and includes Munsell, Natural and OSA UCS colour systems etc. The scales of the systems are chosen to repeat attributes of perceived colours. The systems in this group are sometimes called colour appearance systems^[56]. A brief account of some colour appearance systems are given below.

2.2.2.1 Munsell Colour System

The Munsell system was originated by A.H. Munsell to show the perceptual arrangement of colours^[57]. It based on a collection of many painted samples to represent equal intervals of visual perception between adjacent samples, and to describe all possible colours in terms of its three coordinates: Munsell Hue, Munsell Value, and Munsell Chroma. Value describes the attribute of lightness, ranging from 0 for perfect black to 10 for perfect white. Chroma indicates the amount of chromatic content in a colour. In other words, it is the degree to which a chromatic sample differs from an achromatic sample with the same Value. Chroma scale starts from 0 for neutral sample (no hue trace at all) and extends to a maximum value, (12 or 14) being achievable for actual colorants. Its Hue descriptors consist of five primaries: red (designated 5R), yellow (5Y), green (5G), blue (5B), and purple (5P). The five intermediates are designated as: 5YR, 5GY, 5BG, 5PB, 5RP. Totally, there are 100 hue steps. A complete designation of a colour in Munsell terminology is Hue Value/Chroma, such as 10YR 7/10. Figure 2.10 illustrates the relationships between Munsell Hue, Munsell Value and Munsell Chroma^[46]. The physical exemplifications of Munsell Colour System is shown in the Munsell Book of Colour. The samples in the Book consist of painted paper chips. Each of these is arranged by Value versus Chroma on each page showing a specific hue. In 1943, Optical Society of America (OSA) Committee on Colorimetry smoothed, adjusted the spacing of the Munsell Colour, and related the results to the 1931 CIE system. The

revised system is usually referred to as the Munsell Renotation System^[58,59]. The notation is specified for the 1931 CIE standard observers and standard illuminant C. This improves the visual uniformity of the colour spacing. The book includes both glossy and matt chips based on the renotation^[60].

2.2.2.2 Natural Colour System (NCS)

NCS system is a colour-order system of which the colours are described in terms of the relative amounts of six basic colours perceived^[61]. This system was developed by Jahansson and Hesselgren, and more recently, further modified by Hard and Tonnquist^[62]. A colour in the system is characterised in terms of colour content by six primary colours: red (r), yellow (y), green (g), blue (b), black (s), and white (w). The arrangement of these six primary is schematically shown in Figure 2.11. A typical specification might be $y_{20}r_{20}s_{35}w_{25}$ which means that the sample have 20% yellowness, 20% redness, 35% blackness, and 25% whiteness^[63]. The hue of this colour would be determined by the ratio of the content of the two neighbouring hues, that is $20 / 20$, which is the same as $50 / 50$. Thus the colour can be also described as containing 50% yellowness and 50% redness. NCS Hue is expressed by the initial letter of one unique hue, followed by the percentage of the second unique hue, and then the initial letter of the second hue. The hues are always followed the order Y, R, B, G, Y. The total content of hues is 40%. In this case this gives the total chromatic content and is termed as the NCS Chromaticness (c). Three of four values are sufficient to express NCS system due to $w + s + y + r = 100$. To satisfy this, the whiteness, w is omitted. Thus the NCS specification for the above typical colour is 35 40 Y50R. The values are always given in the order of blackness, chromaticness, and hue.

2.2.2.3 OSA UCS Colour System

The Optical Society of America Uniform Chromaticity Scale is dedicated primarily to produce a system in which samples are arranged in a regular rhombohedral lattice. The distances between a sample and each of its 12 nearest neighbours correspond to

equal perceived colour differences at any point in the lattice^[64]. An OSA specification includes three numbers such as 3:1:5. The first number represents the lightness l , ranging from about -7 to +5 with 0 standing for a medium lightness. The second, j , (from French *jaune*) represents the yellowness-blueness of the colour (j is positive for yellowish colours and negative for bluish colours). The values of j range from about -6 to +11. The third number, g , represents the greenness-redness of the colour (g is positive for greenish colours and negative for reddish colours) with a range from -10 to +6. Figure 2.12 illustrates the geometrical (cubo-octahedral) basis of the OSA system^[16].

2.3 COLOUR APPEARANCE

Hunt^[17] divided the development of colorimetry into three stages: matching, difference, and appearance. Measures used to indicate whether or not two stimuli match each other include tristimulus values and chromaticity coordinates. Measures used to quantify colour difference (e.g., in lightness, chroma, or hue) are devised so that equal scale intervals represent approximately equal perceived differences in the attributes considered, such as those measures in the CIE $L^*a^*b^*$, CIE $L^*u^*v^*$ colour spaces. However, these measures are limited to be used under a set of fixed viewing conditions and can not be used to quantify colour appearance under various viewing conditions. The measures representing the magnitudes of perceived attributes should be devised. These are particularly important in the colour reproduction industry. There is a lack of understanding of the properties of human colour perception in various viewing conditions used for original scenes and for different media. Accurate measurement of colour appearance requires knowledge of the reaction of human vision to each fixed set of viewing conditions.

Adaptation is a visual process of adjustment by an organism to environmental conditions^[65]. Colour appearance of an object is greatly affected by the state of adaptation of the eye^[66]. Light is a key factor to influencing adaptation. According to the mode of light source change, two types of adaptation exist. One occurs when only the luminance level of a light source is changed. The other is due to the change the colour of light source^[67].

2.3.1 Light Adaptation and Dark Adaptation

In the case of changing the luminance level of a light source, adaptation can be divided into light and dark adaptation. Light adaptation is defined as the general reduction in retinal sensitivity resulting from stimulation at a higher intensity level than that the eye adapted. When reference is made to the levels at which cone vision is fully operative, light adaptation is often referred to photopic adaptation^[28]. Dark adaptation

is the reverse process of light adaptation and is often called scotopic adaptation^[28]. This type of adaptation has a significant effect on perceived brightness and brightness discrimination. Light adaptation has been extensively studied over the past decade. Various equations were formulated between the physical stimulus and human responses^[68].

2.3.2 Chromatic Adaptation

When the colour of a light source is changed, the adjustment of the visual system is known as chromatic adaptation. In this process, appropriate compensation is made for changes in the colours of stimuli, especially in the case of changes in light sources^[16]. Normally, the chromatic adaptation is incomplete under common sources such as daylight and incandescent illumination. If we could completely adapt to the changes in the colour of illumination with a rapid time course, we would be unable to discriminate colour change. Because colour appearance varies with chromatic adaptation, the study of chromatic adaptation always includes the accumulation of visual responses for describing colours, the assessment of color-rendering properties of illumination systems, and the derivation of colorimetric transformations for predicting the changes of color appearances between the specific corresponding illuminations^[65].

When an observer takes an array of coloured objects from natural daylight into a room illuminated by an incandescent filament source, he notices that the perceived colours of objects change to a marked degree. The blues become darker and much less saturated; the greens, yellower; and the purples much redder. These changes can be predicted by computation from the spectral reflectance of the objects by means of the CIE standard observer changed from a standard daylight illuminant to standard illuminant A (representative of an incandescent filament source). These predictions hold well for the daylight adapted eye. Unfortunately, the observer's eye changes almost immediately when entering the artificially illuminated room. After a short period of time, the eye increases its sensitivity to the short-wave part of the spectrum so that objects are perceived to have approximate same colours as seen in daylight^[69]. This can be seen

clearly in Figure 2.13^[70]. The long vector on the graph indicates the considerable "blue-yellow" shift in CIE specification of a spectrally nonselective grey object when it is illuminated by CIE sources C and A respectively. The colour difference represented by this vector is called the colorimetric colour shift^[33]. A spectrally nonselective surface in everyday life, however, retains a near-neutral appearance under either daylight (source C) or tungsten (source A) illumination. The actual small change in appearance would be represented by a short vector known as the resultant colour shift (as shown in Figure 2.13). The reason is that the CIE standard assumes an observer viewing at two adjacent areas through a dark tube. The light illuminating any one side or both areas has no effect on the assumed constant adaptation of the (single) standard eye except the light being (theoretically) reflected or transmitted to corresponding adjacent central areas of the standard retina.

In everyday life, identical adjacent areas are not usually illuminated with widely varying illuminants, nor viewed at through dark tubes. It is more typical to find one kind of illumination incident on all objects in view. The general adaptation of the eye is not determined by small patches in a dark surrounding area but the spectral quality of a prevailing illumination. When the illumination is changed from daylight to tungsten light, the eyes adjust their spectral sensitivities to such an extent that, at the beginning, they largely compensate for the change in quality of the general illumination. The eyes continuously adjust their sensitivities to the general illumination, and compensate sufficiently to a change in its quality so that colours of objects tend to retain a characteristic colour appearance regardless of the kind or amount of illumination. Most colours remain relatively stable in appearance^[71], which is called colour constancy. Thus it is important to specify the shifts in colour appearance accurately.

The perception of the colours of objects in a room illuminated by chromatic illumination is thus a combination of two effects. The first is from the changed spectral character of the radiant energy. This is complicated but understood. The second is caused by the changed state of adaptation of the eye. This has not been fully understood^[69].

2.3.3 Some Common Types of Transformation for Chromatic Adaptation

The goal of chromatic adaptation theories is to predict the corresponding colours with same appearance under two different types of illumination^[5]. Corresponding colours are the sets of tristimulus values that describe the stimuli which evoke the same colour appearance^[72]. This is produced by deriving equations translating from one condition of adaptation to another^[73]. Currently there are two types of chromatic adaptation models and theories. The linear models, first proposed in 1877 by von Kries and bearing his name, assume that the changes in sensitivity of the eye associated with the three types of cone receptors are linearly related to the changes in the tristimulus values as the illumination changes. Many other models were also developed. One of these has been recommended by CIE and was proposed by Nayatani and coworkers^[22,74-76] based on the assumption of a nonlinear relationship.

Bartleson compared and divided various transformations into two types^[65,77] according to whether the postulates were associated with the von Kries coefficient rule. Figure 2.14 shows a representative of the type I (top) and type II (bottom) prediction contours with respect to CIE illuminant A evoking the same colour appearances as the samples seen under adaptation to CIE illuminant D65. Type I is somewhat in accordance with the von Kries postulates and includes data from Bartleson^[10], Pointer et al.^[12], Richter^[78], Takahama et al.^[79] and Burnham et al.^[80] The second type was developed by Helson et. al.^[69] and MacAdam^[81] and bore little relation to the von Kries postulates. Linear theory is usually adequate for simple transformation, such as that from daylight to incandescent light at constant illuminance. However in more complex situations, such as changing the luminance level of the illuminant or the background reflectance^[5], a nonlinear theory is required.

The procedures for predicting corresponding colours under chromatic adaptation are as follow: after the reference and test illuminants are defined, the CIE tristimulus values of the sample are transformed to a set of fundamental cone primaries R, G, B.

$$\begin{bmatrix} R \\ G \\ B \end{bmatrix} = A \begin{bmatrix} X \\ Y \\ Z \end{bmatrix} \quad (2.19)$$

Where A is a coefficient matrix.

Then, the R, G, B fundamental tristimulus values are transformed linearly or non-linearly to the fundamental tristimulus values of corresponding colours.

$$R' = f_r(R), \quad G' = f_g(G), \quad B' = f_b(B) \quad (2.20)$$

Where the f_r, f_g, f_b are the functions of R, G, B respectively.

Finally, the new fundamental tristimulus values of the sample in the test illuminant are transformed back to the CIE tristimulus values.

$$\begin{bmatrix} X' \\ Y' \\ Z' \end{bmatrix} = A^{-1} \begin{bmatrix} R' \\ G' \\ B' \end{bmatrix} \quad (2.21)$$

Where A^{-1} is the inverse matrix of A. The unknown part above is the functions f_r, f_g , and f_b .

Two transforms are used to represent the others and described below.

2.3.3.1 Von Kries Transformation

Johannes Adolf von Kries first proposed a quantitative account of chromatic adaptation^[82]. His "coefficient law" assumed that the visual mechanism contained three fundamental sensitivity processes remaining invariant in relative spectral distribution. Changes in spectral sensitivities are in inverse proportion to the strength of their activation by the illuminant. If the fundamental sensitivities are symbolised as $\bar{r}_\lambda, \bar{g}_\lambda, \bar{b}_\lambda$ and tristimulus values R, G, B, and their altered states in response to a change in illuminant spectral power as $\bar{r}_\lambda', \bar{g}_\lambda', \bar{b}_\lambda'$ and tristimulus value R', G', B'. Von Kries'

coefficient rule may be represented in terms of fundamental tristimulus values as

$$R' = a_r R, \quad G' = a_g G, \quad B' = a_b B \quad (2.22)$$

Where a_r , a_g , and a_b are constants.

2.3.3.2 Nayatani's Transformation

Nayatani's model on chromatic adaptation has been recommended by the CIE for field trial^[83]. It consists of two steps^[74-76]. The first step is a linear von Kries transformation:

$$\begin{aligned} R &= k_r (R + R_n) \\ G &= k_g (G + G_n) \\ B &= k_b (B + B_n) \end{aligned} \quad (2.23)$$

Where the R_n , G_n , B_n are the noises. k_r , k_g , and k_b are constants. The nonlinear of the second step is expressed by exponents β .

$$\begin{aligned} R' &= a_r (R)^{\beta_r(R_0)} \\ G' &= a_g (G)^{\beta_g(G_0)} \\ B' &= a_b (B)^{\beta_b(B_0)} \end{aligned} \quad (2.24)$$

Where a_r , a_g , and a_b are constants. $\beta_r(R_0)$, $\beta_g(G_0)$, and $\beta_b(B_0)$ are exponents for the three response mechanisms and are functions of R_0 , G_0 , and B_0 respectively. R_0 , G_0 , and B_0 are the R , G , B values for the non-selective background.

2.3.4 Some Phenomena on Colour Appearance

2.3.4.1 Hunt Effect

The effect on colourfulness of changes in luminance level was first investigated by

Hunt^[84]. This is also called the Hunt Effect^[84]. Considering a series of chromatic colours with various hues, when raising the adapting luminance from low to high, their chroma and colourfulness evaluations increase.

2.3.4.2 Helmholtz-Kohlrausch Effect

Considering lightness, one kind of effect is the Helmholtz-Kohlrausch Effect^[10] which is also called heterochromatic brightness matching. Consider two colours under the same illumination, one is achromatic and the other is chromatic having the same Y value. Generally the perceived lightness (or brightness) is different between the two colours.

2.3.4.3 Helson-Judd Effect

The Helson-Judd Effect^[85-87] is demonstrated when a series of achromatic samples on a grey background is illuminated by a highly chromatic light, for example a yellow light. The light samples are perceived to have the hue of the illuminant (yellow hue), and the dark samples as having the opponent hue of the illuminant (purplish-blue hue). The mid-grey sample is still perceived as achromatic. Other chromatic illuminants (red, green, and blue) also show the same trend. This effect was found by Helson and demonstrates the effectiveness of the opponent colour theory.

2.3.4.4 Effect of Colour Temperature

Illuminants of different colour temperature result in the different illuminant colours. When, at a given level of illumination, changes are made in the colour of the illuminants in which related colours are seen, the observer's state of adaptation usually changes so as to reduce the resulting changes in colour appearance. This has been discussed in Section 2.3.2 and known as the chromatic adaption effect. Another example is illustrated in Figure 2.15 using the grids of lines of constant hue and saturation obtained by subjective scaling with adaptation to standard illuminants D65 and A^[12]. The results are presented in the form of mean loci of constant hue and saturation within the framework

of the u',v' diagram under each conditions of adaptation. The conditions of adapting fields are that luminance is 110 cd/m^2 and angular subtense is 18° ; the test colours have luminance 55 cd/m^2 and angular subtense 2° .

2.3.4.5 Stevens Effect

Another effect on brightness response under changing luminance level is Stevens effect^[88,89]. Given a series of achromatic samples on a white background, if the luminance is increased, the brightness of the medium-dark grey (Y/Y_{white} is about 0.16) maintains approximately constant brightness, darker grey decrease in brightness and lighter grey and the white surround increase in brightness, i.e. the brightness contrast increases. The same tendency was also found for unrelated colours.

2.3.4.6 Simultaneous Contrast

Simultaneous contrast is the change in appearance of a colour through the influence of a contrasting colour in the immediate environment^[90] or surround. The larger surrounding colour will influence the appearance of the smaller colour area. If the angular subtense of the colour is not too small (greater than about 1°) then simultaneous contrast usually occurs^[91,92], i.e. the colour tends to appear more like the opposite of the surround; thus colours on dark surrounds appear lighter, those on light surrounds appear darker; colours on green surrounds appear more magenta, those on magenta surrounds appear greener, and similarly for other hues. If a colour is seen at a very small angular subtense (less than $1/2^\circ$) and particularly if it is in the form of an intricate pattern on the surround, the spreading effect usually occurs^[93]: the colour then tends to appear more like the surround, light surrounds lightening the appearance, green surrounds making the appearance greener, and so on. These simultaneous contrast and spreading effects can be very important for designers in designing fabrics, wall paper and packaging, etc. Considering a grey test area seen on a grey surround of medium reflectance, if the surround reflectance is increased, the formerly grey test patch now looks darker. This is a common brightness (lightness) contrast effect. If the background is changed from

neutral to, say, red, then the formerly grey test patch takes on an apparent greenish hue. This is a common chromatic contrast effect^[94].

The simultaneous contrast effect is usually studied in a centre-surround paradigm. The colour in the centre area is also called induced colour or test colour. The surround colour is called its inducing colour or induction colour. Hue, saturation, brightness and spatial parameters of the centre and surround all have an effect on the change in perceived colour of the centre area^[95]. Although chromatic induction has been a subject of prime interest throughout the history of vision research, this phenomenon is only partly understood.

Adaptation and contrast effects are essential aspects of everyday visual perception and warrant an important place in colour theory. In order to explain chromatic adaptation, von Kries (see section 2.3) simply postulated the coefficient principle which suggested that dim and brightness stimuli should be attenuated in the same proportion. It is now well established that this rule does not account for the contrast effect^[95,96], the general finding being that bright stimuli are attenuated less than dim stimuli. The classical results most frequently cited in relation to colour contrast phenomena are those of Kirschmann's law^[97]. This law states that the chromatic contrast is at a maximum when the luminance contrast is at a minimum. The saturation of the induced colour increased with increasing the size and saturation of inducing colour and the reduction of brightness contrast between the two areas.

In order to study the factors affecting induced colour by chromatic surround, Kinney employed a Bausch & Lomb projection colorimeter with illuminant A to provide the stimuli. Four inducing colours (Red, Blue, Green, Yellow) were used^[98]. His results on colour contrast agree with Kirschmann's law that the saturation of the induced colour increases with increasing size and increasing saturation of inducing colour, but do not agree with Kirschmann's law of increasing saturation of induced colour with decreasing brightness contrast between the two areas. Kinney's experimental result showed that the amount of colour induced increased as the size of the inducing field is increased, as the

luminance ratio between inducing and induced field is increased and, to a small extent, as the purity of the inducing colour is increased. The brightness of the induced colour decreases with increasing luminance ratio. Jameson and Hurvich also found more colour induction with larger luminance ratios between inducing and induced fields^[99]. They made a quantitative evaluation of the effect of simultaneous contrast by simple connection between induced and inducing colours^[100]. They have shown that the amount of colour induced in a focal area is inversely proportional to the opponent response of the inducing surround. Other studies have concluded that receptor sensitivity changes by the chromatic adaptation and incremental (or decremental) contributions to colour signals by the colour background are responsible for chromatic induction^[96-101]. These studies all quantified the effect of the surround on the centre. They applied only a limited number or range of the centre colours.

Scrivener et al.^[102,103] provided historical reviews of the study of simultaneous contrast and conducted a psychological experiment. Their experiment was designed to investigate the effect of simultaneous contrast on colour appearance by varying the lightness, colourfulness, and hue of induction field surrounding the test colour presented on a CRT display and viewed under more natural viewing conditions. They used a total of 333 test-surround presentations estimated using a magnitude estimation method, and concluded that for the lightness perception, when the surround had a higher lightness value than the test, the test appeared darker than when seen against the grey background (with a reflection factor of 20%) and vice versa. For the colourfulness scaling a colour appeared more colourful when surrounded by the neutral grey background and appeared most colourful when surrounded by the colour with hue in opponent hue of the test colour. The decrease in colourfulness of a test patch is greatest when surrounded by an inducing field of the same hue but different lightness. The hue of a test patch shifted in the direction of the opponent hue of the induction field, which is in line with the findings of other researchers.

2.3.5 Experimental Methods to Determine Colour Appearance

Four experimental methods have been developed to measure colour appearance. These are:

2.3.5.1 Haploscopic Matching Technique

Haploscopic matching, also called binocular septum or interocular matching^[8,29], is an often used technique. This method was developed by Wright^[104] and subsequently applied by Wassef^[105], Hunt^[106], Wyszecki and Stiles^[29], etc. It utilised a colorimeter which allowed a test field and an adjacent matching field to be seen by different eyes. It employs observing conditions quite different from those used in the real world (i.e., view with both eyes on one target) and assumes that the two eyes have no interference with each other. This, however, has been pointed out to be not completely true by a number of workers^[107-109]. Hence, the validity of results obtained using this method has to be taken with some reservation.

2.3.5.2 Differential Retinal Conditioning

This method is similar to the haploscopic technique except that the comparison and matching are made between two retinal areas in the same eye. The experiment uses a large 10° colorimeter field in which the two halves of the field are filled with different adapting colours^[110].

2.3.5.3 Memory Matching

In this method, each observer is trained to recognise colour appearance in terms of colour systems, such as Munsell system, and to remember notations for hue, chroma, and lightness. If an object is shown under various conditions, the subject gives its notation, relying on memory.

This method was employed by Helson et al^[69]. In his experiment, a group of nine observers was trained for a period of 8 hours to recognise and correctly identify the

Munsell samples according to the scale values to be used in the experiment. Memory matching method poses some experimental problems^[65]. Observers have a limited capacity for retaining information^[111,112]. It took longer training periods than that used by Helson et al. Furthermore whenever memory is involved, one must recognise the possibility that distortion may occur through the memory trace^[113].

2.3.5.4 Direct Scaling and Magnitude Estimation

Each observer is asked to make a subjective estimate of the magnitude of visual attributes. The attributes might be lightness, brightness, colourfulness, saturation, chroma, and hue. The observer simply assigns a number that in his or her view corresponds to the magnitude of the chosen attribute in the sample being viewed. Alternatively, the observer might be asked to make a subjective estimate of the attribute on some more clearly defined scale, usually an equal-interval scale, or to compare two samples for an estimating parameter^[114,115].

The magnitude estimation technique was first tested by Stevens et al.^[116] and has recently gained in general acceptance. It is a subjective scaling technique by which the magnitudes of perceived attributes are scaled. Rowe^[117] and Padgham^[118] carried out their work to scale hue and saturation. They concluded that a surprising degree of precision can be achieved using this technique. In Ishak et al's study^[115], two observers made estimations in terms of hue, saturation and lightness for 60 surface colours on seven backgrounds (Black, Grey, White, Red, Yellow, Green, and Blue background). They compared their results to these by Helson et al.^[69] (using the memory method), Wassef^[105], Hunt^[106] and Gibson^[119] (using the binocular matching method). The results showed that the magnitude estimation method was reliable in producing results similar to those found using other methods. They concluded that the method was suitable for measuring colour appearance under a variety of viewing conditions. Following their study, Nayatani et al.^[120] examined the precision of this method between and within observers, and reconfirmed its effectiveness. They made assessments for three attributes of 100 object colours by a panel of fifteen observers. A fluorescent lamp with a high

colour-rendering index was used. Results showed a good agreement with those obtained by Ishak et al. This method was later employed by Bartleson^[9], Pointer^[11,12], and Luo et al^[121,122].

In using a magnitude estimation technique, an observer simply views the test sample and assigns numbers or names that correspond to the colour attributes of its subjective appearance. Normally they are lightness, brightness, saturation, colourfulness, and hue.

Lightness is a subjective attribute that has been studied thoroughly by Stevens et al. and by many others^[115, 121, 122]. As far as the method applied to reflecting surfaces, it was relatively grey content that was examined^[89].

Brightness is defined by the CIE as the attribute of a visual sensation according to which an area appears to exhibit more or less light^[123]. It is a perceptually absolute quantity and has an absolute zero modulus without upper limit. For many years attempts have been made to characterise perceived brightness as a function of stimulus luminance. A variety of predictive equations has been proposed. Stevens et al.^[89] specified brightness as a power function of luminance. Bartleson's brightness-scaling experiments with a complex stimulus field showed that the resulting brightness vs luminance functions are not simple power functions but are nonlinear in log-log coordinates^[124].

For estimating hue, four to six names of basic or unique colours are commonly used, among which are Red, Yellow, Green, Blue and the two intermediate hue orange and yellowish-green. For colour appearance between the unique colours interpolations are used either in numerical form^[125] such as "80% green, 20% yellow", or as combination names such as Blue-Green^[126]. This method is closely associated with NCS Colour System (Section 2.2.2.2).

Earlier magnitude estimation experiments were conducted using saturation rather than colourfulness. Saturation assessments were reported by Maxwell^[127], Indow and Stevens^[125], and Warren^[128], etc.. In these studies, observers were asked to scale the

saturation of a test colour on a scale which had fixed points at both ends. One end (zero) represented a colour with no saturation (a neutral colour), and the other end (100) represented the most saturated colour that the observer could imagine having the same hue as the test colour. The test colour was then scaled as a number between these two end points. This led to difficulties in analysing the data because the most saturated colour varied in absolute saturation for different hues, for example, a most saturated blue could be more saturated than a most saturated yellow^[11].

The concept of colourfulness was introduced by Hunt^[66] to denote the attribute of a visual sensation according to which an area appears to exhibit more or less chromatic colour. Pointer's^[129] results showed that this concept is meaningful to the observers who were asked to rank colour chips in order of colourfulness and also able to scale the colourfulness of each individual chip. In his experiment, colourfulness was scaled under various luminance levels and backgrounds. A correlation coefficient of 0.97 was obtained between mean of saturation and colourfulness. This suggested that there was a high degree of correlation between these two attributes. He concluded that colourfulness was a useful concept which observers were well able to scale, and may be more easily scaled than saturation or chroma. If a full measure of the appearance of a colour is required, colourfulness can provide changes in chromatic response caused by the luminance levels.

2.3.6 Prediction of Colour Appearance

A chromatic adaptation model can predict the tristimulus values of a corresponding colour in a reference field but not its colour appearance. Prediction of colour appearance by a model includes at least three procedures: first to gain a typical set of colour vision cone spectral sensitivity functions, then to obtain a quantitative relationship between the spectral sensitivity functions and various adaptation conditions, and finally to establish a model capable of predicting colour appearance in terms of perceived colour attributes, such as lightness, colourfulness, and hue.

Current colour appearance models (also called colour vision models) combine a

simplified theory of colour vision with correction for chromatic adaptation and the use of a uniform colour space. These models require the CIE X, Y, Z tristimulus values of a colour and predict colour appearance attributes (lightness, brightness, colourfulness, chroma, hue, etc.), by taking into account a wide range of viewing conditions. Figure 2.16 schematically outlines two existing models, the Hunt and Nayatani models. Three types of cone receptors (ρ , γ , β) are corrected into two forms of chromatic adaptation, linear and nonlinear forms. Both are input into two opponent channels, R-G and Y-B, and one achromatic channel A. A positive signal in the R-G channel is an indication of redness whereas a negative signal indicates greenness. Similarly, a positive signal in the Y-B channel is an indication of yellowness whereas a negative signal indicates blueness. The signals from these three channels are then combined to produce the sensations of hue, colourfulness, chroma, saturation, lightness and brightness.

2.3.6.1 Hunt Colour Appearance Models

Hunt model emerged in 1982 (Hunt82 model)^[19]. Based on the data obtained by Hurvich^[130], Breneman^[131], Pitt and Winter^[132], and other researchers^[9,12,14,61,73,118,133], this model was established to formulate quantitative empirical relationships between the main trends of these appearance data using a typical set of cone spectral sensitivity functions. The data used were obtained under a set of standard viewing conditions. The model gave a good prediction for the Munsell colour spacing. The Estevez cone spectral sensitivity functions^[134] was utilised. The transformation of cone response to the opponent colour stage was on the basis of physiological and psychophysical information. Figure 2.17 schematically shows the procedures of the model. It describes nonlinear responses of three cone receptors (zone I to zone II), and then combines the three responses in groups. The model derives the outputs of one achromatic signal channel and four chromatic channels (zone II). The latter chromatic signals are further transformed to the hue (the redness-greenness, and the yellowness-blueness signals), colourfulness, saturation, brightness, and chroma (zone III). This model can predict various colour appearance phenomena and accurately predict NCS hues. However it has been confined to a single mid-photopic level of daylight illumination.

In 1985, the original model was extended to cover a wide range of illuminants. This is named the Hunt85 model^[135]. This modified model applied the CIE 1931 standard colorimetric observer rather than Estevez's data. Comparison of the two cone spectral sensitivity curves are given in Figure 2.18^[135]. The modified model also changed the achromatic signal A from $(R+G)^{1/2}$ to $2R^{1/2} + G^{1/2} + (1/20)B^{1/2}$. This was based on physiologically considerations for the signals comprising A . The Hunt85 model gives reasonably good prediction of unique-hue loci, of constant-hue loci, and of constant-chroma loci, as judged by the comparison with the NCS systems (Figures 2.19 and 2.20) under a medium photopic level of daylight illumination. Figure 2.19 shows the predicted grids of the Nayatani and Hunt models for constant hue and colourfulness loci from formula, and that from NCS systems, plotted on the CIE 1976 uniform chromaticity diagram. The Figure shows the two systems are quite similar in predicting the hue and chroma spacing of the NCS data^[23,135]. In Figure 2.20, the lines of unique hue predicted by the Hunt model are compared to the unique hue lines located in the NCS. The lines are associated with the definitions of the four elementary hues (red, yellow, green, and blue)^[135]. When combined with a chromatic-adaptation transform with von Kries type, the model also gives a quite good prediction for surface colours seen in tungsten-light (S_A) illumination and typical fluorescent illumination of medium photopic levels.

The Hunt85 model was further modified to provide predictions of brightness and colourfulness, for both related and unrelated colours at any level of illumination (photopic, mesopic, or scotopic) (Hunt87 model)^[20]. In addition to these, the Hunt87 model covers a wide range of stimulus intensities, as well as reflectance factors of backgrounds. Prediction of colourfulness is achieved by using hyperbolic functions advocated by Seim and Valberg^[136] instead of using power or logarithmic functions. Considering the many viewing parameters in the visual system that are not quantified at the present state of knowledge, Hunt's model utilised readily identifiable parameters such as chromatic and brightness induction factors (N_c and N_b). These factors were easily incorporated into a particular effect so that, in practice, appropriate values of these parameters can be found in the light of the experience of the users. In fact this model exhibits more flexibility than the previous ones.

After field trials by Luo et al.^[121,122] using a large set of experimental data (LUTCHI Colour Appearance Data, which will be detailed in section 2.4.2) of scaling hue, lightness, and colourfulness, under a wide range of viewing conditions, the Hunt87 model was further modified yielding Hunt89^[137]. In 1991, Hunt published his latest version of colour appearance model (Hunt91). This revision was made to predict a more realistic balance between the relative contributions from cones and rods to the achromatic signal at various levels of adaptation, and thus can be used to predict colour appearance accurately under a wide range of viewing conditions^[21]. Previous models were found to include too many proportions of contribution from the cones at low levels of illumination and from rods at high levels of illumination. Also there was not included consideration of adaptation caused by the backgrounds with various luminance factors. Further more, for unrelated colours, the dependence of hue on stimulus luminance was not included. All of these shortcomings was rectified in the Hunt91 model which give definitions of adapting field, surround, background and proximal field.

2.3.6.2 Nayatani Colour Appearance Models

In 1981, Nayatani et al. published their nonlinear chromatic adaptation model^[74] (see section 2.3.3) which was recommended for field trials by CIE. A chromatic adaptation model cannot predict the colour appearance of an object colour directly. Hence, they formulated a model for predicting the colour appearance of an object colours under various states of chromatic adaptation by combining their nonlinear model on chromatic adaptation and the idea of the Hunt82 model^[22]. This becomes the Nayatani86 model. The outline of Nayatani model is shown schematically in Figure 2.21^[22]. Zone 1 corresponds to a modified von Kries transform, zone 2 to a nonlinear transformation in the three-receptor stages and also in the post-receptor stages. These include the combinative process of **R**, **G**, **B** responses. Zone 3 corresponds to interpretative stages. The notation AL stands for the effective adapting level of receptor. The Nayatani86 model introduced the idea of the Hunt model in the transformation from trichromatic to opponent-colour responses, especially in using the parameters e_s (eccentricity) and θ (hue angle). The main difference between the two models is that the

nonlinear characteristics of cones in the Nayatani model are represented by power functions (Figure 2.21) and in the Hunt model by hyperbolic functions. This model can be used to predict the colour appearance of object colours for the change of adaptation caused by the change of illuminant colour and adapting illuminance, but it can only be applied to colours on a medium gray background.

Following a study of the Hunt85 model, Nayatani reformulated their 86 model (to Nayatani87 model) by changing the fundamental functions from Pitt to Estevez-Hunt-Pointer primaries^[24]. The normalising illuminant D65 was used in the transformation from the CIE tristimulus values to those in the fundamental-primary system. Luminance level was kept at 3,000 lux. The reformulated model gave better correlation with the Munsell and the NCS schemes than the original one. Figure 2.19 shows the predicted result of Nayatani87 model compared with NCS data^[24]. Formulae for various colour appearance metrics were included in this model, such as colourfulness, chroma, saturation, brightness, etc..

After field trials on the colour appearance of chromatic object colours under various adapting-illuminance levels of a specified light source and an adapting light source at a specified illuminance level^[138,139], a new scale, whiteness and blackness response of achromatic object colours was included^[25]. The model was further extended into the Nayatani90 model which can take into account the white and light-gray achromatic backgrounds with tristimulus values $Y_0 \geq 20$ ^[23] in addition to the medium-gray background in the original models.

2.4. THE IMPLICATION OF COLOUR APPEARANCE MODELS

2.4.1 Application Area

A colour appearance model can be applied in many areas, e.g. in measuring the colour fidelity between colour reproduction systems^[140], in assessing colour rendering index ^[26] (Colour rendering index is a method assessing the degree to which a test illuminant renders colours similar in appearance to their appearance under a reference illuminant^[16]), and in quantification of the colour constancy of object colour. Another current need of colour appearance model is to predict the effects on colour appearance of adaptation to illuminants of various intensities and colours^[26].

2.4.2 Field Trials of Models

The differences between the Hunt and Nayatani models are the concept of chroma and colourfulness, the formulae of whiteness-blackness, brightness, and lightness and the method to deal with the adaptation (chromatic and brightness) effect. There are many similarities between the two models^[26]. First, both models consist of three colour responses at receptor stage and the responses at the succeeding opponent-colour response stage. Secondly, nonlinear characteristics of colour responses under chromatic adaptation are taken into account. And finally, both models can predict various colour appearance phenomena. The predictions can be directly compared with the data obtained from magnitude estimation experiments.

In 1986, a consortium was formed in Britain to develop an objective method for assessing the appearance of colour in dissimilar media (especially video monitors and printing samples) under various viewing conditions. The results were used to determine the impact of various viewing parameters (such as light source, background, etc) on colour appearance^[103,121,122]. A series of experiments was devised. These experiments comprised 23 phases. Each phase was conducted using 6 to 7 observers by applying a magnitude estimation method (Each observer was asked to scale the lightness,

colourfulness, and hue for a wide range of colours in a complex field). The parameters studied were (1) four light sources: D65, D50, white fluorescent and tungsten; (2) two luminance levels: about 40 and 240 cd/m²; (3) five background conditions: white, grey and black backgrounds, grey background with a white border, and grey background with a black border; (4) two media: luminous colours which were displayed on a high-resolution colour monitor, and nonluminous colours presented in a viewing cabinet. In total, 43,332 estimations were made. These formed the LUTCHI Colour Appearance Data which has been used to test various colour spaces and models, as well as to modify the Hunt colour appearance model. The new model give a quite accurate prediction of the visual results and performed much better than the other spaces and models. It is known as Hunt-Alvey Colour Appearance Model (Hunt-ACAM), later Hunt91 model. The deviation of the predictions by this model to the visual response is close to the typical deviation between each observer's response and mean visual response. This performance is considered to be very satisfactory. The model is therefore believed to provide a reasonable means for evaluating colour fidelity across colour reproduction systems. However, it is only applicable to luminance level around 240 and 40 cd/m² and does not include any transparency colours. Further experiment are required to extend the range of luminance.

A technical committee under the Color Science Association of Japan has also conducted an extensive study for assessing the chromatic-adaptation transform proposed by CIE for further test. The committee also developed a colour appearance model^[26] based on this transform. They obtained their experimental data by the visual assessment of object colours under various artificial light sources^[139] and adapting illuminance levels^[138]. The technique of haploscopic matching was used throughout the study. The light sources used are illuminants C and A, and also five fluorescent lamps previously used by Mori and Fuchida^[141]. The result was used to test various models. It is concluded that the goal for predicting various colour appearance phenomena from fundamental concepts is still far beyond current understanding. Thus further developments are required.

2.5 OUTLINE OF RESEARCH

It is clear from the literature review that the current methods in predicting colour appearance can not fully satisfy the requirements of applications. Hence funding was provided from the DTI and SERC in 1990 (the consortium including LUTCHI, Crosfield Electronics Ltd. and Coats Viyella plc). The aim was to widen the experimental viewing conditions in the earlier studies and to increase the accuracy of prediction by Hunt91 model.

This work developed into three concurrent studies. The objective of the first phase was to gain further understanding of the change in colour appearance under a wide range of viewing conditions. Five psychological experiments were conducted to assess colour appearance according to various media which included cut-sheet transparency, slide film, reflection print, and colour monitor.

The second stage was to test three uniform spaces, and two colour appearance models by using the data obtained in the first stage.

Finally, modelling of colour appearance was carried out based on the Hunt91 model. The newly developed model enables us to predict more accurate visual responses under a wide range of application. The model is also reversible.

3. EXPERIMENTAL METHODS

Effects of various media and viewing conditions on colour appearance were studied via five experiments. The first experiment, the training experiment, aimed to study observers' performance. The others were carried out by using cut-sheet transparency, 35mm slide, reflection print, and monitor colours (colours were displayed on a CRT). The details of the experiments are given in Table 3.1.

Ten observers were employed for the experiments. They all had normal colour vision according to the Ishihara and City University colour vision tests.

3.1 TEST OF DEFECTIVE COLOUR VISION

Defective colour vision is unknown to the person who is colour defective. The incidence of defective colour vision is as high as 8% of men in Britain^[32] so that each observer was tested before the experiments to avoid error in colour scaling caused by subjects with colour defective vision.

Defective colour vision includes complete and partial colour blindness. Colour blindness is usually associated with more serious visual defects where the subject is unable to distinguish one colour from another or to see any colours at all. Partial colour blindness causes some people to experience great confusion in the red-yellow-green range of the spectrum, particularly when looking at subtle gradations of tone. Many of them cannot distinguish one complementary colour from another, such as green from red. It is rare to find anyone who confuses yellow with blue.

Tests of colour vision are designed chiefly to detect protanopes (ρ cone missing), deuteranopes (γ cone missing) and anomalous trichromats (β cone missing) having extremely weak red-green discrimination. The various tests differ essentially as to the form of response required of a subject. The Ishihara and The City University Colour-Vision Tests were used in this study.

The Ishihara chart is provided in the form of coloured plates. The colours in each plate can be perceived by observers with normal colour vision. Each plate consists of a circle of about 4 inches diameter made up of a series of coloured dots forming numbers or lines. The colours were carefully selected by Ishihara to confuse those with defective colour vision. In this work, the test was conducted by presenting the plates to the observers under a D65 simulator in a Verivide viewing cabinet (see later). The plates were held about 70 cm away from the subject and tilted so that the plane of the paper was at right angle to the line of vision^[142].

The City University colour vision test uses coloured paper samples. In each page, four colours surround a central colour against a black background. The observer is required to identify one of the surrounding colours which is identical or most similar to the central colour. Each page provides possible protan (ρ cone missing), deutan (γ cone missing) or tritan (β cone missing) confusions which may be mixed with a normal response since some observers may find more than one match to the central colour. This test was also conducted for all observers attended in this study. The viewing conditions are the same to these for the Ishihara test^[143].

3.2 MAGNITUDE ESTIMATION OF COLOUR ATTRIBUTES

As mentioned in section 2.3.5, four methods are commonly used to assess colour appearance: binocular matching, memory matching, and magnitude estimation.

The method of magnitude estimation was used in this study. This technique is considered to be easy to use, because it does not require colour appearance assessment in terms of some colour system, for example Munsell, illuminated by a reference source, and also does not need any visual colorimeter which is necessary for the binocular matching. In addition, the magnitude estimation can avoid problems associated with either memory or haploscopic matching, i.e. extended training periods and distorted memory traces on the one hand, and binocular interactions on the other hand. The viewing condition for magnitude estimation is essentially the same as that in everyday life. The aim of this work was to investigate the changes of colour appearance under a wide range of viewing conditions. Magnitude estimation is well suited to this purpose.

Using the magnitude estimation technique, an observer simply looks at a test colour and assigns values or names that correspond to the subjective colour attributes: Lightness, Brightness, Colourfulness, and Hue. A brief introduction to magnitude estimation for each of these attributes is given below.

3.2.1 Lightness Scaling

For lightness estimation, a white sample assigned as a standard having a lightness of 100 was used as a reference and viewed simultaneously with the test samples. The black sample in observer's imagination has a lightness of 0. With reference to the lightness of the white sample and the imaginary black, observers estimated the lightness of test samples as a proportion of the reference lightness. For example, an estimated lightness 30 refers to a sample of which the lightness would be of 30 per cent of the lightness of the reference white.

3.2.2 Brightness Scaling

For brightness estimation, an imaginary black was assigned to zero without a reference white. Observers were asked to give a reasonable number to describe brightness of test colours. This is an open-ended scale since no top limit is set. The reference brightness colour is displayed in the test pattern, having say a brightness of 50. Thus a sample estimated to have brightness of 130 would be the one judged to have 2.6 times of the brightness of the reference sample.

3.2.3 Hue Scaling

Hue judgments were given with reference to the four unique hues: Red, Yellow, Green and Blue. These four colours can be arranged as points around a circle and lie at opposite ends of x and y axes, green vs. red and yellow vs. blue (these two are known as opponent hues). Hues lying at opposite ends of each axis cannot be sensed simultaneously. The space between two unique neighbouring hues was assigned the number of 100 on the subjective scale, and a hue circle was divided into 400 steps. There is no hue for a neutral sample. The observer estimated two percentages of two neighbouring unique hues that perceived in the sample. Thus, an estimation of 80%Yellow-20%Red expresses a hue on the red side of pure yellow, with a ratio between perceived yellowness and redness of 80/20. Observers were not permitted to induce response such as "60% red and 40% green". For unique hues, estimations would be 100 Red, 100 Yellow, etc.

3.2.4 Colourfulness Scaling

For colourfulness estimation, an achromatic sensation (black, grey or white) was assigned to zero, and a standard reference sample was also given, say 40. Observers were asked to give a reasonable number to describe the test colours. This was an open-ended scale since no top limit was set. The reference colour was presented in the test pattern. Thus a sample estimated to have colourfulness of 60 would be one estimated to have 1.5 times of the colourfulness of the reference sample.

3.3 MAGNITUDE ESTIMATION EXPERIMENTS

Ten normal colour vision observers took part in the experiments in this work. Most of the observers were either research students or members of staff from the University and had no working experience in the colour industry. The magnitude estimation technique was used throughout the experiments. Five experiments were conducted according to the media studied.

The training experiment (Experiment 1) was conducted first. The cut-sheet transparency medium experiment (Experiment 2) consisted of eleven phases and was performed with variations of viewing parameters such as borders, backgrounds, flare light and luminance levels. The 35 mm slide medium experiment (Experiment 3) included six phases and was carried out under two light sources, luminance levels, and viewing patterns. The reflection print experiment (Experiment 4) was divided into twelve phases according to six luminance levels. Furthermore, observers scaled colour attributes of lightness, colourfulness, and hue, and in addition also brightness, colourfulness, and hue. Monitor colours were used to investigate simultaneous contrast effect (Experiment 5).

3.3.1 Experiment 1: Training Experiment

3.3.1.1 The Apparatus

The training experiment was carried out using a Verivide viewing cabinet. The viewing cabinet provided a set of standard lighting conditions for viewing surface colours. Figure 3.1 shows the front view of a Verivide viewing cabinet. The complex pattern displayed in the middle was used in Experiment 4. This cabinet has four light sources: D65, D50, white fluorescent and tungsten. The luminance level of light sources were controlled by built-in regulators. The interior of the cabinet was finished in a grey emulsion paint widely used in British textile industry. The interior space of the booth is 65 x 53 x 40 cm³.

A Bentham Telespectroradiometer (TSR) was used to measure colours. The TSR

comprises a telescope to collect the light from a target colour, a monochromator with a detached photomultiplier to measure the radiant power of light ranging from 380 nm to 780 nm in a 5 nm interval, and a host computer to analyze data and report results in terms of CIE 1931 colorimetric data, colour temperature, and luminance. Figure 3.2 is a photograph of the Bentham TSR system. The sphere on the top is a standard lamp used for calibrating the instrument. The lamp was originally calibrated at NPL with correlated colour temperature of 2853 K, luminance of 7089.954 cd/m² and chromaticity of $x = 0.4505$ and $y = 0.4129$. Its spectral power distribution is within the accuracy of 0.01% uncertainty. It takes about 2 minutes to measure a sample when the integration time is set to 0.1 second and about 3 minutes for 0.5 second integration time.

Figure 3.3 illustrates the experiment situation. The viewing field was illuminated by a fluorescent tube (Phillips DELUXE) approximating to CIE Illuminant D50 (with the colour temperature about 5000 K). A luminance of 50 cd/m² was obtained by a TSR against the reference white. A neutral background with a luminance factor of 20% was used. Table 3.2 lists the CIE chromaticity coordinates of this light source, the background on which the colour samples were placed, and the standard deviations of these measurements. Measurements of the light sources and backgrounds were carried out several times before, during and after the experiment. The standard deviations of these measurements, in CIE 1931 chromaticity coordinates, were $x = \pm 0.00034$ and $y = \pm 0.00038$. This suggests that the viewing condition was steady during the period of the training experiment which lasted about two weeks. Thus the errors induced by the experimental facilities are very small.

Observers sat in front of the viewing cabinet with a viewing distance about 60 cm and a viewing geometry of 0/45. 40 glossy paint samples were selected from the OSA Uniform Colour Scale. These were chosen to cover a reasonable colour gamut and had Y values ranging from 6 to 64 (Munsell Value of 3 to 8.4). Each sample has a size of 4 x 4 cm². These samples were divided into two groups which were designated as sets A and B. Each group consists of 20 representative samples. Each sample subtended a visual angle of 4° x 4°. The colorimetric data of these forty samples were measured using the TSR. The measuring conditions were: 3.5 mm aperture size and 0.1 second integration

time with a measuring distance of 100 cm from the target sample. The chromaticity coordinates of forty samples are plotted on the CIE $u'v'$ diagram in Figure 3.4. The positive and open circle signals represent samples used in sets A and B respectively.

3.3.1.2 Experimental Procedure

Table 3.3 summarises experimental conditions. Eight observers attended the experiment, four males and four females with age ranging from 22 to 36 years old. Seven had little experience in performing colour scaling experiment. One had considerable experience.

Before commencing the experiment, the definitions (see section 2.1.4) of lightness, colourfulness and hue were introduced to the observers. Various colour images reproducing Munsell and NCS colour systems were displayed on a Sigmex colour monitor to assist the understanding of these perceptual attributes. When all observers fully understood the concepts of these colour attributes, the training experiment was conducted.

Each observer commenced the experiment by adapting to the surround field for a period of 5 minutes. After being introduced to the reference lightness sample having a lightness of 100 and a reference colourfulness sample having a colourfulness of 40, he or she arranged 20 test colours in a Lightness versus Colourfulness plane (two-dimensional ranking). Then, the observer estimated each sample's magnitude of lightness and colourfulness. A typical estimate might be "lightness is 53, colourfulness is 48". Figure 3.5a shows the experimental situation for scaling lightness and colourfulness. For hue scaling, these colours were placed in a Yellow-Blue (y-axis) versus Red-Green (x-axis) plane. These samples were first arranged around a circle according to the contents of two neighbouring unitary hues. Then, observers were asked to give their estimates, such as "the hue of this sample is red with blue, red 78% and blue 22%". Figure 3.5b illustrates the experimental hue circle.

All observers performed the experiment in 4 sessions (each group of samples being

assessed twice). The sequence for presenting samples was randomised for each observer. Each session lasted about 40 minutes. Half of the observers started using set A and the other half using set B. This experiment conducted over a period of two and half weeks.

3.3.2 Experiment 2: Cut-sheet Transparency Medium

This experiment was divided into eleven phases and was carried out using a Verivide transparency illuminator with a single light source, a D50 simulator. Table 3.4 summarises the details of the experimental phases. The parameters investigated were: three luminance levels (2259 cd/m^2 (high), 689 cd/m^2 (medium), and 325 cd/m^2 (low)), two achromatic backgrounds (with $Y\%$ values of 17% and 10%), three borders (a white, a white paper and a black borders), and with and without side flare light.

3.3.2.1 The Apparatus

This experiment was carried out using a Verivide transparency back-lit illuminator which is shown in Figure 3.6. This illuminator was designed to agree closely with ISO 3664 for viewing cut-sheet transparencies. The whole illuminator was painted with a mid-grey colour except for the viewing area ($30 \times 40 \text{ cm}^2$). The viewing pattern was placed in the centre ($17 \times 23 \text{ cm}^2$). This arrangement enables the light presented around four sides of the transparency (designated as white border) to give enough flare light to approximate the typical reflection print viewing condition. Alternatively, this effect was simulated by surrounding the viewing pattern with an opaque sheet of print substrate (designated as white paper border) illuminated using frontal flare lights. For the black border condition, the surrounding white light area was covered by a mid-grey mask. Thus only the viewing pattern can be seen in the viewing area. In Figure 3.6, 3.6a is the viewing pattern with black border (used in phases 5, 6, 7 and 11), 3.6b with white paper border under flare light (used in phase 8), 3.6c with white border (phases 1, 2, 3, 9 and 10), and 3.6d with white border under flare light (phase 4). The exterior volume of the illuminator is $82 \times 43 \times 75 \text{ cm}^3$ and interior volume of $58 \times 29 \times 63 \text{ cm}^3$. Its light source is a D50 (with correlated colour temperature about 4700 K) simulator having CIE 1931 chromaticity coordinates x and y of 0.3564 and 0.3771 respectively. (CIE D50 illuminant

has $x = 0.3457$ and $y = 0.3586$). There are two extra light sources (D50 simulators) located on both sides of the viewing area for introducing extra frontal flare light onto the transparency image. The chromaticity coordinates of this diffusing flare light from either side are $x = 0.3566$ and $y = 0.3774$ with luminance about 2500 cd/m^2 (measured in the centre point of the side area).

The illuminator includes three buttons for controlling luminance levels. Only maximum and minimum controls were used here and were named high and medium levels. For the low luminance level conditions (phases 3 and 7), the luminance was produced by using the minimum control with a neutral filter (density was 0.3) to cover the viewing area. Figure 3.7 illustrates the experimental situation. Observers sat in front of illuminator about 60 cm away with a subtended visual angle about $2^\circ \times 2^\circ$ for a test colour (the centre colour in the pattern of Figure 3.6) in a darkened room with viewing geometry of 0/0.

Two viewing patterns were used in the experiment. The only difference between them was the luminance factors (Y%) of the neutral backgrounds 17% (used in phases 1, 2, 3, 4, 9 and 11) and 10% (used in phases 5, 6, 7, 8 and 10). In each pattern, the reference white and decorating colours were fixed, but not for the test and the reference colourfulness colours.

The chromaticity coordinates in CIE x, y units and luminance in the unit of cd/m^2 of the experimental parameters for each phase are given in Table 3.5. These are illuminant, side flare light, background, reference white sample, and the surround border around the viewing pattern. The measurement was carried out by means of TSR. The conditions of phases 2 and 9 used were the same. Only one set of measurement was listed. The luminances of the four borders surrounding the viewing pattern were different. These measurements were taken at the centre of each border. The mean measurement of the four borders together with standard deviations was also given in Tables 3.5 and 3.6. These results show that for all experimental phases, the neutral background and reference white colour appeared to be slightly more reddish and yellowish (x and y values larger) than those of illuminator and border.

The data in Table 3.5 is the mean results of ten readings obtained before, during, and after the experiment. Table 3.6 lists the standard deviations of the mean measurements for the reference white colour as well as illuminator. In almost all the phases (except phase 8), the SD values were very small, ranging from 0.0004 to 0.0022 for x and y, and from 0.40% to 2.69% for L, which implies that the luminance level of the illuminator was quite stable in each experimental session. For phase 8, the SD values ranged from 0.0042 to 0.0059 for x and y. The white paper border seemed to scatter flare light unevenly producing larger variation in the measurement.

3.3.2.2 Sample Preparation

Ninety-eight test colours were used in the experiment. The test samples were selected according to a RGB 16 x 16 x 16 cube transparency chart which is the standard test chart used in Crosfield Electronics for calibrating their Magnatran film reproduction system. Using 105 OSA samples in the earlier colour project (ALVEY colour project^[121,122]) as target colours, a visual interpolation method was used to approximate the R, G, and B values for each colour. The 105 OSA colours were chosen to give an adequate coverage of colour space (the area of the chromaticity diagram bounded by the optimal colour limits (spectrum colours)). These R, G, B values were then transformed to C, M, Y values using Crosfield's Studio 880 system for producing image pages stored into the disk pack. Subsequently the disk pack then was output into Magnatran system. (Magnatran is a high-precision colour film recorder which produces positive or negative transparencies from the image stored on the disks and films). The films were then developed (at Crosfield) and the transparency samples were obtained. The test colours covered a wide range of colour gamut having Y value from 1 to 56 and Munsell Value from 1 to 8. In addition, two viewing patterns as shown in the bottom of Figure 3.7 with different luminance factors of neutral background were produced. The size of the viewing pattern is 17 x 23 cm² which is shown in Figure 3.7. All colours in this pattern had a size of 2 x 2 cm². The centre colour in the viewing pattern was the test colour which was changed successively during the experiment. The reference colourfulness sample was fixed in each phase but varied in different phases. The reference white sample had a lightness of 100 presented in all phases. The others were the decorating colours fixed

through out the experiment. These decorating colours were randomly chosen to form a complex viewing pattern.

These ninety-eight test colours were presented one after another in a random order, and were assessed by a panel of seven to eight observers in terms of lightness, colourfulness and hue in each phase. For each phase, test colours were measured by a Bentham TSR under the experimental conditions used in each phase. The TSR measuring conditions were: 3.5 mm aperture size and 0.5 second integration time with measuring distance of 100 cm. Figures 3.8 to 3.17 show the chromaticity coordinates of 98 samples plotted on the CIE $u'v'$ diagram for phases 1 to 11 respectively.

3.3.2.3 Experimental Procedure

The reference colourfulness sample for each phase was fixed. They were selected to have various hues but of similar colourfulness. Before commencing each observing session, observers were asked to scale the colourfulness of this reference sample against a standard sample (selected from OSA Uniform Colour Space) assigned colourfulness of 40 viewed in the viewing cabinet. The standard sample has x , y and L values of 0.409, 0.330 and 75.4 cd/m^2 respectively.

Eight observers performed the experiment according to the following sequences:

- (1) Each observer firstly adapted to the Verivide viewing cabinet for about 5 minutes (see Figure 3.1) and was given the instructions for scaling lightness, colourfulness, and hue. The viewing conditions were illuminant D50 with luminance of 250 cd/m^2 and chromaticity of $x = 0.3431$ and $y = 0.3539$.
- (2) There was a viewing pattern with mid-grey background in the viewing cabinet. The observer was asked to remember a standard sample ($2 \times 2 \text{ cm}^2$) in the viewing pattern with colourfulness of 40 (the pink colour as shown in Figure 3.1).
- (3) The lights in the viewing cabinet were switched off and the transparency illuminator

turned on. The observer was asked to adapt to the new viewing conditions for another 5 minutes.

(4) A transparency reference colourfulness sample was presented in the viewing pattern (shown in Figure 3.6). The observer was asked to scale this sample against memory of the standard reference colourfulness sample. The new colourfulness sample was then fixed in the pattern throughout this individual experimental phase.

(5) Subsequently, the reference white sample fixed in the viewing pattern was introduced with a lightness of 100. The estimation experiment was started by using these reference samples.

Each phase was divided into 2 sessions. Fifty samples were estimated in each session which lasted about 1 hour. Eight observers, 4 females and 4 males, took part in the experiment. A typical answer for a colour estimated might be "lightness 67, colourfulness 23, and hue with 60% green and 40% yellow".

3.3.3 Experiment 3: 35mm Projected Slide Medium

This experiment was divided into six phases which are specified in Table 3.7. The viewing parameters investigated were: two light sources (Halogen and Xenon), two luminance levels (about 110 and 45 cd/m²), and two viewing patterns with different display.

3.3.3.1 The Apparatus

Figure 3.18 illustrates the experimental situation. The slide image was projected on a white matte screen (with a size of 120 x 120 cm²) using a Kodak Carousel S-AV 2050 projector in a darkened room. The projector has a Halogen lamp with 250 W. The lamp alignment procedures were routinely carried out for the projector in order to yield maximum brightness, and to ensure symmetric illumination on the screen. When projected on a white screen, the projector had a luminance of about 110 cd/m² and

correlated colour temperature of about 4000K. The white screen was a piece of hardboard painted with Dulux white emulsion paint. The distance between projector and screen was 400 cm and between observer and screen 360 cm (three times of screen width, similar to the typical cinema seat).

Two projector light sources were used: a Halogen lamp (4000K) and a simulated Xenon light (5600K) source which was converted by using a Cokin 80C blue filter in front of Halogen lamp. Their spectral power distributions are plotted in Figure 3.19 for Halogen high level and simulated Xenon low level conditions. Two luminance levels were studied: 113 cd/m² luminance of high level and 46 cd/m² of low level. The Halogen lamp in the projector was used with normal voltage (250 W) throughout. The Halogen low level condition was generated by using the Halogen lamp covered with a Polyester neutral filter having density of 0.4 (supplied by Lee Filter Ltd.).

Ninety-nine test colours were used. Each test colour was presented as a single slide. The slides were again made at Crosfield Electronics' laboratory using the Studio 880 and Magnatran system (the procedures are the same as those used to produce the cut-sheet transparencies mentioned earlier). Each slide corresponds to a test colour with a size of 35 x 21 mm². These colours cover a large range of colour gamut having Y factors ranging from 6 to 88 (Munsell Value of 1 to 9). The slide image when projected on a white screen is shown in Figure 3.20. The image used in phases 1 to 4 is shown in Figure 3.20a. The centre includes three colours, the left one is the reference white sample, the right one the reference colourfulness and the bottom one the test colour. The others are decorating colours. All colours except the test colour for all slides were almost the same. Figure 3.20b gives the viewing pattern used in the phases 5 and 6. The reference lightness and reference colourfulness colours in this pattern were placed further away from the test colour. The centre colour is the test colour, the reference white is located on the top right of the test colour and the reference colourfulness colour on the bottom right. The size of the entire projected image was 110 x 80 cm². The size of each colour patch shown in the image was 7 x 7 cm² (Figure 3.20). This resulted in a visual angle of about one degree. The u',v' chromaticity coordinates of all the test colours used in phases 1 to 6 are plotted in Figures 3.21 to 3.25.

The chromaticity coordinates in CIE x , y units and the luminance in the unit of cd/m^2 of the experimental parameters in each phase are given in Table 3.8. These are: illuminant (open gate which is the projected image without any slide), background (the grey background of the projected image of the slide), reference white (the left and top right colour in the central three colours in Figure 3.20), reference colourfulness (the top right square in the central three colours in Figure 3.20a, and bottom right one of the central 3 colours in Figure 3.20b). The measurement distance was 360 cm from the screen. The measuring conditions were: 1.17 mm aperture size and 0.5 second integration time. As the conditions of phases 1 and 4 were the same, only one set of measurements is listed.

In Table 3.8 the mean results of many readings collected before, during and after the experimental period are given. Table 3.9 provides the standard deviations of mean x , y , and L for the reference white, open gate, reference colourfulness, and background. For all the phases, the SD values were very small, ranging from 0.0003 to 0.0018 for x and y , and 0.74% to 5.16% for L . This again implies that illuminant was quite stable within each experimental session. All slides had almost identical measurements for the reference white, reference colourfulness and the background. This indicates that the colour repeatability of each slide is quite good.

3.3.3.2 Experimental Procedure

Ninety-nine test colours were used in phases 1 to 4. Ninety five and thirty six test samples were employed in phases 5 and 6 respectively. These colours were assessed in a random order in each phase by a panel of six observers in terms of lightness, colourfulness and hue using the technique of magnitude estimation. The experiment procedure was the same as that used in the cut-sheet experiment except that the transparency illuminator used in the cut-sheet experiment was replaced by a slide projector for this experiment.

Each phase was divided into 2 sessions. There were 50 samples estimated in each session which lasted about 45 minutes.

3.3.4 Experiment 4: Reflection Print Medium

Experiment 4 was designed to extend the scope of earlier experiment^[121,122] by investigating the changes of perceived brightness, lightness, colourfulness, and hue under a wide range of luminance levels. The experiment was divided into twelve phases, summarised in Table 3.10.

3.3.4.1 Apparatus

This experiment was carried out using a Verivide viewing cabinet (see section 3.3.1.1) with a grey background. The light source with a correlated colour temperature of about 5000K consisted of six fluorescent tube of Phillips DELUXE. A white transparent diffuser (made by ICI) was used to evenly distribute light in the viewing area. Five large half-tone transparencies (65 x 53 cm²) with neutral densities of 0.6, 1.1, 1.7, 2.1, and 3.3 were used to cover the diffuser so that the six luminance levels required in the experiment could be achieved. For the highest luminance level, only the diffuser was used. A grey background at a luminance factor of 20 was used. Observers sat in front of the viewing cabinet with a viewing distance of 60 cm. The viewing geometry was 0/45. Each colour sample was placed in a complex viewing pattern of size of 35 x 25 cm², divided into two zones. Zone one included 27 decorating colours to make a complex pattern. Zone two included the reference white and the reference colourfulness samples (see in Figure 3.1). The decorating colours were randomly selected from the Pantone Color Paper Selector. Forty OSA samples (4 x 4 cm²) were selected. Their Y values ranged from 7 to 72 (Munsell Value of 3 to 9). These samples were covered with a neutral colour the same as the background to make the sample size of 2 x 2 cm². This size subtended a visual angle about two degree. The chromaticity coordinates of these forty samples under each of the six experimental conditions are plotted on CIE u'v' diagram in Figures 3.26 to 3.31. The measuring conditions were the same as these used in Experiment 1 (section 3.3.1). Figure 3.1 illustrates the experimental set up.

The chromaticity coordinates and luminance of a pressed BaSO₄ tile, reference white sample, and background are given in Table 3.11. The viewing conditions of phases

1 and 7, phases 2 and 8, etc. are exactly the same, therefore one measurement for each of the two phases is listed. The difference between these two groups is the colour attributes scaled. In the first six phases, the attributes scaled were lightness, colourfulness, and hue. Brightness, colourfulness, and hue were estimated in the last six phases. The errors of the measurements are provided in Table 3.12. The standard deviation for the reference white for each phase ranged from 0.0004 to 0.0098 for x and y , and ranged from 2.38% to 14.81% for luminance. These figures again indicate that the experimental conditions were reasonably stable.

3.3.4.2 Experimental Procedure

Four observers attended Experiment 4: 3 males and 1 females. The procedure in the first six phases was the same as those used in Experiment 2 (section 3.3.2.3) except step (3):

(3) The reference colourfulness sample was taken away from the viewing pattern and the white diffuser with suitable neutral filter for that phase was put on. The observer adapted to the new viewing conditions for another 5 minutes.

Before commencing the last six phases of the experiment (in which brightness, colourfulness, and hue were scaled), a special training session was arranged for scaling the brightness attribute. The basic concept of brightness (see section 2.1.4) was introduced. Special attention was paid to distinguish brightness from lightness. The Barco colour monitor with colour demonstration software was used to help the observers to understand the difference between brightness and lightness when luminance level was increased and decreased.

Once observers fully understood the concept of brightness, the last six phases were carried out. The reference white sample in the viewing pattern was removed in the last six phases. This was considered to be necessary to prevent observers scaling lightness instead of brightness. For the colourfulness and brightness scaling, only one reference sample was given for scaling both attributes throughout each phase. The experimental

procedures were the same as those in section 3.3.2.3 except steps (2) and (4):

(2) Each observer was asked to remember the standard sample used in the earlier experiments, assigned colourfulness of 40 and brightness of 100.

(4) A new reference colourfulness and brightness sample was used in the viewing pattern. The observer was asked to scale the colourfulness and brightness for this new reference sample according to his memory of the standard (pink colour in Figure 3.1) reference. This new reference sample was placed in the viewing pattern throughout assessing phase.

3.3.5 Experiment 5: Monitor Colour Medium

This experiment was designed to investigate the simultaneous contrast effect. A high resolution Barco colour monitor was used to generate the luminous colours in the experiment. Its display area is 16" x 12" (40 x 30 cm²) with a resolution of 1448 x 1024 pixels. Before commencing first observing section every day, the monitor was calibrated to illuminant D65 viewing conditions with a constant luminance level of 50 cd/m². The calibration is necessary if accurate colour appearance is to be maintained. The calibration procedures were divided into two stages: internal and external calibrations taking approximate ten minutes^[144]. The first stage simply invokes the calibrator's own internal calibration routines which adjust various internal parameters of the monitor based on the measurements made by an external optical sensor. The second stage compensates for variations in the external video board used to drive the display.

The monitor display was arranged as shown in Figure 3.32, with the test field (having a size of 2 x 2 cm²) subtending a visual angle of approximately 2° and the induction field (having a size of 6 x 6 cm²) with a 6° viewing angle at a distance around 60 cm, the same as that in the earlier study^[103] (This experiment was an extension of the earlier experiment to include more test colours). The chromaticity coordinates and luminance values of the reference white, background, and reference colourfulness samples are listed in Table 3.13.

Thirteen test colours and thirty-seven surrounding colours were used in the experiment. These colours were defined in terms of L^* , C^* , and h_{ab} from CIE $L^*a^*b^*$ uniform colour space. Then they were transformed to their corresponding x , y , and Y values. The generation for each luminous colour on the monitor was completed after transforming its x , y , and Y values to the monitor R , G , and B values using the formula between them. This formula was developed through an extensive study of three Barco monitors' performance at beginning of the project^[145]. The typical variation was found to be around 0.5 CMC(1:1) colour difference units between measured and predicted tristimulus values for this formula. This difference is very small and the performance of the formula is therefore considered quite satisfactory.

The chromaticity coordinates of thirteen test colours measured by means of the TSR and the corresponding CIE L^* , C^* , and h_{ab} expressed in CIE $L^*a^*b^*$ UCS terms are listed in Table 3.14. Figure 3.33 shows the positions of these thirteen test colours on the CIE $L^*a^*b^*$ diagram. Colours of YR, GY, BG, and RB were used in the earlier studies^[103]. Each test colour was presented under 37 different induction surrounds as shown in Table 3.15. The table includes the chromatic data of 37 induction colours as well as CIE L^* , C^* , and h_{ab} . In total there were 481 test-induction combinations used in this experiment.

The reference white and colourfulness patches in the viewing pattern were fixed, the reference white having a lightness of 100 and the reference colourfulness patch having a colourfulness of 40.

The experimental procedure was as follows:

- (1) Each observer adapted to the monitor display for about 5 minutes in a darkened room.
- (2) The observer was asked to scale the lightness, colourfulness, and hue of the test colour referring to the reference white and colourfulness samples.

There was a control panel on the right of the display (not shown in Figure 3.32) for recording the observers' estimations and controlling the next display using a tablet. If an observer was satisfied with his/her answer, he/she could simply select the "accept" panel by clicking the mouse. Otherwise he/she could select the "reject" panel and reestimate his/her answer. After completion of each estimation, the combination was replaced by the next one with the mouse.

Six observers took part in the experiment, 3 females and 3 males. In each session, each observer estimated 40 or 41 combinations displayed in a random order. The whole experiment took a period of over two months.

4. EXPERIMENTAL RESULTS AND DISCUSSION

4.1 DATA ANALYSIS

4.1.1 Methods for calculating mean visual responses

4.1.1.1 Lightness

Lightness was scaled as a relative attribute with two ends of 0 (imaginary black) and 100 (reference white). The arithmetic mean was used to represent an average result, i.e., the mean visual response. This is valid for the ratio scale with two fixed end points.

4.1.1.2 Hue

The method for scaling hue was given in section 3.2.3. Hue attribute was scaled using Hering's opponent theory of colour vision, i.e., employing red, green, yellow and blue psychological primaries. A typical orange colour could have a hue of 40% yellow and 60% red. This was transformed to a scale of 0-400 [0-100, R-Y; 100-200, Y-G; 200-300, G-B; 300-400(0), B-R], i.e. 40 for this orange colour. The arithmetic mean was used to calculate hue mean visual response.

4.1.1.3 Colourfulness

As defined in section 3.2.4, colourfulness was scaled applying an open-ended scale. Observers were unconstrained in their use of numbers and normalisation. The geometric mean was considered to be the best measure of the stimulus magnitude^[11,123]. Each individual observer's scaling data should be related to the mean set by a power function:

$$R = aS^b \quad (4.1)$$

Where **R** is the response magnitude and **S** the stimulus magnitude which is the geometrical mean from several observations, **a** and **b** are the constants obtained by a least-square technique by fitting the log of the geometric mean set of data with each individual observer's data set. The gradient of the best-fit straight line is equivalent to

the exponent b and the antilog of the intercept is equal to a . These factors are then used to normalise each individual observer's data to a common scale using Eq.(4.2)

$$R' = \left(\frac{R}{a} \right)^{-b} \quad (4.2)$$

Where R' is the normalised response, R , a and b are the same as those defined in Eq.(4.1).

In this study, the mean colourfulness response for a stimulus was computed using geometric mean by Eq.(4.3)

$$m = \sqrt[n]{x_1 x_2 \dots x_n} \quad (4.3)$$

where m is the geometric mean and x_i the estimate by the i -th observer.

4.1.1.4 Brightness

In the experiments, the observers scaled the brightness using an open-ended scale. Hence the data analysis is similar to that of colourfulness. The geometric mean was again used to determine the average measurement of a stimulus magnitude using Eq.(4.3).

4.1.2 Investigation of Changes of Colour Appearance Between Different Viewing Parameters

In order to indicate the degree of agreement between two sets of data, i.e., x and y sets, coefficient of variation (CV) was used as a measurement. The calculation of CV is given in Eq.(4.4)

$$CV = \frac{\sqrt{\frac{\sum (x_i - y_i)^2}{n}}}{\frac{\sum y_i}{n}} \times 100 \quad (4.4)$$

Where n is number of colour samples, and x_i, y_i are the i th data of two sets respectively.

CV is a measurement of the distance along the y axis of the points from the 45° line in a y against x plot. It expresses the root-mean-square deviation of the distances of the points from the line as a percentage of the mean value of the y set. This measure is independent of the magnitude of set y and can be thought of as relative percentage deviation, for example a CV value of 10 means 10% variation. For a perfect agreement of two sets of data, the CV value should be zero.

The changes of colour appearance between different viewing parameters were investigated using four measures: correlation coefficient (r), coefficient of variation (CV), gradient (b), and intercept (a). For each of the lightness, colourfulness, or brightness comparisons, two CV values were computed: CV(o) and CV(s). CV(o) was computed using the unscaled data from X and Y phases. CV(s) was calculated using unscaled data from Y phase, and linearly scaled data using gradient and intercept from X phase. The gradient and intercept were obtained using the least-square method. For lightness comparison, two different methods were used. One was to get the best fit line using a least-square method and designated as the "nonconstrained" method. The other one was to force the best-fit line to pass through the white point ((100,100) point) by assuming that each observer used the reference white as an anchor point in each phase. This method was designated as "constrained" method. For colourfulness comparison, only the gradient was calculated as the best-fit line being constrained to pass through the origin (for neutral colours). The difference between these two CV values provides further information concerning the degree to which the agreement can be improved following linear rescaling. For hue comparison, only the CV(o) measure was used.

The significance test using Student's t-distribution^[146] was carried out to determine whether there is a significant difference from 1.0 for gradient or from zero for the intercept. The values will be given in parentheses, which means that these are insignificant within a 95% confidence limit. Scatter diagram was also used to illustrate the tendency due to the change of viewing parameters.

4.1.3 Evaluation of Performance of Colour Spaces And Models

The aim of this study was to derive a generalised model of colour vision capable of predicting changes in colour appearance under various viewing conditions. The strategic approach was first to obtain a comprehensive set of reliable experimental data, second to test the ability of various colour spaces and models for predicting these data, and finally, to modify a particular model in order to improve the fit to the current experimental data. The experimental visual responses from the experiments were used to evaluate the predictive performance of three colour spaces (CMC(1:1), CIE L*a*b* and CIE L*u*v*, see section 2.2.1) and two colour appearance models (Nayatani and Hunt91, see section 2.4.1). Coefficient of variation (CV), correlation coefficient (r), gradient (b), and intercept (a) were used to indicate the agreement between visual data and those predicted by spaces and models. To compare the visual with predicted lightness or hue data, no scaling factor (SF) was used for each space and model. As mentioned earlier, colourfulness and brightness were defined as an absolutely attribute with one zero end and one open end. To make comparison between visual and predicted colourfulness or brightness, a scaling factor was first calculated using a least-square method to adjust the predicted colourfulness (chroma or brightness) onto the same scale as the mean visual data for each experimental phase. The calculation of SF was as follow:

$$SF = \frac{\sum x_i y_i}{\sum x_i^2} \quad (4.5)$$

where x_i is predicted colourfulness (chroma or brightness), y_i is mean visual colourfulness (or brightness) for the i -th sample.

4.2 EXPERIMENT 1: STUDIES ON THE PERFORMANCE OF OBSERVERS

The aim of Experiment 1 was to study observers' repeatability and accuracy. It was carried out using a Verivide viewing cabinet illuminated by a D50 source. Table 3.3 summarises the experimental conditions. The detail of these are described in Section 3.3.1. Ten observers joined the experiments. Some of them only attended a few experiments. The characteristics of these observers who took part in all the experiments are given in Table 4.1. They were divided into 3 categories according to the experience in doing magnitude estimation experiment, i.e. with high, moderate, and none experience. Observers HML and MCL attended to later experiments and did not take part in this experiment.

4.2.1 Observers' Repeatability and Accuracy Performance

Each observer assessed the same colour twice. The correlation coefficient (r) and coefficient of variation (CV) measures were calculated between the two repeated mean visual responses of all observers and are given in Table 4.2 for sets A and B experiments respectively. These represent the repeatability of experimental data. The CV values were 5, 14, and 3 for lightness, colourfulness, and hue respectively. These small CV values suggest that the experimental visual data were highly reproducible. These figures show that hue response was the most repeatable and colourfulness the worst. This was expected in the subjective estimation experiment^[10].

Table 4.3 summarises the observer's accuracy performance using r and CV measures calculated between each individual's and the mean data for each of 8 observers. For colourfulness attribute, the geometric mean was used to represent the mean visual responses. The arithmetical mean was used for lightness and hue attributes. The table shows that all r values are close to 1 for the three attributes studied. This indicates that each observer's results correlated well with the mean response. The average CV values are 13, 20, and 6 for the assessments of lightness, colourfulness, and hue results respectively. These figures represent the accuracy of experimental visual responses. The observers differed from one another on their colourfulness response more

than that in their lightness and hue responses. This indicates that larger variation occurs when scaling colourfulness than the other attributes. The results also show that the more experienced observers generally performed better than those inexperienced ones. For example, observers SH and RL who were classified as highly experienced had the lowest deviations, an average of 13, 16, 5 CV values in scaling lightness, colourfulness and hue respectively, while for the inexperienced observers SS, RJ and SC, the average CV values for lightness, colourfulness and hue were 15, 20, 6 respectively. This implies that individuals accuracy could be improved by gaining more experience.

4.2.2 Observers' Consistency

The observers' performance was further investigated by comparing the b factors calculated between each individual and mean visual data. For the lightness and hue responses, Eq.(4.6) was used.

$$R = a + b M \quad (4.6)$$

and Eq.(4.7) for colourfulness responses.

$$\log R = a + b \log M \quad (4.7)$$

Where R is each individual observer's response and M is the arithmetic mean in Eq. (4.6) or geometric mean in Eq. (4.7).

The a factors in Eqs.(4.6) and (4.7) indicate the multiplicative constants used in each session for a particular observer. These values varying among observers indicate that each observer chose a somewhat different modulus in each experimental session^[10].

The factor b indicating the variation of scales used throughout all sessions can be used to show the consistency of each observer. Table 4.4 gives the b scaling factors between observer's response (Y set) and the mean response (X set) for each observer together with range variation in b factor which is calculated using Eq.(4.8)^[147]

$$\text{Range Variation} = \frac{\text{Max} - \text{Min}}{m} \quad (4.8)$$

Where Max and Min are the maximum and the minimum values respectively and m the

mean value in a given set of data. For a perfect consistency between two sets of data, range variation should be zero. The results show that all the observers are highly consistent in scaling hue attribute with an average range variation of 4.5% and a reasonable degree of consistency in scaling lightness (an average of 23.9% variation). In scaling colourfulness, observer RJ was the most consistent over sessions, from 0.66 to 0.86, a range of 25.6%. Observer JX was the least consistent, from 0.78 to 1.63, a range of 83% variation. The average variation of b factor for colourfulness is 41.8%. This is still considered to be good in magnitude estimation experiment. The current results represent a typical variations in this type of experiment.

In conclusion, observers' precision can be improved by gaining more experience. So training programme is essential to get reliable results and to check observer's understanding of colour concepts. Hue response is more accurate than the other two attributes with the colourfulness the worst. All observers have good understanding of hue concept. The reason might be that the hue is the most common attribute to describe a colour. The accuracy of hue scaling was about two times of that of lightness. The colourfulness scaling was less accuracy than that of hue by a factor of 3.

The typical experimental accuracy obtained from this study are 13, 20 and 6 for lightness, colourfulness and hue respectively. This is very similar to Luo's results^[122]. These figures represent the typical experimental deviations in the magnitude estimation experiment. If a model of colour vision can predict the mean visual response better than or close to these figures, that model should be considered good enough to predict human perception to a colour.

4.3 EXPERIMENTS 2 AND 3: TRANSMISSIVE MEDIA

4.3.1 Introduction

Colour appearance models were evaluated using various experimental data sets which were mainly obtained using the reflection print and monitor media^[121,122,141,148,149]. In the graphic arts industry, the source image, or "original", is frequently presented using transmissive materials and needs to be reproduced on paper. To obtain successful colour reproduction needs various adjustments because of the different viewing conditions used for the transparent original and the reproduction on paper^[124]. The research work described in this section was divided into two parts according to the types of the transmissive samples used: cut-sheet transparency (Experiment 2) and 35mm projected film (Experiment 3). The viewing conditions used for these two types of transparency were vastly different: the cut-sheet film was viewed using a back-lit illuminator against a dim surround(see Figure 3.6), and the 35-mm slide was observed by projecting image onto a white screen against a dark surround. The experimental data were again used to investigate the changes in colour appearance caused by different viewing parameters, and to test the predictive accuracy of five colour spaces and colour appearance models.

Experiment 2 consisted of 11 phases according to the viewing parameters studied. The experimental conditions are summarised in Table 3.4 and described in section 3.3.2. Each sample was assessed by a panel of 8 observers. The parameters investigated were grey backgrounds with two luminance factors, three luminance levels, with and without extra flare lights, and white, black, and white paper borders.

Projected slide with size of 35 x 21 mm² is another type of transparency medium used in Experiment 3. Each slide was projected on a screen. The experiment was divided into six phases. The difference between all phases are summarised in Table 3.7 and described in section 3.3.3. The viewing parameters investigated were different light sources, luminance levels, and spatial arrangement of colours in the viewing pattern. Phases 1 to 4 experiments were first carried out. Phases 5 and 6 were conducted at a later stage to verify the results from previous phases.

4.3.2 Observers' Performance

In each of the Experiments 2 and 3, two phases were conducted in the same experimental conditions, i.e. phases 2 and 9 in Experiment 2 and phases 1 and 4 in Experiment 3. Six observers took part in all the phases. The repeatability of experimental data were again studied using r , CV, a , and b values between two repeated mean assessments (see section 4.1). The mean visual responses from these two sessions were compared and the quantitative measurements [i.e., CV(0), CV(s), gradients, and intercepts] are given in Table 4.5. The a and b values in parentheses in the table show that there is no significant difference between two set of mean data for each experiment. The CV(o) values for lightness, colourfulness and hue responses were 7, 11, and 3 respectively for Experiment 2 and 7, 9, and 4 respectively for Experiment 3. These small CV values indicates that the visual data are highly repeatable and the magnitude estimation method is quite reliable in quantifying colour appearance.

Tables 4.6 and 4.7 list each observer's consistency performance for Experiments 2 and 3 respectively. The r and CV measures indicate the accuracy of experimental visual data. The average CV for each observer's response against mean values are 15, 17, and 6 in Experiment 2 and 16, 16, and 7 in Experiment 3 for lightness, colourfulness, and hue respectively. These figures are similar to those found in Experiment 1 (13, 20, 6) and represent the typical observer deviations involved in the magnitude estimation experiments. The accuracy of visual data for both experiments are almost the same. This suggests that the degree of consistency in the two experiments is reasonable close. Generally the present perceived colourfulness are more accurate than that in Experiment 1 including many inexperienced observers. In Experiment 2, the mean CV values gradually reduced for lightness and colourfulness responses. This implies that observers were gaining more experience as the experiment progressing, and also the training experiment (Experiment 1) served a useful purpose.

4.3.3 Effect of Different Viewing Parameters

The visual responses from different phases for each experiment were compared to

reveal the effects of the different viewing parameters studied. These effects are high, medium and low luminance levels, lighter and darker mid-grey backgrounds, white and black borders, with and without extra flare side lights and illuminants. The quantitative measures (r , CV, a , and b as described in section 4.1.2) and scatter diagrams were used to show the agreement and trend of difference between two sets of visual results.

4.3.3.1 Effect of Luminance Levels

Six comparisons were made between the data for the different luminance levels in Experiment 2. The quantitative measures are given in Table 4.8. As mentioned earlier, lightness is defined as a relative brightness scale. The reference white colour in the visual field is always defined with a lightness of 100. This seems that the luminance levels should have little effect on the perceived lightness. The experimental data show that the perceived lightness changed when the luminance level varied. For lightness responses, dark colours look lighter when viewed under the highest luminance level (with intercept larger than 3), but not much lightness difference between the medium and low levels. For colourfulness responses, the results show that colours tend to appear more colourful under the highest than the lowest levels (with gradient 1.09) against lighter background, but there is no significant changes under the other luminance levels (with gradients in parentheses). There is little effect on the perceived hue attribute when luminance level was changed. These trends can be clearly seen in Figure 4.1. In this figure, hue response were plotted in the scale of 0-100, i.e., 0-25 for R-Y, 25-50 for Y-G, 50-75 for G-B and, 75-100 for B-R.

In Experiment 3, there were two luminance levels under Halogen projected source, i.e, 113 and 45 cd/m^2 . A comparison between phases 1 and 3 was made to investigate the changes of perceived appearance caused by changing the screen luminance. The results are given in Table 4.9 and illustrated in Figure 4.2. It can be seen that colours appear more colourful under high than low level. There is hardly any difference between two phases' hue and lightness results.

4.3.3.2 Effect of Extra Flare Light

In Experiment 2, the only difference between phases 2 and 4 was the introduction of flare light. The viewing conditions of phase 4 had side flare light from both sides of illuminator, but not for phase 2. The experimental situations of these two phases were photographed and shown in Figure 3.6 (c and d). The comparison results are given in Table 4.10 and the effect is illustrated in Figure 4.3 which shows the perceived lightness, colourfulness and hue of phase 2 (in X axis) plotted with those of phase 4 (in Y axis). These results clearly show that, for most samples they appeared lighter ($a=0$ and $b=1.06$) and more colourful ($b=1.03$) in phase 4 than in phase 2. This implies that flare light increased the perceived lightness and colourfulness but little influence on hue response.

4.3.3.3 Effect of Luminance Factors of Backgrounds

In Experiment 2, the effect of luminance factors of backgrounds was investigated by comparing visual responses from a lighter ($Y=17$) and a darker ($Y=10$) grey backgrounds, i.e. phases 2 and 10 (with white border) and phases 11 and 6 (with black border).

In Figure 4.4 the data are plotted between phases 2 (X axis) and 10 (Y axis), and between phases 11 (X axis) and 6 (Y axis) for lightness (top), colourfulness (middle), and hue (bottom) responses. Figure 4.4 and Table 4.10 show that the darker background causes colours more colourful. For the lightness comparison, the dark colour appears lighter under the darker than the lighter background for white border conditions. There is very little difference for the black border conditions.

4.3.3.4 Effect of Borders

In Experiment 2, border means the area immediately surrounding the viewing pattern (see Figure 3.6). The difference between viewing conditions in phases 2 and 11 and phases 10 and 6, was the border. The comparison results are also given in Table 4.10 and illustrate in Figure 4.5. It is shown that dark samples appeared lighter under black border than under white border. There was no significant colourfulness and hue

differences found between white and black borders.

4.3.3.5 Helmholtz-Kohlrausch Effect

The Helmholtz-Kohlrausch Effect (see section 2.3.4) was found in Experiment 2. The visual responses for some chosen samples are given in Table 4.11 to illustrate this effect. These include 4 neutral samples and their corresponding chromatic samples with same luminance factors. The data were obtained from phase 2 (white border with lighter background), phase 6 (dark border with darker background), phase 10 (white border with darker background) and phase 11 (dark border with lighter background). All these phases had same luminance level about 680 cd/m^2 . The average standard deviation for the mean lightness response for the 4 neutral samples was 5 units. In most cases, the perceived lightness is different more than 5 units between achromatic and chromatic colours with same Y factors. This suggests that achromatic and chromatic lightness for samples with identical luminance factors differ considerably, especially for the darker colours.

4.3.3.6 Effect of Colour Temperature

In Experiment 3, no significant shift on hue and colourfulness responses was found when colour temperature changed from 4000K to 5600K. The colourfulness and hue responses of phases 3 and 2 are presented graphically on response diagram in Figure 4.6. Response diagram is a 2 dimension colour diagram in polar coordinates. The angle and radius represent hue and colourfulness responses respectively. These coordinates provide a graphic presentation of the relationships of perceptual magnitudes for hue and colourfulness ^[11]. In Figure 4.6, the "o" markers correspond to the colour appearance under illuminant of 4000K (phase 3) and the "x" markers to the appearances of the same stimuli under illuminant of 5600K (phase 2). The length from the "o" to "x" differs according to their positions in the diagram. The illuminant of 4000K appears yellower than that of illuminant 5600K (close to achromatic light). The response diagram shows that for most of colour stimuli, their colour appearance do not change significantly when illuminant changed from 4000K to 5600K. Also there is little evidence to show a

systematic colour shift. Because the response for most achromatic stimuli were perceived being neutral colour by most observers, there was no Helson-Judd effect (see section 2.3.4) being found. This suggests that most of the samples used in Experiment 3 are colour constant ones.

4.3.4 Testing Performance of Various Colour Spaces and Models

The visual data from the above experiments were used to evaluate the predictive performance of three uniform colour spaces (CMC(1:1), CIE L*a*b*, and CIEL*u*v*, see Section 2.21) and two colour appearance models (Nayatani and Hunt91 models, Section 2.3.6). Correlation coefficient (r) and coefficient of variation (CV) were again used to indicate the agreement between the visual data and those predicted by the spaces and models. To compare visual with predicted lightness and hue, no scaling factor (SF) was used for each space or model. To compare the visual colourfulness with predicted chroma or colourfulness, different mean SFs were used for Experiments 2 and 3 to adjust predicted data onto the same scale as the visual data and allow for different magnitudes in the spaces and models studied (using Eq.(4.5) in Section 4.1.3). Tables 4.12 and 4.13 summarise the comparison results for lightness, colourfulness, chroma, and hue attributes in Experiments 2 and 3 respectively. For testing colourfulness predictions, only Hunt91 and Nayatani models can gave predictions and hence were tested.

Colour spaces are mainly used to describe the colour difference between two stimuli such that equal scale intervals represent approximately equal perceived differences in the attribute considered. The hue scales of the spaces are designed to quantify the hue difference, not appearance. Thus hue comparison between perceived and predicted hue by the spaces is meaningless. The models of colour vision were designed to estimate the colour appearance under different viewing conditions and are able to take into account all the parameters studied in the experiments. Therefore their hue predictions were tested.

4.3.4.1 Lightness Predictions

As CIEL*a*b* and CIEL*u*v* have the same lightness scale, four lightness predictions were tested. The r values in Table 4.12 (Experiment 2) for the four lightness predictions are about 0.96 which suggests that all the predictions of lightness were linearly correlated very well with the observed lightness. The visual responses from phases 1 and 5 are plotted in Figure 4.7 against four lightness scales tested. The data from these two phases are used to typify the trend of predictions from these spaces and models. These figures show that CIE, Nayatani's and Hunt's scales predict the visual responses too dark; CMC predictions are the closest to the 45° line with the CV value of 16. The Hunt91 lightness scale fits very well to the monitor and surface media data^[121], but not sufficient to this set of data. This strongly indicates large difference in perceived lightness presented between the monitor and surface colours and the current cut-sheet transparency viewing conditions. Based on these results, further modifications were made to the Hunt91 lightness scale. This will be described later.

The mean CV values in Table 4.12 represent the average deviation of predicted from observed lightness. These are 16, 20, 20, 29 for CMC(1:1), CIE L*, Nayatani and Hunt91 scales respectively. Almost all spaces and models performed disappointingly, i.e., their predictions are worse than the typical observer's accuracy (15 CV units).

The test results from Experiment 3 are summarised in Table 4.13. In comparison with perceived lightness, the CIE scale (mean CV = 18) gave the most accurate prediction and the CMC (mean CV = 35) the worst. The CMC performs the best for cut-sheet transparency medium and the worst for 35-mm projected slide. This implies large differences in perceived lightness between the two transparency viewing conditions. The visual lightness from phases 1 and 2 are plotted in Figure 4.8 against the four lightness scales tested. This figure clearly shows that none of the lightness scales predict well to the visual responses, i.e., all over-predict lighter colours for all phases and the CMC over-predict all colours. This discrepancy was thought to be caused by a lightness contrast effect resulting from the reference white in the viewing pattern being too close to the test colour (see Figure 3.20a). Hence, phases 5 and 6 experiments were carried out to verify this. Both phases used a different viewing pattern in which the reference white was further away from the test colour (see Figure 3.20b). In phase 6 of the

experiment, three test colours were identical to the reference white. In Figure 4.9, phases 5 and 6 visual data are plotted against predictions by the four models studied. Again, these figures show the same trend found as those in previous phases regardless of the spatial arrangement in the viewing pattern. Additionally, all observers scaling the lightness of 100 for three test colours which were identical to the reference white. All evidence suggests that this phenomenon is genuine and a modified lightness scale for Hunt91 model is required to take into account 35mm projection conditions.

4.3.4.2 Chroma and Colourfulness Predictions

The chroma predictions from three spaces and two colour appearance models were tested. Before comparison, a scaling factor (SF) for each of spaces and models was found using Eq.(4.5). These are also given in Tables 4.12 and 4.13 for Experiments 2 and 3 respectively together with their mean SFs. These scaling factors were used to adjust predicted data onto the same scale as the visual data. The final comparison was made using MCV values obtained using mean SF from all phases in each experiment.

In Experiment 2, a comparison of the chroma predictions of the spaces and models show that the predictive accuracy of Hunt91 chroma scale was the highest. An example is shown in Figure 4.10 in which the perceived colourfulness from phase 1 are plotted against predicted chroma by the five chroma scales studied. It shows that the largest and smallest spread of data points occur for the CIE $L^*u^*v^*$ and Hunt91, respectively. The performance of the colourfulness predictions by the Nayatani and Hunt91 models were not better than their chroma predictions with CV values of 28 and 30 respectively. The CV values of 20, 22, 26, 22 and 18 were found by chroma predictions of CMC(1:1), CIE $L^*a^*b^*$, CIE $L^*u^*v^*$, Nayatani, and Hunt91 respectively. Because the typical observer's deviation in scaling colourfulness is 17, Hunt91 model performs as well as the average observer's and the best among the 5 scales.

For Experiment 3, the r values of 0.92, 0.91, 0.88, 0.65, and 0.87, and 19, 19, 25, 35, and 23 of CV values in Table 4.13 are found for the chroma predictions by CMC(1:1), CIE $L^*a^*b^*$, CIE $L^*u^*v^*$, Nayatani, and Hunt91 respectively. The results

show that the CMC and CIE L*a*b* scales performed better than the other scales. The visual colourfulness from phases 1 and 2 are plotted in Figure 4.11 against predictions by the five chroma scales studied. Again, like the cut-sheet transparency samples, the colourfulness response are more accurately predicted by chroma scales of both models than by their colourfulness scales.

4.3.4.3 Hue Predictions

The hue predictions from two colour appearance models are very similar as shown in Figures 4.12 and 4.13 for Experiments 2 and 3 respectively. CV values of 8 and 11 for Experiments 2 and 3 suggest that both models predicted hue more accurately for cut-sheet than for 35mm slide media. This is due to the large difference between the two viewing conditions.

4.3.5 Modifying Hunt91 Colour Appearance Model

As shown in section 4.3.2, a typical observer accuracy for scaling lightness, colourfulness, and hue are 15, 17, and 6 CV units respectively in Experiment 2, 16, 16, and 7 respectively in Experiment 3. Hunt91 model's deviation of predictions for lightness, chroma, colourfulness, and hue are 29, 17, 27, and 7 respectively for Experiment 2 and 22, 23, 30, and 11 respectively in Experiment 3. Some effort is therefore desirable to modify this model in order to improve its predictive accuracy for transmissive media.

4.3.5.1 Modification of Hunt Model's Lightness Scale

In the Hunt91 models, lightness (J) is calculated as follows:

$$J = 100 \left(\frac{Q}{Q_w} \right)^z \quad (4.9)$$

$$z = 1 + \left(\frac{Y_b}{Y_w} \right)^{\frac{1}{2}} \quad (4.10)$$

$$Q = [7(A + M/100)]^{0.6} N1 - N2 \quad (4.11)$$

where

$$N1 = (7Aw)^{0.5} / (5.33 Nb^{0.13}) \quad (4.12)$$

$$N2 = 7 Aw Nb^{0.362} / 200 \quad (4.13)$$

and Q and Q_w are the brightness of the stimulus considered and reference white respectively. A and Aw are the achromatic signals of the sample and reference white respectively. M is the colourfulness of the stimulus. Y_b and Y_w are the Y factors for the background and reference white respectively. Nb is the brightness induction factor. For the television and visual displays unit in dim surround condition, Nb should be 25 as approximation^[21].

It is easy to modify the model by optimising the Nb and z values until the minimum CV between the visual and predicted data is obtained. For cut-sheet transparency displays, it was found that the factor z were 1 for the lighter background and 0.85 for the darker background with Nb of 25. For projected slide, $Nb = 10$, and $z = 1.2$. Hence, the original suggested values for Nb were confirmed and new z values were obtained. The comparison using these new z values were carried out and their results are listed in Table 4.14 for Experiment 2. The scatter diagram were again produced between the visual and predicted data. Figure 4.14 shows lightness responses of phases 1 and 5 in Experiment 2 plotted against those predicted using the modified lightness scale. In comparison with those in Figure 4.7, all data points in Figure 4.14 are closer to the 45° line. Although a little improvement did occur for 35mm slide experiment, the model still over-predicted lighter colours as shown in Table 4.13. Therefore, a revised formula of lightness scale was derived and expressed in Eq.(4.14):

$$J_{new} = J_{old} \left[\left(1 - \left(\frac{J_{old}}{100} \right)^3 \right) 1.14 + \left(\frac{J_{old}}{100} \right)^5 \right] \quad (4.14)$$

Where J_{new} and J_{old} are new and original lightness scales respectively with $Nb = 10$, and $z = 1.2$. The prediction by the new lightness scale are plotted with observers' lightness

response in Figure 4.15 for the first two phases of Experiment 3. The quantitative measures are given in Table 4.15. It can be seen that much better agreement between visual and predicted data can be found for lighter colours in Figure 4.15 than those in Figure 4.8.

4.3.5.2 Modification of Hunt Models Chroma and Hue Scales

In Hunt91 model, there are some variables to take into account the state of adaptation in a particular viewing conditions, i.e., $F_\rho, F_\gamma, F_\beta, \rho_D, \gamma_D$ and β_D . When the Helson-Judd effect (as described in section 2.3.4.3) is ignored $\rho_D = \gamma_D = \beta_D = 0$. If the illuminant is discounted or the observer is fully adapted, $F_\rho = F_\gamma = F_\beta = 1$ (this would also make $\rho_D = \gamma_D = \beta_D = 0$). These modifications would affect the chroma, colourfulness, and hue predictions in the original model. These were used to test the data of Experiments 2 and 3 and the results are also given in Tables 4.14 and 4.15 respectively. Table 4.14 shows that in almost all phases, the model with $F_\rho = F_\gamma = F_\beta = 1$ fit chroma and hue visual data slightly better than the original model and the model with $\rho_D = \gamma_D = \beta_D = 0$. This implies that observers seem fully adapted in the cut-sheet viewing conditions. It is arguable that the model with $F_\rho = F_\gamma = F_\beta = 1$ should be recommended in cut-sheet viewing conditions because of the limited improvement (1 or 2 units in CV) from the original model.

In testing the modified model using Experiment 3 data (see Table 4.15), it is quite encouraging that great improvements in chroma and hue predictions (but not for colourfulness) were found for both modified scales. The model with $\rho_D = \gamma_D = \beta_D = 0$ performed the best and is recommended to be used in predicting colours under 35-mm slide viewing conditions. Figure 4.16 shows the visual colourfulness and hue from phases 1 and 2 plotted against the modified model's chroma and hue predictions respectively. It can be seen that the agreement between the visual and predicted data is much better than those in Figures 4.11 and 4.13 with 5 and 4 less CV units for chroma and hue predictions respectively than that of original model.

The CV values for all the predictions are summarised in Tables 4.16 and 4.17 for

Experiments 2 and 3 respectively. In conclusion, the experiment described here extends other researchers' study^[121,122] to cover transmissive media. Two experiments were conducted according to the types of transparency used, i.e., large cut-sheet size and 35-mm slide. In analysing the visual data, it shows good observer accuracy and repeatability performance.

Various viewing parameters were employed to show how these would affect the perceived colour appearance. For the cut-sheet experiment, as the luminance increases colours appear more colourful and lighter (particularly between the highest and lowest luminance levels). The similar effect was also presented when the background changes from lighter to darker. Adding extra flare to the image increases colourfulness and lightness responses. In Experiment 3, again the colours appear more colourful under high than low luminance, but very little difference in perceived lightness was found. There is little difference in hue response when viewing conditions were changed.

The testing results for various colour spaces and models using the two sets of data suggest that the Hunt91 colour appearance model needs to further modify to meet the requirement of the applications for the current media and viewing conditions studied. There are large perceptual differences between the transmissive and non-transmissive media viewing conditions.

Modifications were made to the Hunt91 model afterwards. Two different versions were developed to model the cut-sheet and 35-mm projection visual data separately. Fixing the z factors in the Hunt91 lightness scale gives big improvement with 20 less CV values in Experiment 2. A new lightness scale (J_{new}) together with removal of the Helson-Judd effect in the Hunt91 model produced the best fit to the 35mm projection data. This suggests that observers were effectively adapted in the dark surround conditions.

4.4 EXPERIMENT 4: REFLECTION PRINT MEDIUM

4.4.1 Introduction

Reflection samples were widely used in studying colour appearance by many researchers as stated in section 2.4.2^[121,122,148]. In their experiments, the viewing parameters studied were illuminants, backgrounds, and borders. Two luminance levels were employed. This experiment extended their experimental conditions to cover a wide range of luminances. In addition, a brightness attribute was added to the lightness, colourfulness, and hue attributes for describing colour appearance. The experimental conditions are given in Table 3.10 and described in section 3.3.4.

4.4.2 Observers' Performance

In this experiment, forty OSA samples were assessed by four observers in each of 12 phases. The quantitative measures (r , CV, a , and b) between each individual's and mean responses for colour attributes of lightness, brightness, colourfulness, and hue are given in Table 4.18. The results show that observer WY was less accurate than those of the others. The average CV values for lightness, brightness, hue, and colourfulness were 10, 10, 16, and 6 respectively. These data are similar to those found in transmissive media experiments except for the lightness. There was about 5 more CV values in scaling lightness for transmissive media than for reflection medium studied in this experiment. The results show that observers' variations for scaling colourfulness considerably increased for the lowest luminance level (phases 6 and 12) with average 8 more CV values. Table 4.19 gives exponent factor b (see section 4.2) for the brightness and colourfulness response. The average range variations were 33.1% for brightness and 18.1% for colourfulness estimations. In Experiment 1, the average range variation in b for colourfulness was 41.8%. This implies that observers did improve their accuracy in scaling colourfulness by gaining more experience.

A repeatability study was also carried out using the colourfulness and hue data. These two attributes were scaled twice by each observer, i.e., in phases 1 and 7, 2 and

8, etc. The mean colourfulness and hue responses for the two corresponding phases having the same viewing conditions were compared. These results are summarised in Table 4.20. The results reveal that for hue comparison, the agreements from all six pairs of phases are excellent, with an average CV value of 3. For colourfulness attributes, the poorest agreement (CV=20) occurs between phases 6 and 12. This is due to somewhat large experimental deviation occurred in the darkest adapting luminance. The average CV value of 12 for colourfulness was similar to that found in the transmissive media study. The gradients for all comparisons are all close to 1, except between phases 1 and 7. This could be due to perceived colourfulness being affected by the scaling of either lightness or brightness. In phase 7, the highest luminance level was used. The observers scaled higher brightness values than those in the other phases. This encouraged observers to give higher colourfulness value. A decision was made to recalculate the mean colourfulness and hue results using data from eight observing sessions (4 observers x 2 equal-luminance phases) in order to simplify the subsequent data analysis. These data, together with the mean lightness from phases 1 to 6, and the mean brightness from phases 7 to 12 were merged, and formed the new combined phases (CPs) 1 to 6.

4.4.3 Effect of Various Adapting Luminance Levels

In this experiment, six different luminance levels of D50 light source were studied.

The mean responses from combined phase (CP) 1 (the highest luminance) were compared with those from the other phases. These provide information about the changes in colour appearance under different adapting luminances. The measures used previously were again calculated and are given in Table 4.21. In Figures 4.17 and 4.18, the visual data from CP1 are plotted against those of the other phases from left to right for lightness, brightness, colourfulness and hue respectively.

It can be seen that CV values are getting larger when comparisons are made between the highest and lower luminances. The reason is that increasing luminance increased the difference of colour appearance under two luminance level conditions. The results also show that there was not only significant evidence for the majority of gradients

and intercepts different from 1 and 0 respectively, but also $CV(0)$ values are much larger than $CV(s)$ for all comparisons. This clearly indicates that strong linear relationships exist between each of three attributes (lightness, brightness and colourfulness) in different adapting luminances.

For the hue comparison, the CP 1 data agree very well with those of the other CPs (with an average CV of 4). However a systematic discrepancy was found that most colours in the green to blue areas appeared bluer in the lower levels than in the highest one. These are shown in Figures 4.17 and 4.18.

For the lightness comparison, there is a consistent trend for the gradients to reduce and intercepts to increase under the low luminance phases. This means that dark colours appear darker under low luminance than high luminance (see the left side of Figures 4.17 and 4.18). This phenomenon agrees well with that found in Experiment 2.

For the brightness comparison, the results clearly show that both gradients and intercepts increase in magnitude for lower luminance. This implies that all colours appear darker under lower luminance than under higher luminance.

For the colourfulness comparison, there is a clear trend for the gradients to increase under the lower luminance. This implies that colours appear to be more colourful under high luminance levels than under low levels. However there is no increase in colourfulness between CPs 1 and 2. This suggests that perceived colourfulness may not rise when luminance exceeds 200 cd/m^2 .

4.4.4 Testing Performance of Colour Spaces and Models

Three uniform colour spaces of CMC(1:1), CIE $L^*a^*b^*$ and CIE $L^*u^*v^*$, and two colour appearance models of Nayatani and Hunt91, were again tested. The comparison between visual and predicted data by spaces and models were carried out. The correlation coefficient (r), CV values, intercept (a) and gradient (b) are all tabulated in Table 4.22 for the lightness, brightness, chroma, colourfulness, and hue attributes for the

six combined phases of Experiment 4. In addition, the r and CV measures for each model calculated from the first 5 phases and all 6 phases are also given. It is clear from the data in Table 4.2.2 that the CV values from phase 6 (the lowest luminance phase) are always much larger than those in the other phases. This is the reason that two mean CV values were used. Scatter diagrams were produced from the visual data and the predictions by two models for qualitative comparison. Figures 4.19 and 4.20 present the visual responses (Y axis) plotted against the predictions of lightness, brightness, chroma, and hue (X axis) for all phases from Nayatani and Hunt91 models, respectively.

4.4.4.1 Lightness Predictions

Four lightness scales were tested. These are CMC(1:1), CIE L^* , Nayatani, and Hunt91. For Hunt91 lightness scale, the brightness induction factor N_b is set to equal to 75 according to the model's recommendation.

The r values of 0.96, 0.96, 0.95, and 0.95 in Table 4.22 for all models indicate that these lightness scales linearly correlate very well with perceived lightness. This is similar to that found in the previous two experiments.

The Hunt91 model performed the best for prediction of lightness (CV value = 14). Predictions by the CIE and Nayatani models were good. Large CV value (38) was obtained when using the CMC space. Comparing with the average observer's deviation of 10, Hunt91 model is quite good and may not require further modification.

4.4.4.2 Brightness Predictions

For testing brightness scales, only Hunt91 and Nayatani models were used, as the colour spaces do not include brightness scales. Each model's predictions were scaled using a mean scaling factor obtained using Eq.(4.5) before comparisons. The r , CV a , and b measures are also given in Table 4.22 together with the mean CV values from all 6 CPs. The CV values are 13 and 11 for Nayatani and Hunt91 brightness scales. Both models gave good predictions to the visual response. Figures 4.19 and 4.20 show that the

brightness data are close to the 45° line for both models. Both colour appearance models' brightness scales gave very similar overall performance and their predictions for this attribute were quite accurate.

4.4.4.3 Chroma and Colourfulness Predictions

For comparisons of chroma or colourfulness scales of spaces and models, a scaling factor was first calculated between the visual colourfulness data and those predicted by the spaces and models. These are listed in Table 4.22. For three spaces (which were not designed to predicted the changes of appearance under different luminance), as expected, there is a clear pattern showing that their SFs reduce from high to low luminance phases. This indicates that perceived colourfulness is reduced under lower luminance, and this is particularly marked between CPs 5 and 6. There is a very large spread of SFs between high- and low-luminance phases. The range variations in SF for these spaces and models are ranged from 33.3% to 133.2%. The SF from CP 6 for each space or model is very low in comparison with those of the other phases. Using the mean SFs calculated from all six CPs would produce a poorer overall performance than from just the first five CPs. The mean SF from CPs 1 to 5 was calculated for each space or model (see the last column of Table 4.22) and these were used to indicate the overall performance of the spaces and models. The results show that the predictive accuracy of Hunt91 chroma scale was the highest. As described above, the SFs obtained from phase 6 are quite different from those of the other phases. The results reveal that the mean CV values obtained from five CPs are much smaller than those from six CPs. The performance of the colourfulness predictions from the Nayatani and Hunt91 models were not better than their chroma predictions.

4.4.4.4 Hue Predictions

The hue prediction by Hunt91 model with CV of 8 over-performed that of Nayatani model with CV of 13. However, the perceived hue appears bluer in low-luminance levels (less than 20 cd/m²) than those of predictions in the green to blue area as shown in Figure 4.20. Both models assumed that there is no hue variation with change in

luminance. As mentioned in 4.4.3, colours in the green to blue areas appear bluer under low luminance than high luminance. The Hunt91 model predict well for the hue visual results under high luminance. However this may not be expected in the case under low luminance.

Table 4.23 gives the summary of testing various colour spaces and models for Experiment 4. In conclusion, Experiment 4 investigated the changes of perceived lightness, brightness, colourfulness and hue attributes under six different luminance level ranging from 0.4 to 800 cd/m². Observer's accuracy and repeatability performances were examined. It was found that there is a very good repeatability in the experimental results. Several comparisons were made to understand the changes in each perceived attribute under various luminance levels. The results clearly show that for all attributes under adapting luminances, strong correlation exists in the changes. For lightness, the dark colours appear to be darker in low luminance than in high luminance. For brightness, all colours appear darker in low luminance than in high luminance. For colourfulness, all colours increase in colourfulness when viewed under high luminance, but exhibit no further change for luminance exceeding 200 cd/m². Hue is not affected by differences in luminance apart from colours in the green to blue area. These colours appear bluer in lower than in higher luminance. All spaces and models perform worse for the lower luminance phases, i.e., the worst prediction always occurs in CP 6. This is because larger experimental deviations occurred in the darker conditions. All models were not designed for use under very low luminance conditions. The Hunt91 model fits all visual responses very well. The CV values of 13, 10, 19 and 7 (from the mean of five phases) are very close to those of 11, 11, 18 and 8 (typical observer accuracy performance) for lightness, brightness, colourfulness and hue attributes respectively. This once again show that the Hunt91 colour appearance model outperformed the other spaces and models. It is encouraging that the predictive deviation from this model is very close to that of typical observer accuracy. As mentioned in Section 2.3.6, Hunt colour appearance model was derived from data obtained partially using surface colours. This suggests that there is a good agreement between this set of data and other researchers' datum sets.

4.5 EXPERIMENT 5: SIMULTANEOUS CONTRAST EXPERIMENT

4.5.1 Introduction

Experiment 5 was designed to extend earlier study^[102] as described in Section 2.3.4.6. Instead of 9 test colours studied before, 13 colours were used in this experiment. Thirty seven induction colours were the same as those used in the earlier experiment. Totally, 481 test-induction combinations were estimated. In addition to quantification of simultaneous contrast effects, the Hunt91 colour appearance model was also tested using the data obtained so that simultaneous contrast effects could be included in the model. The detailed experimental conditions were described in Section 3.3.5.

4.5.2 Observers' Performance

The mean visual responses were calculated using arithmetic mean for lightness and hue attributes and geometric mean for colourfulness. The accuracy of visual data for each attribute by each subject is summarised in Table 4.24 using r and CV values. The CV values for each observer in scaling lightness, colourfulness and hue are 17, 22, and 9 respectively. The deviation of colourfulness scaling is larger than those in Experiments 1 to 4. This implies that monitor colour with various surroundings is more difficult to scale than other media.

4.5.3 Simultaneous Colour Contrast Effect

When a test field was surrounded by an induction field, the perceived colour of the test field is usually different from this test field surrounded only by a large grey background (with size of 40 x 20 cm²) as shown in Figure 3.32 for the experimental display. The lightness, colourfulness and hue differences between the visual responses of the test patch surrounded by an induction field, and those surrounded only by the mid-grey ($L^*=50$) induction fields, were first calculated. The mid-grey induction field was the same colour as the background. Hence, the visual results for this test-induction combination for each test colour represented its colour appearance without an induction

field. For Experiments 1 to 4, all test stimuli were estimated against a grey background, and Hunt colour appearance model can predict these visual estimations very well. Therefore, the test colour against the mid-grey induction field (same colour as background) was used to establish the base line here, ie., how response from the other induction fields differed from this particular conditions. These differences were plotted against CIE LAB L^* , C^* , and hue angles of various induction field respectively to reveal the contrast effects.

4.5.3.1 Effect on Lightness

A. Lightness on lightness

Figures 4.21 to 4.23 show lightness difference ($L_{\text{test-with-surround}} - L_{\text{test-against-grey}(L^*=50)}$) (Y axis) for each of 13 test colours plotted against the L^* of the inducing field (X axis). Each graph includes 37 test-induction combinations. All data points are plotted using pluses ("+") except the circle ("o") for the five neutral induction fields. The L^* values of the induction fields are given in Table 3.15. For each test colour, a vertical dashed line was draw at the point where the L^* at x axis equal to the L^* of test colour. Therefore when the L^* of the induction field is smaller than that of the test field, the marker is plotted on the left side of the vertical line, and vice verse. For the identical L^* , the marker is on the vertical line.

For the test colours with L^* less than 80 (10 out of 13 test colours), the figures indicate that the test patch appeared lighter when the induction field became darker. For the lighter test colours with L^* larger than or equal to 80, such as YYG, GGY and GGB, all data are above the zero line. This indicates that they looked lighter against any induction field than against grey background. Also when a test colour was seen against the lightest grey (white, the circle marker located at the end of right side of graph with $x=100$) and the darkest-grey (black, the circle located at the end of left side of the graph) induction field, larger contrast effect was formed (both circle markers located further away from the zero line than the most of markers for each of the test colours).

B. Hue on lightness

For each test field with a given hue surround, there are four surrounds varying in L^* (e.g. red surround at L^* equal to 30, 40, 50, and 70), yielding a test-surround set located at the same vertical line in the graphs. Figures 4.24 gives lightness difference plotted against the hue angles of the inducing fields for the four representative test colours. The hue angles of the inducing field are the CIE $L^*a^*b^*$ hue angles (see Table 3.15). The smaller marker represents the lighter induction fields for that particular hue, while circle plus marker "+" represents each of five achromatic surrounds and the circle without plus the darkest surround. The pluses located in the joint line represent that the induction fields for those combinations have the same L^* as the test field ($L^*=50$) has. It can be seen clearly that the joint line is very close to the zero line. This suggests that any surround with the same L^* as that in the test field gave little effect on the lightness response of test colour. When a test field was surrounded by an induction field with identical hue but smaller L^* (darker) value than the test colour (red, green and blue belonged to this case), the test field appeared the lightest among all the induction fields. The larger pluses locating above the smaller pluses for each hue angle in x axis indicates that for an induction field, a given hue with lighter surround made test colour darker. Additionally, the test colours surrounded by the white colour gave the darkest appearance (circle with smallest plus located lowest).

C. The size of test patch on lightness

The change of the size of a test field also changed its lightness response when seen against grey background. Figure 4.25 shows lightness difference of test colours between small and large sizes ($2 \times 2 \text{ cm}^2$ and $6 \times 6 \text{ cm}^2$ respectively) when seen against grey background plotting against the hue names for each of Red, Yellow, Green, and Blue test colours (top graph) (used in this experiment) and for each of Red, YR, Yellow, GY, Green, BG, B, and RB test colours (bottom graph) (scaled in the earlier studies^[102]). It is clear that for 10 out of 12 cases the colour appears lighter when the size of test colour increases in the case of lightness difference less than zero.

4.5.3.2 Effect on Colourfulness

A. Lightness and Hue on colourfulness

Figures 4.26 to 4.29 show colourfulness difference ($C_{\text{test-with-surround}} - C_{\text{test-against-grey}(L^*=50)}$) plotting against hue angles of induction fields for all test colours. The sizes of the markers have the same meaning as those stated in the last section. The colourfulness of a test colour is affected by the L^* of the surround: the smallest pluses (lighter surrounds) are nearly always located at the bottom part of diagram. This trend occurred in 75% cases, which implies that for each particular hue surround, the colourfulness of the test colour decreased when surrounded by lighter induction fields.

In Figures 4.26 to 4.29, for most test colours (10 out of 12 cases), there are joint lines connecting pluses with their neighbouring hues. The L^* of surround for each plus (representing a test-induction combination) in the lines is close to the L^* of the test field. This difference is less than 10 L^* units. There is a clear pattern that almost all the pluses in the joint lines are located at the lower part of each graph, while the pluses located at higher positions always have the opponent hue of the test colour. This suggests that induction hue affects the colourfulness of test colours. The colourfulness of a test patch reduced when surrounded by an induction field with a similar hue and increased when surrounded by an opponent hue. In general the darker of this opponent hue surround was (or close to the opponent hue), the more colourful of the test colour appeared, because larger plus (darker) is located above smaller one (lighter). The largest colourfulness reduction occurred when a test colour was surrounded by an induction field with closer hue and similar L^* to the test colour (most joint lines located at the lowest part of the graph). For achromatic surround fields, lighter surround made a test colour less colourful. Taking green colour in Figure 4.28 as an example, the joint line connects five pluses with its neighbouring hue surrounds. These five sets of markers are located lower than the others, while two sets of markers at the end of left and right sides of the graph respectively are located higher. These two sets of higher markers have hue of induction fields close to red, ie., the opponent hue of green. Additionally, larger (darker) pluses located above smaller (lighter) ones. This indicates that darker surrounds with

opponent hue cause test colour more colourful. Among the five pluses in the joint line, the lowest one has hue of GB and L^* of 50 (the same as the L^* of the green test colour), ie., largest contrast effect occurred when a test colour was surrounded by a colour with closer hue and similar L^* to the test colour.

B. The size of test patch on colourfulness

The size of a test field gave an influence on the colourfulness response under grey background. Figure 4.30 plots the colourfulness difference of test field colours between small and large sizes ($2 \times 2 \text{ cm}^2$ and $6 \times 6 \text{ cm}^2$) against hue names. The top one is for test colours used in this experiment, while the bottom one is for the earlier experiment^[102]. When the sample size increased, the colourfulness was decreased (with colourfulness difference greater than zero), i.e., large size colour appears less colourful than small size one.

4.5.3.3 Effect on Hue

Many studies indicated that the effect of an induction field on hue of a test field is to shift the hue of the test colour in the direction of the opponent hue of the induction field (see Section 2.3.4.6). Hence, if a yellow-red were surrounded by red, we would expect the yellow-red to move in the direction of green, thus appearing yellower. This effect has been confirmed in the current study. Figures 4.31 to 4.34 plot the hue difference ($H_{\text{test-with-surround}} - H_{\text{test-against-grey}(L^*=50)}$) for each of 12 test field colours against the hue angles of the induction fields as listed in Table 3.15. The meanings of the size of the marks in these graph are the same as above (in Section 4.5.3.1.B), i.e., lighter induction field plotted in smaller plus. For each test colour, if markers are located above the zero line, the colour shifts towards its neighbouring hue anticlockwise, otherwise, the test colour shift towards its clockwise adjacent hue. Taking red in Figure 4.31 as an example, if markers are located above zero line, the red test colours shift towards yellow, otherwise blue. There is a clear trend that the test colour surrounded by the induction fields with two adjacent hues have the larger and smaller differences respectively, i.e., shifts largely. When red test colour in Figure 4.31 was surrounded by red-yellow and

yellow-red (the markers in R-Y area) or red-blue (the markers in B-360 area) colours, the red test colour shifted largely. These pluses are located below zero line (appeared bluer) when surrounded by red-yellow and above zero line (appeared yellower) when surrounded by red-blue. The markers located in G area (opponent hue of red) scatter a little and are close to zero line. When a test colour was surrounded by its closest adjacent colour, the hue of the test field shifted largest (the markers scatter further away from the zero line) and smallest by its opponent colour surrounding. When the red test colour in Figure 4.31 was surrounded by red-yellow and yellow-red, it shifted largely by red-yellow than by yellow-red surrounds, because red-yellow hue is closer to red. Blue colour shifted smallest among all hues. For the less colourful test patches, RRY, GGB and BBG with C^* of 20, 20 and 10 respectively, their hues shifted largely against any induction field. The reasons could be either that larger deviations occurred when observers scaling test colours close to neutral, or that there was large contrast effect for the less colourful colours.

When the size of test field from $2 \times 2 \text{ cm}^2$ is increased to $6 \times 6 \text{ cm}^2$, the hue difference of Red, Yellow, Green, and Blue test colours between two size patches are very small. There is no systematic effect on hue by changing size.

4.5.6 Testing of The Hunt Colour Appearance Model for Prediction of The Simultaneous Contrast Effect

Only the Hunt model proposed functions to predict the simultaneous contrast effect through modifying the reference white cone responses $\rho_w, \gamma_w, \beta_w$ into $\rho'_w, \gamma'_w, \beta'_w$ calculated as follows^[21]:

$$\rho'_w = \frac{\rho_w \left[(1-p) p_\rho + \frac{1+p}{p_\rho} \right]^{\frac{1}{2}}}{\left[(1+p) p_\rho + \frac{1-p}{p_\rho} \right]^{\frac{1}{2}}} \quad (4.15)$$

$$\gamma'_w = \frac{\gamma_w \left[(1-p) p_\gamma + \frac{1+p}{p_\gamma} \right]^{\frac{1}{2}}}{\left[(1+p) p_\gamma + \frac{1-p}{p_\gamma} \right]^{\frac{1}{2}}} \quad (4.16)$$

$$\beta'_w = \frac{\beta_w \left[(1-p) p_\beta + \frac{1+p}{p_\beta} \right]^{\frac{1}{2}}}{\left[(1+p) p_\beta + \frac{1-p}{p_\beta} \right]^{\frac{1}{2}}} \quad (4.17)$$

Where

$$p_p = \frac{\rho_p}{\rho_b}, \quad p_\gamma = \frac{\gamma_p}{\gamma_b}, \quad p_\beta = \frac{\beta_p}{\beta_b} \quad (4.18)$$

and $\rho_p, \gamma_p, \beta_p$ are the ρ, γ, β signals for the proximal field, i.e. the induction field, and $\rho_b, \gamma_b, \beta_b$ are those for the background. The value of p depends on the size and shape of the proximal field and will be between 0 and -1 for the simultaneous contrast as Hunt proposed as an approximation.

Table 4.25 lists the comparison between the mean visual response (Y axis) and the Hunt model's predictions (X axis) for the representative p values being 0 and -0.5 respectively. For each comparison between the visual data and model's predictions, the CV measure is again used. For model's predictions, various p values were tested to obtain the least CV values. It was found that using one particular p value, there were good fits between predictions and some hues, but not for all colours. Simultaneous contrast is too complicated to predict thoroughly. Further investigations and modifications of Hunt91 model are required on this area.

In conclusion, this experiment was carried out to investigate the effect of simultaneous contrast on the colour appearance of self-luminous colours, by varying the lightness, colourfulness, and hue of an induction field surrounding the test colour. A total

of 481 test-induction combinations were assessed by a panel of six observers using a magnitude estimation technique. In general, for most colours (with $L^* < 80$), the perceived lightness increases with decreasing of L^* values of surrounds. When a test colour is surrounded by an induction field with the identical hue but a smaller L^* than the test colour, it appears the lightest. Additionally, a white surround always causes a test colour to be the darkest. For colourfulness attribute, both lightness and hue of an induction field affect perceived colourfulness. When surrounded by an induction field with its neighbouring hue and similar L^* , a test colour appears less colourful. Darker opponent hue surround causes a test colour more colourful. Lighter achromatic surround also change a test colour less colourful. Smaller size of colour looks more colourful and darker than larger one. The contrast effect of an induction field on hue is to shift the hue of a test colour in the direction of the opponent hue of the induction field.

4.6 SUMMARY

4.6.1 Summary Results of All the Experiments

4.6.1.1 Summary of Observer Accuracy Performance

The typical observer accuracy results for the five experiments are summarised in Table 4.26 in terms of CV values. It shows that for the hue estimation, the accuracy for all experiments is the highest and similar to each other with about 6 CV units in average. This suggests that the accuracy of perceived hue is independent of media and viewing conditions. The accuracy of lightness for the reflection print medium has CV value of only 10, which is much lower than that for the monitor colours under various colour surrounds with CV of 17. Colourfulness is the least accurate attribute to estimate during the experiments. But a CV value of 17 is still considered to be reasonably accurate and acceptable. The perceived brightness is also very accurate with only 10 CV units. The mean CV values of 13, 10, 17 and 6 for lightness, brightness, colourfulness and hue respectively form a base line to evaluate the performance of colour models.

4.6.1.2 Summary of the Performance of Colour Spaces and Models

Three uniform colour spaces and two colour appearance models were tested. These are CMC(1:1), CIE $L^*a^*b^*$, CIE $L^*u^*v^*$, Nayatani, and Hunt91.

The performance of these spaces and models tested using three experimental data are summarised in Table 4.27 for lightness, brightness, chroma, colourfulness, and hue attributes using CV measure. It shows that the modified Hunt91 model performed the best with the least deviations for all the colour attributes studied. For various media, different scaling factors were employed for each space or model. These are given in Table 4.28. A clear trend can be found that most spaces and models except CIE $L^*u^*v^*$ used a larger SF for reflection colours (Experiment 4) than for transparency media (Experiments 2 and 3). In comparison with each other of the two sets of transparency data, the SFs from all spaces' and Hunt91 chroma scales are larger in Experiment 2 than

in Experiment 3. These results suggest that to achieve a colourfulness appearance match would require a slight increase in CIE metric chroma for 35-mm slide medium matching cut-sheet medium and a significant increase for transparency media matching reflection medium.

In using Hunt91 colour appearance model, scaling factors of 0.68, 0.64, and 0.75 were obtained for cut-sheet, 35mm slide transparencies and reflection media respectively.

4.6.2 Further Modifying Hunt Chroma and Colourfulness Scales

The deviation of colourfulness by Hunt91 model are much larger than that of chroma prediction as shown in Table 4.27. Further modification for colourfulness scale was made. The new chroma and colourfulness formulae are expressed by Eqs.(4.19) and (4.20):

$$\text{Colourfulness} = \text{Chroma } F_1^{0.15} \quad (4.19)$$

$$\text{Chroma} = 2.44 s^{0.69} \left(\frac{Q}{Q_w} \right)^{\frac{Y_b}{Y_w}} (1.64 - 0.29 \frac{Y_b}{Y_w}) \quad (4.20)$$

Where s is saturation, Y_b and Y_w are the luminance factors for background and reference white respectively. F_1 is the luminance level factor for the cone response.

The only difference between the old and new chroma formulae is the coefficient. The original coefficient for chroma was 4 instead of 2.44 in Eq.(4.20). When the predictions of new chroma scale are compared with the visual colourfulness data, the performance of this scale is very similar to that from the old chroma scale except the scaling factor.

The measures for the comparison between predicted colourfulness by the new formula and perceived colourfulness are tabulated in Table 4.29 for each of Experiments

2 to 4. The data show that the new colourfulness formula performed much better than the original one with much less deviations. For example, the deviation by the original colourfulness scale for Experiment 2 is 30, but only 19 by the new one. The accuracy of predictions by the chroma and new colourfulness scales is almost the same. In Experiment 2, there are 17 and 19 CV values for the chroma and new colourfulness predictions respectively. Thus in the future application, either chroma or colourfulness prediction can be employed to predict perceived colourfulness with similar precision.

For the new chroma formula expressed in Eq.(4.20), scaling factors of 1.11, 1.05, and 1.23 were obtained for cut-sheet, 35mm slide transparencies and reflection print colours.

4.7 THE REVISED HUNT COLOUR APPEARANCE MODEL

In the previous discussion, a revised Hunt91 model was derived and tested to be the best of all spaces and models studied. Followed this work, reversing of the modified model was also attempted. With this reversing form, it is possible to compute a colour from a set of visual attributes (lightness, colourfulness and hue) to obtain its corresponding tristimulus values under a given set of viewing conditions. The modified model is named Hunt93. This together with its reversing form will be supplemented in this section.

4.7.1 Comparison of Revised Hunt91 Model with NCS and Munsell Data

4.7.1.1 Constant-Hue Loci

The Hunt model defines constant hue with fixed ratios ($C_1: C_2: C_3$). This corresponds to loci of constant hue being straight lines in its "chromaticity" diagram (m_{RG} vs m_{YB} , see Section 4.7.2). When these lines are transformed to the $u'v'$ chromaticity diagram, they become curved as shown by the solid curves with marker "o" in Figure 4.35. The constant hue loci R, YR, Y, GY, G, BG, B, and BR predicted by the new Hunt model are plotted. The criteria for the unique hues are:

Unique Red:	$C_1 = C_2$.
Unique Green:	$C_1 = C_3$.
Unique Yellow:	$C_1 = C_2 / 11$.
Unique Blue:	$C_1 = C_2 / 4$.

The model is normalised for the CIE Standard Illuminant C ($x = 0.3101$, $y = 0.3162$) with factors: luminance of 500 cd/m^2 , the luminance factor of 20 for the background, $N_b = 25$, and $N_c = 1$. The hue YR is the half way between R and Y in a Red-Green against Yellow-Blue hue diagram as shown in Figure 2.11, so are the GY, BG, and BR hues.

Also shown in Figure 4.35, the dashed curves with marker "+" are the constant-hue loci of the Swedish NCS scheme. The constant hues of R, Y50R, Y, G50Y,

G, B50G, B, and R50B in the NCS scheme are plotted (The blackness for these NCS hues is 40). The close correspondence between the solid and dashed curves in Figure 4.35 indicates that two systems agree with each other quite well.

Figure 4.36 gives the comparison of the constant-hue loci predicted by modified Hunt91 model (solid curves with marker "o") and the constant-hue loci plotted using Munsell data (dashed curves with marker "+"). The Munsell constant hues are 5R, 5YR, 5Y, 5GY, 5G, 5BG, 5B, 5PB, 5P, and 5RP. The constant hues predicted by the model are the same as those in Figure 4.35. As far as the angular positions of the unique-hue loci concerned, the two systems do not agree with each other very well. Munsell 5R and 5G curves are close to the predicted red and green respectively. However Munsell 5Y is a little bit redder than the predicted yellow, and 5B is greener than the predicted blue. This difference is probably caused in part, by the division of equal apparent hue difference in five groups for the Munsell system instead of four groups used by the model.

4.7.1.2 Constant-Chroma Loci

In Figure 4.37, the dashed curves show the gird with the Munsell Chroma data for Munsell Value 5. The Munsell Chroma contours plotted are 2, 4, 6, 8, 10, and 12. Those plotted with solid curves with marker "o" are the predictions from the Hunt93 model for a series of values of chroma: 20, 40, 60, 80, 100, and 120. The model was employed with the Standard Illuminant C, luminance level of 500 cd/m^2 , the Y factor of 20 for the grey background, $N_b = 25$, and $N_c = 1$. Because Munsell Value 5 corresponds to Hunt93's lightness (J) about 43, the solid line curves in Figure 4.37 were computed with constant lightness of 43. The values of chroma were scaled by a factor of 0.75 to make the predicted chroma are in the same scale with Munsell Chroma.

Referring to the shape of both solid and dashed curves in Figure 4.37, the Munsell Chroma is quite different from those predicted by the model, especially in the blue-red area.

4.7.2 The Formulae of Forward Revised Hunt91 Model

To utilize the revised Hunt91 model requires the input of the tristimulus values of a sample and its viewing conditions to predict colour appearance attributes. The detail procedures of the forward model are given below. Its C programme is supplemented in Appendix A.

4.7.2.1 Input Data:

1. x, y, Y : colorimetric data of an object colour.
2. Viewing parameters:
 - L_w : Photopic luminance of the reference white in cd/m^2 .
 - Y_b : luminance factor of the background.
 - L_A : Photopic luminance of adapting field in cd/m^2 .

$$L_A = L_w \left(\frac{Y_b}{100} \right) \quad (4.21)$$

L_{AS} : Scotopic luminance of adapting field in cd/m^2 . If the value L_{AS} is not available, an approximation to it can be derived from L_A as

$$\frac{L_{AS}}{2.26} = L_A \left(\frac{T}{4000} - 0.4 \right)^{\frac{1}{3}} \quad (4.22)$$

Where T is the correlated colour temperature of the illuminant. For instance,

When $T=4000\text{K}$, $L_{AS}/(2.26L_A)=0.84$

When $T=5000\text{K}$, $L_{AS}/(2.26L_A)=0.95$

When $T=5600\text{K}$, $L_{AS}/(2.26L_A)=1.00$

x_w, y_w, Y_w : colorimetric data for the reference white.

N_b : Brightness induction factor.

$N_b = 75$ for normal scenes, e.g., reflection colours.

$N_b = 10$ for projected transparency in dark surrounds, such as 35mm-projected colours.

$N_b = 25$ for television and VDU displays in dim surrounds,

including cut-sheet transparency colours.

N_c : Colourfulness induction factor

$$N_c = 1.$$

x_E, y_E, Y_E : colorimetric data for equi-energy white ($Y_E=100$).

4.7.2.2 Computing procedures of the Hunt93 model

Step 1. Calculate X, Y, Z (Tristimulus values):

$$\begin{aligned} X &= xY/y \\ Y &= Y \\ Z &= (1 - x - y)Y/y \end{aligned} \quad (4.23)$$

Step 2. Calculate the cone signals ρ, γ, β :

$$\begin{aligned} \rho &= 0.38971 X + 0.68898 Y - 0.07868 Z \\ \gamma &= -0.22981 X + 1.18340 Y + 0.04641 Z \\ \beta &= 1.00000 Z \end{aligned} \quad (4.24)$$

Step 3. Calculate the cone bleach factors $B_\rho, B_\gamma, B_\beta$:

$$\begin{aligned} B_\rho &= \frac{10^7}{10^7 + 5L_A \left(\frac{\rho_w}{100} \right)} \\ B_\gamma &= \frac{10^7}{10^7 + 5L_A \left(\frac{\gamma_w}{100} \right)} \\ B_\beta &= \frac{10^7}{10^7 + 5L_A \left(\frac{\beta_w}{100} \right)} \end{aligned} \quad (4.25)$$

Where the $\rho_w, \gamma_w, \beta_w$ are the ρ, γ, β values of the reference white.

Step 4. Calculate luminance-level adaptation factor F_L :

$$F_L = 0.2 k^4 (5L_A) + 0.1 (1-k^4)^2 (5L_A)^{1/3} \quad (4.26)$$

Where

$$k = \frac{1}{5L_A + 1} \quad (4.27)$$

Step 5. Calculate Chromatic adaptation factors F_ρ , F_γ , F_β :

$$F_\rho = \frac{1 + L_A^{\frac{1}{3}} + h_\rho}{1 + L_A^{\frac{1}{3}} + \frac{1}{h_\rho}}$$

$$F_\gamma = \frac{1 + L_A^{\frac{1}{3}} + h_\gamma}{1 + L_A^{\frac{1}{3}} + \frac{1}{h_\gamma}} \quad (4.28)$$

$$F_\beta = \frac{1 + L_A^{\frac{1}{3}} + h_\beta}{1 + L_A^{\frac{1}{3}} + \frac{1}{h_\beta}}$$

Where

$$h_\rho = \frac{3\rho_w}{\rho_w + \gamma_w + \beta_w}$$

$$h_\gamma = \frac{3\gamma_w}{\rho_w + \gamma_w + \beta_w} \quad (4.29)$$

$$h_\beta = \frac{3\beta_w}{\rho_w + \gamma_w + \beta_w}$$

Step 6. Calculate the Helson-Judd coefficients $\rho_D, \gamma_D, \beta_D$:

$$\begin{aligned}\rho_D &= f_n \left[\left(\frac{Y_b}{Y_w} \right) F_L F_Y \right] - f_n \left[\left(\frac{Y_b}{Y_w} \right) F_L F_\rho \right] \\ \gamma_D &= 0 \\ \beta_D &= f_n \left[\left(\frac{Y_b}{Y_w} \right) F_L F_Y \right] - f_n \left[\left(\frac{Y_b}{Y_w} \right) F_L F_\beta \right]\end{aligned}\quad (4.30)$$

For the 35 mm projected colours

$$\rho_D = \gamma_D = \beta_D = 0.$$

Step 7. Calculate the cone response after adaptation $\rho_a, \gamma_a, \beta_a$:

$$\begin{aligned}\rho_a &= B_\rho \left[f_n \left(F_L F_\rho \frac{\rho}{\rho_w} \right) + \rho_D \right] + 1 \\ \gamma_a &= B_\gamma \left[f_n \left(F_L F_Y \frac{\gamma}{\gamma_w} \right) + \gamma_D \right] + 1 \\ \beta_a &= B_\beta \left[f_n \left(F_L F_\beta \frac{\beta}{\beta_w} \right) + \beta_D \right] + 1\end{aligned}\quad (4.31)$$

Where

$$f_n(I) = 40 \frac{I^{0.73}}{I^{0.73} + 2} \quad (4.32)$$

Step 8. Calculate colour-difference signals:

$$\begin{aligned}C_1 &= \rho_a - \gamma_a \\ C_2 &= \gamma_a - \beta_a \\ C_3 &= \beta_a - \gamma_a\end{aligned}\quad (4.33)$$

Step 9. Calculate hue angle h_s :

$$h_s = \arctan \frac{\frac{1}{9} (C_2 - C_3)}{C_1 - \frac{C_2}{11}} = \arctan \left(\frac{t}{t'} \right) \quad (4.34)$$

$0^\circ \leq h_s < 90^\circ$ when $t \geq 0, t' > 0$,
 $90^\circ < h_s < 180^\circ$ when $t > 0, t' < 0$,
 $180^\circ \leq h_s < 270^\circ$ when $t < 0, t' < 0$
 $270^\circ < h_s < 360^\circ$ when $t < 0, t' > 0$

Step 10. Calculate hue H :

$$H = H_i + \frac{100 \frac{(h_s - h_i)}{e_i}}{\frac{(h_s - h_i)}{e_i} + \frac{(h_{i+1} - h_s)}{e_{i+1}}} \quad (4.35)$$

Where

	Red	Yellow	Green	Blue	Red
i	1	2	3	4	5
H_i	0	100	200	300	400
h_i	20.14	90.0	164.25	237.53	380.14
e_i	0.8	0.7	1.0	1.2	0.8

(4.36)

Step 11. Calculate eccentricity factor e_s :

$$e_s = e_i + \frac{(e_{i+1} - e_i) (h_s - h_i)}{(h_{i+1} - h_i)} \quad (4.37)$$

Where the values of e_i and h_i are given in Eq. (4.36).

Step 12. Calculate low luminance tritanopia factor F_t :

$$F_t = \frac{L_A}{L_A + 0.1} \quad (4.38)$$

Step 13. Calculate Yellowness-Blueness response M_{YB} and Redness-Greenness response M_{RG} :

$$M_{YB} = 100 \left[\frac{(C_2 - C_3)}{9} \right] \left[e_s \frac{12}{13} N_c N_{cb} F_t \right] \quad (4.39)$$

$$M_{RG} = 100 \left[C_1 - \frac{C_2}{11} \right] \left[e_s \frac{12}{13} N_c N_{cb} \right] \quad (4.40)$$

Where

$$N_{cb} = 0.725 \left(\frac{Y_w}{Y_b} \right)^{0.2} \quad (4.41)$$

$$N_c = 1$$

Step 14. Calculate colourfulness content factor M :

$$M = (M_{YB}^2 + M_{RG}^2)^{\frac{1}{2}} \quad (4.42)$$

Step 15. Calculate relative Yellowness-Blueness m_{YB} , relative Redness-Greenness m_{RG} and Saturation s :

$$m_{YB} = \frac{M_{YB}}{\rho_a + \gamma_a + \beta_a} \quad (4.43)$$

$$m_{RG} = \frac{M_{RG}}{\rho_a + \gamma_a + \beta_a} \quad (4.44)$$

$$S = \frac{50M}{\rho_a + \gamma_a + \beta_a} \quad (4.45)$$

Step 16. Calculate scotopic luminance level adaptation factor F_{LS} :

$$F_{LS} = 3800j^2 \frac{5L_{AS}}{2.26} + 0.2(1-j^2)^4 \left(\frac{5L_{AS}}{2.26} \right)^{\frac{1}{6}} \quad (4.46)$$

Where

$$j = \frac{0.00001}{\frac{5L_{AS}}{2.26} + 0.00001} \quad (4.47)$$

Step 17. Calculate rod bleach or saturation factor B_s :

$$B_s = \frac{0.5}{1 + 0.3 \left(\frac{5L_{AS}}{2.26} \right) \left(\frac{S}{S_w} \right)^{0.3}} + \frac{0.5}{1 + 5 \left(\frac{5L_{AS}}{2.26} \right)} \quad (4.48)$$

Step 18. Calculate rod response after adaptation A_s :

$$A_s = B_s (3.05) \left[f_n \left(F_{LS} \frac{S}{S_w} \right) \right] + 0.3 \quad (4.49)$$

Where f_n is calculated by Eq. (4.32).

Step 19. Calculate photopic part of the achromatic signal A_a :

$$A_a = 2\rho_a + \gamma_a + \frac{1}{20}\beta_a - 3.05 + 1 \quad (4.50)$$

Step 20. Calculate total achromatic signal:

$$A = N_{bb} [A_a - 1 + A_b - 0.3 + (1^2 + 0.3^2)^{\frac{1}{2}}] \quad (4.51)$$

Where

$$N_{bb} = 0.725 \left(\frac{Y_w}{Y_b} \right)^{0.2} \quad (4.52)$$

Step 21. Calculate Brightness Q:

$$Q = \left[7 \left(A + \frac{M}{100} \right) \right]^{0.6} N_1 - N_2 \quad (4.53)$$

Where

$$N_1 = \frac{(7A_w)^{0.5}}{5.33N_b^{0.13}} \quad (4.54)$$

$$N_2 = \frac{7A_w N_b^{0.362}}{200} \quad (4.55)$$

and A_w is the value of A for the reference white.

Step 22. Calculate lightness J and J_{NEW} :

$$J = 100 \left(\frac{Q}{Q_w} \right)^z \quad (4.56)$$

Where Q_w is the value of brightness for the reference white and

$z = 1 + (Y_b/Y_w)^{1/2}$ for the reflection colours;

$z = 0.85$ for the cut-sheet transparency colours under darker background;

$z = 1$ for the cut-sheet transparency colours under lighter medium-grey

background;

For the 35mm projected slide colours $z = 1.2$ and

$$J_{NEW} = J \left[1.14 \left(1 - \left(\frac{J}{100} \right)^3 \right) + \left(\frac{J}{100} \right)^5 \right] \quad (4.57)$$

Step 23. Calculate Chroma c_b and Colourfulness M_c

$$c_b = 2.44 S^{0.69} \left(\frac{Q}{Q_N} \right)^{\frac{Y_b}{Y_N}} (1.64 - 0.29 \frac{Y_b}{Y_N}) \quad (4.58)$$

$$M_c = c_b F_L^{0.15} \quad (4.59)$$

Where F_L is calculated using Eq.(4.26)

Step 24. Calculate whiteness-Blackness Q_{WB} :

$$Q_{WB} = 20 (Q^{0.7} - Q_b^{0.7}) \quad (4.60)$$

Where Q_b is the value of Q for the background.

4.7.3 Reversing HUNT93 Model

From a set of appearance attributes (Hue, Chroma, and Lightness) and a fixed set of viewing conditions, the reversed model enables us to obtain this colour's tristimulus values. Appendix B gives a C program for the Reversing Hunt93 Model using the optimisation method of Hooke and Jeeves together with the golden method^[150]. The input data are lightness, chroma, and hue, the output data are x , y , Y , and X , Y , Z .

4.7.3.1 Input Data

1. H , C_b , J : Hue, chroma, and lightness of the colour stimulus.

2. Viewing parameters:

L_w : Photopic luminance of reference white in cd/m^2 .

Y_b : Luminance factor for the background.

L_A : Photopic luminance of adapting field in cd/m^2 .

$$L_A = L_w \left(\frac{Y_b}{100} \right) \quad (4.61)$$

L_{AS} : Scotopic luminance of adapting field in cd/m^2 . If the value L_{AS} is not available, an approximation to it can be derived from L_A as

$$\frac{L_{AS}}{2.26} = L_A \left(\frac{T}{4000} - 0.4 \right)^{\frac{1}{3}} \quad (4.62)$$

Where T is the correlated colour temperature of the illuminant.

For instance,

When $T = 4000 \text{ K}$, $L_{AS} / (2.26 L_A) = 0.84$

When $T = 5000 \text{ K}$, $L_{AS} / (2.26 L_A) = 0.95$

When $T = 5600 \text{ K}$, $L_{AS} / (2.26 L_A) = 1.00$

x_w , y_w , Y_w : colorimetric data for the reference white.

N_b : Brightness induction factor.

$N_b = 75$ for normal scenes.

$N_b = 10$ for projected photographs in dark surrounds

$N_b = 25$ for TV and VDU displays in dim surrounds

Nc: Colourfulness induction factor

$$Nc = 1.$$

x_E, y_E, Y_E : colorimetric data for equi-energy white ($Y_E=100$).

4.7.3.2 Calculating Procedures for Reversing Hunt93 Model

Step 1. Calculate X_w, Y_w, Z_w (Tristimulus values):

$$\begin{aligned} X_w &= x_w Y_w / y_w \\ Y_w &= Y_w \\ Z_w &= (1 - x_w - y_w) Y_w / y_w \end{aligned} \quad (4.63)$$

Step 2. Calculate r_w, g_w, b_w for reference white, and r_E, g_E, b_E for the equi-energy white.

$$\begin{aligned} \rho_w &= 0.38971 X_w + 0.68898 Y_w - 0.07868 Z_w \\ \gamma_w &= -0.22981 X_w + 1.18340 Y_w + 0.04641 Z_w \\ \beta_w &= 1.00000 Z_w \end{aligned} \quad (4.64)$$

Similarly ρ_E, γ_E and β_E are calculated by using X_E, Y_E , and Z_E .

Step 3. Calculate the cone bleach factors $B_\rho, B_\gamma, B_\beta$:

$$\begin{aligned} B_\rho &= \frac{10^7}{10^7 + 5L_A \left(\frac{\rho_w}{100} \right)} \\ B_\gamma &= \frac{10^7}{10^7 + 5L_A \left(\frac{\gamma_w}{100} \right)} \\ B_\beta &= \frac{10^7}{10^7 + 5L_A \left(\frac{\beta_w}{100} \right)} \end{aligned} \quad (4.65)$$

Step 4. Calculate luminance-level adaptation factor F_L :

$$FL = 0.2 k^4 (5L_A) + 0.1 (1-k^4)^2 (5L_A)^{1/3} \quad (4.66)$$

Where

$$k = \frac{1}{5L_A + 1} \quad (4.67)$$

Step 5. Calculate Chromatic adaptation factors F_p , F_y , F_β :

$$F_p = \frac{1 + L_A^{\frac{1}{3}} + h_p}{1 + L_A^{\frac{1}{3}} + \frac{1}{h_p}}$$

$$F_y = \frac{1 + L_A^{\frac{1}{3}} + h_y}{1 + L_A^{\frac{1}{3}} + \frac{1}{h_y}} \quad (4.68)$$

$$F_\beta = \frac{1 + L_A^{\frac{1}{3}} + h_\beta}{1 + L_A^{\frac{1}{3}} + \frac{1}{h_\beta}}$$

Where

$$h_p = \frac{3\rho_w}{\rho_w + \gamma_w + \beta_w}$$

$$h_y = \frac{3\gamma_w}{\rho_w + \gamma_w + \beta_w} \quad (4.69)$$

$$h_\beta = \frac{3\beta_w}{\rho_w + \gamma_w + \beta_w}$$

Step 6. Discounting the Helson-Judd coefficients ρ_D , γ_D , β_D :

$$\rho_D = f_n \left[\left(\frac{Y_b}{Y_w} \right) F_L F_\gamma \right] - f_n \left[\left(\frac{Y_b}{Y_w} \right) F_L F_\rho \right]$$

$$\gamma_D = 0 \quad (4.70)$$

$$\beta_D = f_n \left[\left(\frac{Y_b}{Y_w} \right) F_L F_\gamma \right] - f_n \left[\left(\frac{Y_b}{Y_w} \right) F_L F_\beta \right]$$

For the 35 mm projected slide

$$\rho_D = \gamma_D = \beta_D = 0.$$

Step 7. From hue H to calculate h_s and e_s :

$$h_s = \frac{(H - H_i) (h_i e_{i+1} - h_{i+1} e_i) - 100 h_i e_{i+1}}{(H - H_i) (e_{i+1} - e_i) - 100 e_{i+1}} \quad (4.71)$$

$$e_s = e_i + \frac{(e_{i+1} - e_i) (h_s - h_i)}{h_{i+1} - h_i} \quad (4.72)$$

Where H_i , h_i and e_i values are given in Eq.(4.36).

Step 8. Calculate A_w , Q_w :

$$A_w = N_{bb} [A_{aw} - 1 + A_{sw} - 0.3 + 1.09^{1/2}] \quad (4.73)$$

$$Q_w = \left[7 \left(A_w + \frac{M_w}{100} \right) \right]^{0.6} N_1 - N_2 \quad (4.74)$$

Where A_{aw} , A_{sw} and M_w are the values of A_a , A_s , and M for the reference white and can be obtained by Eqs.(4.50), (4.49) and (4.42) respectively. N_{bb} can be obtained from Eq.(4.52).

Step 9. From lightness J to calculate brightness Q :

$$Q = \left(\frac{J}{100} \right)^{\frac{1}{2}} Q_w \quad (4.75)$$

Where z is calculated according to the step 22 in section 4.7.2.2. If the colour is slide medium, the J can be obtained through iteration method using Eq. (4.57) by input J_{new} .

Step 10. From chroma c_b to calculate saturation s :

$$s = \left[\frac{c_b}{2.44 \left(\frac{Q}{Q_w} \right)^{\frac{Y_w}{Y_b}} (1.64 - 0.29 \frac{Y_w}{Y_b})} \right]^{\frac{1}{0.69}} \quad (4.76)$$

Step 11. Express following formula as functions of Y .

From Eqs.(4.48) and Eq.(4.49), B_s and A_s can be got:

$$B_s = \frac{0.5}{1 + 0.3 \left[\left(\frac{5L_{AS}}{2.26} \right) \left(\frac{Y}{Y_w} \right) \right]^{0.3}} + \frac{0.5}{1 + 5 \left(\frac{5L_{AS}}{2.26} \right)} \quad (4.77)$$

$$A_s = B_s (3.05) \left[f_n \left(F_{LS} \frac{Y}{Y_w} \right) \right] + 0.3 \quad (4.78)$$

Where f_n is the function using Eq.(4.32), and Y/Y_w is the approximation of S/S_w

Step 12. Preliminary discussion for an iterative procedure towards the optimisation of Y value.

Let

$$\begin{aligned} C_{12} &= C_1 - C_2/11 \\ C_{23} &= (C_2 - C_3)/9 \end{aligned} \quad (4.79)$$

Then

$$C_1 = \frac{22C_{12} + 9C_{23}}{23}$$

$$C_2 = 11 \frac{9C_{23} - C_{12}}{23} \quad (4.80)$$

$$C_3 = \frac{-108C_{23} + 11C_{12}}{23}$$

From Eq.(4.34),

$$\operatorname{tg}(h_s) = C_{23}/C_{12} \quad (4.81)$$

From Eqs.(4.39) to (4.42), (4.79) and (4.81),

$$\frac{M}{100} = e_s \frac{12}{13} N_c N_{cd} |C_{12}| \sqrt{1 + F_t^2 \operatorname{tg}^2(h_s)} \quad (4.82)$$

From Eq.(4.45),

$$\frac{M}{100} = \frac{s(p_a + \gamma_a + \beta_a)}{50 \cdot 100} \quad (4.83)$$

Therefore from above two equations

$$\begin{aligned} \frac{s(p_a + \gamma_a + \beta_a)}{50 \cdot 100} &= e_s \frac{10}{13} N_c N_{cb} \sqrt{1 + F_t^2 \operatorname{tg}^2(h_s)} |C_{12}| \\ &= k_1 |C_{12}| \quad (4.84) \end{aligned}$$

Where let

$$k_1 = e_s \frac{10}{13} N_c N_{cb} \sqrt{1 + F_t^2 \operatorname{tg}^2(h_s)} \quad (4.85)$$

From Eq.(4.53) and above:

$$A = \frac{\left(\frac{Q+N_2}{N_1}\right)^{\frac{1}{0.6}}}{7} - \frac{M}{100} = \frac{\left(\frac{Q+N_2}{N_1}\right)^{\frac{1}{0.6}}}{7} - K_1 |C_{12}| \quad (4.86)$$

From Eq.(4.51)

$$A = N_{bb} [A_a - 1 + A_s - 0.3 + (1^2 + 0.3^2)^{1/2}]$$

Therefore, from above two equations:

$$\frac{(\frac{Q+N_2}{N_1})^{\frac{1}{0.6}}}{7} - K_1 |C_{12}| = N_{bb} [A_a - 1 + A_s - 0.3 + (1^2 + 0.3^2)^{\frac{1}{2}}]$$

$$==> \quad A_a = - K_1 |C_{12}| / N_{bb} + K_2 \quad (4.87)$$

Where

$$K_2 = \frac{(\frac{Q+N_2}{N_1})^{\frac{1}{0.6}}}{7 N_{bb}} + 1 - A_s + 0.3 - (1^2 + 0.3^2)^{\frac{1}{2}} \quad (4.88)$$

From Eqs.(4.83) and (4.33),

$$s (C_1 + 2 C_2 + 3 \beta_a) = 5000 K_1 |C_{12}| \quad (4.89)$$

From Eqs.(4.50) and (4.33):

$$\begin{aligned} A_a &= 2\rho_a + \gamma_a + 1/20 \beta_a - 3.05 + 1 \\ &= 2C_1 + 3C_2 - 2.05 + 61/20 \beta_a \end{aligned} \quad (4.90)$$

==>

$$\beta_a = (A_a + 2.05 - 2C_1 - 3C_2) 20/61 \quad (4.91)$$

Put Eq.(4.91) into Eq.(4.89):

$$C_1 + 2C_2 + 60/61 (A_a + 2.05 - 2C_1 - 3C_2) = 5000K_1/s |C_{12}| \quad (4.92)$$

==>

$$-\frac{59}{61} C_1 - \frac{58}{61} C_2 + \frac{60}{61} 2.05 + \frac{60}{61} A_a = \frac{5000K_1}{s} |C_{12}| \quad (4.93)$$

Put Eqs.(4.80) , (4.81) and (4.87) into Eq.(4.93):

$$C_{12} [-\frac{59}{61} (\frac{22+9 \operatorname{tg}(h_s)}{23}) - \frac{58}{61} (\frac{11.9 \operatorname{tg}(h_s) - 11}{23})] =$$

$$\frac{5000K_1}{s}|C_{12}| - \frac{60}{61} \left(K_2 - \frac{K_1}{N_{bb}}|C_{12}| \right) - \frac{60}{61} 2.05 \quad (4.94)$$

==>

$$C_{12} = \frac{60K_1 + 60 \cdot 2.05}{K_3} \quad (4.95)$$

Where when $90 < h_s < 270$ then $C_{12} < 0$, therefore

$$K_3 = 59 [22 + 9 \operatorname{tg}(h_s)] + 58 [11.9 \operatorname{tg}(h_s) - 11] - \left(\frac{61 \cdot 5000}{s} K_1 + 60 K_1 \right) \quad (4.96)$$

otherwise

$$K_3 = 59 [22 + 9 \operatorname{tg}(h_s)] + 58 [11.9 \operatorname{tg}(h_s) - 11] + \left(\frac{61 \cdot 5000}{s} K_1 + 60 K_1 \right) \quad (4.97)$$

Step 13. Iterative procedure to get Y.

- (1). From Eqs. (4.85), (4.88), and (4.96) calculates K_1 , K_2 , and K_3 .
- (2). From Eq. (4.95) to get C_{12} .
- (3). Form Eq.(4.81)

$$C_{23} = C_{12} \operatorname{tg}(h_s) \quad (4.98)$$

- (4). From Eq.(4.79)

$$C_1 = \frac{22C_{12} + 9C_{23}}{23}$$

$$C_2 = 11 \frac{9C_{23} - C_{12}}{23} \quad (4.99)$$

$$C_3 = \frac{-108C_{23} + 11C_{12}}{23}$$

(5). From Eq.(4.86)

$$A = \frac{1}{7} \left(\frac{Q + N_2}{N_1} \right)^{\frac{1}{0.6}} - K_1 |C_{12}| \quad (4.100)$$

(6). From Eq.(4.51)

$$A_a = A / N_{bb} + 1 + 0.3 - (1^2 + 0.3^2)^{1/2} - A_s \quad (4.101)$$

(7). From Eq.(4.91)

$$\beta_a = (A_a + 2.05 - 2C_1 - 3C_2) 20/61 \quad (4.102)$$

From Eq.(4.33)

$$\gamma_a = C_2 + \beta_a \quad (4.103)$$

$$\rho_a = C_1 + \gamma_a \quad (4.104)$$

$$\text{if any of } \frac{\rho_a^{-1}}{B_\rho} - \rho_D, \frac{\gamma_a^{-1}}{B_\gamma} - \gamma_D, \frac{\beta_a^{-1}}{B_\beta} - \beta_D < 0, \text{ then}$$

let $C_{12} = -C_{12}$, $C_{23} = -C_{23}$ (because from Eq. (4.33) $C_1 + C_2 + C_3 = 0$ then $-C_1 - C_2 - C_3 = 0$) and go back to Step 13(1).

Step 14. From Eq.(4.31)

$$\rho = \frac{f_n^{-1} \left[\frac{\rho_a^{-1}}{B_\rho} - \rho_D \right]}{F_L F_\rho} \rho_w$$

$$\gamma = \frac{f_n^{-1} \left[\frac{\gamma_a^{-1}}{B_\gamma} - \gamma_D \right]}{F_L F_\gamma} \gamma_w \quad (4.105)$$

$$\beta = \frac{f_n^{-1} \left[\frac{\beta_a^{-1}}{B_\beta} - \beta_D \right]}{F_L F_\beta} \beta_w$$

Where

$$f_n^{-1}(I) = \left(\frac{2I}{40-I} \right)^{\frac{1}{0.73}} \quad (4.106)$$

and $I \neq 40$ and $2I/(40-I) > 0$.

Step 15. From Eq.(4.24)

$$Y_{NEW} = [(\gamma - 0.04641 \beta) 0.38971 + (\rho - 0.07868 \beta) 0.22981] / P \quad (4.107)$$

Where

$$P = 0.38971 \times 1.18340 + 0.68898 \times 0.22981 \quad (4.108)$$

Using a proper optimisation method can solve the Y value from steps 11, 13 to 15 to make

$$|Y - Y_{NEW}| < \epsilon \quad (4.109)$$

Where Y is a given value in Step 11, ϵ can be any given error limit.

Step 16. Final result from Eq.(4.24):

$$\begin{aligned} X &= [(\rho - 0.07868 \beta) 1.18340 - (\gamma - 0.04641 \beta) 0.68898] / P \\ Y &= [(\gamma - 0.04641 \beta) 0.38971 + (\rho - 0.07868 \beta) 0.22981] / P \\ Z &= 1.0000 \beta \end{aligned} \quad (4.110)$$

Where P is given in Eq.(4.108)

4.7.3.3 Testing a Reverse Hunt93 Model

A C program given in Appendix B illustrates the reversed Hunt model which uses

the Hooke and Jeeves' optimisation method together with the Golden method^[150]. The testing data used is the Munsell database^[29] including 2713 colours. The viewing source applied was standard illuminant C varied with luminance levels of 500, 40, and 2 cd/m², and the reflectance factor of background of 100%, 20%, and 2%. The testing procedure is described as follows:

- (1). Input the Munsell database with x , y , Y to the forward Hunt model as given in Appendix A and calculate the lightness, chroma, and hue predictions.
- (2). Input the lightness, chroma, and hue obtained from (1) to the reverse Hunt model as given in Appendix B to obtain x' , y' , Y' .
- (3). Calculate the colour difference (ΔE) between x , y , Y and x' , y' , Y' .

The difference between two groups of x , y , Y is expressed by mean difference of x , y , Y together with CIE LAB, CIE LUV, and CMC(1:1). All these data are tabulated in Table 4.30. The results show that this reverse Hunt model works very satisfactorily with average CIELAB, CIELUV, and CMC(1:1) colour differences less than 0.1. In addition, the optimisation method used in the software is suitable to derive the reverse Hunt model.

5. CONCLUSIONS

Modelling of colour appearance was attempted based on the investigations on the effects of four types of media and various viewing conditions on colour appearance. The results obtained can be summarised below:-

(1) Colour appearance is affected by adapting luminance levels. In the case of luminance less than 200 cd/m^2 , most reflection samples appear lighter, brighter and more colourful as luminance level increases. When luminance is increased from the lowest (325 cd/m^2) to the highest (2259 cd/m^2) levels, cut-sheet transparencies with lighter background increases their perceived colourfulness and appear lighter for dark colours under the highest luminance levels. Projected slides appear more colourful as luminance increases.

(2) Colour appearance is also affected by side flare light, background and borders. For cut-sheet transparency media, colours appear lighter and more colourful either when a side flare light is used, or under darker backgrounds. A black border causes colours to be lighter than a white border does. Neither the spatial arrangement of viewing pattern nor the changes of illuminants from 5600K to 4000K influence colour appearance of projected colours. The changes of viewing conditions give little effect on perceived hue for these three types of media.

(3) Simultaneous contrast effect was obtained using monitor displays. Most monitor colours appear lighter when surrounded by darker induction fields. The perceived colourfulness of a test patch decreases when surrounded by an induction field with similar hue and L^* , and increases with an opponent hue. Both lighter opponent hue induction field and lighter achromatic surround can cause a test colour less colourful. The effect of an induction field on hue of a test colour is to shift the hue of the test colour in the direction of the opponent hue of the induction field. Closer adjacent hue surrounding largely shifts the hue of a test colour.

(4) Three colour spaces of CIELAB, CIELUV, CMC and two colour appearance models of the Nayatani and Hunt91 were tested using the visual data obtained in this study. For

the reflection samples, the Hunt91 lightness scale performs the best. The predictions from the Hunt91 is close to the average observer's estimation. The two colour appearance models give similar and accurate predictions in brightness. The accuracy of the predictions of Hunt91 chroma scale is the highest for the cut-sheet transparency and reflection colours. Scaling factors of 0.68, 0.64 and 0.75 were found for this scale to predict cut-sheet, projected slide transparencies, and reflection samples respectively. Colourfulness scale of both models does not performs better than their chroma scales. The Hunt91 model give better hue predictions than the Nayatani model.

(5) In modification of the Hunt91 model, a new lightness scale was developed and the Helson-Judd effect was removed. This results in the best fit to the visual data of projected slides. By using the factor z with 1 and 0.85 for lighter and darker background respectively, lightness prediction for cut-sheet films was considerably improved. A new colourfulness scale was also developed. In the new chroma scale, scaling factors of 1.11, 1.05 and 1.23 are well suitable for cut-sheet film, projected slide, and reflection colours respectively.

(6) Considerable improvement in prediction was obtained using the modified Hunt91 model (Hunt93). The model predicts visual data with CV values of 12, 11, 18 and 8 for lightness, brightness, colourfulness and hue respectively.

6. RECOMMENDATIONS FOR FUTURE WORK

In this thesis, Hunt91 colour appearance model was tested and modified into Hunt93 model. From the discussion of section 4.6, it can be recommended that Hunt93 model predicts colour appearance as accurate as average observer's responses. In the future work, Hunt93 model can be applied to the colour industry where colour appearance will be take into account.

6.1 Application of Hunt Colour Appearance Model to the Colour Communication System

Many manufactures have produced large volumes of standard merchandise to satisfy customer requirements for quick response and a wide choice of fashionable goods. A lot of Computer-Aided Design (CAD) systems have been developed to support this goal and are improving efficiency in making design proofing and reducing lead time from design to product. However, these systems suffer the common problem of poor colour fidelity between dissimilar media, e.g. the mismatch between the colours on screen and those on paper, or between the colours printed on the mail-order catalogue and those on garment. The future work should develop a demonstrator that not only supports multiple individuals working together with computer systems but also preserves high colour fidelity between different systems and the media by means of Hunt93 colour appearance model .

6.2 Applications to the Textile Industry

It is well known that same recipe will produce different colour appearance when it is employed to different substrates. If the same colour is required for different substrates materials, Hunt93 colour appearance model should be applied together with Ink Recipe Prediction Formula (work package 4 in this project) to give different recipes for different substrates.

7. REFERENCES

- [1]. Bartleson, C.J., **On Chromatic Adaptation and Persistence**, *Color Res. Appl.*, **6**, 153-160, 1981.
- [2]. Billmeyer, F.W.Jr., Saltzman, M., **Principles of Color Technology**, 2nd ed, John Wiley & Sons, New York, 1981.
- [3]. Judd, D.B., **Color Appearance**, *Die Farbe*, **14**, 2-26, 1965.
- [4]. Pointer, M.R., **Progress Towards Measuring Colour Reproduction**, In AIC COLOR 89, 166-168, Buenos Aires, Argentina, 1989.
- [5]. Billmeyer, F.W.Jr., **Quantifying Color Appearance Visually and Instrumentally**, *Color Res. Appl.* **12**, 140-145, 1988.
- [6]. Young, T., **On the Theory of Light and Colours**, *Phil. Roy. Soc., London*, **92**, 12, 1802.
- [7]. Helmholtz, H.V., **Handbook of Physiological Optics**, Vol.II, Ed., Southall, J.P.C., Optical Society of American, New York, 1924.
- [8]. Wright, W.D., **The Measurement of Colour**, 96-118, 3rd ed, Hilger & Watts Ltd, London, 1964.
- [9]. Bartleson, C.J., **Changes in Color Appearance with Changes in Adaptation**, *Color Res. Appl.*, **4**, 119-138, 1979.
- [10]. Bartleson, C.J., **Factor Affecting Colour Appearance and Measurement by Psychophysical Methods**, Ph.D. Thesis, The City University, London, 1977.
- [11]. Pointer, M.R., **The Concept of Colourfulness and Its Use for Deriving Grids for**

-
- Assessing Colour Appearance, *Color Res. Appl.*, 5, 99-107, 1980.**
- [12]. Pointer, M.R., Ensell, J.S., & Bullock, L.M., **Grids for Assessing Colour Appearance, *Color Res. Appl.*, 2, 131-136, 1977.**
- [13]. Troscianko, T.S., **Factor Affecting Colour Saturation, PhD Thesis, The City University, London, 1978.**
- [14]. Troscianko, T.S., **Analysis of Colour Scaling Data, *Colour Res. Appl.*, 4, 225-228, 1979.**
- [15]. Hunt, R.W.G., **Problems in Colour Reproduction, *Colour* 73, 53-76, Billing, 1973.**
- [16]. Hunt, R.W.G., **Measuring Colour, John Wiley & Sons, New York, 1987.**
- [17]. Hunt, R.W.G., **The Specification of Colour Appearance. I. Concepts and Terms, *Color Res. Appl.* 2, 55, 1977.**
- [18]. Hunt, R.W.G., **The Specification of Colour Appearance. II. Effects of Changes in Viewing Conditions, *Color Res. Appl.* 2, 109-120, 1977.**
- [19]. Hunt, R.W.G., **A Model of Colour Vision for Predicting Colour Appearance, *Color Res. Appl.* 7, 95-112, 1982.**
- [20]. Hunt, R.W.G., **A Model of Colour Vision for Predicting Colour Appearance In Various Viewing Conditions, *Color Res. Appl.* 12, 297-314, 1987.**
- [21]. Hunt, R.W.G., **A Revised Colour Appearance Model for Related and Unrelated Colours, *Color Res. Appl.*, 16, 146-165, 1991.**
- [22]. Nayatani, Y., Takahama, K., & Sobagaki, H., **Prediction of Colour Appearance under Various Adapting Conditions, *Color Res. Appl.*, 11, 62-71, 1986.**
-

-
- [23]. Nayatani, Y., Takahama, K., Sobagaki, H., A Non-linear Color-Appearance Model Using Estevez-Hunt-Pointer primaries, *Color Res. Appl.* 12, 231-242, 1987.
- [24]. Nayatani, Y., Umemura, Y., Hashimoto, K., Takahama, K., Sobagaki, H., Analysing the Natural Color System's Color-Order System by Using a Nonlinear Color-Appearance Model, *Color. Res. Appl.* 14, 59-63, 1989.
- [25]. Nayatani, Y., Takahama, K., Sobagaki, H., Hashimoto, K., Color-Appearance Model and Chromatic-Adaptation Transform, *Color Res. Appl.*, 15, 210-221, 1990.
- [26]. Nayatani, Y., Color Appearance and Its Application to Illuminating Engineering, CIE Proceedings 22nd Session Melbourne 1991, 1, 73-82, Australia, 1991.
- [27]. Shevell, S.K., Wesner, M.F., Color Appearance under Conditions of Chromatic Adaptation and Contrast, *Color Res. Appl.* 14, 309-317, 1989.
- [28]. Burnham, R.W., Hanes, R.M., Bartleson, C.J., *Color: A Guide to Basic Facts and Concepts*, John Wiley & Sons, New York, 1963.
- [29]. Wyszecki, G. & Stiles, W.S., *Color Science, Concept and Methods, Quantitative Data and Formulas*, John Wiley & Sons, New York, 1967.
- [30]. Robertson, A.R., The Future of color Science, *Color. Res. Appl.* 7, 16-18, 1982.
- [31]. Judd, D.B., *Color in Business, Science, and Industry*, John Wiley & Sons, New York, 1975.
- [32]. Taylor, F.A., *Colour Technology*, Oxford University Press, 1962.
- [33]. Bouma, P.J. *Physical Aspects of Colour*, 2nd edition, W. De Groot, A.A., Kruithof, and J.L., Ouweltjes, editors, Macmillan, New York, 1971.
-

- [34]. Newton, Sir Isaac, **Optiks**, 4th ed, London, Bell, 1952.
- [35]. Judd, D.B., David, L.M., & Wyszecki, G., **Spectral Distribution of Typical Daylight As a Function of Correlated Color Temperature**, *J. Opt. Soc. Am.*, **54**, 1031-1040 & 1382, 1964.
- [36]. Hering, E., **Outline of a Theory of The Light Source**, Translated by Hurvich, L. & Janeson, D., Harvard University Press, Massachusetts, 1964.
- [37]. Muller, G.E., **Ueber die Farbenempfindungen**, *Z. Psychol., Ergänzungsbaude* 17 and 18, 1930.
- [38]. Guild, J., **The Colorimetric Properties of the Spectrum**, *Phil. Trans. Royal Society, A*, **230**, 149, 1931.
- [39]. Wright, W.D., **A Re-determination of the Trichromatic Coefficients of the Spectral Colours**, *Trans. Optical Society*, **30**, 141, 1928-1929.
- [40]. Optical Society of America, Committee on Colorimetry, **The Science of Color**, T.Y. Crowell Co., Reprinted by the Optical Society of America, New York, 1963.
- [41]. CIE Publication No. 17, **International Lighting Vocabulary**, Commission Internationale de l'Eclairage, Paris, 1970.
- [42]. Evans, R.M., **Variables of Perceived Color**, *J. Opt. Soc. Am.*, **54**, 1467-1474, 1964.
- [43]. Wyszecki, G., **Current Developments in Colorimetry**, in *Colour* 73, 21-50, Adam Hilger, London, 1973.
- [44]. Wright, W.D., **The Historical and Experimental Background to the 1931 CIE System of Colorimetry**, In *Golden Jubilee of COLOUR in the CIE*, Bradford, SDC, England, 1981.

- [45]. International Commission on Illumination, **Colorimetry: Official Recommendations of the International Commission on Illumination**, Publication CIE no. 15, Bureau Central de la CIE, Paris, 1971.
- [46]. Hunter, R.S., & Harold, R.W., **The Measurement of Appearance**, 2nd ed, John Wiley & Sons, New York, 1987.
- [47]. Henderson, S.T., **Daylight and Its Spectrum**, Adam Hilger Ltd., London, 1970.
- [48]. Jacobson, A.E., **Non-Adaptability of the ICI System to Some Near-White which Show Absorption in the Far Blue Region of the Spectrum**, *J. Opt. Soc. Am.*, **38**, 442-444, 1948.
- [49]. Stiles, W.S. and Burch, J.M., **NPL Colour-matching Investigation: Final Report (1958)**, *Opt. Acta*, **6**, 1, 1959.
- [50]. Speranskaya, N.I., **Determination of Spectrum Colour Coordinates for Twenty-Seven normal Observers**, *Optical Spectroscopy*, **7**, 424-428, 1959.
- [51]. International Commission on Illumination, **Recommendations on Uniform Colour Spaces, Colour Difference Equations, and Psychometric Terms**, CIE Supplement no 2 to Publication CIE no. 15, Bureau Central de la CIE, Paris, 1978.
- [52]. International Commission on Illumination, **Colorimetry**, Publication CIE no. 15.2, 2nd ed, 1986.
- [53]. Luo, M. R. and Rigg, B., **Uniform Colour Space Based on The CMC (l:c) Colour-difference Formula**, *J. Soc. Dyers Colour.*, **102**, 164-171, 1989.
- [54]. Luo, M. R. and Rigg, B., **BFD (l:c) Colour-difference Formula, Part II: Performance of the Formula**, *J. Soc. Dyers Colour.*, **103**, 126-132, 1987.

- [55]. Alman, D. H., Berns, R. S., Snyder, G. D. and Larsen, W. A., **Performance Testing of Colour-difference Matrix Using a Colour Tolerance Data Set**, *Color Res. Appl.*, **14**, 139-151, 1989.
- [56]. Robertson, A.R., **Colour Order Systems: An Introductory Review**, *Color Res. Appl.*, **9**, 234-240, 1984.
- [57]. Nickerson, D., **History of the Munsell Color System and Its Scientific Application**, *J. Opt. Soc. Am.*, **30**, 575-586, 1942.
- [58]. Kelly, K.L., Gibson, K.S., & Nickerson, D., **Tristimulus Specification of the Munsell Book of Color from Spectrophotometric Measurements**, *J. Opt. Soc. Am.*, **33**, 355-376, 1942.
- [59]. Billmeyer, F.W., Jr., **Survey of Color Order Systems**, *Color Res. Appl.*, **12**, 173-186, 1987.
- [60]. **Munsell Book of Color**, Munsell Color Corporation, Maryland, 1929 to date.
- [61]. Hard, A. & Sivik, L., **NCS - Natural Colour System: A Swedish Standard for Colour Notation**, *Color Res. Appl.*, **6**, 129-138, 1981.
- [62]. Tonnquist, G., **Comparison between CIE and NCS Colour Spaces**, FOA Report No. 30032-EI, Forsvarets Forskningsanstalt, Stockholm, 1975.
- [63]. NCS, **NCS Colour Atlas**, 2nd ed, Stockholm, Sweden, 1989.
- [64]. Nickerson, D., **History of the OSA Committee on Uniform Color Scales**, *Opt. News*, **3**(1), 8-17, 1977.
- [65]. Bartleson, C.J., **A Review of Chromatic Adaptation**, in Fred W. Billmeyer, Jr., and G. Wyszecki, editors, *AIC Color 77*, Adam Hilger, Bristol, 63-96, 1978.

-
- [66]. Hunt, R.W.G., **Light and Dark Adaptation and the Perception of Color**, *J. Opt. Soc. Am.*, **42**, 190-199, 1952.
- [67]. Von Kries, J., **Influence of Adaptation on the Effect Produced by Luminous Stimuli**, in D.L.MacAdam ed. *Sources of Color Science*, the MIT Press, England, 1970.
- [68]. Valeton, J.W., **Photoreceptor Light Adaptation Models: An Evaluation**, *Vision Res.*, **23**, 1549-1554, 1983.
- [69]. Helson, H, Judd, D.B., & Warren, M.H., **Object-Color Changes From Daylight to Incandescent Filament Illumination**, *Illum. Engin.*, **47**, 221-233, 1952.
- [70]. Burnham, R.W., **Predictions of Shift in Color Appearance with a Change from Daylight to Tungsten Adaptation**, *J. Opt. Soc. Am.*, **49**, 254-263, 1959.
- [71]. Burnham, R.W., Evens, R.M., & Newhall, S.M., **Influence on Color Perception of Adaption to Illumination**, *J. Opt. Sci. Am.*, **42**, 597-605, 1952.
- [72]. Fairchild, M.D, **Formulation and Testing of an Incomplete Chromatic Adaptation Model**, *Color Res. Appl.*, **16**, 243-250, 1991.
- [73]. Bartleson, C.J., **Predicting Corresponding Colors with Changes in Adaptation**, *Color Res. Appl.*, **4**, 143-155, 1979.
- [74]. Nayatani, Y., Takahama, K., Sobagaki, H., **Formulation of a Non-linear Model of Chromatic Adaptation**, *Color Res. Appl.* **6**, 161-171, 1981.
- [75]. Nayatani, Y., Takahama, K., Sobagaki, H., Hirono, H., **On Exponents of a Nonlinear Model of Chromatic Adaptation**, *Color Res. Appl.* **7**, 34-45, 1982.
- [76]. Takahama, K., Sobagaki, H., Nayatani, Y., **Formulation of a Nonlinear Model of**
-

-
- Chromatic Adaptation for a Light-Gray Background, *Color Res. Appl.* 9, 106-115, 1984.**
- [77]. Bartleson, C.J. **Comparison of Chromatic-Adaptation Transforms, *Color Res. Appl.*, 3, 129-136, 1978.**
- [78]. Richter, K., **Das Auge Als Farbreizempfänger, Rep. LSSN 0431-5343, Forschung Und Entwicklung in der BAM, Bundesanstalt für Materialprüfung, Berlin, 1976.**
- [79]. Takahama, K., Sobagaki, H, and Nayatani, Y., **Analysis of Chroma-adaptation Effect by A Linkage Model, *J. Opt. Soc. Am.*, 67, 651-656, 1977.**
- [80]. Burnham, R. W., Evans, R. M. and Newhall, S. m., **Prediction of Color Appearance with Different Adaptation Illuminations, *J. Opt. Soc. Am.*, 47, 35-42, 1975.**
- [81]. MacAdam, D. L., **Chromatic Adaptation II: Non-linear Hypothesis, *J. Opt. Soc. Am.* 53, 1441-1445, 1963.**
- [82]. Von Kries, J.A., **Chromatic Adaptation, in Sources of Color, D.L MacAdam ed., The MIT Press, England, 1970.**
- [83]. Mori, L., Sobagaki, H., Komatsubara, H., Ikeda, K., **Field Trials on CIE Chromatic Adaptation Formula, CIE Proceedings 22nd Session Melbourne 1991, 1, 55-58, Australia, 1991.**
- [84]. Hunt, R.W.G., **The Effects of Daylight and Tungsten Light-Adaptation on Color Perception, *J. Opt. Soc. Am.*, 40, 362-371, 1950.**
- [85]. Pearson, D.E., Rubinstein, C.B., and Spivack, G.J., **Comparison of Perceived Color in Two-Primary Computer-Generated Artificial Images with Prediction Based on the Helson-Judd Formulation, *J. Opt. Soc. Am.*, 59, 644-658, 1969.**
-

- [86]. Helson, H., **Fundamental Problems in Colour Vision I: The Principle Governing Changes in Hue, Saturation and Lightness of Non-Selective Samples in Chromatic Illumination**, *J. Exp. Psychol.* **23**, 439-476, 1938
- [87]. Judd, D. B., **Hue, Saturation , And Lightness of Surface Color with Chromatic Illumination**, *J. Res. NBS* **24**, 293-333, 1940.
J. Opt. Soc. Amer. **30**, 2-32, 1940.
- [88]. Stevens, S.S., **To Honour Fechner and Repeat His Laws**, *Science*, **133**, 80-86, 1961.
- [89]. Stevens, J.C., & Stevens, S.S., **Brightness Function: Effect of Adaptation**, *J. Opt. Soc. Am.*, **53**, 375-385, 1963.
- [90]. Gerritsen, F., **Theory and Praticce of Color**, Studio Vista, London, 1975.
- [91]. Takasaki, H., **Lightness Change of Greys Induced by Change in Reflectance of Grey Background**, *J. Opt. Soc. Am.*, **56**, 504-506, 1966.
- [92]. Takasaki, H., **Von-Kries Coefficient Law Applied to Subjective Color Change Induced by Background Color**, *J. Opt. Soc. Am.*, **59**, 1370-1376, 1969.
- [93]. Evans, R., **An Introduction to Color**, John Wiley & Sons, New York, Plate XI, 1948.
- [94]. Jameson, D., and Hurvich, L.M., **Theory of Brightness and Color Contrast in Human Vision**, *Vision Res.*, **4**, 135-154, 1964.
- [95]. Blackwell, K.T., and Buchsbaum, G., **The Effect of Spatial and Chromatic Parameters on Chromatic Induction**, *Colour Res. & Appl.*, **13**, 166-173, 1988.
- [96]. Walraven, J., **Discounting the Background ---- The Missing Link in the Explanation of Chromatic Induction**, *Vision Res.*, **16**, 289-295, 1976.

-
- [97]. Kirschmann, A., **Über Die Quantitative Verhältnisse Des Simultanen Helligkeits-und Farben-Contrastes**, Psychol, Stud. (Wundt), 6, 417-491, 1890.
- [98]. Kinney, Jo Ann S., **Factors Affecting Induced Color**, *Vision Res.*, 2, 503-525, 1962.
- [99]. Jameson, D., & Hurvich, L.M., **Perceived Color and Its Dependence on Focal Surrounding, and Preceding Stimulus Variables**, *J. Opt. Soc. Am.*, 49, 890-898, 1959.
- [100]. Jameson, D., & Hurvich, L.M., **Opponent Chromatic Induction: Experimental Evaluation and Theoretical Account**, *J. Opt. Soc. Am.*, 51, 46-53, 1961.
- [101]. Shevell, S., **The Dual Role of Chromatic Backgrounds in Colour Perception**, *Vision Res.*, 18, 1649-1661, 1978.
- [102]. Scrivener, S.A.R., Luo, M.R., Clarke, A.A., MacDonald, L.M., **Colour Appearance and the Effect of Simultaneous Contrast**, Colour and Light'91 AIC, Sydney, 1991.
- [103]. MacDonald, L.W., Luo, M.R. and Scrivener, S.A.R., **Factors Affecting the Appearance of Coloured Images on a Video Display Monitor**, *J. Photogr. Sci.*, 38, 177-186, 1990.
- [104]. Wright, W.D., **The Measurement and Analysis of Colour Adaptation Phenomena**, *Proc. Roy. Soc.*, 115B, 49, London, 1934.
- ∇ [105]. Wassef, E.G.T., **Application of the Binocular Matching Method to the Study of the Subjective Appearance of Surface Colours**, *Optica Acta*, 2, 144-150, 1955.
- ∫ [106]. Hunt, R.W.G., **Measurement of Colour Appearance**, *J. Opt. Soc. Am.*, 55, 1540-1551, 1965.
- [107]. DeValois, R.L. and Walraven, J., **Monocular and Binocular after Effects of Chromatic Adaptation**, *Science N.Y.*, 155, 463-465, 1967.
-

-
- [108]. Tschermak, A.V., Segsenegg, **Introduction to Physiological Optics**, Spring Field, 111, Charles C Thomas, 1952.
- [109]. Thomas, F.H., Pimmick, F.L., and Luria, S.M., **A Study of Binocular Colour Mixture**, *Vision Res.*, I, 108-116, 1961.
- [110]. MacAdam, D.L., **Chromatic Adaptation**, *J. Opt. Soc. Am.*, 46, 500-513, 1956.
- [111]. Miller, G.A., **The Magical Number Seven, Plus or Minus Two: Some Limits on Our Capacity for Processing Information**, *Psychol. Rev.*, 63, 81-97, 1956.
- [112]. Bartleson, C.J., and Woodbury, W.W., **Psychophysical Methods for Evaluating The Quality of Color Transparencies. III. Effect of Nunber of Categories, Anchors, And Types of Instructions on Quality Ratings**, *Photogr. Sci. Eng.*, 9, 323-330, 1965.
- [113]. Newhall, S.M., Burnham, R.W., and Clark, J.R., **Comparison of Successive with Simultaneous Color Matching**, *J. Opt. Soc. Am.*, 47, 43-56, 1957.
- ✓ [114]. Wright, W.D., **Why and How Chromatic Adaptation Has Been Studied**, *Color Res. Appl.*, 6, 147-152, 1981.
- ✓ [115]. Ishak, I.G.H., Bouma, H., & van Bussel, J.J., **Subjective Estimates of Colour Attributes for Surface Colours**, *Vision Res.*, 10, 489-500, 1970.
- [116]. Stevens, S.S. and Galanter, E.H., **Ratio Scales and Category Scales for a Dozen Perceptual Continua**, *J. Exp. Psychol.*, 54, 377-411, 1957.
- ✓ [117]. Rowe, S.C.H., **The Subjective Scaling of Hue and Saturation**, in *Color 73*, 391-393, Adam Hilger, London, 1973.
- ✓ [118]. Padgham, C.A, and Rowe, S.C.H., **A Mass Colour Scaling Experiment**, in *Color*
-

73, 393-398, Adam Hilger, London, 1973.

- ✓ [119]. Gibson, N., **The Measurement of Subjective Colour**, *Optica Acta*, **14**, 219-243, 1967.
- [120]. Nayatani, Y., Yamanaka, T., and Sobagaki, H., **Subjective Estimation of Color Attributes for Surface Colours (Part 1: Reproducibility of Estimations)**, *Acta Chromatica*, **2**, 129-138, 1972.
- [121]. Luo, M.R., Clarke, A.A., Rhodes, R.A., Schappo, A., Scrivener, S.A.R., Tait, C.J., **Quantifying Colour Appearance, Part I, LUTCHI Colour Appearance Data**, *Color Res. Appl.*, **16**, 166-179, 1991.
- [122]. Luo, M.R., Clarke, A.A., Rhodes, R.A., Schappo, A., Scrivener, S.A.R., Tait, C.J., **Quantifying Colour Appearance, Part II, Testing Colours Models Performance Using LUTCHI Colour Appearance Data**, *Color Res. Appl.*, **16**, 181-197, 1991.
- [123]. Bartleson, C.J., **Measures of Brightness and Lightness**, *Die Farbe*, **28**, 132-148, 1980.
- [124]. Bartleson, C.J., and Breneman, E.J., **Brightness Perception in Complex Fields**, *J. Opt. Soc. Am.*, **57**, 1967, 953-975, 1967.
- [125]. Indow, T., and Stevens, S.S., **Scaling of Saturation and Hue**, *Perception & Psychophysics*, **1**, 253-271, 1966.
- [126]. Kruithof, A.A. and Bouma, P.J., **Hue-estimation of Surface Colours as Influenced by the Colours of the Surroundings**, *Physica.*, **9**, 957-966, 1942.
- [127]. Maxwell, R.S., **The Quantitative Estimation of the Sensation of Colour**, *Br. J. Psychol.*, **20**, 181-189, 1929.
-

-
- [128]. Warren, R.M., **Quantitative Judgments of Colour: the Square Root Rule**, *Percept. Psychophys.*, **2**, 448-452, 1967.
- [129]. Pointer, M.R., **Colourfulness: A New Concept**, in F.W. Billmeyer, Jr., and G. Wyszecki, ed., *AIC Colour 77*, Adam Hilger, Bristol, England, 327-330, 1978.
- [130]. Hurvich, L.M., **Two Decades of Opponent Processes**, in Fred W. Billmeyer, Jr., and G. Wyszecki, editors, *AIC Color 77*, Adam Hilger, Bristol, 33-61, 1978.
- [131]. Breneman, E.J., **Perceived Saturation in Complex Stimuli Viewed in Light and Dark Surround**, *J. Opt. Soc. Am.*, **67**, 657-662, 1977.
- [132]. Pitt, I.T., and Winter, L.M., **Effect of Surround on Perceived Saturation**, *J. Opt. Soc. Am.*, **64**, 1328-1331, 1974.
- [133]. Sobayaki, H., Yamanaka, T., Takahama, K., and Nayatani, Y., **Chromatic Adaptation Study by Subjective Estimation Method**, *J. Opt. Soc. Am.*, **64**, 743-749, 1974.
- [134]. Estevez, O., **On the Fundamental Data-Base of Normal and Dichromatic Colour Vision**, Ph.D. thesis, University of Amsterdam, 1979.
- [135]. Hunt, R.W.G., Pointer, M.R., **A Colour-appearance Transform for the CIE 1931 Standard Colorimetric Observer**, *Color Res. Appl.*, **10**, 165-179, 1985.
- [136]. Seim, T., and Valberg, A., **Towards a Uniform Color Space: a Better Formula to Describe the Munsell and OSA Color Scales**, *Color Res. Appl.*, **11**, 11-24, 1986.
- [137]. Hunt, R.W.G., **Procedures for Using A Revised Colour Appearance Model**, *J. Photogr. Sci.*, **38**, 109-113, 1990.
- [138]. Nayatani, Y., Takahama, K., & Hashimoto, K., **Field Trials on Color Appearance**
-

-
- and Brightness of Chromatic Object Colours under Different Adapting Illuminance Levels, *Color Res. Appl.*, 13, 298-305, 1988.**
- [139]. Nayatani, Y., Takahama, K., & Sobagaki, H., **Field Trials on Color Appearance of Chromatic Colours under Various Light Sources, *Color Res. Appl.*, 13, 307-317, 1988.**
- [140]. Pointer, M.R., **Measuring Colour Reproduction, *J. Photogr. Sci.*, 34, 81-90, 1986.**
- [141]. Mori, L., and Fuchida, T., **Subjective Evaluation of Uniform Color Spaces Used for Color-Rending Specification, *Color Res. Appl.*, 7, 285-293, 1982.**
- [142]. Ishihara, S., **The Series of Plates Designed as a Test for Colour-Blindness, 38 plates ed., Kanehara Shuppan Co. Ltd., Tokyo, Japan, 1985.**
- [143]. Fletcher, R., **The City University Colour Vision Test, 2nd ed, Keeler, London, 1980.**
- [144]. Barco, **The Calibrator® Explained, Part I, Barco Video & Communications, Belgium, 1990.**
- [145]. Luo, M.R., Xin, J.H., Rhodes, P.A., Scrivener, S.A.R., and MacDonald, L.W., **Stusying the Performance of High Resolution Colour Displays, CIE Proceedings 22nd Session Melbourne, 97-100, Australia, 1991.**
- [146]. Clarke, G.M., & Cooke, D., **A Basic Course in Statistics, Edward Arnold Ltd, London, 1978.**
- [147]. Hoel, P.G., **Introduction to Mathematical Statistics, 3rd ed., John Wiley & Sons, New York, 1966.**
- [148]. Nayatani, Y., Takahama, K., Sobayaki, H., & Hashimoto, K., **Field Trials of a**
-

Nonlinear Model for Predicting Color Appearance under Various Conditions of Chroma Adaptation, in Proceedings of the 5th Congress of the International Color Associations 85, Monaco, 25, 1985.

- [149]. Fuchida, T. and Mori, L., **Comparison of Correcting Methods for Chromatic Adaptation Used for Color-rendering Specification**, *Color Res. Appl.*, 7, 294-301, 1982.
- [150]. Bunday, B.D., **Basic Optimisation Methods**, Edward Arnold Ltd, London, 1984.

APPENDIX A. HUNT 93 MODEL IN C CODE

```

#include<sys/file.h>
#include<sys/types.h>
#include<sys/stat.h>
#include<stdio.h>
#include<math.h>

static double la,las,lw,Lp,flas,Nb,Nc,sxe,sye,Ye,sxw,syw
&          ,Yw,sxb,syb,Yb,Nbb,Ncb;
static double J,Mc,Hue,chroma,Q;
main(argc, argv)
int argc;
char *argv[];
{
    char infile1[15],infile2[15];
    FILE *ip1, *ip2,*ip3,*ip4;
    char title[81];
    int j,nch,nsum1,nsum2,i,m,count,neutral,neu[10];
    double Cc[3000],Qqwb[3000],Qq[3000], Jj[3000],Mm[3000],Hh[3000];
    double sx[3000],sy[3000],Y[3000];
    double Qb;
    void hunt89_xg();

    if(argc == 3)
{
    strcpy(infile1,argv[1]);
    strcpy(infile2,argv[2]);
}
    else
{

```

```
    printf("Hunt91:what is the name of x,y,Y data file?");
    gets(infile1);
    printf("... and viewing parameters file?--");
    gets(infile2);
}
if((ip1 = fopen(infile1,"r")) == NULL)
{
    printf("Can't open %s\n",infile1);
    exit(1);
}
if((ip2 = fopen(infile2,"r")) == NULL)
{
    printf("Can't open %s \n",infile2);
    exit(1);
}

    i =0;
do
{
    fscanf(ip1,"%lf %lf %lf",&sx[i],&sy[i],&Y[i]);

    i = i+1;
} while(getc(ip1)!=EOF);

    nsum1 = i-1;
    printf("\n There are %d samples in file %s\n",nsum1,infile1);

/* Luminance factor of reference white (cd/m2). */
    fscanf(ip2,"%s",title);
    fscanf(ip2,"%lf",&Yw);
/* Luminance of perfect diffuser (cd/m2). */
    fscanf(ip2,"%s",title);
```

```

        fscanf(ip2,"%lf",&Lp);
/* Photopic luminances of reference white in cd/m2. */
        lw = Lp * Yw /100;
/* Luminance factor of the background considered. */
        fscanf(ip2,"%s",title);
        fscanf(ip2,"%lf",&Yb);

/* Photopic luminances of adapting fields in cd/m2. */
la=lw*Yb/100;
/* Scotopic luminance level conversion factor flas factors are 1.071,0.97,
* 0.776 and 0.663 for D65, D50, WF and A light sources respectively.
*/
fscanf(ip2,"%s",title);
        fscanf(ip2,"%lf",&flas);
las=la*flas;
/* Brightness induction factor Nb=75 for nonluminous colours
*
        Nb=25 for luminous colours.
*/
fscanf(ip2,"%s",title);
        fscanf(ip2,"%lf",&Nb);
/* printf(" lw Lp Yb Nb flas are %lf %lf %lf %lf %lf \n",lw,Lp,Yb,Nb,flas); */

/* Colourfulness induction factor for luminous and nonluminous colours
*
        Nc=0.93 for high luminance level
*
        Nc=1.18 for low luminance level
*/
fscanf(ip2,"%s",title);
        fscanf(ip2,"%lf",&Nc);
/* Colorimetric data for reference level. */
fscanf(ip2,"%s",title);
        fscanf(ip2,"%lf %lf %lf",&sxw,&syw,&Yw);
/* Colorimetric data for equi-energy white (Ye=100). */

```

```

fscanf(ip2,"%s",title);
    fscanf(ip2,"%lf %lf %lf",&sxe,&sye,&Ye);
/* Colorimetric data for background. */
fscanf(ip2,"%s",title);
    fscanf(ip2,"%lf %lf %lf",&sxb,&syb,&Yb);

Ncb = 0.725 *pow( Yw/Yb ,0.2);
Nbb = 0.725 * pow(Yw/Yb,0.2);

printf("Working ...\n");
ip3=fopen("Hunt91-end","w");
fprintf(ip3,"\n No. Lightness Colourful Hue Chroma  brightness white-black \n");
ip4=fopen("Hunt91.lch","w");

hunt89_xg(sxb,syb,Yb);
Qb = Q;

for(i=0;i<nsum1;i++)
{
    hunt89_xg(sx[i],sy[i],Y[i]);
    Jj[i] = J;
    Mm[i] = Mc;
    Hh[i] = Hue;
    Cc[i] = chroma;
    Qq[i] = Q;
    Qqwb[i] = 20.0 * (pow(Qq[i],0.7) - pow(Qb,0.7));
    fprintf(ip3,"%3d %8.4lf %8.4lf %8.4lf %8.4lf %8.4lf %8.4lf\n",i,Jj[i],Mm[i],Hh[i],Cc[i],Qq[i],Qqwb[i]);
    fprintf(ip4,"%8.4lf %8.4lf %8.4lf \n",Jj[i],Cc[i],Hh[i]);
    printf("The %d th lightness is %lf \n",i,Jj[i]);
}

printf("\n The predict result file is Hunt91-end\n");

```

```
printf("\n The predict LCH file is Hunt91.lch\n");

fclose(ip1);
fclose(ip3);
fclose(ip4);
fclose(ip2);
}

com_xw(nx,ny,x,y)
int nx,ny;
double x[100],y[100];
{
    double ff,cv1,cv2,sst,rmq,mean,f,mst,sumd,sumdsq,thigamax,thigamay;
    double d[100],dsq[100],t,sd,sde;
    int i;
    sumd=0.0;
    sumdsq=0.0;
    sst =0.0;
    for(i=0;i<nx;i++)
    {
        d[i] = x[i] -y[i];
        dsq[i] = d[i] *d[i];
        if(d[i]< 0.0)
            sumd = sumd - d[i];
        else
            sumd = sumd + d[i];
        sumdsq = sumdsq + dsq[i];
        sst = sst + x[i] + y[i];
    }

    mean = sst/2.0;
```

```

sumd = sumd ;
sumdsq = sqrt(sumdsq/nx) ;
printf(" The SUM|x-y| is %lf \n",sumd);
printf(" The sqrt(S(x-y)(x-y)/n) is %lf \n",sumdsq);
return;
}

int not_neutral(n,neu,sam)
int n,neu[10],sam;
{
    int ok;
    int i;
    ok=0;
    for(i=0;i<n;i++)
    {
        if(sam==neu[i]);
        ok=1;
    }
    return(ok);
}

void hunt89_xg(sx,sy,Y)
/* sx,sy,Y: input data
 * J:Lightness;Mc:Colourfulness,H:Hue;C: Chroma; Qwb:whiteness-blackness.
 * Q:Brightness.
 */
    double sx,sy,Y;
{
    /* rgb[0,i] standard for test colour r,g,b
     * rgb[1,i] for white reference colour,
     * rgb[2,i] for equal-energy stiumous
     * rgb[3,i] for background.
     * xyz[i,j] for X,Y,Z of ith colour,i is same as the i in rgb[i,j] */

```

```

double rgb[4][3],xyz[4][3];
double rd,fl,k,fr,fg,fb,ge,be,Aa,Aab,Aaw;
double hr,hg,hb,gd,bd,ra,ga,ba,raw,gaw,baw;
double rorw,gogw,bobw,rgbsum;
double H[6],sh[6],e[6],shs,rorb,gogb,bobb,bbf,gbf,rbf;
double ft, Myb,Mrg,smYB,smRG,s,sw,Mw,fls,sa,saw,A,Aw;
double Qw,N1,N2,C1,C2,C3,sz,sab,Ab,C1w,C2w,C3w,C1b,C2b,C3b;
double rb,gb,bb,re,Sbf,Sab,Saw,Sbfbw,Sb,l,ybw;
double Mwyb,Mwrg,Mbrg,Mb,es,sb,sbf,sj,Mbyb,sbfbw,Sa;
double tt,hangle,hwangle,esw,Huew,bll,ftw,M,Jw,Cw,Mwc;
double k1,k2,k3;
int i;
double fn();
double es_factor();

```

```

/* A.1 Calculate X,Y,Z ( Tristimulus values) */
l=Lp*Y/Yw;
xyz[0][0] = sx * Y / sy;
xyz[0][1] = Y;
xyz[0][2] = ( 1-sx - sy) * Y / sy;
xyz[1][0] = sxw * Yw / syw;
xyz[1][1] = Yw;
xyz[1][2] = ( 1-sxw - syw) * Yw / syw;
xyz[2][0] = 100;
/* printf("r,g,b,values are %lf %lf %lf \n",r,g,b); */
xyz[2][1] = 100;
xyz[2][2] = 100;
xyz[3][0] = sxb * Yb / syb;
xyz[3][1] = Yb;
xyz[3][2] = ( 1-sxb - syb) * Yb / syb;

```

```

/* A.2 Calculate red, green and blue primaries. */
/* A.3 Calculate R/Rw,G/Gw,B/Bw; (Rw,Gw,Bw: The values of R,G,B for the
 * reference white in the effective adapting illuminant.)
 * re,ge,be: the value of r,g,b for the equi-energy white(YE = 100).
 */
for(i=0;i<3;i++)
{
rgb[i][0] = 0.38971 * xyz[i][0] + 0.68898 * xyz[i][1] - 0.07868 * xyz[i][2];
rgb[i][1] = - 0.22981 * xyz[i][0] + 1.18340 * xyz[i][1] + 0.04641 * xyz[i][2];
rgb[i][2] = 1.00000 * xyz[i][2];
}

rorw = rgb[0][0] / rgb[1][0];
gogw = rgb[0][1] / rgb[1][1];
bobw = rgb[0][2] / rgb[1][2];

/* A.4 Calculate Fl ( Adaptation parameter for luminance level) */
/* LA : The effective illuminance of the adapting background in cd/m2
 * 5LA: The luminance of a reference white.
 */
k = (1.0/(5.0*la+1.0));
k = k*k*k*k;
fl = 0.2* k * 5*la + 0.1 *(1-k)*(1-k)* pow((5*la),0.33333);
/* printf("rorw,gogw,bobw = %lf %lf %lf\n",rorw,gogw,bobw); */

/* A.5 Calculate FR,FG,FB: ( Chromatic daptation parameters)
 * RE,GE,BE: The value of R,G,B for the equi-energy stimulus
 * hr,hr,hb: A measure of the purity of the colour of the
 * adapting illuminant.
 */
rgbsum = rgb[1][0] + rgb[1][1] + rgb[1][2];

```

```

    hr = 3*rgb[1][0] / rgbsum;
    hg = 3*rgb[1][1] / rgbsum;
    hb = 3*rgb[1][2] / rgbsum;
    fr = ( 1.0 + pow(la ,0.33333) + hr) / ( 1.0 + pow(la ,0.33333) + 1/hr);
    fg = ( 1.0 + pow(la ,0.33333) + hg) / ( 1.0 + pow(la ,0.33333) + 1/hg);
    fb = ( 1.0 + pow(la ,0.33333) + hb) / ( 1.0 + pow(la ,0.33333) + 1/hb);

/* A.6 Calculate RD,GD,BD ( adaptation parameters to discounting the colour
* of the illuminant).
*/
rd = fn((Yb/Yw) * fl *fg) - fn((Yb/Yw) * fl *fr);
gd = 0.0;
bd = fn((Yb/Yw) * fl *fg) - fn((Yb/Yw) * fl *fb);

/* A.7 Calculate ra,ga,ba and raw, gaw, baw
*
*      ra,ga,ba : Cone responses after adaptation;
*      raw,gaw,baw : the value of ra,ga,ba for reference white.
*      rb,gb,bb for background.
*/
rbf = 10000000/(10000000 + 5*la * (rgb[1][0]/100));
gbf = 10000000/ ( 10000000 + 5*la * (rgb[1][1]/100));
bbf = 10000000/ ( 10000000 + 5*la * (rgb[1][2]/100));

/* printf("rbf,gbf,bbf,rd,bd,fl= %lf %lf %lf %lf %lf %lf\n",rbf,gbf,bbf,rd,bd,fl); */
ra = rbf * (fn(fl*fr*rorw) + rd ) +1 ;
ga = gbf * (fn(fl*fg*gogw) + gd ) +1 ;
ba = bbf * (fn(fl*fb*bobw) + bd ) +1;
raw = rbf * (fn(fl*fr) + rd ) + 1 ;
gaw = gbf * (fn(fl*fg) + gd ) + 1 ;
baw = bbf * (fn(fl*fb) + bd ) + 1 ;

/* printf("ra+ga+ba is %lf\n", k1); */

```

```

/* printf("hr,fr,rd,rbf,ra,raw = %lf %lf %lf %lf %lf %lf\n",hr,fr,rd,rbf,ra,raw);
*/
/* printf("ra,ga,ba= %lf %lf %lf\n",ra,ga,ba);*/

/* A.8 Calculate% Aa, Aaw, C1,C2,C3, C1w,C2w,C3w
*      Aa : Photopic a(*chroma)tic signal;
*      Aaw: the value of Aa for reference white;
*      C1,C2,C3: (*chroma) difference signal;
*      C1w,C2w,C3w: the values of C1,C2,C3 for reference white.
*/
Aa = 2 * ra + ga + ba/20 - 3.05 + 1 ;
Aab = 2 * rb + gb + bb/20 - 3.05 + 1 ;
Aaw = 2 * raw + gaw + baw/20 - 3.05 + 1 ;
C1 = ra-ga;
C2 = ga-ba;
C3 = ba-ra;
C1w = raw - gaw;
C2w = gaw - baw;
C3w = baw - raw;

/* printf("C1,C2,C3,C1w,C2w,C3w,Aa,Aaw=%lf %lf %lf %lf %lf %lf %lf
%lf\n",C1,C2,C3,C1w,C2w,C3w,Aa,Aa); */
/* A.9 Calculate hs ( Hue angle) */
/* A.10 Calculate H ( Hue response) */

tt=es_factor(C1,C2,C3,&es,&hangle,&Hue);
tt=es_factor(C1w,C2w,C3w,&esw,&hwangle,&Huew);
/* printf("hs,es,hs,esw are %lf %lf %lf %lf\n",hangle,es,hwangle,esw);*/
/* printf("c12,c23 ,hangle, C23/c12,tan(hangle), %lf %lf %lf %lf
%lf\n",C1-C2/11.0,(C2-C3)/9.0,hangle,(C2-C3)/9.0/(C1-C2/11.0),tan(hangle*3.1415/180.
0)); */

```

```
/* A.13 Calculate Ft ( Low-luminance tritanopia factor )*/
```

```
ft =la/(la+0.1);
```

```
/* A.14 Calculate MYB, MRG, M,Mw, mYB,mRG,s
```

```
*      MYB : Yellowness-Blueness response;
*      MRG : Redness-greenness response;
*      M   : (*chroma)fulness response;
*      Mw  : The value of M for reference white;
*      mYB : Relative yellowness-blueness response;
*      mRG : Relstive redness-greenness response;
*      s   : Saturation response.
```

```
*/
```

```
Myb = 100* (C3-C2)/9 * (es* 10/13 * Nc * Ncb * ft ) ;
```

```
Mrg = 100*(C1- C2/11) * ( es * 10/13 * Ncb * Nc ) ;
```

```
M = pow( Myb*Myb + Mrg*Mrg ,0.5);
```

```
Mc = M;
```

```
tt = (C2-C3)/9.0/((C1-C2/11.0));
```

```
tt = tan(hangle *3.1415/180.0);
```

```
/* printf("k1,es is %lf %lf\n",es*Nc*Ncb*10.0/13.0*pow(tt*tt*ft*ft+ 1.0,0.5),es);*/
```

```
smYB = Myb / (ra+ga+ba);
```

```
smRG = Mrg / (ra+ga+ba);
```

```
s = 50 * Mc / (ra+ga+ba);
```

```
Mwyb = 100*(C3w-C2w)/9 * (esw* 10/13 * Nc * Ncb * ft ) ;
```

```
Mwrg = 100*(C1w- C2w/11) * ( esw * 10/13 * Ncb * Nc ) ;
```

```
Mw = pow((Mwyb*Mwyb + Mwrg*Mwrg), 0.5);
```

```
Mwc=Mw;
```

```
sw = 50 * Mwc / (raw+gaw+baw);
```

```

/* A.15 Calculate FLS ( Scotopic luminance-level adaptation factor);
*      LAS': Scotopic liminance of the adapting background.
*/

/* sj = 0.00001 / (5*las/2.26 + 0.00001);
* fls = 3800.0*sj*sj* 5 * las/2.26 + 0.2*pow((1-sj*sj),4) * pow((5*las/2.26),1/6);
*/
sj = 0.00001 / (5.0*las + 0.00001);
fls = 3800.0* sj*sj*5.0*las+0.2*pow((1.0-sj*sj),4.0)*pow((5.0*las),1.0/6.0);

/* A.16 Calculate Sa ans Saw
*      Sa : the rod response after adaptation;
*      Saw : the value of Sa for the reference white;
*      Sw : the value of S for the reference white;
*      S/Sw: Scotopic luminances relative to reference white.
*/
sbf = 0.5/(1 + 0.3* pow((5*las * l/lw),0.3) ) + 0.5/(1 + 5 * ( 5*las));
sbfw = 0.5/(1 + 0.3* pow((5*las),0.3 )) + 0.5/(1.0 + 5.0 * ( 5.0*las));

Sa=sbf * 3.05 * fn(fls*(l/lw)) + 0.3 ;
/* Sa = 0.3; */

/* Saw = 122 * Sbfw * pow(fls,0.73) / (pow(fls ,0.73) + 2) +0.3; */
Saw = sbfw * 3.05 * fn(fls) + 0.3 ;
printf("sbfw,saw,fls,las = %lf %lf %lf %lf\n",sbfw,Saw,fls,las);

/* A.17 Calculate A and Aw
*      A : the total a(*chroma)tic response;
*      Aw: the value of A for reference white.
*/

```

```

A = Nbb * ( Aa - 1.0 + Sa - 0.3 + pow(1.09,0.5));
Aw = Nbb * ( Aaw - 1.0 + Saw - 0.3 + pow(1.09,0.5));

/* printf("A is %lf \n",A); */
/* A.18 Calculate A+M /100 ( The parameter on which brightness depends) */

/* A.19 Calculate Q and Qw.
* Q : Brightness response;
* Qw: The value of Q for reference white;
* Nb: Induction factor for brightness;
*/
N1 = sqrt( 7 *Aw) / (5.33 * pow(Nb,0.13));
N2 = (7 * Aw) * pow(Nb,0.362) / 200;
Q = pow( (7 * (A+M/100)),0.6) * N1 - N2 ;
/* Qw = pow( 7* ( Aw + Mw/100 ),0.6) * N1 - N2; */
Qw = pow((7*(Aw + Mw/100)),0.6) * N1 - N2 ;

/* printf("Nbb,Aw,Mw,Saw,N1,N2,las are
%lf,%lf,%lf,%lf,%lf,%lf,%lf\n",Nbb,Aw,Mw,Saw,N1,N2,las);*/

/* A.20 Calculate J (Lightness response) */
sz = 1 + pow((Yb/Yw),0.5); /* For surface colours */
/* sz = 1.0; */
J = 100 * pow((Q/Qw),sz);
/* **** For cut-sheet transparency experiment, J=100(Q/Qw)**sz,sz nearly 1 **** */
/* For projected slide, sz =1.2, J = J(1.14(1-(J/100)**3 + G/100) **5) */
Jw=100;

/* A.21 Calculate C (Chroma response) */

/* chroma=s*J/100.0; */
ybw = Yb/Yw;

```

```

/* chroma = 4.0 * pow(s,0.69) *pow((Q/Qw),ybw) * (1.31 - pow(0.31,ybw));*/
chroma = 2.44 * pow(s,0.69) *pow((Q/Qw),ybw) * (1.64 - pow(0.29,ybw));

Mc = chroma * pow(fl,0.15);
Cw=sw*Jw/100;
k3 = 2*ra+ga + 1.0/20.0*(50.0*Mc/s-C1-2.0*C2)/3.0;
k2 = tan(hangle *3.1415/180.0);
k2 = (C2-C3)/9.0/(C1-C2/11.0);
k1 = es*Nc*Ncb*10.0/13.0*pow(k2*k2*ft*ft+1.0,0.5);

tt=pow((Q+N2)/N1,1.0/0.6)/7.0/Nbb+1.3-Sa-pow(1.09,0.5)+2.05; /*
-k1*fabs(C1-C2/11.0)/Nbb;*/

k3= 61.0/60.0*50.0*k1*fabs(C1-C2/11.0)*100.0/s + 59.0/60.0*C1+29.0/30.0*C2;
k3 = (C1-C2/11.0);
/* printf("Mc,s,Q,J,C,Hue preA are %lf %lf %lf %lf %lf %lf
%lf\n",Mc,s,Q,J,chroma,Hue,tt); */
/* printf("preA,c12,N2,Q,Sa,Nbb are %lf %lf %lf %lf %lf %lf\n",tt,k3,N2,Q,Sa,Nbb);
*/

/* printf("Mwc,sw,Qw,Jw,Cw,Huew are %lf %lf %lf %lf %lf
%lf\n",Mwc,sw,Qw,Jw,Cw,Huew);
*/
/*printf("ga,ra,ba,A,Aa Q Qw are %lf %lf %lf %lf %lf %lf %lf\n",ga,ra,ba,A,Aa,Q
,Qw);*/
}

double fn(c)
double c;
{
double pow();
double p;

```

```
p= 40.0 * pow(c,0.73)/(pow(c,0.73) + 2.0);
return(p);
}
```

```
double es_factor(C1,C2,C3,es,angle,hue)
double C1,C2,C3,*hue,*es,*angle;
{
double H[5],sh[5],e[5];
double shs,de,nu;
int i,j;
H[0] = 0,    H[1] = 100, H[2] = 200,  H[3] = 300,  H[4] = 400;
sh[0] = 20.14, sh[1] = 90.0, sh[2]=164.25, sh[3]=237.53, sh[4]=380.14;
e[0] = 0.8,   e[1] = 0.7, e[2] = 1.0,  e[3] = 1.2,  e[4] = 0.8;

nu = (C2-C3)/9.0;
de = C1 - C2/11.0;
if(fabs(de) < 0.000001)
{
    if(nu > 0.0)
        shs = 90.0;
    else
        shs = 270.0;
}
else
{
shs = atan(fabs(nu)/fabs(de));
shs = shs * 180.0/3.1415;
if ( fabs(nu) < 0.000001)
{
    if(de < 0.0)
        shs = shs + 180.0;
}
}
```

```

if(nu > 0 && de <0 )
shs = 180.0 - shs ;
else
if(nu < 0 && de <0 )
shs = shs + 180.0;
else
if(nu < 0 && de >0 )
shs = 360.0 - shs ;

if (shs>0.0 && shs<sh[0])
shs = shs + 360.0;
}
*angle=shs;

for(j=0;j<5;j++)
{
    if (shs>= sh[j] && shs < sh[j+1])
        i=j;
}

*es = e[i] + ( e[i+1] - e[i] )*( shs - sh[i] ) / (sh[i+1] -sh[i]);

/* A.10 Calculate H ( Hue response) */

*hue = H[i] +(100.0*(shs-sh[i])/e[i])/((shs-sh[i])/e[i] +(sh[i+1]-shs)/e[i+1]);
/* printf("es i angle Hue are %lf %d %lf %lf \n",*es,i,*angle,*hue); */
return (1.0);
}

```

APPENDIX B. REVERSE HUNT93 MODEL IN C CODE

```
#include <sys/file.h>
#include <sys/types.h>
#include <sys/stat.h>
#include <stdio.h>
#include <math.h>

/* The method of Hooke and Jeeves together with golden method. */

static double la,las,lw,Lp,flas,Nb,Nc,sxe,sye,Ye,sxw,
&          syw,Yw,sxb,syb,Yb,Nbb,Ncb;
static double XXX,YYY,ZZZ,Ycdm;
main(argc, argv)
int argc;
char *argv[];
{
    char infile1[15],infile2[15];
    FILE *ip1, *ip2,*ip3,*ip4;
    char title[81];
    int j,nch,nsum1,nsum2,i,m,count,neutral,neu[10];
    double Cc[3000],Qqwb[3000],Qq[3000], Jj[3000],Mm[3000],Hh[3000];
    double sx[3000],sy[3000],Y[3000];
    double Qb;
    void hunt89_xg();

    if(argc == 3)
{
    strcpy(infile1,argv[1]);
    strcpy(infile2,argv[2]);
}
```

```
        else
{
    printf("Hunt91:what is the file-name of L,C,H data file?");
    gets(infile1);
    printf("... and viewing parameters file?--");
    gets(infile2);
}
if((ip1 = fopen(infile1,"r")) == NULL)
{
    printf("Can't open %s\n",infile1);
    exit(1);
}
if((ip2 = fopen(infile2,"r")) == NULL)
{
    printf("Can't open %s \n",infile2);
    exit(1);
}

    i =0;
do
{
    fscanf(ip1,"%lf %lf %lf",&Jj[i],&Cc[i],&Hh[i]);

    i = i+1;
} while(getc(ip1)!=EOF);

    nsum1 = i-1;
    printf("\n There are %d samples in file %s\n",nsum1,infile1);

/* Luminance factor of reference white (cd/m2). */
    fscanf(ip2,"%s",title);
    fscanf(ip2,"%lf",&Yw);
```

```

/* Luminance of perfect diffuser (cd/m2). */
    fscanf(ip2,"%s",title);
    fscanf(ip2,"%lf",&Lp);
/* Photopic luminances of reference white in cd/m2. */
    lw = Lp * Yw /100;
/* Luminance factor of the background considered. */
    fscanf(ip2,"%s",title);
    fscanf(ip2,"%lf",&Yb);

/* Photopic luminances of adapting fields in cd/m2. */
la=lw*Yb/100;
/* Scotopic luminance level conversion factor flas factors are 1.071,0.97,
 * 0.776 and 0.663 for D65, D50, WF and A light sources respectively.
 */
fscanf(ip2,"%s",title);
    fscanf(ip2,"%lf",&flas);
las=la*flas;
/* Brightness induction factor Nb=75 for nonluminous colours
 *
 * Nb=25 for luminous colours.
 */
fscanf(ip2,"%s",title);
    fscanf(ip2,"%lf",&Nb);
/* printf(" lw Lp Yb Nb flas are %lf %lf %lf %lf %lf \n",lw,Lp,Yb,Nb,flas); */

/* Colourfulness induction factor for luminous and nonluminous colours
 *
 * Nc=0.93 for high luminance level
 *
 * Nc=1.18 for low luminance level
 */
fscanf(ip2,"%s",title);
    fscanf(ip2,"%lf",&Nc);
/* Colorimetric data for reference level. */
fscanf(ip2,"%s",title);

```

```

        fscanf(ip2,"%lf %lf %lf",&sxw,&syw,&Yw);
/* Colorimetric data for equi-energy white (Ye=100). */
fscanf(ip2,"%s",title);
        fscanf(ip2,"%lf %lf %lf",&sxe,&sye,&Ye);
/* Colorimetric data for background. */
fscanf(ip2,"%s",title);
        fscanf(ip2,"%lf %lf %lf",&sxb,&syb,&Yb);

Ncb = 0.725 *pow( Yw/Yb ,0.2);
Nbb = 0.725 * pow(Yw/Yb,0.2);

printf("Working ...\n");
/* ip3=fopen("Iteration-H91-XYZ","w"); */
ip4=fopen("Iter.ch.2-H91-xyY","w");
/* fprintf(ip3,"\n No.    X        Y        Z        Y(cd/m2) \n"); */
fprintf(ip4,"\n No.        x        y        Y\n");

for(i=0;i<nsum1;i++)
{
    hunt89_xg(Jj[i],Cc[i],Hh[i]);
    Ycdm = YYY*Lp/100.0;
    sx[i] = XXX/(XXX+YYY+ZZZ);
    sy[i] = YYY/(XXX+YYY+ZZZ);
/* fprintf(ip3,"%3d %8.4lf %8.4lf %8.4lf %8.4lf \n",i,XXX,YYY,ZZZ,Ycdm); */
fprintf(ip4,"%3d %9.5lf %9.5lf %9.5lf \n",i,sx[i],sy[i],YYY);
    printf("The %d th Y is %lf \n",i,YYY);
}
/*      printf("\n The predict result XYZ file is Iteration-H91-XYZ\n"); */
    printf("\n The predict result xyY file is Iter.ch.2-H91-xyY\n");
    system("date");

fclose(ip1);

```

```

fclose(ip3);
fclose(ip2);
}

com_xw(nx,ny,x,y)
int nx,ny;
double x[100],y[100];
{
    double ff,cv1,cv2,sst,rmq,mean,f,mst,sumd,sumdsq,thigamax,thigamay;
    double d[100],dsq[100],t,sd,sde;
    int i;
    sumd=0.0;
    sumdsq=0.0;
    sst =0.0;
    for(i=0;i<nx;i++)
    {
        d[i] = x[i] -y[i];
        dsq[i] = d[i] *d[i];
        if(d[i]< 0.0)
            sumd = sumd - d[i];
        else
            sumd = sumd + d[i];
        sumdsq = sumdsq + dsq[i];
        sst = sst + x[i] + y[i];
    }

    mean = sst/2.0;
    sumd = sumd ;
    sumdsq = sqrt(sumdsq/nx) ;
    printf(" The SUM|x-y| is %lf \n",sumd);
    printf(" The sqrt(S(x-y)(x-y)/n) is %lf \n",sumdsq);

```

```
return;
```

```
}
```

```
int not_neutral(n,neu,sam)
```

```
int n,neu[10],sam;
```

```
{
```

```
    int ok;
```

```
    int i;
```

```
    ok=0;
```

```
for(i=0;i<n;i++)
```

```
{
```

```
    if(sam==neu[i]);
```

```
    ok=1;
```

```
}
```

```
    return(ok);
```

```
}
```

```
void hunt89_xg(l,c,h)
```

```
/* sx,sy,Y: input data
```

```
* J:Lightness;Mc:Colourfulness,H:Hue;C: Chroma; Qwb:whiteness-blackness.
```

```
* Q: Brightness.
```

```
*/
```

```
    double l,c,h;
```

```
{
```

```
/* rgb[0,i] standard for test colour r,g,b
```

```
* rgb[1,i] for white reference colour,
```

```
* rgb[2,i] for equal-energy stiumous
```

```
* rgb[3,i] for background.
```

```
* xyz[i,j] for X,Y,Z of ith colour,i is same as the i in rgb[i,j] */
```

```
    double rgb[4][3],xyz[4][3],Bs,low0;
```

```
    double rd,fl,k,fr,fg,fb,ge,be,Aa,Aab,Aaw;
```

```

double hr,hg,hb,gd,bd,Ra,Ga,Ba,raw,gaw,baw;
double rgbsum,As,rrr,bbb,ggg,Yresult,rowcolumn;
double H[6],sh[6],e[6],shs,rorb,gogb,bobb,bbf,gbf,rbf;
double ft, Myb,Mrg,smYB,smRG,s,sw,Mw,fls,sa,saw,A,Aw;
double Qw,N1,N2,C1,C2,C3,sz,sab,Ab,C1w,C2w,C3w,C1b,C2b,C3b;
double rb,gb,bb,re,Sbf,Sab,Saw,Sbfbw,Sb,ybw,testhue;
double Mwyb,Mwrg,Mbrg,Mb,es,sb,sbf,sj,Mbyb,sbfbw,Sa;
double tt,hangle,hwangle,esw,Huew,bll,ftw,M,Jw,Cw,Mwc;
double c12,c23,tghs,Q,hs,prer,preg,preb,temes,temhs,temhue;
double k1,k2,k3,preA,step1,low,top,count[3],testY,testlow,testtop;
double X1,X2,X0,X3,Fx1,Fx2,step2,length;
int i,nc12,nc23,timecount,numiter,Fnum;
double fn();
double inverse_fn();
double es_factor();
double es_factor_w();

```

```

/* B.1 Calculate FI */

```

```

    /* A.4 Calculate FI ( Adaptation parameter for luminance level) */

```

```

/* LA : The effective illuminance of the adapting background in cd/m2

```

```

 * 5LA: The luminance of a reference white.

```

```

*/

```

```

k = (1.0/(5.0*la+1.0));

```

```

k = k*k*k*k;

```

```

fl = 0.2* k * 5*la +0.1 *(1-k)*(1-k)* pow((5*la),0.33333);

```

```

/* B.2 Calculate Fls */

```

```

    /* A.15 Calculate FLS ( Scotopic luminance-level adaptation factor);

```

```

 *    LAS': Scotopic liminance of the adapting background.

```

```

*/

```

```

/* sj = 0.00001 / (5*las/2.26 + 0.00001);
   *fls = 3800.0*sj*sj* 5 * las/2.26 + 0.2*pow((1-sj*sj),4) * pow((5*las/2.26),1/6);
   */

```

```

sj = 0.00001 / (5.0*las + 0.00001);
fls = 3800.0*sj*sj* 5.0*las+ 0.2*pow((1.0-sj*sj),4.0)*pow((5.0*las),1.0/6.0);
/* printf("fls,sj,las, is %lf,%lf,%lf\n",fls,sj,las);*/

```

```

/* B.3 Calculate Rw,Gw,Bw and Re,Ge,Be. */
xyz[1][0] = sxw * Yw / syw;
xyz[1][1] = Yw;
xyz[1][2] = ( 1-sxw - syw) * Yw / syw;
xyz[2][0] = 100;
/* printf("r,g,b,values are %lf %lf %lf \n",r,g,b); */
xyz[2][1] = 100;
xyz[2][2] = 100;
xyz[3][0] = sxb * Yb / syb;
xyz[3][1] = Yb;
xyz[3][2] = ( 1-sxb - syb) * Yb / syb;

```

```

/* A.2 Calculate red, green and blue primaries. */

```

```

/* A.3 Calculate R/Rw,G/Gw,B/Bw; (Rw,Gw,Bw: The values of R,G,B for the
   * reference white in the effective adapting illuminant.)
   * re,ge,be: the value of r,g,b for the equi-energy white(YE = 100).
   */

```

```

for(i=1;i<3;i++)
{
/* xyz[i][0]= xyz[i][0] * lw/100.0; */
/* xyz[i][1]= xyz[i][1] * lw/100.0; */
/* xyz[i][2]= xyz[i][2] * lw/100.0; */
/* rgb[i][0] = 0.40024 * xyz[i][0] + 0.70760 * xyz[i][1] - 0.08081 * xyz[i][2];

```

```

* rgb[i][1] = - 0.22630 *xyz[i][0] + 1.16532 * xyz[i][1] + 0.04570 * xyz[i][2];
* rgb[i][2] =
*                               0.91822 * xyz[i][2];
*/
rgb[i][0] = 0.38971 * xyz[i][0] + 0.68898 * xyz[i][1] - 0.07868 * xyz[i][2];
rgb[i][1] = - 0.22981 * xyz[i][0] + 1.18340 * xyz[i][1] + 0.04641 * xyz[i][2];
rgb[i][2] =
                               1.00000 * xyz[i][2];
/* printf("r,g,b are %lf, %lf, %lf\n",rgb[i][0],rgb[i][1],rgb[i][2]);*/
}

```

```

/* B.4 calaulate Fr,Fg,Fb. */

```

```

/* A.5 Calculate FR,FG,FB: ( Chromatic daptation parameters)

```

```

*           RE,GE,BE: The value of R,G,B for the equi-energy stimulus
*           hr,hr,hb: A measure of the purity of the colour of the
*
*                   adapting illuminant.
*/

```

```

rgbsum = rgb[1][0]/rgb[2][0] + rgb[1][1]/rgb[2][1] + rgb[1][2]/ rgb[2][2];
hr = (3*rgb[1][0]/ rgb[2][0])/ rgbsum;
hg = (3*rgb[1][1]/rgb[2][1]) / rgbsum;
hb = (3*rgb[1][2]/rgb[2][2]) / rgbsum;
fr = ( 1.0 + pow(la ,0.33333) + hr) / ( 1.0 + pow(la ,0.33333) + 1/hr);
fg = ( 1.0 + pow(la ,0.33333) + hg) / ( 1.0 + pow(la ,0.33333) + 1/hg);
fb = ( 1.0 + pow(la ,0.33333) + hb) / ( 1.0 + pow(la ,0.33333) + 1/hb);

```

```

/* B.5 Calculate Rd,Gd,Bd. */

```

```

/* A.6 Calculate RD,GD,BD ( adaptation parameters to discounting the colour
* of the illuminant).

```

```

*/
rd = fn((Yb/Yw) * fl *fg) - fn((Yb/Yw) * fl *fr);
gd = 0.0;
bd = fn((Yb/Yw) * fl *fg) - fn((Yb/Yw) * fl *fb);
/* printf("rd,gd,bd are and try es_factor %lf %lf %lf\n",rd,gd,bd); */

```

```
/* B.6 calculate hs,es, according to the h value. */
```

```
if(h >= 400.0)
```

```
h = h - 400.0;
```

```
if(h < 0.0)
```

```
h = h + 400.0;
```

```
nc12 = 0;
```

```
nc23 = 0;
```

```
tt=es_factor(h,&es,&hs);
```

```
hangle = hs;
```

```
if(hangle >= 0.0 && hangle <90.0)
```

```
{
```

```
nc12=0;
```

```
nc23=0;
```

```
}
```

```
    if(hangle >= 90.0 && hangle <180.0)
```

```
    {
```

```
        nc12=1;
```

```
        nc23=0;
```

```
    }
```

```
        if(hangle >= 180.0 && hangle <270.0)
```

```
        {
```

```
            nc12=1;
```

```
            nc23=1;
```

```
        }
```

```
            if(hangle >=270.0 && hangle <=360.0)
```

```
            {
```

```
                nc12=0;
```

```
                nc23=1;
```



```

    }
/* printf("hs,nc12,nc23, %lf %d %d \n",hangle,nc12,nc23); */

/* B.7 Calculate Ft . */
/* A.13 Calculate Ft ( Low-luminance tritanopia factor )*/

ft =la/(la+0.1);

/* B.8 Calculate C1,C2,C3 from c,hs. */

/* C1 = (22.0*c12 + 9.0*c23)/23.0;
 * C2 = 11.0*(9.0*c23-c12)/23.0;
 * C3 = - (108.0*c23+11.0*c12)/23.0;
 */
/* printf("C1 C2 C3 tghs,c12 c23 l c h are %lf %lf %lf %lf %lf %lf %lf %lf
%lf\n",C1,C2,C3,tghs,c12,c23,l,c,h); */
/* *** Assume S/Sw = 0 *** */

/* B.9 raw,gaw,baw */
/* A.7 Calculate ra,ga,ba and raw, gaw, baw
 *      ra,ga,ba : Cone responses after adaptation;
 *      raw,gaw,baw : the value of ra,ga,ba for reference white.
 *      rb,gb,bb for background.
 */
rbf = 10000000/(10000000 + 5*la * (rgb[1][0]/100));
gbf = 10000000/ ( 10000000 + 5*la * (rgb[1][1]/100));
bbf = 10000000/ ( 10000000 + 5*la * (rgb[1][2]/100));

/* printf("rbf,gbf,bbf,rd,bd,fb= %lf %lf %lf %lf %lf %lf\n",rbf,gbf,bbf,rd,bd,fb); */
raw = rbf * (fn(fl*fr) + rd ) + 1 ;

```

```

gaw = gbf * (fn(fl*fg) + gd ) + 1 ;
baw = bbf* (fn(fl*fb) + bd ) + 1 ;
/*printf("hr,fr,rd,rbf,ra,raw = %lf %lf %lf %lf %lf %lf\n",hr,fr,rd,rbf,ra,raw);
*/
/* printf("raw,gaw,baw,=%lf %lf %lf\n",raw,gaw,baw);*/
/* B.10 C1w,C2w,C3w */
/* A.8 Calculate% Aa, Aaw, C1,C2,C3, C1w,C2w,C3w
*           Aa : Photopic a(*chroma)tic signal;
*           Aaw: the value of Aa for reference white;
*           C1,C2,C3: (*chroma) difference signal;
*           C1w,C2w,C3w: the values of C1,C2,C3 for reference white.
*/
Aaw = 2.0 * raw + gaw + baw/20.0 - 3.05 + 1.0 ;
C1w = raw - gaw;
C2w = gaw - baw;
C3w = baw - raw;

/* printf("C1,C2,C3,C1w,C2w,C3w,Aa,Aaw=%lf %lf %lf %lf %lf %lf %lf
%lf\n",C1,C2,C3,C1w,C2w,C3w,Aa,Aa); */
/* A.9 Calculate hs ( Hue angle) */
/* A.10 Calculate H ( Hue response) */

/* tt=es_factor(C1,C2,C3,&es,&hangle,&Hue); */
tt=es_factor_w(C1w,C2w,C3w,&esw,&hwangle,&Huew);

/* printf("hs,es,hs,esw are %lf %lf %lf %lf\n",hs,es,hwangle,esw);*/
/* B.11 Calculate Mw. */
/* A.14 Calculate MYB, MRG, M,Mw, mYB,mRG,s
*           MYB : Yellowness-Blueness response;
*           MRG : Redness-greenness response;
*           M  : (*chroma)fulness response;
*           Mw : The value of M for reference white;

```

```

*           mYB : Relative yellowness-blueness response;
*           mRG : Relstive redness-greenness response;
*           s   : Saturation response.
*/

Mwyb = 100.0*(C3w-C2w)/9.0 * (esw* 10.0/13.0 * Nc * Ncb * ft );
Mwrg = 100.0*(C1w- C2w/11.0) * ( esw * 10.0/13.0 * Ncb * Nc );
Mw = pow((Mwyb*Mwyb + Mwrg*Mwrg), 0.5);
Mwc=Mw;
sw = 50.0 * Mwc / (raw+gaw+baw);

/* B.12 Sw */
/* A.16 Calculate Sa ans Saw
*           Sa : the rod response after adaptation;
*           Saw : the value of Sa for the reference white;
*           Sw : the value of S for the reference white;
*           S/Sw: Scotopic luminances relative to reference white.
*/

sbfw = 0.5/(1.0 + 0.3* pow((5.0*las),0.3 )) + 0.5/(1.0 + 5.0 * ( 5.0*las));

/* Saw = 122 * Sbfw * pow(fls,0.73) / (pow(fls ,0.73) + 2) +0.3; */
Saw = sbfw * 3.05 * fn(fls) + 0.3 ;
/* printf("sbfw,saw,fls,las = %lf %lf %lf %lf\n",sbfw,Saw,fls,las);*/

/* B.13 Aw */
/* A.17 Calculate A and Aw
*           A : the total a(*chroma)tic response;
*           Aw: the value of A for reference white.
*/

Aw = Nbb * ( Aaw - 1.0 + Saw - 0.3 + pow(1.09,0.5));

/* B.14 Qw */

```

```

/* A.19 Calculate Q and Qw.
* Q : Brightness response;
* Qw: The value of Q for reference white;
* Nb: Induction factor for brightness;
*/
N1 = sqrt( 7.0 *Aw) / (5.33 * pow(Nb,0.13));
N2 = (7.0 * Aw) * pow(Nb,0.362) / 200.0;
/* Qw = pow( 7* ( Aw + Mw/100 ),0.6) * N1 - N2; */
Qw = pow((7.0*(Aw + Mw/100)),0.6) * N1 - N2 ;

/*printf("Nbb,Aw,Mw,Saw,N1,N2,las are
%lf,%lf,%lf,%lf,%lf,%lf,%lf\n",Nbb,Aw,Mw,Saw,N1,N2,las);*/
/* A.20 Calculate J (Lightness response) */
sz = 1 + pow((Yb/Yw),0.5); /* For surface colours */
/* sz = 1.0; */
/* J = 100 * pow((Q/Qw),sz); */
/* **** For transparency experiment, J=100(Q/Qw)**sz,sz nearly 1 **** */
Q = Qw * pow(1/100.0,1.0/sz);
/* s = c/(4.0*pow(Q/Qw,Yb/Yw)*(1.31-pow(0.31,Yb/Yw))); */
s = c/(2.44*pow(Q/Qw,Yb/Yw)*(1.64-pow(0.29,Yb/Yw)));
s = pow(s,1.0/0.69);
/* A = pow((Q+N2)/N1,1.0/0.6)/7.0 - c/100.0; */

/* printf("s,Q are %lf %lf\n",s,Q); */

rowcolumn = 0.38971*1.18340 + 0.22981*0.68898;
step1 = 0.381966; /* ta = 1.68033989, step = 1/ta**2. */
step2 = 1.0 - step1;
low = 0.0 ;
top = 100.0;
length = top - low;
X0 = low; X1=low + step1*(top-low); X2=low+step2*(top-low); X3=top;

```

```
testlow = 10000.0;
low0 = low;
testY = 10000.0;
timecount = 0;
    testhue = 80.0;

numiter = 2;
Yresult = X1;
Fnum = 5;

/* do
 * {
 */
do
{
for(i=0;i<numiter;i++)
{
    if(Yresult<0.0)
    {
        Yresult = 0.0;
/*        step = 0.6*step; */
    }
    if(Yresult > 100.0)
    {
        Yresult = 100.0;
/*        step = 0.6*step; */
    }

/* if((fabs(Yresult-low)>0.001) || fabs(Yresult-top)>0.001) */

/* printf("Low, Y,step are %lf %lf %lf\n",low,Yresult,step); */
```

```

/* Yresult = 56.29;*/
Bs=0.5/(1.0+0.3*pow((5.0*las*Yresult/Yw),0.3))+0.5/(1.0+5.0*(5.0*las));
/* Bs[1]=0.5/(1.0+0.3*pow((5.0*las*low/Yw),0.3))+0.5/(1.0+5.0*(5.0*las));
 * Bs[2]=0.5/(1.0+0.3*pow((5.0*las*top/Yw),0.3))+0.5/(1.0+5.0*(5.0*las));
 */
As = Bs * 3.05 * fn(fl*Yresult/Yw) + 0.3;
/* printf("Bs, Sa are %lf %lf \n", Bs[0],As[0]); */
/* As[1] = Bs[1] * 3.05 * fn(fl*low/Yw) + 0.3;
 * As[2] = Bs[2] * 3.05 * fn(fl*top/Yw) + 0.3;
 */
preA = pow((Q+N2)/N1,1.0/0.6)/7.0/Nbb + 1.3 -As -pow(1.09,0.5)+2.05;

/* printf("preA N1,N2,Nbb As Bs is %lf %lf %lf %lf %lf %lf
\n",preA,N1,N2,Nbb,As,Bs);*/

if((hs>89.0 && hs <91.0) || (hs>269.0 && hs<271.0))
{
k3 = es*Nc*Ncb*ft*10.0/13.0;
k2 = 61.0*500.0*k3/(s*6.0)+k3/Nbb;
    if(nc23 == 1)
k2 = -k2 + 59.0*9.0/(60.0*23.0)+29.0*99.0/(30.0*23.0);
    else
k2 = k2 + 59.0*9.0/(60.0*23.0)+29.0*99.0/(30.0*23.0);
    c23 = preA/k2;
    c12 = 0.0;
A = pow((Q+N2)/N1,1.0/0.6)/7.0 - fabs(c23)*k3;
}
else
{
tghs = tan(hs*3.1415/180.0);
k1 = (es*Nc*Ncb*10.0/13.0)*pow(tghs*tghs*ft*ft+1.0,0.5);
k2 = k1/Nbb+k1*61.0*500.0/(6.0*s) ;

```

```

if(nc12 == 1)
    k2 = -k2+ 59.0*(9.0*tghs+22.0)/(60.0*23.0)+29.0*(99.0*tghs-11.0)/(30.0*23.0);
else
    k2 = k2 + 59.0*(9.0*tghs+22.0)/(60.0*23.0)+29.0*(99.0*tghs-11.0)/(30.0*23.0);

c12 = preA/k2;
c23 = tghs * c12;
/*printf("nc12 is %d \n",nc12); */
A = pow((Q+N2)/N1,1.0/0.6)/7.0 - fabs(c12)*k1;
}
/* printf("c12,c23,A,k1,es,c23/c12,tghs,hs,k2*c12, is %lf %lf%lf %lf %lf %lf %lf %lf
%lf \n",c12,c23, A,k1,es,c23/c12,tghs,hs,k2*c12); */

/*printf("A is %lf\n",A);*/

k1 = -1.0;
do
{
    C1 = (22.0*c12 + 9.0*c23)/23.0;
    C2 = 11.0*(9.0*c23-c12)/23.0;
    C3 = - (108.0*c23+11.0*c12)/23.0;
/* C1 =0.017736 ;
* C2 =0.496359 ;
* C3 =-0.514094;
*/

Aa = A/Nbb +1.3-1.044 - As;
Ga = (Aa-2.0*C1+2.05-(C3+C1)/20.0)/(3.0+1/20.0);
Ra = C1 + Ga;
Ba = Ga - C2;

prer = (Ra-1.0)/rbf-rd;

```

```
preg = (Ga-1.0)/gbf-gd;
preb = (Ba-1.0)/bbf-bd;
/* printf("rbf,gbf,bbf,prer,preg,preb Aa are %lf %lf %lf %lf %lf %lf
%lf\n",rbf,gbf,bbf,prer,preg,preb,Aa); */

if(prer<0.0 || prer<0.0 || prer<0.0)
{
    if(k1<0.0)
    {
        c12 = -c12;
        c23 = -c23;
        k1 = k1 + 1.0;
    }
    else
    {
        prer=0.0;
        preg=0.0;
        preb=0.0;
    }
}

}while(prer<0.0 || prer<0.0 || prer<0.0);

/* printf("C1,C2,C3 %lf %lf %lf \n",C1,C2,C3); */

/* printf("ra,ga,ba are %lf %lf %lf\n",(Ra[i]-1.0)/rbf-rd,(Ga[i]-1.0)/gbf,(Ba[i]
-1.0)/bbf-bd); */

/* printf("count[i] is %lf \n",count[i]); */
```

```

if(fabs(prer)<0.00001 && fabs(preg)<0.00001 && fabs(preb)<0.00001)
testY = 10000.0;
else
{
rrr = inverse_fn((Ra-1.0)/rbf - rd);
rrr = rrr*rgb[1][0]/fl/fr;
ggg = inverse_fn((Ga-1.0)/gbf);
ggg = ggg/fl/fg*rgb[1][1];
bbb = inverse_fn((Ba-1.0)/bbf - bd);
bbb = bbb/fl/fb*rgb[1][2];

testY = Yresult - (0.38971*ggg + 0.22981*rrr - 0.000005*bbb)/rowcolumn;
}
/* printf("testY,rrr,ggg,bbb are %lf %lf %lf %lf\n",testY,rrr,ggg,bbb); */
if( numiter > 1)
if(i==0)
{
        Fx1=testY;
        Yresult = X2;
}
if(i==1)
        Fx2=testY;
else
        {
if(Fnum == 1)
        Fx1 = testY;
if(Fnum == 2)
        Fx2 = testY;
        }
/* printf("testY is %lf\n",testY); */
}

```

```
/* printf("testY is %lf\n",testY);
 * printf("Begin: X0,X1,X2,X3,Fx1,Fx2,length are,
%lf,%lf,%lf,%lf,%lf,%lf,%lf\n",X0,X1,X2,X3,Fx1,Fx2,length);
 */
if(fabs(Fx2) < fabs(Fx1))
    {
        length = X3 - X1;
        X0 = X1;
        X1 = X2;
        X2 = X0 + step2*length;
        Fx1 = Fx2;
        Yresult = X2;
        Fnum = 2;
/*          printf("testY < testlow\n"); */
    }
else
    {
        length = X2-X0;
        X3 = X2;
        X2 = X1;
        X1 = X0 + step1*length;
        Fx2 = Fx1;
        Yresult = X1;
        Fnum = 1;
/*          printf("testY>testlow\n"); */
    }
    numiter = 1;

/* printf("X0,X1,X2,X3,Fx1,Fx2,length are,
%lf,%lf,%lf,%lf,%lf,%lf,%lf\n",X0,X1,X2,X3,Fx1,Fx2,length); */
/* }while(fabs(length)>0.0005 && fabs(testY)>0.0005);*/
}while(fabs(testY)>0.0005);
```

```
/* printf("C1,C2,C3 are %lf %lf %lf\n",C1,C2,C3); */
/* printf("ga,ra,ba,A,Aa Q Qw are %lf %lf %lf %lf %lf %lf %lf %lf
\n",Ga,Ra,Ba,A,Aa,Q,Qw); */

/* printf("rorw,gogw,bobw are %lf %lf %lf\n",rorw,gogw,bobw); */

xyz[0][2] = bbb;
xyz[0][1] = Yresult;
xyz[0][0] = ((rrr+0.07868*bbb)*1.18340-0.68898*(ggg-0.04641*bbb))/rowcolumn;

XXX = xyz[0][0];
YYY = xyz[0][1];
ZZZ = xyz[0][2];

}

double fn(c)
double c;
{
double pow();
double p;
p= 40 * pow(c,0.73) /(pow(c,0.73) + 2);
return(p);
}

double inverse_fn(c)
double c;
{
double pow();
double p;
p = 2.0/(40.0/c-1.0);
p= pow(p,1.0/0.73);
```

```

/* p= 40 * pow(c,0.73) /(pow(c,0.73) + 2); */
return(p);
}

double es_factor(hue,es,hs)
double hue,*es,*hs;
{
double H[5],sh[5],e[5];
double shs,de,nu;
int i,j;
H[0] = 0.0,   H[1] = 100.0, H[2] = 200.0, H[3] = 300.0, H[4] = 400.0;
sh[0] = 20.14, sh[1] = 90.0, sh[2]=164.25, sh[3]=237.53, sh[4]=380.14;
e[0] = 0.8,   e[1] = 0.7, e[2] = 1.0, e[3] = 1.2, e[4] = 0.8;

shs = hue;

for(j=0;j<5;j++)
{
    if (shs >= H[j] && shs < H[j+1])
        i=j;
}

de = (hue-H[i])*(sh[i]*e[i+1]-sh[i+1]*e[i]) - 100.0*sh[i]*e[i+1];
de = de/((hue-H[i])*(e[i+1]-e[i])-100.0*e[i+1]);
*hs = de;
*es = e[i] + ( e[i+1] - e[i] )*( de - sh[i] ) / (sh[i+1] -sh[i]);

/* printf("es i hs Hue are %lf %d %lf %lf \n",*es,i,*hs,hue); */
return (1.0);
}

```

```
double es_factor_w(C1,C2,C3,es,angle,hue)
double C1,C2,C3,*hue,*es,*angle;
{
double H[5],sh[5],e[5];
double shs,de,nu;
int i,j;
H[0] = 0.0, H[1] = 100.0, H[2] = 200.0, H[3] = 300.0, H[4] = 400.0;
sh[0] = 20.14, sh[1] = 90.0, sh[2]=164.25, sh[3]=237.53, sh[4]=380.14;
e[0] = 0.8,   e[1] = 0.7, e[2] = 1.0, e[3] = 1.2, e[4] = 0.8;

nu = (C2-C3)/9.0;
de = C1 - C2/11.0;
if(fabs(de) < 0.0001)
{
    if(nu > 0.0)
        shs = 90.0;
    else
        shs = 270.0;
}
else
{
shs = atan(fabs(nu)/fabs(de));
shs = shs * 180.0/3.1415;
if ( fabs(nu) < 0.0001)
{
    if(de < 0.0)
        shs = shs + 180.0;
}

if(nu > 0 && de <0 )
shs = 180.0 - shs ;
else
```

```
if(nu < 0 && de < 0 )
shs = shs + 180.0;
else
if(nu < 0 && de > 0 )
shs = 360.0 - shs ;

/* if (shs>0.0 && shs<sh[0])
* shs = shs + 360.0;
*/
}
shs = shs;
i = 0;
for(j=0;j<5;j++)
{
    if (shs>= sh[j] && shs < sh[j+1])
        i=j;
}

*es = e[i] + ( e[i+1] - e[i] )*( shs - sh[i] ) / (sh[i+1] -sh[i]);

/* A.10 Calculate H ( Hue response) */
*hue = H[i] +(100.0*(shs-sh[i])/e[i])/((shs-sh[i])/e[i] +(sh[i+1]-shs)/e[i+1]);
*angle = shs;
/* printf("es i angle Hue are %lf %d %lf %lf \n",*es,i,*angle,*hue); */
return (1.0);
}
```

Table 2.1 The chromaticity coordinates of the CIE illuminants.

Illuminant	x	y
=====		
A	0.4476	0.4074
B	0.3484	0.3516
C	0.3101	0.3162
D65	0.3127	0.3290
D50	0.3457	0.3586
=====		

Table 2.2 Values of k4 to k8 for Eq.(2.14.)

h (degrees)	k4	k5	k6	k7	k8 (degrees)
0-49	133.87	-134.50	-0.924	1.727	340
49-110	11.78	-12.70	-0.218	2.120	333
110-269.5	13.87	10.93	0.140	1.000	83
269.5-360	0.14	5.23	0.170	1.610	233

Table 3.1 Overview of the experimental conditions studied[illegible]

Table 3.2 CIE specifications of the light source and background used in Experiment 1 with the standard deviation (SD) of the TSR measurement results (Luminance (L) in cd/m²).

	x	y	L(cd/m ²)
Illuminant	0.3562	0.3710	43.5
Background	0.3288	0.3469	9.57
SD	0.00034	0.00038	0.52

Table 3.3 Summary of the experimental conditions in Experiment 1.

Phase	Light Source	Luminance	Sample Group	No of Observers	No of Colours	No of Estimations	Scaling Attributes
1	D50	43	Set A	8	20	480	L, C, H *
2	D50	43	Set B	8	20	480	L, C, H
3	D50	43	Set A	8	20	480	L, C, H
4	D50	43	Set B	8	20	480	L, C, H
Total						1920	

* Note: L, C, H represent Lightness, Colourfulness, and Hue.

Table 3.4 Summary of the experimental conditions in Experiment 2.

Phase	Light Source	Y% of Background	Luminance of RW (cd/m ²)	Border	No of Colours	No of Observers	No of Estimation
1	D50	15.9	high (2259)	white	98	7	2058
2	D50	17.1	medium (689)	white	98	8	2352
3	D50	16.7	low (325)	white	98	7	2058
4	D50	17.4	medium + flare (670)	white	98	7	2058
5	D50	9.6	high (1954)	black	98	8	2352
6	D50	9.5	medium (619)	black	98	7	2058
7	D50	9.8	low (319)	black	98	8	2352
8	D50	9.4	medium + flare (642)	white paper	98	8	2352
9	D50	17.1	medium (689)	white	98	6	1764
10	D50	9.6	medium (658)	white	98	7	2058
11	D50	17.5	medium (680)	black	98	7	2058
Total							22668

Table 3.5 Colour measurement results for the viewing conditions in Experiment 2
(Luminance (L) in cd/m^2)

Phase	Illuminator	Reference	Background	Border					SD(%)	
				White	left	right	bottom	top		Mean
1	x	0.3564	0.3649	0.3727	0.3536	0.3532	0.3534	0.3532	0.3534	4
	y	0.3771	0.3920	0.3964	0.3731	0.3727	0.3723	0.3722	0.3726	
	L	3986	2259	360	3395	3615	3390	3346	3437	
2	x	0.3563	0.3665	0.3713	0.3535	0.3542	0.3570	0.3570	0.3554	26
	y	0.3757	0.3931	0.3966	0.3700	0.3716	0.3762	0.3761	0.3735	
	L	1218	689	118	1526	1531	978	953	1247	
3	x	0.3559	0.3661	0.3707	0.3541	0.3546	0.3577	0.3582	0.3562	26
	y	0.3780	0.3964	0.3961	0.3741	0.3758	0.3807	0.3812	0.3779	
	L	591	325	54	799	811	514	496	655	
4	x	0.3577	0.3698	0.3627	0.3540	0.3546	0.3574	0.3576	0.3559	27
	y	0.3777	0.3974	0.3953	0.3713	0.3723	0.3766	0.3766	0.3742	
	L	1310	670	116	1729	1735	1095	1060	1405	
5	x	0.3552	0.3690	0.3739	-	-	-	-	-	
	y	0.3761	0.3955	0.3875	-	-	-	-	-	
	L	3673	1954	186	-	-	-	-	-	
6	x	0.3546	0.3674	0.3716	-	-	-	-	-	
	y	0.3749	0.3942	0.3880	-	-	-	-	-	
	L	1148	619	59	-	-	-	-	-	
7	x	0.3544	0.3673	0.3734	-	-	-	-	-	
	y	0.3786	0.3974	0.3926	-	-	-	-	-	
	L	590	318	31	-	-	-	-	-	
8	x	0.3583	0.3714	0.3737	0.3567	0.3584	0.3566	0.3568	0.3571	47
	y	0.3793	0.3979	0.3875	0.3781	0.3779	0.3777	0.3777	0.3779	
	L	1273	642	60	304	328	143	127	225	
10	x	0.3574	0.3676	0.3743	0.3552	0.3536	0.3571	0.3558	0.3552	27
	y	0.3774	0.3954	0.3921	0.3703	0.3718	0.3764	0.3748	0.3733	
	L	1140	658	63	1551	1563	996	951	1265	
11	x	0.3570	0.3670	0.3724	-	-	-	-	-	
	y	0.3768	0.3945	0.4006	-	-	-	-	-	
	L	1175	680	119	-	-	-	-	-	
Side Light										
Phase	x	y	L (cd/m ²)							
4	0.3566	0.3774	2453							
8	0.3566	0.3774	2453							

Table 3.6 Variation of colour measurement for reference white and the Illuminator in Experiment 2 (luminance (L) in cd/m^2).

Phase	Reference White				Illuminator			
	x(SD)	y(SD)	L(SD)	L(SD%)	x(SD)	y(SD)	L(SD)	L(SD%)
1	0.0008	0.0012	59.20	2.62	0.0008	0.0012	107.20	2.69
2	0.0005	0.0005	4.97	0.72	0.0005	0.0005	5.23	0.43
3	0.0008	0.0007	8.77	2.70	0.0005	0.0006	11.20	1.89
4	0.0005	0.0004	5.38	0.80	0.0007	0.0009	34.50	2.63
5	0.0004	0.0007	70.00	3.58	0.0012	0.0022	132.90	3.61
6	0.0005	0.0009	12.50	2.00	0.0010	0.0015	22.60	1.96
7	0.0005	0.0009	1.40	0.40	0.0009	0.0011	9.50	1.60
8	0.0059	0.0045	9.80	1.50	0.0052	0.0042	14.80	1.16
10	0.0006	0.0008	5.30	0.80	0.0008	0.0011	12.70	1.12
11	0.0006	0.0006	4.90	0.70	0.0006	0.0007	12.60	1.07

Table 3.7 Summary of experimental conditions of Experiment 3.

Phase	Light Source (Colour Temperature)	Y% of Background	Luminance of RW	No of Colours	No of Observers	No of Estimations	Viewing Pattern
1	Halogen (4000 K)	18.88	High (113 cd/m^2)	99	6	1782	1*
2	Xenon (5600 K)	19.18	Low (47 cd/m^2)	99	6	1782	1
3	Halogen (4000 K)	18.91	Low (45 cd/m^2)	99	6	1782	1
4	Halogen (4000 K)	18.88	High (113 cd/m^2)	99	6	1782	1
5	Halogen (4000 K)	16.00	High (75 cd/m^2)	95	5	1425	2*
6	Halogen (4105 K)	16.00	High (75 cd/m^2)	36	5	540	2
Total						9093	

*Note: Viewing pattern 1 is that the test colour, reference white, and reference colourfulness were placed closely in the centre triangle, and further apart in viewing pattern 2.

Table 3.8 Colour measurement results for the viewing conditions in Experiment 3
(Luminance (L) is in the unit of cd/m^2).

Phase		Open Gate	Reference White	Reference Colourfulness	Background	Colour Temperature
1,4	x	0.3879	0.3887	0.4051	0.3768	4000K
	y	0.4088	0.4184	0.5120	0.4217	
	L	190	113	71	21	
2	x	0.3297	0.3307	0.3607	0.3145	5600K
	y	0.3692	0.3814	0.5110	0.3879	
	L	81	47	29	9	
3	x	0.3888	0.3889	0.4060	0.3778	4000K
	y	0.4098	0.4201	0.5129	0.4231	
	L	78	45	28	9	
5	x	0.3928	0.3810	0.3942	0.3725	4000K
	y	0.4109	0.4062	0.5125	0.3938	
	L	187	75	40	12	
6	x	0.3897	0.3833	0.3942	0.3670	4000K
	y	0.4097	0.4021	0.5125	0.3834	
	L	204	75	40	12	

Table 3.9 The standard deviation for open gate, reference white, reference colourfulness, and background by in Experiment 3 (luminance (L) in cd/m^2).

Phase	x(SD)	y(SD)	L(SD)	L(SD%)	x(SD)	y(SD)	L(SD)	L(SD%)
Open Gate					Reference White			
1,4	0.0015	0.0013	1.40	0.74	0.0007	0.0004	2.77	2.46
2	0.0007	0.0005	1.95	2.41	0.0011	0.0007	1.18	2.50
3	0.0006	0.0004	1.98	2.54	0.0013	0.0007	1.29	2.58
5	0.0056	0.0026	4.73	2.53	0.0009	0.0008	1.24	1.66
6	0.0003	0.0005	5.43	2.66	0.0012	0.0006	1.48	1.97
Reference Colourfulness					Background			
1,4	0.0012	0.0009	1.42	2.00	0.0016	0.0016	0.80	3.77
2	0.0012	0.0009	0.87	2.96	0.0011	0.0017	0.47	5.16
3	0.0013	0.0012	0.85	2.95	0.0011	0.0014	0.37	4.31
5	0.0013	0.0008	0.61	1.51	0.0018	0.0010	0.32	2.96
6	0.0013	0.0008	0.61	1.51	0.0006	0.0010	0.34	2.86

Table 3.10 Summary of the experimental conditions in Experiment 4.

Phase	Light Source	Y% Background	Scaled Attributes	Luminance of RW (cd/m^2)	No of Colours	No of Observers	No of Estimations
1	D50	21.8	L, C, H *	843.1	40	4	480
2	D50	23.5	L, C, H	200.3	40	4	480
3	D50	23.4	L, C, H	61.9	40	4	480
4	D50	22.3	L, C, H	16.6	40	4	480
5	D50	23.2	L, C, H	6.2	40	4	480
6	D50	19.2	L, C, H	0.4	40	4	480
7	D50	21.8	B, C, H *	843.1	40	4	480
8	D50	22.5	B, C, H	200.3	40	4	480
9	D50	23.4	B, C, H	61.9	40	4	480
10	D50	22.3	B, C, H	16.6	40	4	480
11	D50	23.2	B, C, H	6.2	40	4	480
12	D50	19.2	B, C, H	0.4	40	4	480
Total							5,760

* Note: L, C, H standard for Lightness, Colourfulness, and Hue,
B, C, H standard for Brightness, Colourfulness, and Hue.

Table 3.11 The colour measurement results of the BaSO₄ tile, reference white, and background in Experiment 4 (luminance (L) in cd/m²).

	<u>BaSO₄</u>			<u>Reference White</u>			<u>Background</u>		
	x	y	L	x	y	L	x	y	L
Phase 1 & 7	0.3411	0.3607	1006.4	0.3484	0.3713	843.1	0.3331	0.3570	221.7
Phase 2 & 8	0.3446	0.3671	271.8	0.3506	0.3751	200.3	0.3362	0.3588	47.0
Phase 3 & 9	0.3488	0.3638	82.8	0.3502	0.3711	61.9	0.3354	0.3565	14.5
Phase 4 & 10	0.3432	0.3660	21.9	0.3504	0.3743	16.5	0.3375	0.3624	3.7
Phase 5 & 11	0.3432	0.3654	8.7	0.3510	0.3774	6.2	0.3356	0.3634	1.5
Phase 6 & 12	0.3393	0.3779	0.50	0.3487	0.3840	0.38	0.3287	0.3740	0.07

Table 3.12 The standard deviation of colour measurement for reference white in Experiment 4.

	<u>Reference White</u>			
	x(SD)	y(SD)	L(SD)	L(SD%)
Phase 1 & 7	0.0011	0.0021	20.12	2.38
Phase 2 & 8	0.0004	0.0028	18.02	9.00
Phase 3 & 9	0.0013	0.0048	5.78	9.33
Phase 4 & 10	0.0010	0.0024	1.10	6.66
Phase 5 & 11	0.0012	0.0048	0.78	12.53
Phase 6 & 12	0.0011	0.0098	0.06	14.81

Table 3.13 Colour measurement results of the reference white, background, and reference colourfulness samples in Experiment 5.

	x	y	Y	L (cd/m ²)
Illuminant	0.3050	0.3232	100.00	50.00
Background	0.3052	0.3232	18.42	9.21
Reference Colourfulness	0.3755	0.3002	26.44	13.00

Table 3.14 CIE chromaticity coordinates x, y, and Y of the 13 test colours as well as corresponding L*,C*,and Hue from CIE L*a*b* uniform colour space in Experiment 5.

x	y	Y	L*	C*	Hue	Colour Name
0.4832	0.3342	18.4186	50.0	50.0	30.0	Red
0.4467	0.4598	18.4186	50.0	50.0	87.0	Yellow
0.2686	0.4277	18.4186	50.0	40.0	155.0	Green
0.2089	0.2428	18.4186	50.0	30.0	253.0	Blue
0.3051	0.3232	18.4186	50.0	0.1	----	Grey
0.4443	0.3573	2.9890	20.0	20.0	42.0	RRY
0.4658	0.4193	40.7494	70.0	60.0	70.0	YYR
0.3963	0.4696	76.3034	90.0	70.0	104.0	YYG
0.3044	0.5129	56.6813	80.0	80.0	138.0	GGY
0.2820	0.3453	56.6813	80.0	20.0	170.0	GGB
0.2552	0.3044	6.2359	30.0	10.0	219.0	BBG
0.1851	0.1452	2.9890	20.0	40.0	294.0	BBR
0.4065	0.2819	6.2359	30.0	30.0	2.0	RRB

Table 3.15 CIE chromaticity coordinates x , y , Y of the 37 induction field colours as well as corresponding L^* , C^* , and Hue from CIE $L^*a^*b^*$ uniform colour space for Experiment

5.					
x	y	Y	L^*	C^*	Hue
0.3052	0.3231	100.00	100.0	0.1	----
0.3052	0.3231	40.74	70.0	0.1	----
0.3051	0.3232	18.41	50.0	0.1	----
0.3050	0.3232	6.23	30.0	0.1	----
0.3044	0.3235	0.55	5.0	0.1	----
0.4422	0.3358	40.74	70.0	50.0	30.0
0.4832	0.3342	18.41	50.0	50.0	30.0
0.5136	0.3312	11.25	40.0	50.0	30.0
0.5552	0.3248	6.23	30.0	50.0	30.0
0.4519	0.3783	40.74	70.0	50.0	53.0
0.4929	0.3857	18.41	50.0	50.0	53.0
0.5218	0.3881	11.25	40.0	50.0	53.0
0.5391	0.3882	8.49	35.0	50.0	53.0
0.4090	0.4246	56.68	80.0	50.0	87.0
0.4195	0.4346	40.74	70.0	50.0	87.0
0.4320	0.4462	28.12	60.0	50.0	87.0
0.4467	0.4598	18.41	50.0	50.0	87.0
0.3489	0.4450	56.68	80.0	50.0	120.0
0.3564	0.4784	28.12	60.0	50.0	120.0
0.3603	0.5023	18.41	50.0	50.0	120.0
0.3620	0.5169	14.54	45.0	50.0	120.0
0.2815	0.3921	56.68	80.0	40.0	155.0
0.2686	0.4277	18.41	50.0	40.0	155.0
0.2606	0.4493	11.25	40.0	40.0	155.0
0.2552	0.4637	8.49	35.0	40.0	155.0
0.2559	0.3391	56.68	80.0	30.0	184.0
0.2432	0.3430	28.12	60.0	30.0	184.0
0.2341	0.3458	18.41	50.0	30.0	184.0
0.2220	0.3494	11.25	40.0	30.0	184.0
0.2367	0.2671	56.68	80.0	30.0	253.0
0.2203	0.2529	28.12	60.0	30.0	253.0
0.2089	0.2428	18.41	50.0	30.0	253.0
0.1942	0.2296	11.25	40.0	30.0	253.0
0.3298	0.2468	40.74	70.0	50.0	335.0
0.3355	0.2278	18.41	50.0	50.0	335.0
0.3394	0.2143	11.25	40.0	50.0	335.0
0.3444	0.1965	6.23	30.0	50.0	335.0

Table 4.1 Characteristics of observers who took part in the experiments studied in this thesis

Observer	Experience	Age	Sex
XG	moderate	28	F
SH	high	30	F
SS	none	33	F
HML	moderate	31	F
RJ	none	26	F
MCL	none	30	F
RL	high	35	M
JX	moderate	28	M
SC	none	30	M
WY	moderate	35	M

Table 4.2 Comparison of the mean visual data between two repeated assessments in Experiment 1

Set		A	B
L	r	0.99	0.99
	CV	5	4
C	r	0.95	0.97
	CV	14	13
H	r	1.00	1.00
	CV	2	3

Table 4.3 Individual observer accuracy performance in Experiment 1 using r and CV measures

			Observer	XG	SH	SS	RJ	JX	RL	SC	WY	Mean
Set	Phase		<u>Lightness</u>									
A	1	r	0.99	0.98	0.98	0.97	0.98	0.96	0.84	0.98	0.96	
		CV	5	8	11	10	17	11	18	8	11	
B	2	r	0.96	0.95	0.99	0.96	0.99	0.96	0.96	0.98	0.97	
		CV	17	11	12	11	6	12	10	11	11	
A	3	r	0.98	0.98	0.96	0.97	0.96	0.99	0.94	0.95	0.97	
		CV	12	13	14	20	12	12	16	15	14	
B	4	r	0.94	0.97	-	0.97	0.98	0.98	0.93	0.94	0.96	
		CV	13	23	-	20	7	9	15	14	14	
Mean CV			12	14	12	17	11	11	15	12	13	
Set	Phase		<u>Colourfulness</u>									
A	1	r	0.89	0.90	0.87	0.90	0.87	0.97	0.88	0.95	0.90	
		CV	21	19	23	18	23	11	22	12	19	
B	2	r	0.93	0.91	0.90	0.96	0.84	0.96	0.86	0.90	0.91	
		CV	15	19	19	14	23	12	21	18	18	
A	3	r	0.96	0.96	0.96	0.93	0.92	0.95	0.97	0.94	0.95	
		CV	19	14	21	22	26	16	13	20	19	
B	4	r	0.92	0.92	-	0.89	0.80	0.96	0.93	0.84	0.89	
		CV	17	22	-	24	27	13	20	29	22	
Mean CV			18	19	21	20	25	13	19	20	20	
Set	Phase		<u>Hue</u>									
A	1	r	0.99	1.00	0.99	0.99	0.99	1.00	0.99	1.00	0.99	
		CV	10	7	6	6	6	5	8	5	7	
B	2	r	0.99	1.00	0.99	1.00	1.00	1.00	1.00	1.00	1.00	
		CV	7	7	7	3	5	4	6	4	5	
A	3	r	1.00	1.00	1.00	1.00	1.00	1.00	0.99	0.99	1.00	
		CV	4	6	5	5	5	3	6	8	5	
B	4	r	1.00	1.00	-	1.00	1.00	1.00	1.00	0.99	1.00	
		CV	4	5	-	5	5	4	6	7	5	
Mean CV			6	6	6	5	5	4	7	6	6	

Table 4.4 The b factors and their range variations in Experiment 1

Observer		XG	SH	SS	RJ	JX	RL	SC	WY	Mean
		<u>Lightness</u>								
Set	Phase									
A	1	1.06	1.05	1.05	1.13	1.15	0.82	0.77	0.98	
B	2	1.05	0.89	1.07	0.88	1.05	1.00	0.96	1.11	
A	3	0.85	0.99	1.12	1.18	0.79	1.01	1.11	0.94	
B	4	0.99	1.00	-----	1.13	0.94	1.11	0.93	0.91	
Range variation(%)		21.1	16.3	6.5	27.8	33.3	29.4	36.1	20.3	23.9
		<u>Colourfulness</u>								
Set	Phase									
A	1	1.05	0.70	0.84	0.86	0.78	1.18	0.72	0.82	
B	2	0.98	0.90	1.05	0.66	0.78	1.08	0.89	1.01	
A	3	0.70	0.64	0.74	0.83	1.63	1.22	0.77	0.68	
B	4	0.89	0.69	-----	0.78	0.88	0.90	0.54	0.85	
Range variation(%)		38.5	35.6	35.2	25.6	83.3	29.1	47.9	39.3	41.8
		<u>Hue</u>								
Set	Phase									
A	1	1.08	0.98	1.01	1.02	0.98	0.98	0.98	0.98	
B	2	0.99	1.00	0.98	1.03	1.02	0.99	1.03	0.97	
A	3	0.98	0.99	1.00	0.98	1.00	1.02	0.97	1.05	
B	4	1.03	1.01	-----	1.00	1.00	1.00	0.99	0.98	
Range variation(%)		4.9	3.0	3.0	5.0	4.0	3.0	6.1	7.0	4.5

Table 4.5 The performance of observer's repeatability in Experiments 2 and 3.
Parentheses indicate that results are not significantly different from 1 for gradient
(b) and intercept (a).

		<u>Experiment 2</u>	<u>Experiment 3</u>
	X	Phase 2	Phase 1
	Y	Phase 9	Phase 4
L			
(nonconstrained)			
	r	0.98	0.99
	CV(o)	7	7
	CV(s)	7	6
	b	1.05	(1.02)
	a	-2	(1)
(constrained)			
	CV(s)	7	6
	b	(1.00)	(0.97)
	a	(0.0)	(3)
C			
	r	0.95	0.98
	CV(o)	11	9
	CV(s)	11	8
	b	(1.02)	(0.97)
H			
	r	1.00	1.00
	CV(o)	3	4

Table 4.6 Individual observer accuracy performance in Experiment 2 using r and CV measures.

		<u>Lightness</u>								
Observer		XG	SH	SS	HML	JX	RL	SC	WY	Mean
Phase										
1	r	0.96	0.96	0.84	0.93	0.94	0.95	0.95	-	0.93
	CV	19	12	19	16	14	13	23	-	16
2	r	-	0.95	0.92	-	0.94	0.96	0.93	0.92	0.93
	CV	-	12	19	-	13	15	19	14	16
3	r	0.96	0.96	0.94	0.93	0.95	0.97	0.96	-	0.95
	CV	19	15	15	21	16	13	13	-	16
4	r	0.96	0.97	0.95	0.95	0.96	0.97	0.95	-	0.96
	CV	12	16	19	20	17	13	13	-	16
5	r	0.95	0.93	0.93	0.93	0.96	0.94	0.94	0.91	0.94
	CV	13	14	20	20	17	13	10	15	15
6	r	0.95	0.95	0.91	0.91	0.94	0.95	-	0.91	0.93
	CV	12	18	20	17	16	13	-	13	16
7	r	0.96	0.97	0.94	0.91	0.94	0.96	0.93	0.93	0.94
	CV	14	11	16	21	17	14	13	14	15
8	r	0.96	0.95	0.95	0.93	0.95	0.96	0.95	0.92	0.95
	CV	12	16	16	22	13	14	12	16	15
9	r	0.97	0.97	0.96	0.95	0.93	0.97	0.95	0.95	0.96
	CV	12	9	17	17	19	12	13	14	14
10	r	0.97	0.96	-	0.93	0.95	0.95	0.96	0.93	0.95
	CV	13	14	-	15	12	12	15	12	13
11	r	0.95	0.97	-	0.94	0.94	0.96	0.96	0.94	0.95
	CV	10	9	-	13	13	14	10	11	11
Mean	CV	13	13	18	18	15	13	14	14	15

To be continued

Colourfulness

Observer		XG	SH	SS	HML	JX	RL	SC	WY	Mean
Phase										
1	r	0.90	0.92	0.87	0.91	0.92	0.90	0.88	-	0.90
	CV	17	16	20	17	16	17	19	-	17
2	r	-	0.92	0.81	-	0.90	0.94	0.83	0.89	0.88
	CV	-	17	24	-	17	13	22	18	19
3	r	0.90	0.92	0.90	0.89	0.90	0.93	0.86	-	0.89
	CV	19	17	26	20	19	16	23	-	20
4	r	0.94	0.92	0.88	0.89	0.88	0.94	0.87	-	0.90
	CV	14	16	20	19	20	14	21	-	18
5	r	0.92	0.93	0.94	0.89	0.92	0.95	0.93	0.90	0.92
	CV	16	16	15	19	16	14	16	18	16
6	r	0.92	0.88	0.91	0.88	0.91	0.95	-	0.90	0.91
	CV	14	18	15	18	16	12	-	16	15
7	r	0.92	0.92	0.90	0.89	0.91	0.92	0.92	0.90	0.91
	CV	15	16	18	18	17	16	16	18	17
8	r	0.93	0.93	0.87	0.89	0.90	0.94	0.87	0.88	0.90
	CV	15	15	20	19	18	14	20	19	17
9	r	0.93	0.90	0.91	0.94	0.91	0.93	0.88	0.89	0.91
	CV	16	19	17	14	18	15	20	19	17
10	r	0.93	0.92	-	0.92	0.92	0.94	0.91	0.90	0.92
	CV	14	15	-	14	14	12	15	15	14
11	r	0.94	0.91	-	0.90	0.92	0.92	0.92	0.90	0.92
	CV	13	17	-	17	15	15	15	17	16
Mean	CV	15	17	19	18	17	15	18	18	17

To be continued

		<u>Hue</u>								
Observer		XG	SH	SS	HML	JX	RL	SC	WY	Mean
Phase										
1	r	1.00	0.99	0.99	0.99	1.00	1.00	0.99	-	0.99
	CV	5	6	7	7	5	5	7	-	6
2	r	-	1.00	0.99	-	1.00	1.00	0.99	0.99	0.99
	CV	-	5	7	-	5	5	7	7	6
3	r	1.00	0.99	0.99	1.00	1.00	1.00	0.99	-	0.99
	CV	5	7	8	5	5	6	8	-	6
4	r	1.00	1.00	0.99	1.00	0.99	0.99	0.99	-	0.99
	CV	5	5	9	5	6	7	8	-	6
5	r	1.00	0.99	0.99	1.00	1.00	1.00	0.99	0.99	0.99
	CV	5	6	7	5	4	5	9	6	6
6	r	1.00	0.99	0.99	0.99	1.00	1.00	-	0.99	0.99
	CV	5	7	9	6	5	6	-	7	6
7	r	1.00	1.00	0.99	0.99	1.00	0.99	0.99	0.99	0.99
	CV	5	6	8	7	5	6	9	7	7
8	r	1.00	1.00	0.99	0.99	1.00	1.00	0.99	0.99	0.99
	CV	5	6	7	6	5	6	8	7	6
9	r	1.00	1.00	0.99	1.00	1.00	1.00	0.99	0.99	0.99
	CV	4	5	8	5	5	5	8	7	6
10	r	1.00	1.00	-	1.00	1.00	1.00	0.99	1.00	1.00
	CV	5	5	-	5	5	5	8	7	6
11	r	0.99	1.00	-	1.00	1.00	1.00	0.99	1.00	1.00
	CV	6	5	-	5	5	5	9	5	6
Mean	CV	5	6	8	6	5	6	8	7	6

Table 4.7 Individual observer accuracy performance in Experiment 3 using r and CV measures.

Observer Phase		XG	SH	HML	JX	RL	WY	Mean
<u>Lightness</u>								
1	r	0.95	0.95	0.92	0.95	0.95	0.89	0.94
	CV	11	24	18	11	18	17	17
2	r	0.95	0.95	0.95	0.95	0.94	0.91	0.94
	CV	13	24	17	13	19	17	17
3	r	0.95	0.96	0.96	0.95	0.96	0.93	0.95
	CV	12	26	15	13	16	14	16
4	r	0.96	0.95	0.94	0.96	0.96	0.93	0.95
	CV	11	23	15	11	15	13	15
5	r	0.98	0.96	-	0.97	0.97	0.92	0.96
	CV	12	25	-	13	15	16	16
6	r	0.98	0.97	-	0.98	0.96	0.95	0.97
	CV	12	16	-	11	17	13	14
Mean	CV	12	23	16	12	15	13	16
<u>Colourfulness</u>								
1	r	0.91	0.93	0.86	0.90	0.92	0.92	0.91
	CV	16	14	20	17	15	16	16
2	r	0.92	0.91	0.94	0.89	0.89	0.90	0.91
	CV	16	17	13	18	19	18	17
3	r	0.93	0.93	0.92	0.92	0.95	0.94	0.93
	CV	15	15	16	16	13	14	15
4	r	0.92	0.92	0.91	0.91	0.96	0.94	0.93
	CV	15	16	17	17	12	13	15
5	r	0.92	0.95	-	0.89	0.95	0.96	0.93
	CV	17	14	-	20	14	13	16
6	r	0.96	0.96	-	0.94	0.97	0.97	0.96
	CV	16	17	-	22	13	14	16
Mean	CV	16	16	17	18	14	15	16
<u>Hue</u>								
1	r	1.00	1.00	1.00	1.00	1.00	1.00	1.00
	CV	6	6	7	6	6	7	6
2	r	1.00	0.99	1.00	1.00	1.00	0.99	1.00
	CV	5	7	7	4	6	7	6
3	r	0.99	0.99	1.00	1.00	1.00	0.99	1.00
	CV	7	7	6	5	6	8	6
4	r	1.00	1.00	1.00	1.00	1.00	0.99	1.00
	CV	6	7	7	5	5	8	6
5	r	0.99	1.00	-	1.00	1.00	0.99	0.99
	CV	8	6	-	5	5	8	7
6	r	0.99	1.00	-	0.99	1.00	0.98	0.99
	CV	8	7	-	10	5	13	8
Mean	CV	7	7	7	6	6	9	7

Table 4.8 Comparison of mean results between different luminances phases in Experiment 2. Paratheses indicate that results are not significantly different from 1 for gradient (b) and 0 for intercept (a).

Y (Phase)	1	1	2	5	5	6
L(cd/m ²)	2259	2259	689	1954	1954	619
X (Phase)	2	3	3	6	7	7
L(cd/m ²)	689	325	325	619	319	319

Lightness

(nonconstrained)

r	0.99	0.99	0.99	0.98	0.98	0.98
CV(o)	10	9	7	10	10	7
CV(s)	6	6	6	6	6	6
b	0.90	0.89	(0.98)	(1.03)	0.93	0.89
a	8	8	(0)	3	8	5

(constrained)

CV(s)	6	6	6	7	6	7
b	0.93	0.94	(1.01)	(0.92)	0.92	(1.00)
a	7	6	-1	8	8	(0)

Colourfulness

r	0.93	0.93	0.95	0.98	0.93	0.96
CV(o)	13	15	11	12	13	10
CV(s)	12	12	10	12	13	9
b	(1.04)	1.09	(1.04)	(0.99)	(1.04)	(1.04)

Hue

r	0.998	0.999	0.999	0.996	0.996	0.999
CV(o)	3	2	3	5	5	3

Table 4.9 Comparison of mean visual results between phases 1 (high luminance) and 3 (low luminance) in Experiment 3. Parentheses indicate that results are not significantly different from 1 for b and o for a.

X	Phase 1
Y	Phase 3

Lightness

(nonconstrained)	
r	0.98
CV(o)	7
CV(s)	7
b	0.96
a	3
(constrained)	
CV(s)	7
b	(0.98)
a	2

Colourfulness

r	0.94
CV(o)	11
CV(s)	9
b	1.06

Hue

r	0.99
CV(o)	3

Table 4.10 Comparison of mean visual results between two phases with different viewing parameters in Experiment 2. Parentheses indicate that results are not significantly different from 1 for gradient (b) and intercept (a) at 95% confidence interval

X (Phase)	2 (off)	2 (17%)	11 (17%)	2 (white)	10 (White)
Y (Phase)	4 (on)	10 (10%)	6 (10%)	11 (black)	6 (black)
parameter	Flare light	Y% of background	Y% of background	Border	Border
<u>Lightness</u>					
(nonconstrained)					
r	0.99	0.98	0.99	0.98	0.98
CV(o)	9	10	7	11	6
CV(s)	6	6	5	6	5
b	1.06	0.85	(1.00)	0.81	0.96
a	(0)	9	0	11	3
(constrained)					
CV(s)	7	7	5	7	5
b	(0.96)	0.95	0.99	0.94	0.98
a	4	5	(1)	6	2
<u>Colourfulness</u>					
r	0.95	0.94	0.95	0.88	0.92
CV(o)	11	14	13	16	11
CV(s)	11	12	9	16	11
b	1.03	1.08	1.10	(0.97)	(0.99)
<u>Hue</u>					
r	0.999	0.998	0.997	0.999	0.999
CV(o)	3	4	4	3	3

Table 4.11 The lightness and hue estimates of some selected achromatic and chromatic samples from phases 2, 6, 10, and 11 in Experiment 2 (Each group with identical luminance factor). The numerical values in parentheses are the colourfulness response

Luminance Factor (Y%)	Sample Number	Perceived Lightness								Hue
		Phase 2		Phase 6		Phase 10		Phase 11		
1.36	98	6	(0)	9	(0)	8	(0)	9	(0)	Neutral
	12	12	(19)	21	(33)	15	(26)	21	(30)	89B11G
	80	13	(20)	21	(36)	17	(29)	23	(35)	96R4B
8.64	97	41	(0)	45	(0)	43	(0)	44	(0)	Neutral
	93	47	(59)	52	(56)	50	(62)	48	(57)	100R
17.45	96	51	(0)	59	(0)	56	(0)	57	(0)	Neutral
	65	51	(32)	51	(34)	53	(37)	53	(28)	78Y22R
24.71	95	70	(0)	79	(0)	77	(0)	80	(0)	Neutral
	52	72	(30)	69	(34)	69	(34)	68	(24)	70R30Y

Table 4.12 Testing colour spaces and models using visual data in Experiment 2.
The lightness results from Hunt91 model were computed using Nb=25. MCV
represent CV values calculated using mean SF.

Phase	1	2	3	4	5	6	7	8	9	10	11	Mean
Border	W	W	W	W	B	B	B	B	W	W	B	
Luminance	2259	689	325	670	1954	619	319	642	689	658	680	
Yof bg	15.9	17.1	16.7	17.4	9.6	9.5	9.8	9.4	17.1	9.6	17.5	
Flare	off	off	off	Flare	off	off	off	Flare	off	off	off	

LIGHTNESS

CMC

r	0.97	0.97	0.97	0.98	0.96	0.96	0.98	0.97	0.98	0.97	0.96	0.97
CV	13	23	19	20	9	14	11	19	22	17	16	16

CIE

r	0.96	0.96	0.97	0.96	0.95	0.96	0.97	0.96	0.97	0.96	0.96	0.96
CV	22	15	16	18	28	22	23	18	15	19	21	20

Nayatani

r	0.95	0.95	0.97	0.96	0.94	0.96	0.96	0.96	0.97	0.97	0.96	0.96
CV	22	16	16	18	28	22	23	17	15	18	21	20

Hunt91

r	0.95	0.95	0.96	0.94	0.94	0.95	0.95	0.94	0.96	0.96	0.96	0.96
CV	30	27	29	30	33	29	31	25	28	26	32	29

CHROMA

CMC

r	0.86	0.88	0.88	0.94	0.87	0.86	0.88	0.90	0.90	0.92	0.85	0.89
CV	20	19	21	15	21	17	19	18	19	15	21	19
SF	1.60	1.56	1.46	1.69	1.61	1.61	1.62	1.54	1.62	1.68	1.45	1.58
MCV	21	19	22	18	21	21	19	18	19	17	23	20

CIE L*a*b*

r	0.83	0.86	0.86	0.93	0.86	0.85	0.85	0.87	0.88	0.88	0.81	0.86
CV	24	22	23	16	22	22	22	21	21	290	25	21
SF	0.86	0.87	0.81	0.97	0.88	0.88	0.84	0.92	0.86	0.93	0.78	0.88
MCV	24	21	24	19	22	22	23	22	21	22	28	22

CIE L*u*v*

r	0.79	0.81	0.84	0.83	0.76	0.79	0.80	0.86	0.87	0.84	0.80	0.82
CV	27	26	24	25	30	27	27	23	22	24	21	26
SF	0.87	0.85	0.82	0.92	0.88	0.88	0.86	0.90	0.85	0.92	0.79	0.87
MCV	27	22	26	25	30	30	27	24	22	24	28	26

To be continued

Phase	1	2	3	4	5	6	7	8	9	10	11	Mean
<u>Nayatani</u>												
r	0.90	0.83	0.88	0.84	0.81	0.90	0.91	0.90	0.89	0.86	0.90	0.87
CV	17	19	24	25	18	16	18	18	22	17	16	20
SF	0.54	0.62	0.65	0.69	0.52	0.63	0.68	0.67	0.61	0.67	0.57	0.62
MCV	23	22	25	27	26	20	20	20	22	19	18	22

<u>Hunt91</u>												
r	0.93	0.92	0.91	0.90	0.90	0.92	0.93	0.93	0.93	0.94	0.94	0.92
CV	15	16	20	19	19	14	16	16	19	13	14	17
SF	0.66	0.66	0.64	0.71	0.68	0.71	0.70	0.72	0.65	0.74	0.61	0.68
MCV	16	19	21	20	19	20	17	17	19	15	18	18

COLOURFULNESS

<u>Nayatani</u>												
SF	0.41	0.55	0.65	0.61	0.40	0.56	0.68	0.59	0.54	0.59	0.50	0.55
MCV	40	24	29	27	45	20	27	19	22	18	18	28

<u>Hunt91</u>												
r	0.78	0.80	0.83	0.86	0.69	0.70	0.72	0.83	0.85	0.81	0.71	0.78
SF	0.66	0.80	0.87	0.86	0.67	0.84	0.93	0.84	0.80	0.87	0.74	0.81
CV	27	25	25	22	33	31	31	25	23	25	31	27
MSF	36	23	26	23	40	35	34	26	23	26	32	30

HUE

<u>Nayatani</u>												
r	0.99	0.99	0.99	0.99	0.99	0.99	0.99	0.99	0.99	0.99	0.99	0.99
CV	8	7	9	8	8	9	10	9	7	8	7	8

<u>Hunt91</u>												
r	1.00	1.00	0.99	0.99	0.99	0.99	0.99	0.99	1.00	0.99	0.99	0.99
CV	8	6	9	7	7	8	8	8	6	6	7	7

Table 4.13 Testing various spaces and models using visual data in Experiment 3.
MCV represent CV values calculated using mean SF.

Phase	1	2	3	4	5	6	Mean
Y of bg	18.88	19.18	18.91	18.88	14.65	15.58	
Luminance in cd/m^2	113	47	45	113	75	75	
LIGHTNESS							
CMC							
r	0.97	0.97	0.97	0.98	0.96	0.97	0.97
CV	37	41	40	32	36	24	35
CIE							
r	0.95	0.95	0.96	0.95	0.94	0.97	0.95
CV	20	20	19	17	20	13	18
Nayatani							
r	0.94	0.95	0.95	0.95	0.95	0.96	0.95
CV	21	22	21	19	21	13	20
Hunt91 (Nb = 10)							
r	0.93	0.94	0.94	0.93	0.93	0.96	0.94
CV	23	21	23	22	23	20	22
Hunt 91 (Nb = 10, z = 1.2)							
r	0.94	0.95	0.95	0.94	0.94	0.96	0.95
CV	20	19	19	18	20	14	18
CHROMA							
CMC							
r	0.89	0.92	0.93	0.92	0.90	0.95	0.92
CV	18	17	16	17	20	20	18
SF	1.49	1.38	1.42	1.45	1.52	1.52	1.43
MCV	18	18	16	17	21	21	19
CIE L*a*b*							
r	0.88	0.91	0.92	0.91	0.88	0.95	0.91
SF	0.80	0.73	0.76	0.78	0.80	0.84	0.77
CV	19	18	17	17	21	18	18
MCV	0	18	17	17	21	19	19

To be continued

Phase	1	2	3	4	5	6	Mean
CHROMA							
<u>CIE L*u*v*</u>							
r	0.85	0.91	0.86	0.87	0.87	0.94	0.88
SF	0.68	0.61	0.66	0.67	0.68	0.70	0.67
CV	27	20	26	25	26	21	24
MCV	27	21	26	25	27	21	25
<u>Nayatani</u>							
r	0.61	0.74	0.54	0.58	0.63	0.79	0.65
SF	0.82	0.92	0.93	0.79	0.86	0.88	0.87
CV	34	28	35	35	36	36	34
MCV	34	29	36	37	36	36	35
<u>Hunt91</u>							
r	0.82	0.91	0.84	0.83	0.82	0.93	0.86
SF	0.65	0.63	0.64	0.63	0.67	0.65	0.64
CV	22	17	23	22	25	27	23
MCV	22	18	23	23	27	27	23
COLOURFULNESS							
<u>Nayatani</u>							
SF	0.98	1.30	1.33	0.95	1.12	1.15	1.14
MCV	38	31	38	41	36	36	37
<u>Hunt91</u>							
r	0.76	0.79	0.80	0.79	0.80	0.85	0.80
SF	0.83	0.92	0.95	0.81	0.87	0.87	0.88
CV	30	29	27	27	31	31	29
MCV	31	29	29	30	31	31	30
HUE							
<u>Nayatani</u>							
r	0.99	0.99	0.98	0.98	0.97	0.98	0.98
CV	12	11	12	12	13	8	11
<u>Hunt91</u>							
r	0.99	0.99	0.99	0.99	0.98	0.98	0.99
CV	11	10	12	12	13	8	11

Table 4.14 Performance of the Modified Hunt91 model tested using visual data in Experiment 2.

Phase	1	2	3	4	5	6	7	8	9	10	11	Mean
Border	W	W	W	W	B	B	B	B	W	W	B	
Luminance	2259	689	325	670	1954	619	319	642	689	658	680	
Yof bg	15.9	17.1	16.7	17.4	9.6	9.5	9.8	9.4	17.1	9.6	17.5	
Flare	off	off	off	Flare	off	off	off	Flare	off	off	off	

LIGHTNESS(Nb = 25)

z	1	1	1	1	0.85	0.85	0.85	0.85	1	0.85	1	
CV	10	10	9	12	10	9	8	11	10	10	12	10
Original												
CV	30	27	29	30	33	29	31	25	28	26	32	29

CHROMA($F_p = F_y = F_\beta = 1$)

CV	15	16	19	17	18	14	15	17	13	14	18	16
----	----	----	----	----	----	----	----	----	----	----	----	----

($\rho_D = \gamma_D = \beta_D = 0$)

CV	16	17	20	17	19	15	16	17	13	15	19	17
----	----	----	----	----	----	----	----	----	----	----	----	----

Original

CV	16	19	21	20	19	20	17	17	19	15	18	18
----	----	----	----	----	----	----	----	----	----	----	----	----

COLOURFULNESS($F_p = F_y = F_\beta = 1$)

CV	38	25	27	24	41	32	35	27	25	27	34	31
----	----	----	----	----	----	----	----	----	----	----	----	----

($\rho_D = \gamma_D = \beta_D = 0$)

CV	36	25	29	24	40	33	36	29	25	28	35	32
----	----	----	----	----	----	----	----	----	----	----	----	----

Original

CV	36	23	26	23	40	35	34	26	23	26	32	30
----	----	----	----	----	----	----	----	----	----	----	----	----

HUE($F_p = F_y = F_\beta = 1$)

CV	6	6	6	5	6	6	6	7	5	5	6	6
----	---	---	---	---	---	---	---	---	---	---	---	---

($\rho_D = \gamma_D = \beta_D = 0$)

CV	6	7	7	6	7	6	6	7	5	6	7	7
----	---	---	---	---	---	---	---	---	---	---	---	---

Original

CV	8	6	9	7	7	8	8	8	6	6	7	7
----	---	---	---	---	---	---	---	---	---	---	---	---

Table 4.15 performance of the Modified Hunt91 model tested using visual data in Experiment 3.

Phase	1	2	3	4	5	6	Mean
Y of bg	18.88	19.18	18.91	18.88	14.65	15.58	
Luminance in cd/m ²	113	47	45	113	75	75	

LIGHTNESS

Modified Hunt91 (Nb = 10, z = 1.2)

$$J_{new} = J_{old} \left[\left(1 - \left(\frac{J_{old}}{100} \right)^3 \right) 1.14 + \left(\frac{J_{old}}{100} \right)^5 \right]$$

CV	13	13	13	11	13	10	12
Original	23	21	23	22	23	20	22

CHROMA

$(F_p = F_y = F_\beta = 1)$ CV	19	16	19	20	24	22	20
-----------------------------------	----	----	----	----	----	----	----

$(\rho_D = \gamma_D = \beta_D = 0)$ CV	17	19	16	17	19	20	18
Original	22	18	23	23	27	27	23

COLOURFULNESS

$(F_p = F_y = F_\beta = 1)$ CV	34	30	32	32	36	35	33
-----------------------------------	----	----	----	----	----	----	----

$(\rho_D = \gamma_D = \beta_D = 0)$ CV	31	33	30	29	31	32	31
Original	31	29	29	30	31	31	30

HUE

$(F_p = F_y = F_\beta = 1)$ CV	7	7	9	8	10	9	8
-----------------------------------	---	---	---	---	----	---	---

$(\rho_D = \gamma_D = \beta_D = 0)$ CV	7	7	7	7	7	7	7
Original	11	10	12	12	13	8	11

Table 4.16 Summary of the spaces and models performance in CV values using visual data in Experiment 2 (cut-sheet transparency)

Model	Lightness	Colourfulness	Chroma	Hue
CMC(1:1)	16		20	
CIEL*a*b*	20		22	
CIEL*u*v*	20		26	
Nayatani	20	28	22	8
Hunt'91	29	30	18	7
Hunt'91	10	31	16	6
(z=1 or 0.85, $F_{\rho} = F_{\gamma} = F_{\beta} = 1$)				

Table 4.17 Summary of the spaces and models performance in CV values using visual data in Experiment 3 (35mm projection).

Model	Lightness	Colourfulness	Chroma	Hue
CMC(1:1)	35		19	
CIEL*a*b*	18		19	
CIEL*u*v*	18		25	
Nayatani	20	37	35	11
Hunt91	22	30	23	11
Hunt91	12	31	18	7
(Jnew, $\rho = \gamma = \beta = 0$)				

Table 4.18 Individual observers accuracy performance in Experiment 4 using r and CV measures.

Observer			XG	RL	JX	WY	Mean
L	Phase						
(cd/m ²)							
<u>Lightness</u>							
843	1	r	0.97	0.97	0.97	0.97	0.97
		CV	8	8	8	11	9
200	2	r	0.98	0.97	0.97	0.92	0.96
		CV	8	9	8	14	10
62	3	r	0.97	0.96	0.96	0.94	0.96
		CV	8	9	8	12	9
17	4	r	0.98	0.97	0.98	0.97	0.98
		CV	7	9	6	9	8
6	5	r	0.99	0.98	0.98	0.96	0.98
		CV	10	11	10	12	11
0.4	6	r	0.99	0.98	0.99	0.98	0.98
		CV	10	10	9	11	10
	Mean CV		9	9	8	12	10
<u>Brightness</u>							
843	7	r	0.96	0.98	0.97	0.95	0.96
		CV	8	7	8	9	8
200	8	r	0.98	0.97	0.97	0.91	0.96
		CV	7	8	8	14	9
62	9	r	0.98	0.97	0.97	0.94	0.96
		CV	8	8	9	13	10
17	10	r	0.98	0.98	0.96	0.92	0.96
		CV	8	6	10	14	10
6	11	r	0.99	0.98	0.94	0.93	0.96
		CV	6	8	14	13	10
0.4	12	r	0.98	0.98	0.96	0.96	0.97
		CV	7	8	13	13	10
	Mean CV		7	8	11	13	10

To be continued

Observer		XG	RL	JX	WY	Mean
Phase		<u>Hue</u>				
1	r	1.00	1.00	1.00	0.99	0.99
	CV	6	4	4	6	5
2	r	0.99	1.00	1.00	0.99	1.00
	CV	5	5	4	6	5
3	r	0.99	1.00	1.00	0.99	1.00
	CV	7	4	4	7	5
4	r	0.99	1.00	0.99	0.98	0.99
	CV	7	4	6	10	7
5	r	0.99	1.00	1.00	0.98	0.99
	CV	7	3	5	10	7
6	r	0.99	0.99	0.99	0.99	0.99
	CV	6	6	7	7	7
7	r	0.99	0.99	0.99	0.99	0.99
	CV	7	6	5	6	6
8	r	0.99	0.99	1.00	0.99	0.99
	CV	7	5	5	8	6
9	r	1.00	1.00	1.00	0.99	0.99
	CV	5	4	4	7	5
10	r	0.99	0.99	0.99	0.99	0.99
	CV	7	6	6	8	7
11	r	1.00	0.99	1.00	0.99	0.99
	CV	4	5	5	7	5
12	r	0.99	0.98	0.97	0.99	0.98
	CV	7	8	7	7	7
Mean CV		6	5	5	9	6

To be continued

Observer		XG	RL	JX	WY	Mean
Phase						
		<u>Colourfulness</u>				
1	r	0.95	0.97	0.93	0.93	0.95
	CV	15	12	17	19	16
2	r	0.97	0.97	0.97	0.96	0.96
	CV	13	14	14	15	14
3	r	0.96	0.96	0.96	0.94	0.95
	CV	15	16	15	18	16
4	r	0.97	0.95	0.94	0.96	0.96
	CV	17	15	18	14	15
5	r	0.97	0.96	0.93	0.94	0.94
	CV	16	17	21	19	18
6	r	0.95	0.92	0.93	0.85	0.91
	CV	22	27	25	34	27
7	r	0.95	0.98	0.97	0.95	0.96
	CV	15	10	13	16	14
8	r	0.96	0.98	0.96	0.97	0.97
	CV	15	10	15	12	13
9	r	0.96	0.98	0.95	0.95	0.96
	CV	14	10	17	16	14
10	r	0.97	0.97	0.96	0.95	0.96
	CV	13	14	15	16	15
11	r	0.96	0.98	0.95	0.95	0.93
	CV	14	10	17	16	14
12	r	0.94	0.95	0.95	0.88	0.93
	CV	20	19	18	27	21
Mean CV		15	14	17	19	16

Table 4.19 Exponent factors for colourfulness and brightness in Experiment 4.

Colourfulness					
Phase	XG	RL	JX	WY	Mean
1	0.77	0.97	0.77	1.11	
2	0.81	1.11	0.84	0.94	
3	0.83	1.08	0.93	0.85	
4	0.83	1.07	0.90	0.86	
5	0.76	1.28	0.76	0.94	
6	0.85	1.28	0.95	0.87	
Mean	0.81	1.13	0.86	0.93	
Range variation(%)	11.1	12.4	20.9	28.0	18.1
Brightness					
7	1.05	0.78	1.06	0.83	
8	0.85	1.01	1.03	1.25	
9	0.82	1.08	1.26	0.99	
10	0.89	1.02	1.39	0.90	
11	0.81	0.98	1.04	0.89	
12	0.90	0.91	1.38	0.84	
Mean	0.89	0.96	1.19	0.95	
Range variation(%)	27.0	31.3	30.3	44.2	33.1

Table 4.20 Performance of observer's repeatiability using Experiment 4 colourfulness and hue results

[illegible]

Table 4.21 Comparison of mean visual results between the highest and the other luminance levels. Parentheses indicate the result is not significantly different from 1 for gradient (b) and 0 for intercept (a).

Y (Combined phase)		1	1	1	1	1
X (Combined phase)		2	3	4	5	6
Lightness						
(nonconstrained)	CV(o)	6	7	7	10	17
	CV(s)	5	5	4	5	6
	b	(0.96)	(0.96)	0.90	0.87	0.77
	a	5	5	9	12	20
(constrained)	CV(s)	5	5	4	5	7
	b	(0.94)	(0.94)	0.93	0.89	0.82
	a	6	6	7	11	18
Brightness						
	CV(o)	25	45	47	57	75
	CV(s)	8	9	10	11	12
	b	1.09	1.23	1.44	1.64	2.32
	a	29	36	34	44	57
Colourfulness						
	CV(o)	7	14	20	27	59
	CV(s)	6	8	10	14	25
	b	(0.98)	1.12	1.20	1.27	2.05
Hue						
	CV(o)	3	3	3	4	9

Table 4.22 Testing of colour spaces and models using visual results (combined phases 1 to 6) in Experiment 4. MCV represents the CV values calculated using mean SF.

CP	1	2	3	4	5	6	Mean of 6 phases	Mean of 5 phases
LIGHTNESS								
<u>CMC</u>								
r	0.95	0.96	0.96	0.98	0.97	0.94	0.96	
CV	29	37	38	38	39	48	38	36
<u>CIE</u>								
r	0.95	0.96	0.95	0.97	0.96	0.94	0.96	
CV	11	14	15	16	16	23	16	14
<u>Nayatani</u>								
r	0.94	0.96	0.94	0.97	0.96	0.93	0.95	
CV	13	16	18	18	18	25	18	17
<u>Hunt91 (Nb=75)</u>								
r	0.95	0.95	0.94	0.96	0.96	0.93	0.95	
CV	14	13	14	12	14	17	14	13
BRIGHTNESS								
<u>Nayatani</u>								
r	0.95	0.96	0.97	0.98	0.96	0.93	0.97	
SF	2.05	1.95	1.80	2.21	2.21	2.02	2.04	2.04
CV	9	9	9	8	11	17	12	
MCV	9	10	17	11	14	17	13	12
<u>Hunt91</u>								
r	0.96	0.97	0.97	0.99	0.97	0.94	0.97	
SF	4.33	4.18	3.76	4.39	4.29	3.97	4.15	4.19
CV	8	9	9	7	11	16	11	
MCV	9	9	14	9	11	16	11	10

To be continued

CP	1	2	3	4	5	6	Mean of 6 phases	Mean of 5 phases
CHROMA								
<u>CMC</u>								
r	0.96	0.94	0.95	0.94	0.91	0.86	0.93	
CV	18	20	18	20	25	36	23	
SF	1.81	1.81	1.58	1.48	1.34	0.78	1.47	1.60
MCV	20	22	16	21	33	122	39	22
<u>CIE L*a*b*</u>								
r	0.94	0.92	0.94	0.92	0.86	0.81	0.91	
SF	1.04	1.03	0.89	0.84	0.75	0.43	0.83	0.91
CV	20	23	20	21	29	36	25	
MCV	24	26	20	25	37	127	43	26
<u>CIE L*u*v*</u>								
r	0.92	0.93	0.94	0.91	0.92	0.89	0.92	
SF	0.81	0.82	0.70	0.66	0.62	0.38	0.67	0.72
CV	22	21	20	24	22	28	23	
MCV	25	25	39	26	29	105	42	29
<u>Nayatani</u>								
r	0.92	0.92	0.89	0.85	0.81	0.72	0.86	
SF	0.88	1.12	1.19	1.46	1.53	1.25	1.24	1.24
CV	21	21	25	29	32	42	28	
MCV	49	25	25	32	32	42	34	33
<u>Hunt91</u>								
r	0.96	0.96	0.97	0.95	0.94	0.78	0.92	
SF	0.80	0.81	0.72	0.71	0.70	0.57	0.72	0.75
CV	15	15	15	19	21	39	21	
MCV	17	17	16	18	27	52	25	19
COLOURFULNESS								
<u>Nayatani</u>								
SF	0.77	1.20	1.59	2.52	3.15	3.66	2.15	1.85
MCV	158	63	30	40	36	69	66	65
<u>Hunt91</u>								
r	0.95	0.92	0.94	0.93	0.90	0.73	0.89	
SF	0.76	0.96	1.04	1.28	1.47	2.22	1.29	1.10
CV	16	21	17	19	24	42	23	
MCV	52	26	18	24	26	69	36	29
HUE								
<u>Nayatani</u>								
r	0.99	0.99	0.97	0.95	0.95	0.94	0.97	
CV	6	7	12	18	17	17	13	
<u>Hunt91</u>								
r	1.00	1.00	0.99	0.99	1.00	0.99	0.99	
CV	6	6	6	8	7	13	8	

Table 4.23 Summary of the performance of the spaces and models with CV values using visual results in Experiment 4.

Combined phase	1	2	3	4	5	6	Mean	Mean
Y of Background	22	24	23	22	23	19	of 6	of 5
Luminance (cd/m ²)	843	200	62	17	6	0.4	phases	phases
Lightness								
CMC(1:1)	27	23	33	35	37	44	35	31
CIE 1976	11	14	15	16	16	23	16	14
Nayatani	13	16	18	18	18	25	18	17
Hunt91	14	13	14	12	14	17	14	13
Brightness SF								
Nayatani	2.04	9	10	17	11	14	17	13
Hunt91	4.15	9	9	14	9	11	16	11
Chroma SF								
CMC(1:1)	1.60	20	22	16	21	33	122	39
CIEL*a*b*	0.91	24	26	20	25	37	127	43
CIEL*u*v*	0.72	25	25	39	26	29	105	42
Nayatani	1.24	49	25	25	32	32	42	34
Hunt91	0.75	17	17	16	18	27	52	25
Colourfulness SF								
Nayatani	1.85	158	63	30	40	36	69	66
Hunt91	1.10	52	26	18	24	26	69	36
Hue								
Nayatani		6	7	12	18	17	17	13
Hunt91		6	6	6	8	7	13	8

Table 4.24 Performance of individual observers' accuracy using r and CV measures in Experiment 5.

Observer	XG	SH	MCL	RL	JX	WY	Mean
<u>Lightness</u>							
r	0.96	0.96	0.97	0.96	0.97	0.94	0.96
CV	16	23	21	14	10	17	17
<u>Colourfulness</u>							
r	0.92	0.93	0.88	0.91	0.95	0.94	0.92
CV	22	21	26	24	19	19	22
<u>Hue</u>							
r	0.99	0.99	0.99	0.99	0.99	0.98	0.99
CV	8	9	8	8	9	10	9

Table 4.25 Testing of performance of Hunt91 model with CV values using results in Experiment 5.

$$N_b=25, \quad z=1+\left(\frac{Y_b}{Y_w}\right)^{\frac{1}{2}}$$

p	0	-0.5	0	-0.5	0	-0.5	0	-0.5
Test colour		Red		RRY		YYR		Yellow
Lightness	16	12	40	32	9	11	13	7
Colourfulness	12	12	51	57	10	12	14	10
SF	0.63	0.65	0.24	0.22	0.73	0.75	0.70	0.70
Hue	25	19	60	236	33	41	33	36
Test colour		YYG		GGY		Green		GGB
Lightness	18	21	7	14	19	16	9	12
Colourfulness	12	9	9	12	17	15	27	45
SF	0.40	0.25	0.71	0.65	0.58	0.52	0.55	0.55
Hue	13	28	1	5	4	5	4	4
Test colour		Grey		Combined				
Lightness	22	22		18	18			
Colourfulness	-	-		26	35			
SF	-	-		0.65	0.60			
Hue	-	-		13	21			

Table 4.26 Summary of observers' accuracy performance using CV values

Experiment	Media	Lightness	Brightness	Colourfulness	Hue
1	Reflection sample	13	-	20	6
2	Transparency	15	-	17	6
3	35mm Projection	16	-	16	7
4	Reflection Sample	10	10	16	6
5	monitor colour	17	-	22	9
	Mean	14	10	18	7

Table 4.27 Summary of performance of colour space and models using CV values

Model	Experiment Number	<u>Lightness</u> CV	<u>Brightness</u> CV SF	<u>Chroma</u> CV	<u>Colourfulness</u> CV	<u>Hue</u> CV
<u>CMC(1:1)</u>						
	2	16	-	20	-	-
	3	35	-	19	-	-
	4	35	-	39	-	-
<u>CIE L*a*b*</u>						
	2	20	-	22	-	-
	3	18	-	19	-	-
	4	16	-	43	-	-
<u>CIE L*u*v*</u>						
	2	20	-	26	-	-
	3	18	-	25	-	-
	4	16	-	42	-	-
<u>Nayatani</u>						
	2	20	-	20	28	8
	3	20	-	35	37	11
	4	18	13, 2.04	34	66	12
<u>Hunt91</u>						
	2	29	-	17	27	7
	3	22	-	23	30	11
	4	14	11, 4.15	25	36	8
<u>Modified Hunt91</u>						
	2	10	-	16	31	6
	3	12	-	18	31	7

Table 4.28 Mean scaling factors (SF) used for scaling chroma and colourfulness predictions in Experiments 2 to 4.

Experiments media	2 cut-sheet	3 35mm-slide	4 (Mean of 5) Reflection
Chroma			
CMC(1:1)	1.58	1.43	1.60
CIEL*a*b*	0.88	0.77	0.91
CIEL*u*v*	0.87	0.67	0.72
Nayatani	0.62	0.87	1.24
Hunt91	0.68	0.64	0.75
Colourfulness			
Nayatani	0.55	1.14	1.85
Hunt91	0.81	0.88	1.10

Table 4.29 The comparison between Experiments 2 to 4 colourfulness data and those predicted by the Hunt91 and revised Hunt models. MCV represents CV value calculated using mean SF

Transparency Sample Experiment (Experiment 2)

Phase	1	2	3	4	5	6	7	8	10	11	Mean
SF	0.60	0.63	0.64	0.69	0.60	0.67	0.68	0.68	0.69	0.59	0.65
CV	15	17	19	16	19	14	16	15	17	12	16
MCV	18	17	19	18	21	15	17	16	17	14	19
Original CV	36	23	26	23	40	35	34	26	26	32	30

35mm Projected Slide Experiment (Experiment 3)

Phase	1	2	3	4	5	6	Mean
SF	0.63	0.61	0.62	0.62	0.65	0.62	0.63
CV	22	17	23	23	20	27	22
MCV	22	18	23	23	21	27	22
<u>($\rho_D = \rho_D = \rho_D = 0$)</u>							
SF	0.63	0.60	0.60	0.60	0.61	0.64	0.61
CV	17	18	16	16	17	19	17
MCV	17	19	16	17	18	19	18
Original CV	31	29	29	30	31	31	30

Reflection Sample Experiment (Experiment 4)

CP	1	2	3	4	5	6	Mean of 5	Mean of 6
SF	0.80	0.88	0.83	0.86	0.88	0.87	0.85	0.85
CV	15	15	15	16	21	39	16	20
MCV of 5	19	15	16	17	22	41	18	22
MCV of 6	17	16	16	17	21	39	17	21
Original CV	52	26	18	24	26	69	29	36

Table 4.30 Testing of the reversibility of the forward and reverse Hunt models using the Munsell data set

Luminance	500	40	2	500	40	2	500	40	2	Mean
Y% of										
Background	100	100	100	20	20	20	2	2	2	
Mean $ x - x' \cdot 10^5$	6	6	5	6	5	30	6	30	100	20
Mean $ y - y' \cdot 10^5$	10	10	10	10	10	10	10	10	20	10
Mean $ Y - Y' \cdot 10^3$	1	1	0.9	4	9	10	2	5	6	40
Mean $\Delta E_{(LAB)}$	0.013	0.013	0.013	0.016	0.018	0.08	0.014	0.076	0.31	0.061
Mean $\Delta E_{(LUV)}$	0.014	0.014	0.014	0.016	0.021	0.10	0.015	0.089	0.38	0.074
Mean $\Delta E_{(CMC)}$	0.010	0.010	0.010	0.012	0.014	0.04	0.012	0.039	0.14	0.032

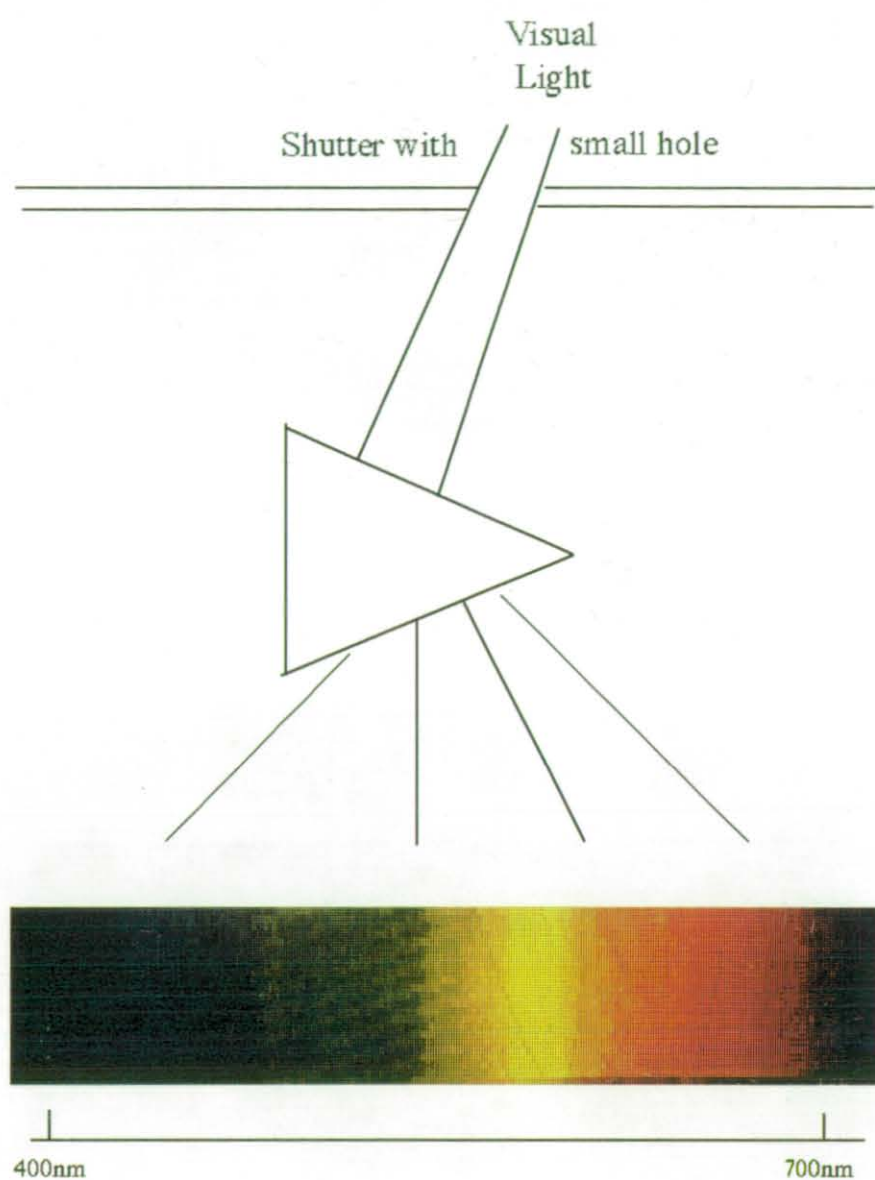


Figure 2.1 Newton's experiment in 1666 [22].

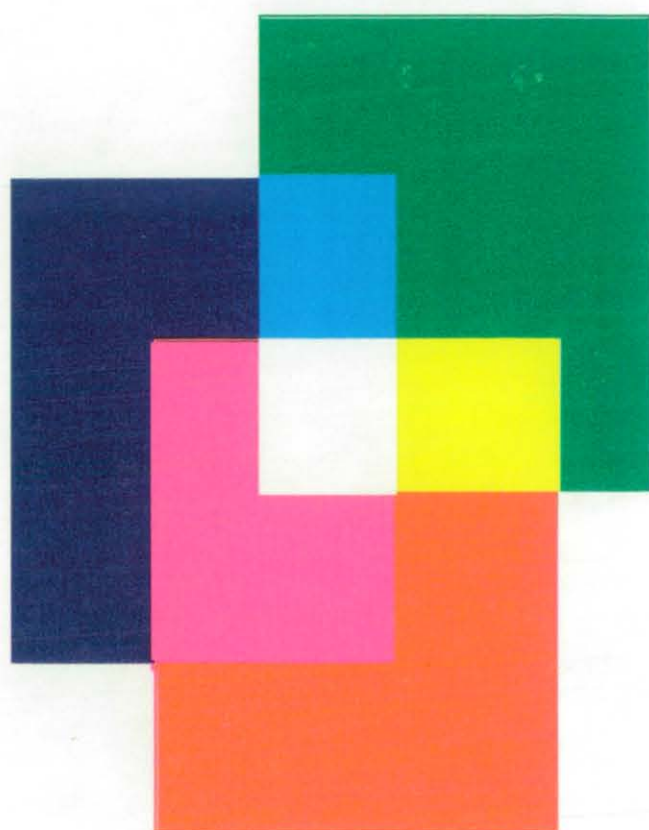


Figure 2.2 An illustration of the result of additive colour mixing.

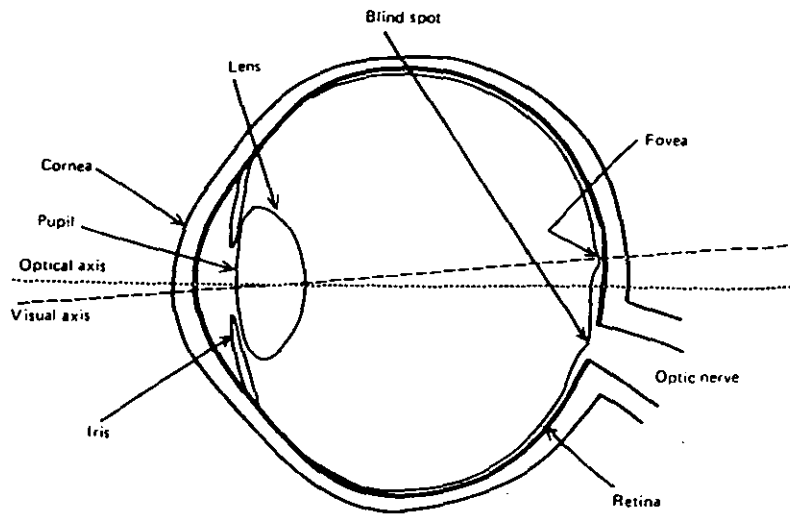


Figure 2.3 Cross-section of a human's eye^[16]

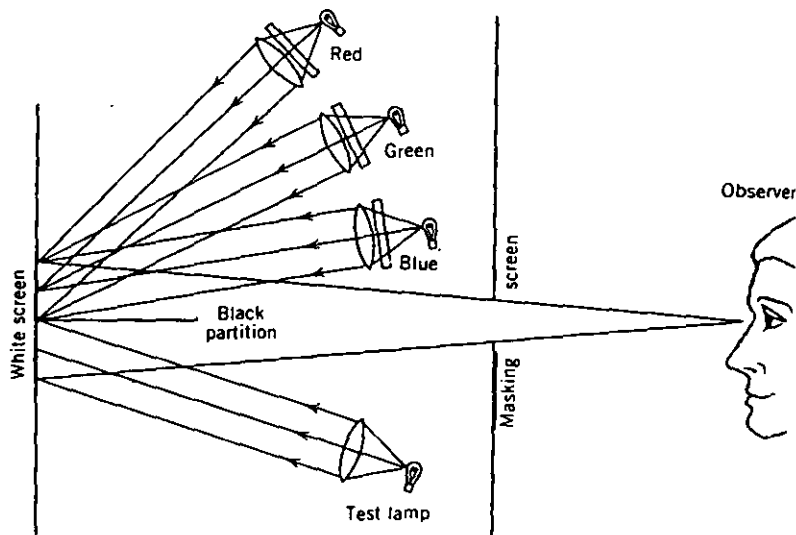


Figure 2.4 A visual arrangement for producing a colour by mixing the light from three different coloured lamps^[2]

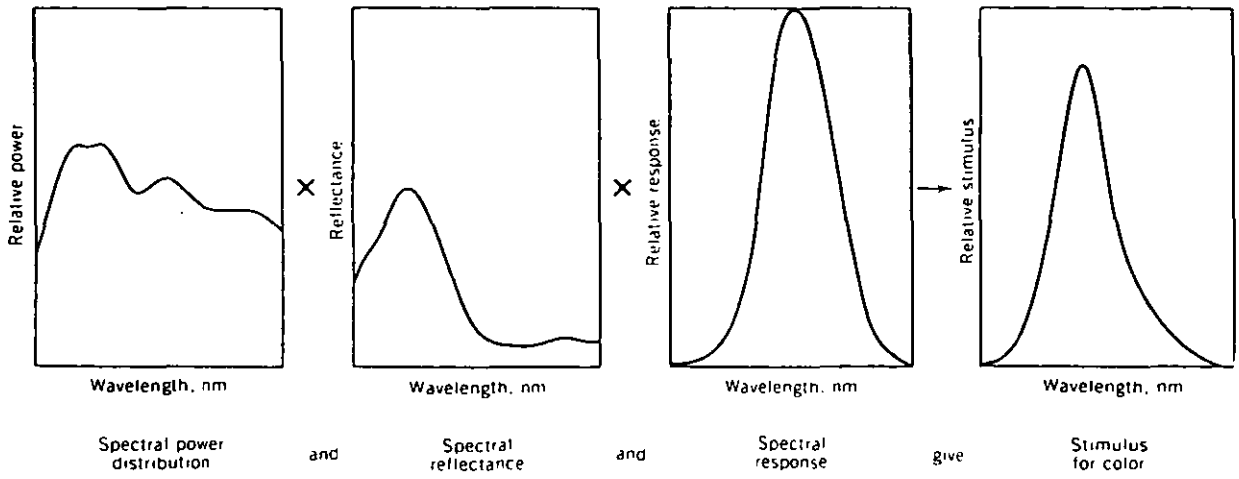


Figure 2.5 Quantitative definition of a stimulus^[2]

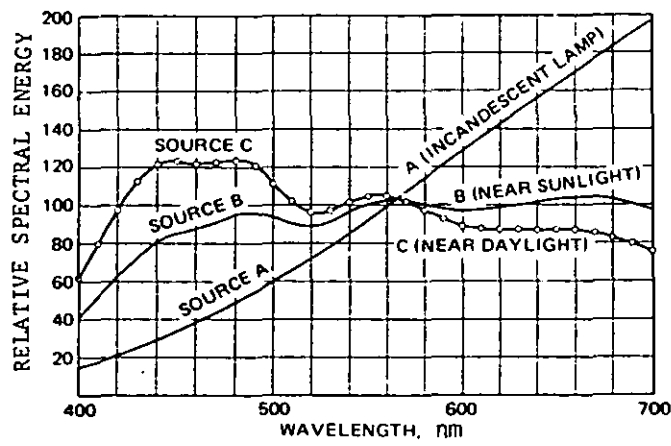


Figure 2.6 The spectral power distribution of CIE sources A, B and C^[46]

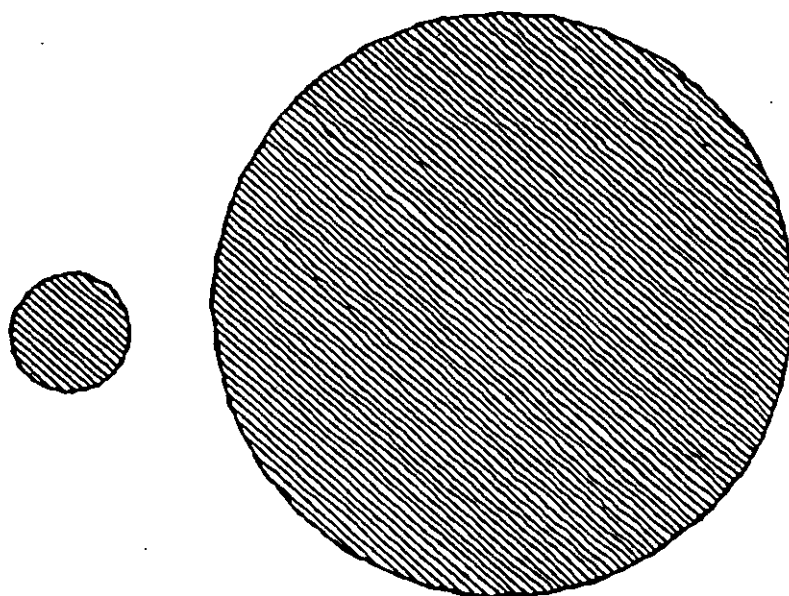


Figure 2.7 The actual sample size of 2° field and 10° field seen at a normal distance of 45 cm (18in)^[2]. The circle on the left represents the 2° field on which the 1931 CIE standard observer is based. The figure on the right is the 10° field on which the 1964 CIE standard observer is based.

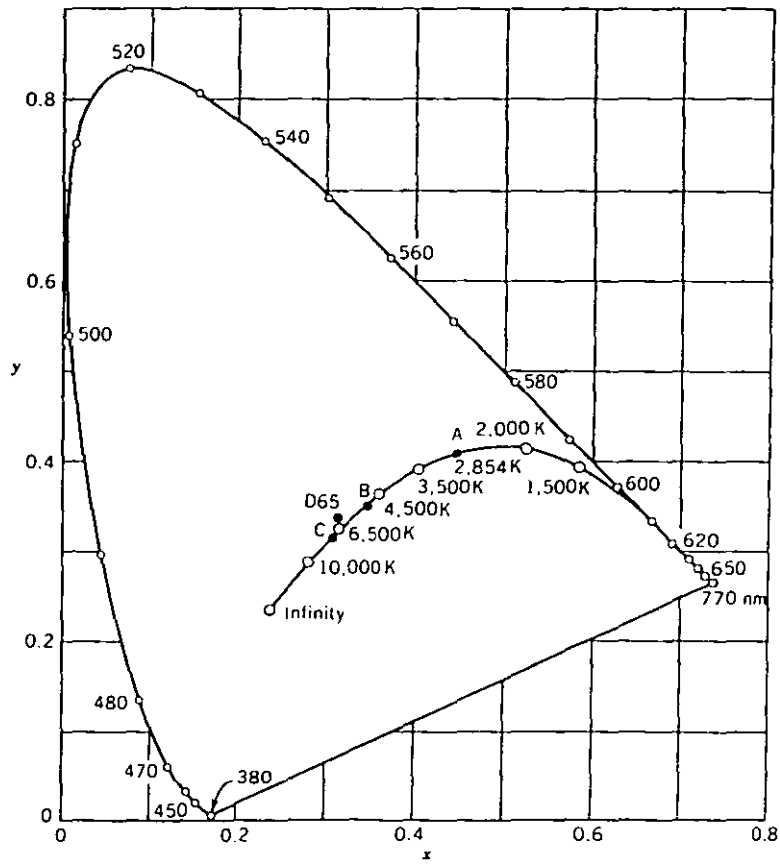


Figure 2.8 The CIE 1931 chromaticity diagram showing horseshoe-shaped spectrum locus with the spectrum colours identified by their wavelength, the purple line joining the ends of the spectrum locus, the locus of blackbody light sources identified by their colour temperatures in Kelvins, and the locations of the CIE standard illuminants A, B, C, and D65 [2].

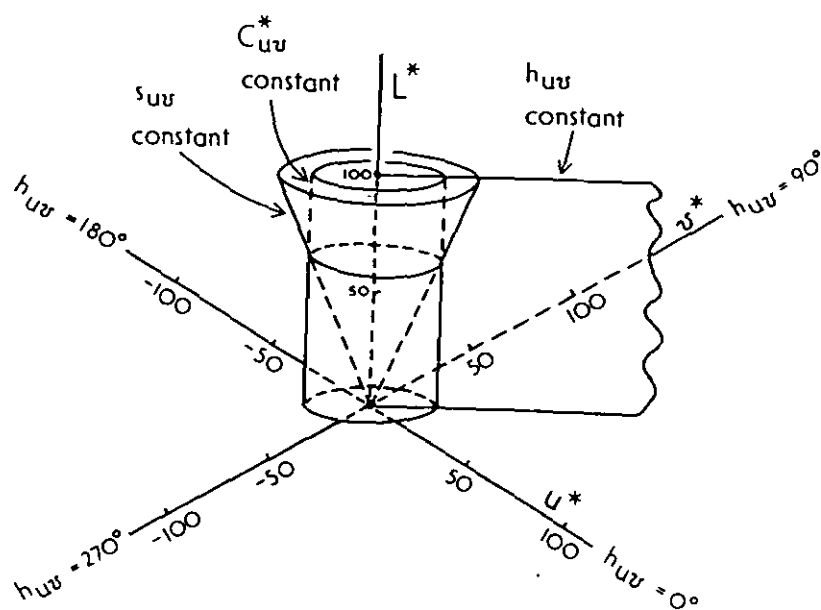


Figure 2.9 A three-dimensional illustration of CIELUV space^[16]

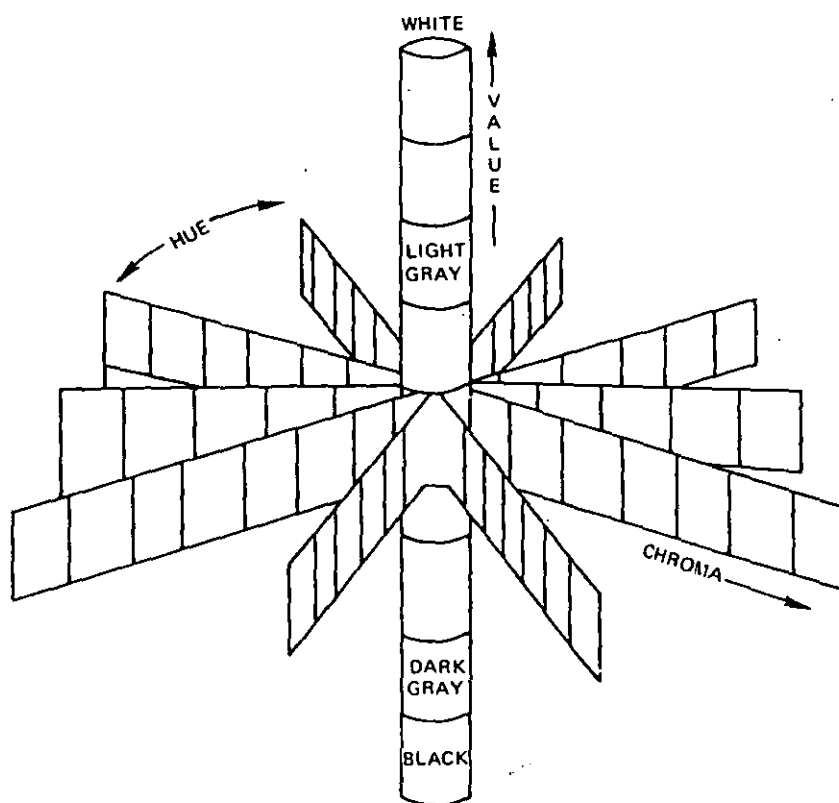


Figure 2.10 The Munsell Colour System^[46]

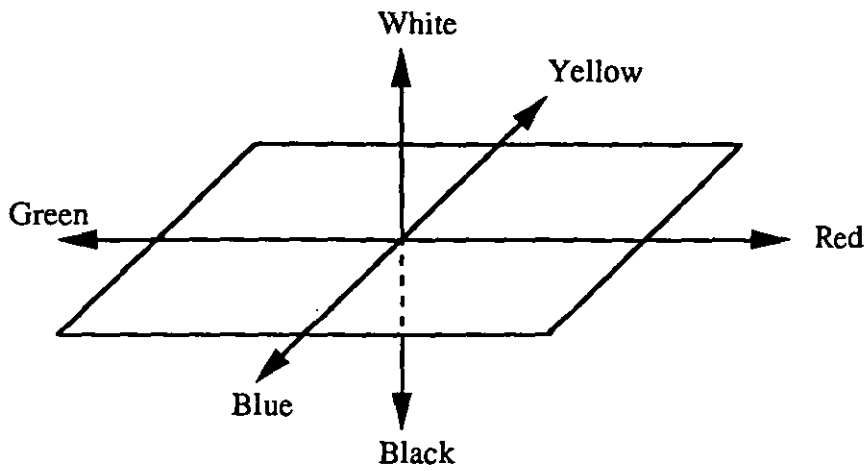


Figure 2.11 Three dimensions of the opponent - colour space

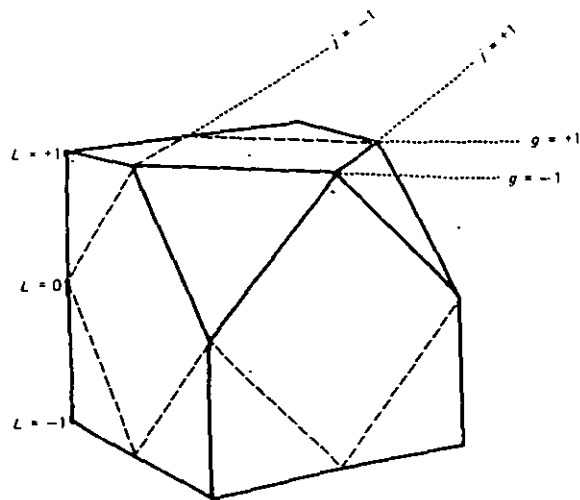


Figure 2.12 The cubo-octahedral basis of OSA system^[16]

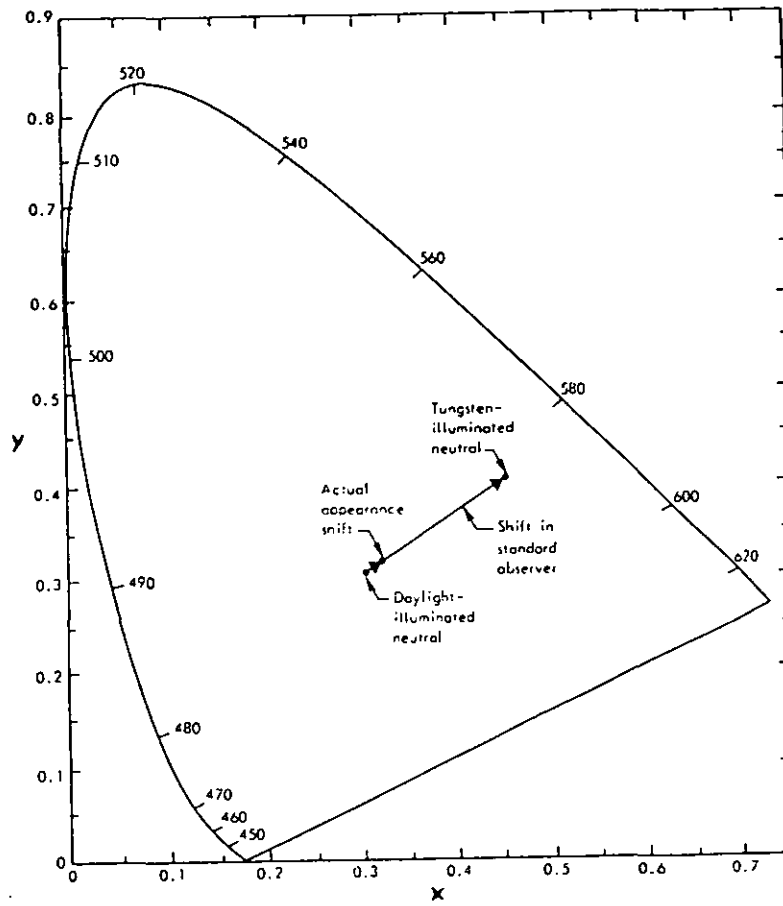


Figure 2.13 Comparison of actual appearance shift and the shift in CIE specification, for a neutral surface in daylight and in tungsten illumination^[70]

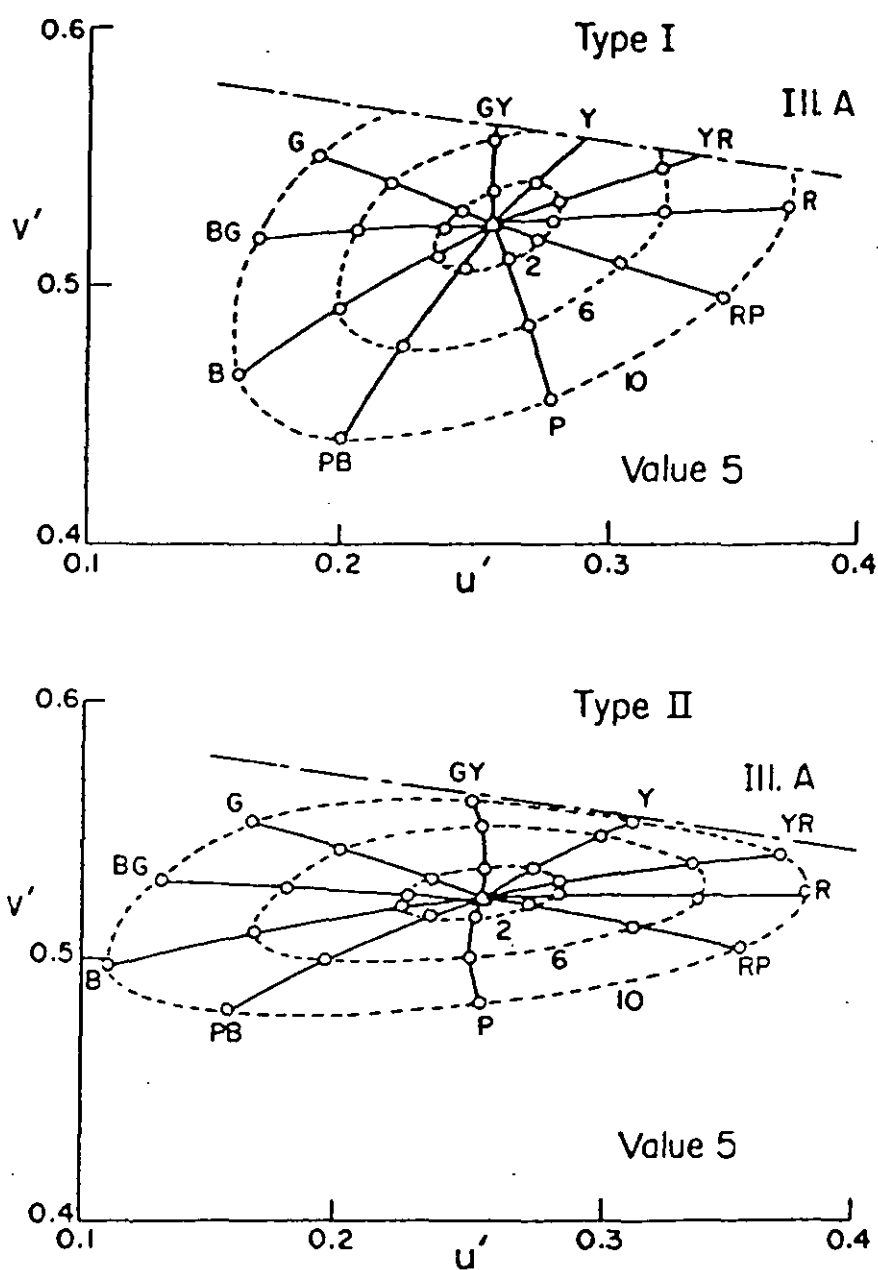


Figure 2.14 Contours of constant Munsell Hue and Chroma, at a Value of 5, as predicted for adaption to CIE illuminant A by Type I (top) and Type II (bottom) transformations^[65]

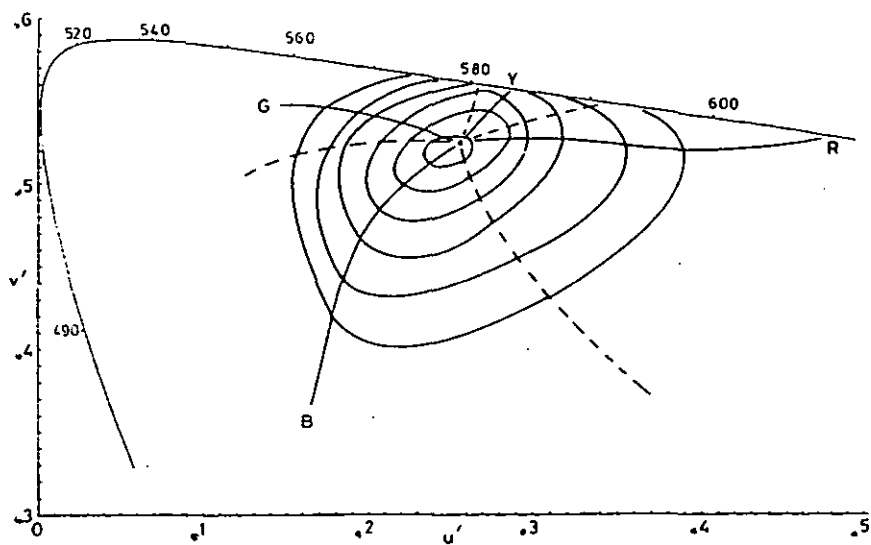
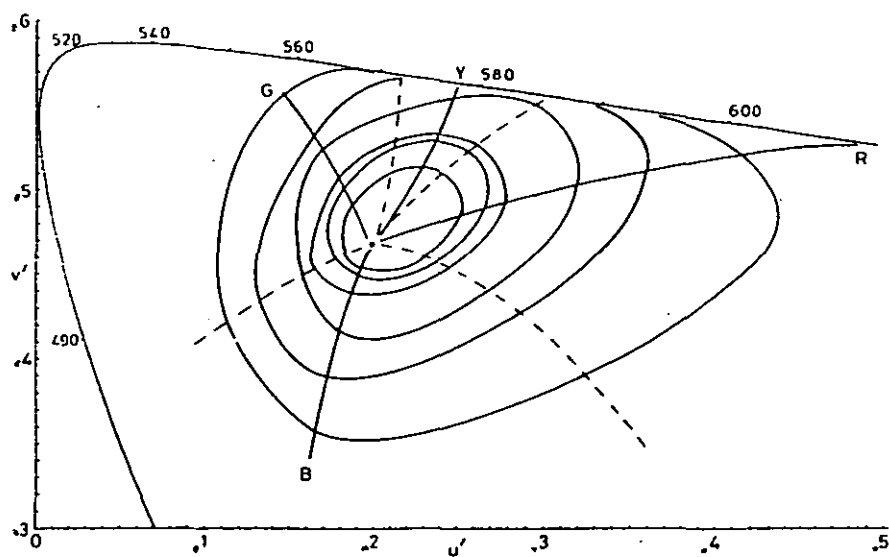


Figure 2.15 Grids of lines of constant hue and saturation obtained by subjective scaling for adaptation to standard illuminants D65 and A^[12]

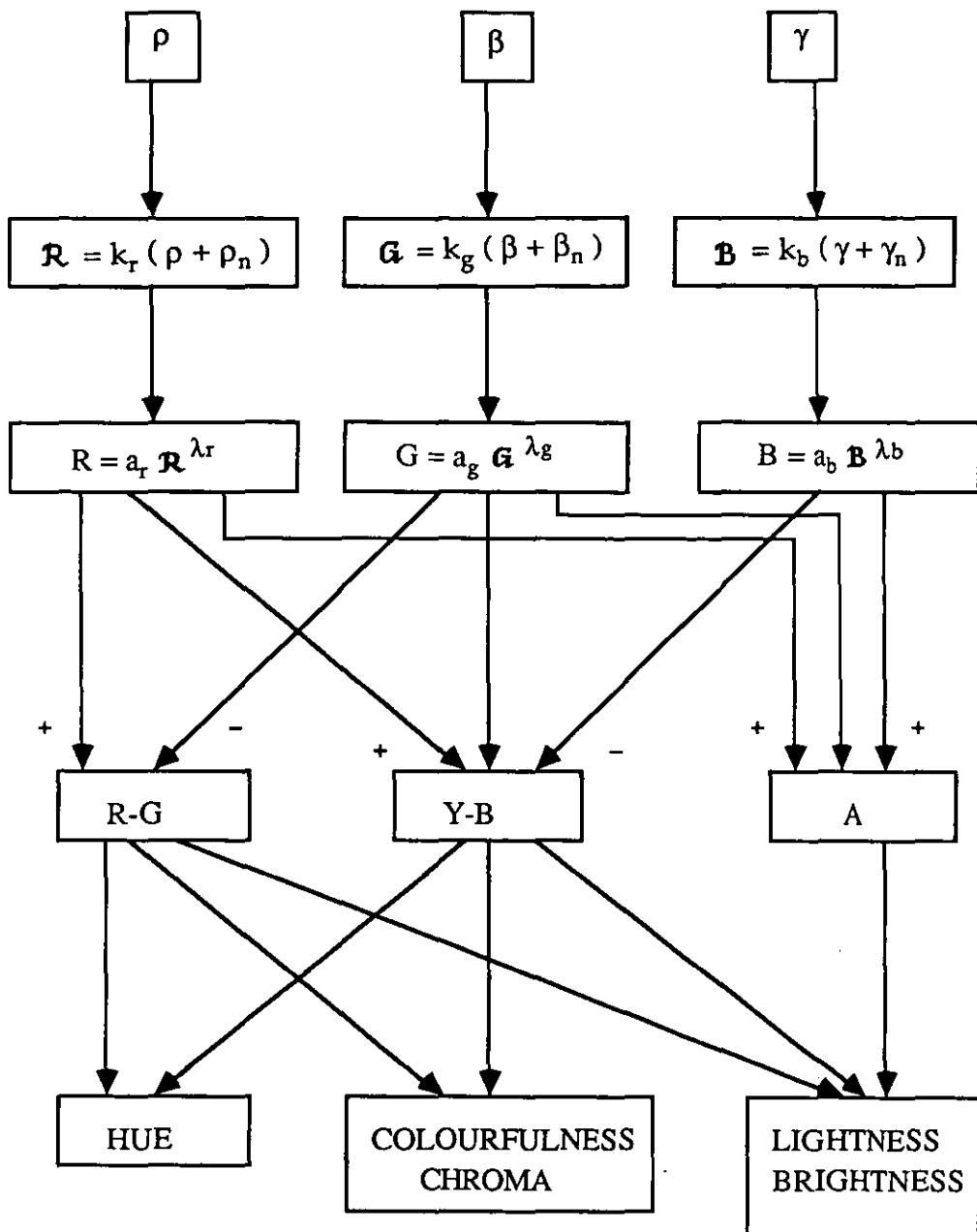


Figure 2.16 Schematic outline of Hunt's and Nayatani's colour vision models for prediction of colour appearance

Figure 2.17 Diagram of Hunt-82 model^[19]

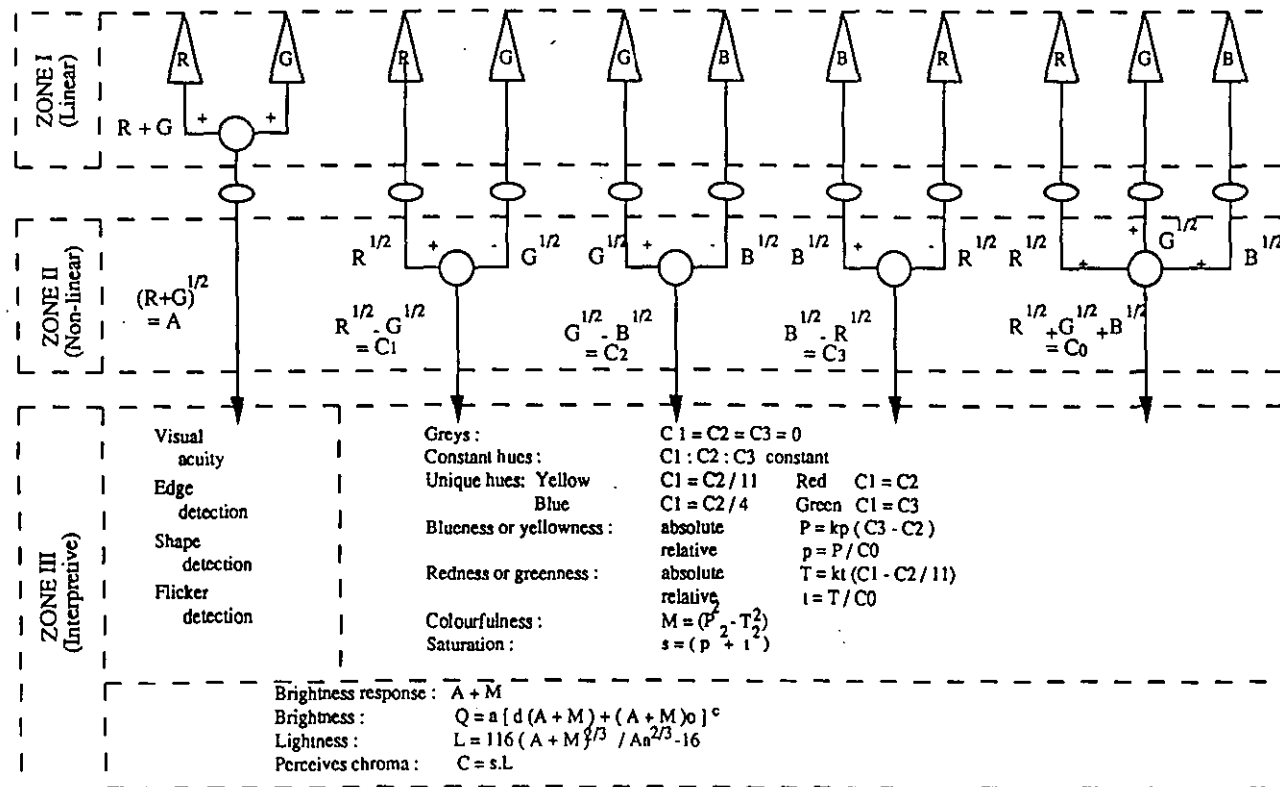
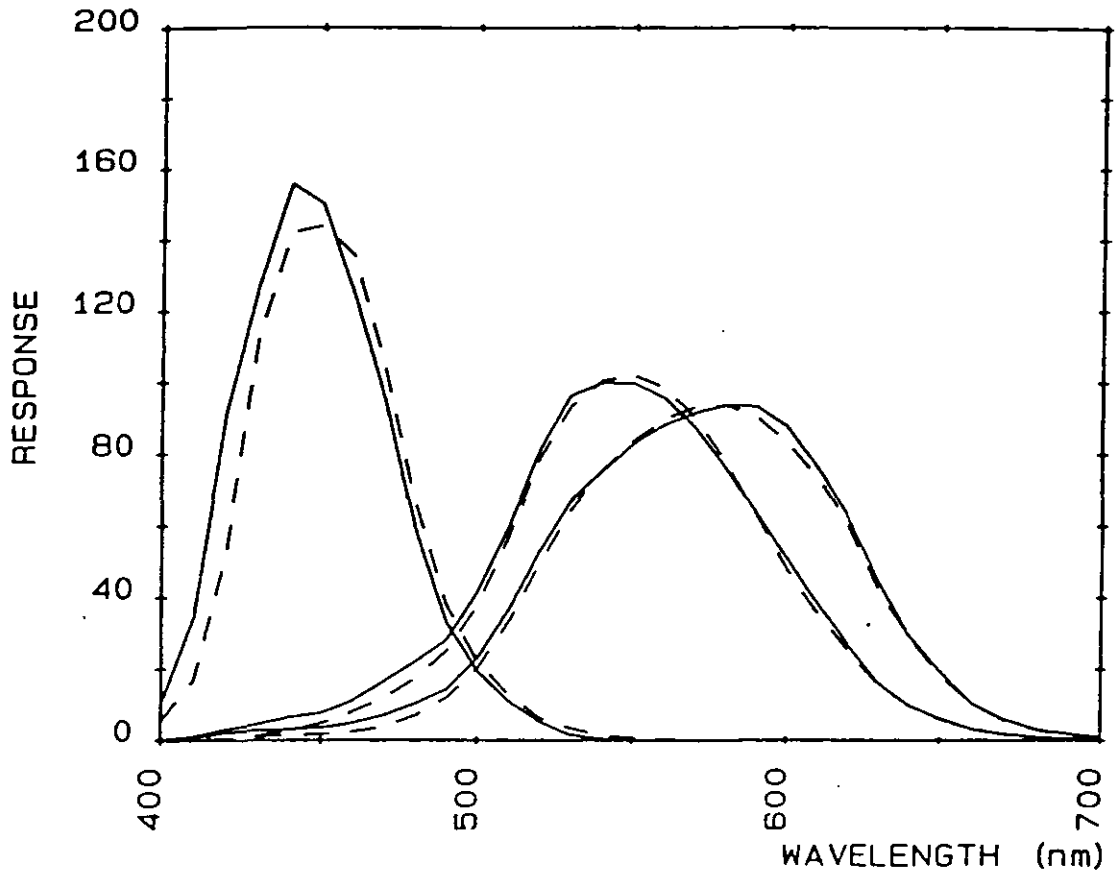


Figure 2.18 Cone spectral sensitivity curves used in Hunt-82 model (—) (after Estevez) and Hunt-85 model (---) (linear combination of CIE 1931 colour-matching functions^[135])



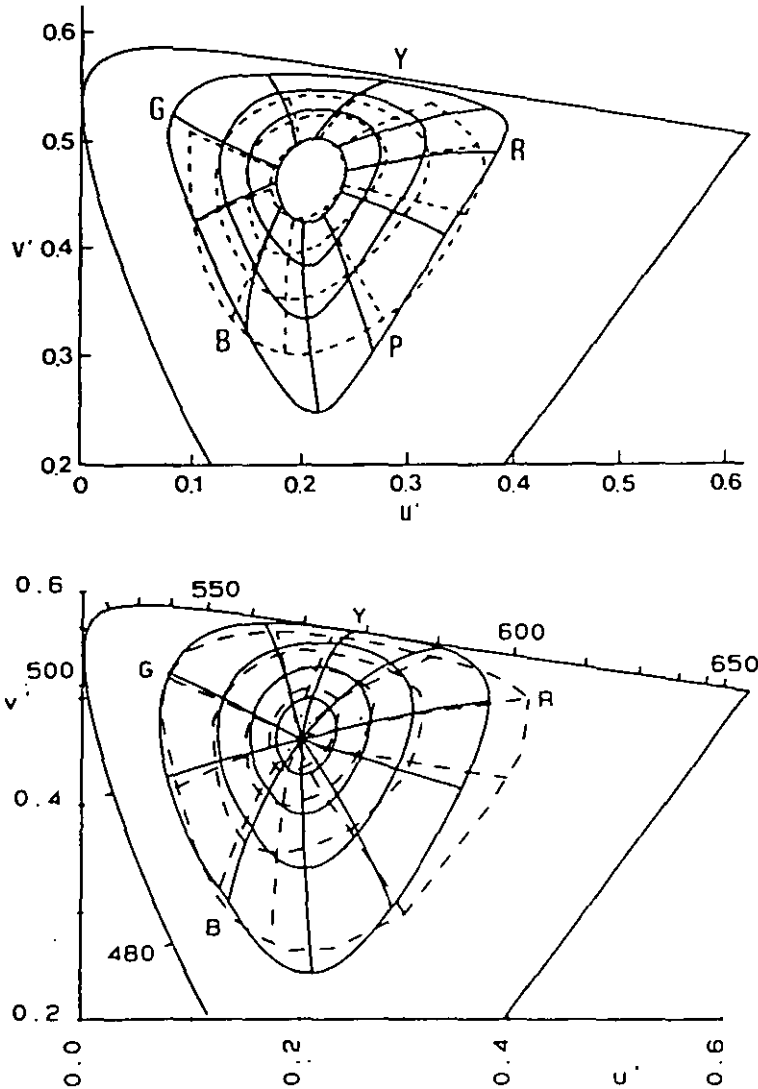


Figure 2.19 NCS constant-hue lines and constant-chroma figures shown on the CIE 1976 $u'v'$ diagram. Dashed lines: NCS data; solid lines: predicted by models of Nayatani (top) and Hunt (bottom)^[23 & 135]

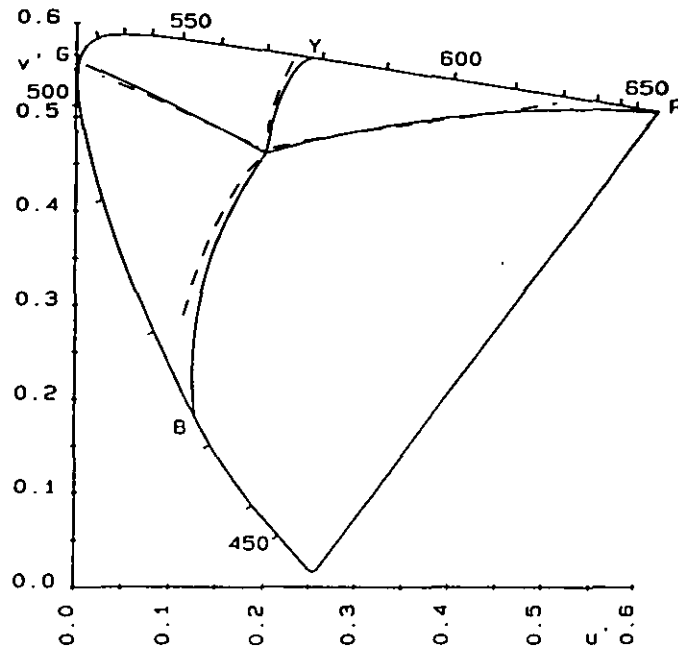


Figure 2.20 NCS constant-hue lines for the unique hues shown on the CIE 1976 u'v' diagram. Dashed lines: predicted by Hunt's model^[135]

Figure 2.21 Schematic illustration of Nayatani's model^[22]

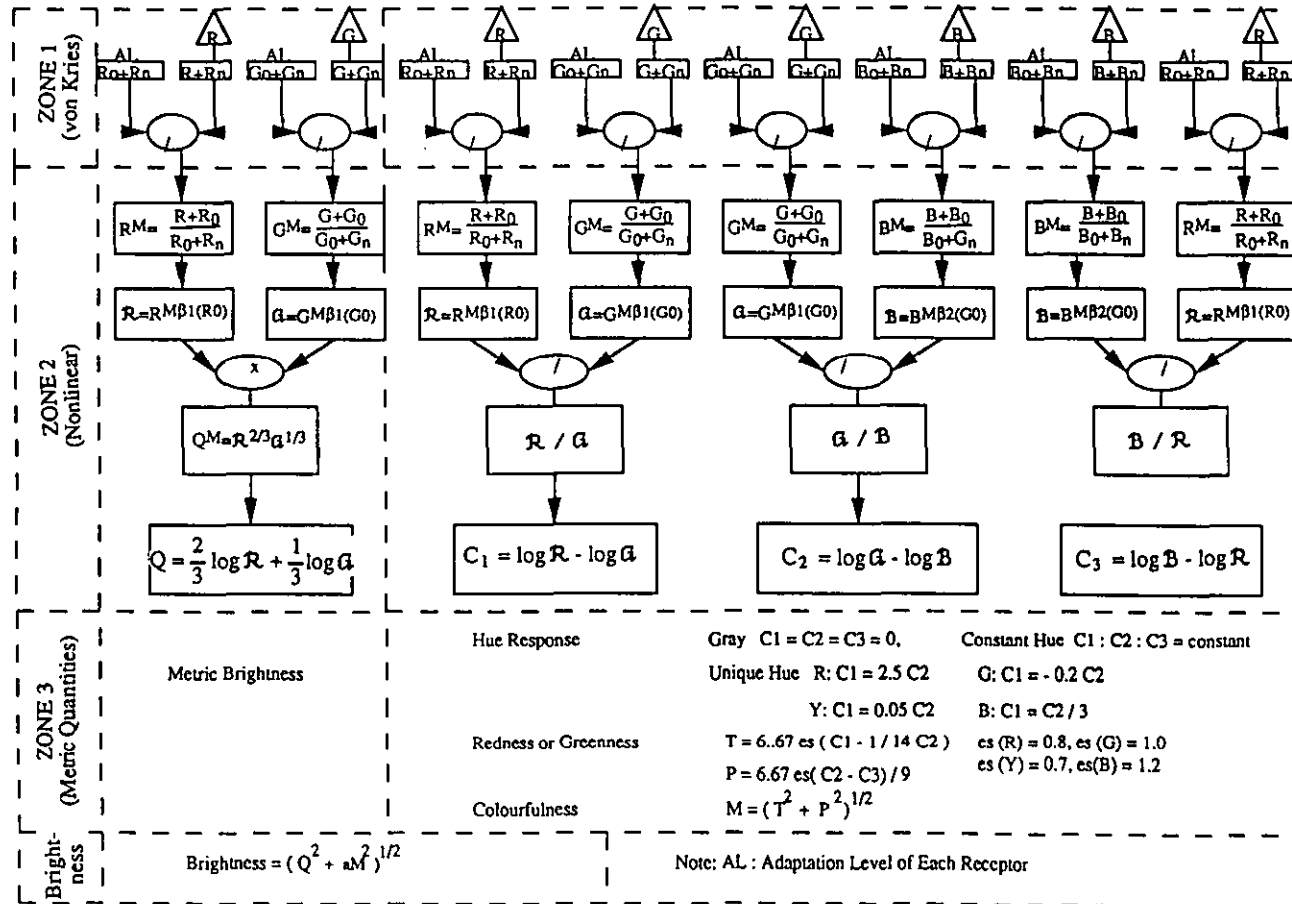


Figure 3.1 The front view of Verivide Viewing Cabinet. The pattern inside is used in Experiment 4



Figure 3.2 Bentham Telespectroradiometer (TSR) system. The sphere on the top is Bentham standard lamp used for calibration



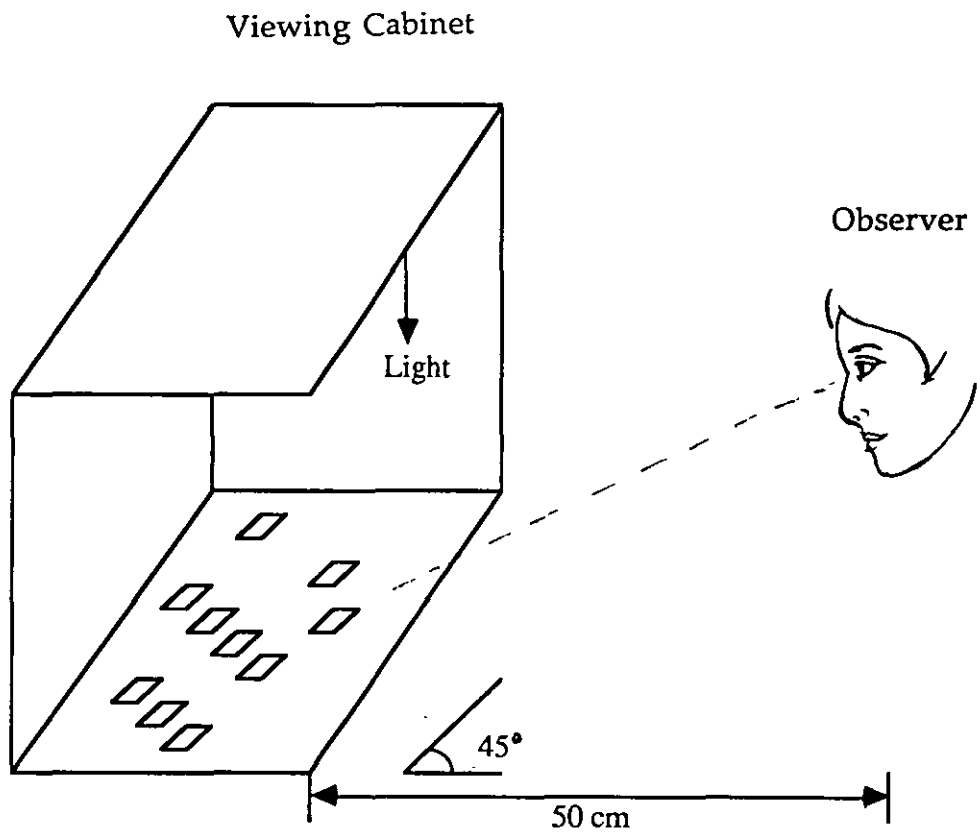


Figure 3.3 Schematic illustration of training experiment

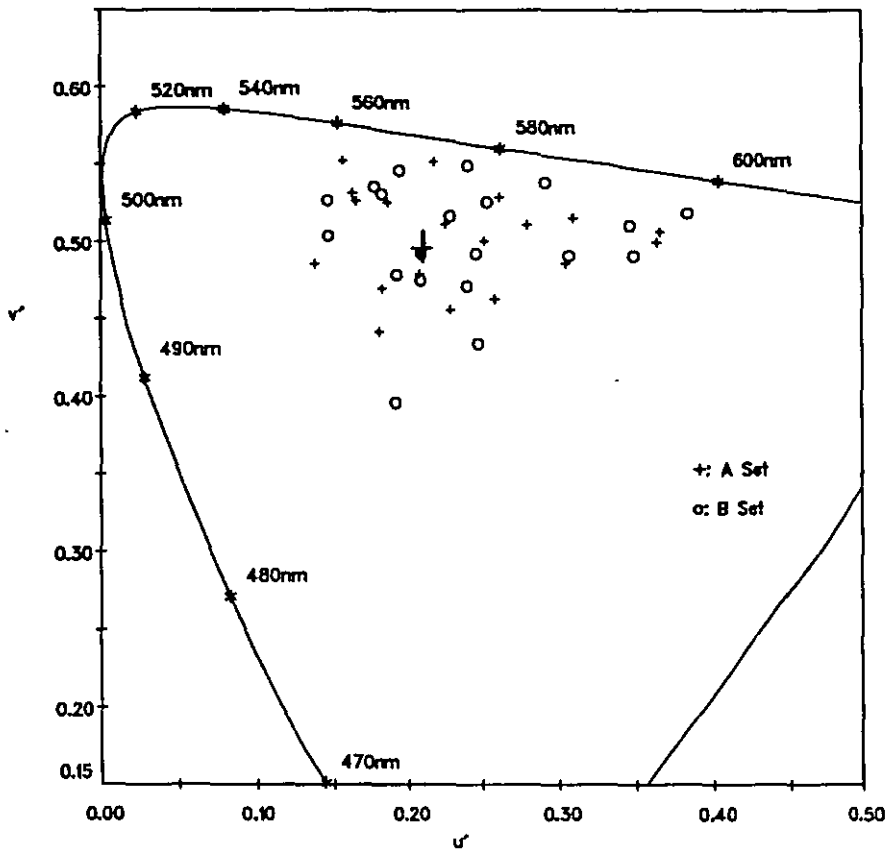


Figure 3.4 Distribution of 40 OSA samples used in Experiment 1 plotted on the CIE $u'v'$ diagram under illuminant D50. The larger plus symbol represents the reference white point.

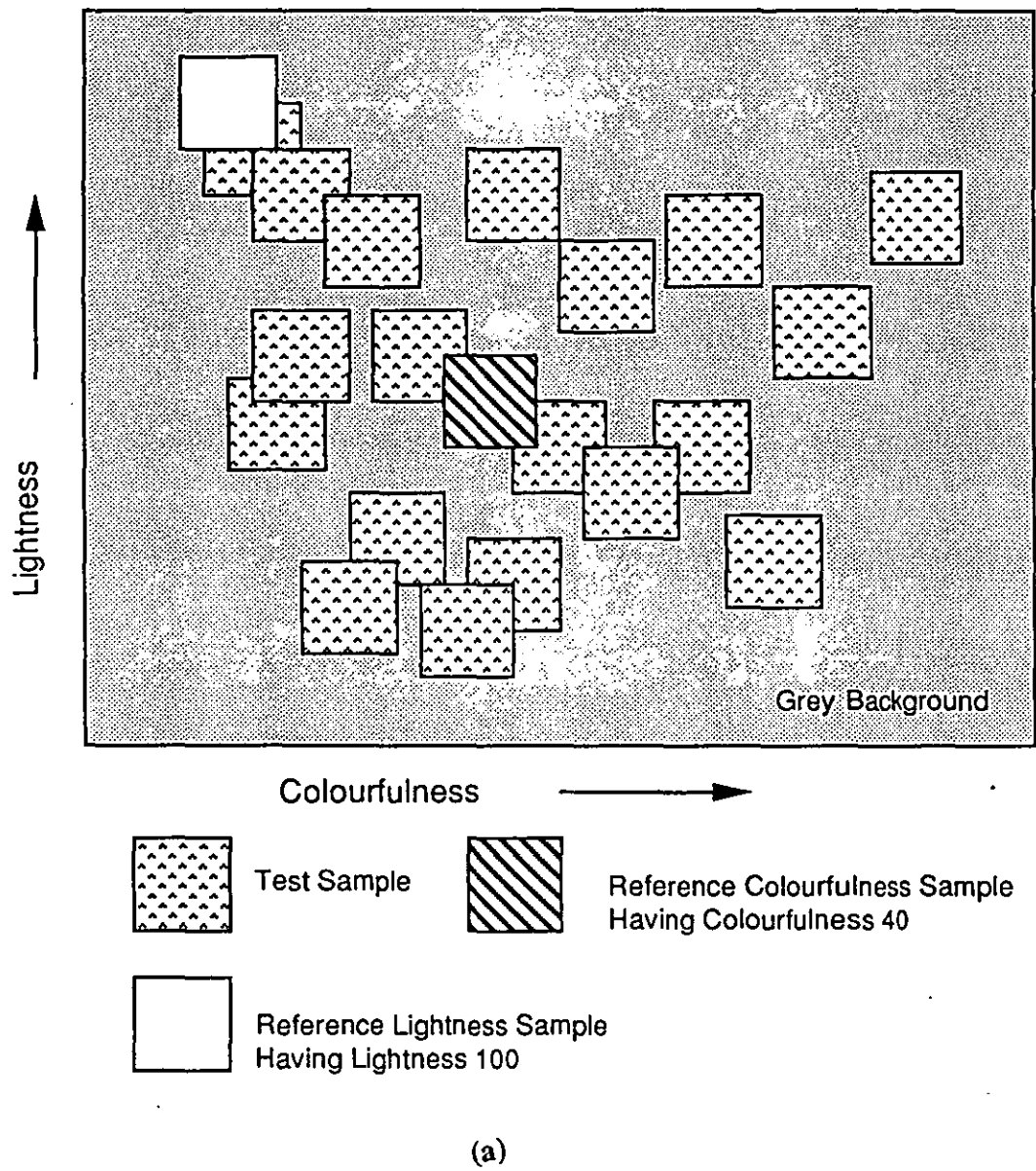
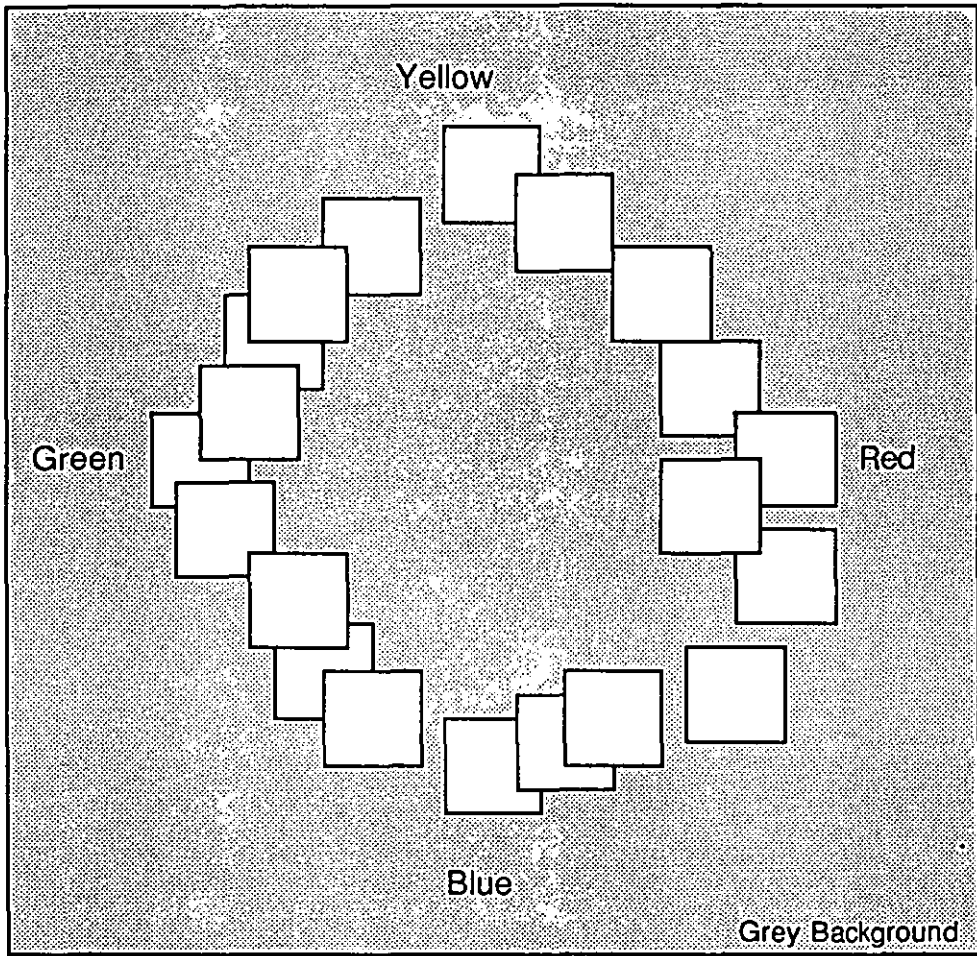
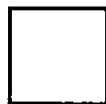


Figure 3.5 (a) Two-dimensional ranking of lightness against colourfulness for training experiment; (b) One-dimensional hue circle used in the training experiment



 Test Sample

(b)

Figure 3.6 The Vervide transparency illuminator



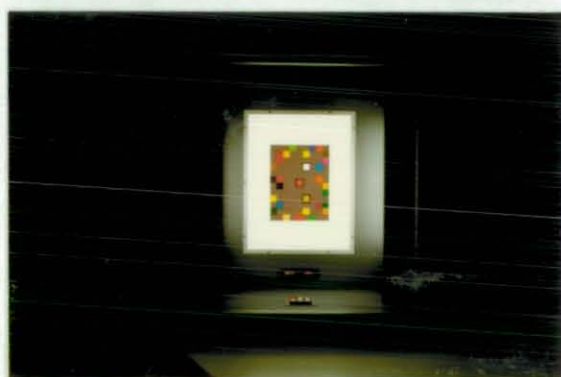
(a) The viewing pattern with black border



(b) The viewing pattern surrounded by a white paper border with flare light



(c) The viewing pattern with white border



(d) The viewing pattern surrounded by a white border with flare

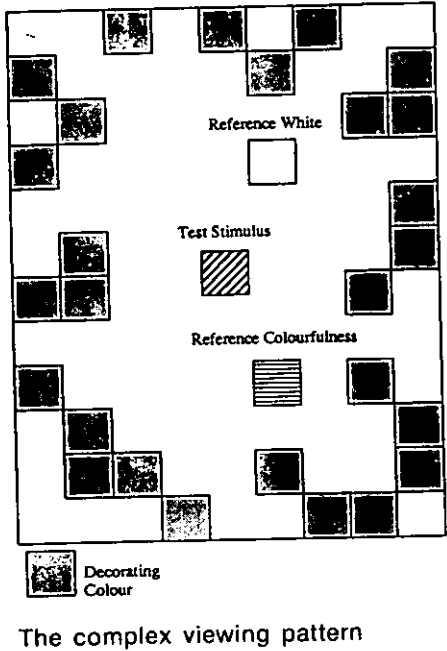
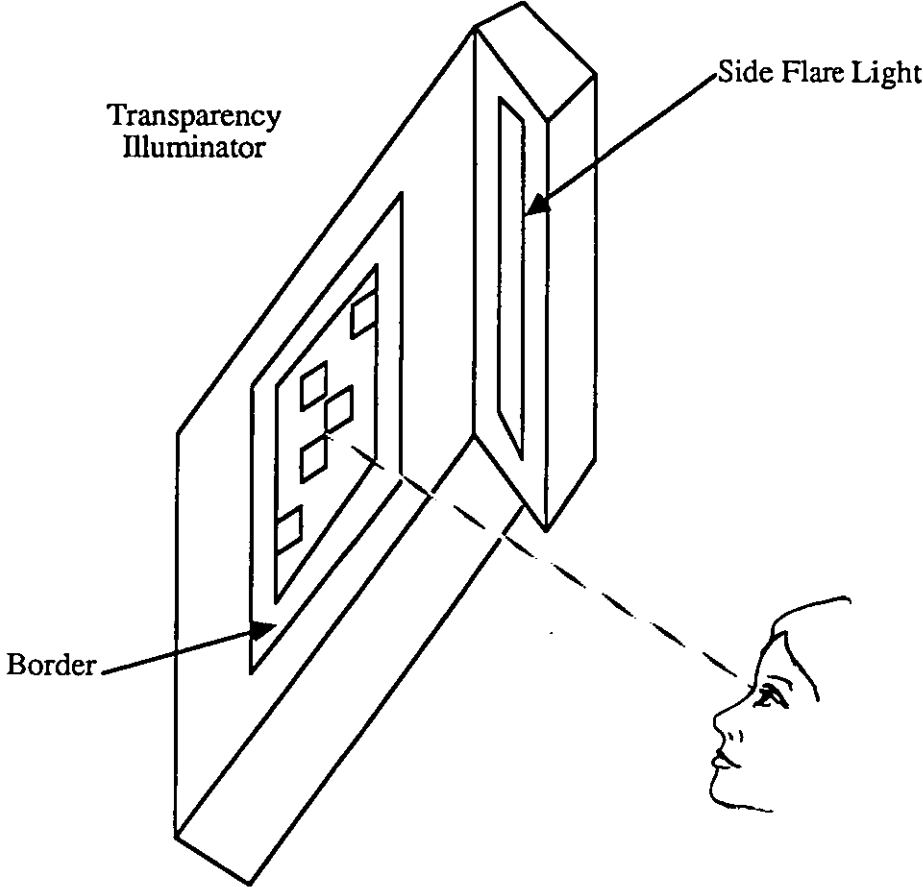


Figure 3.7 Diagram of the set-up of cut-sheet transparency experiment

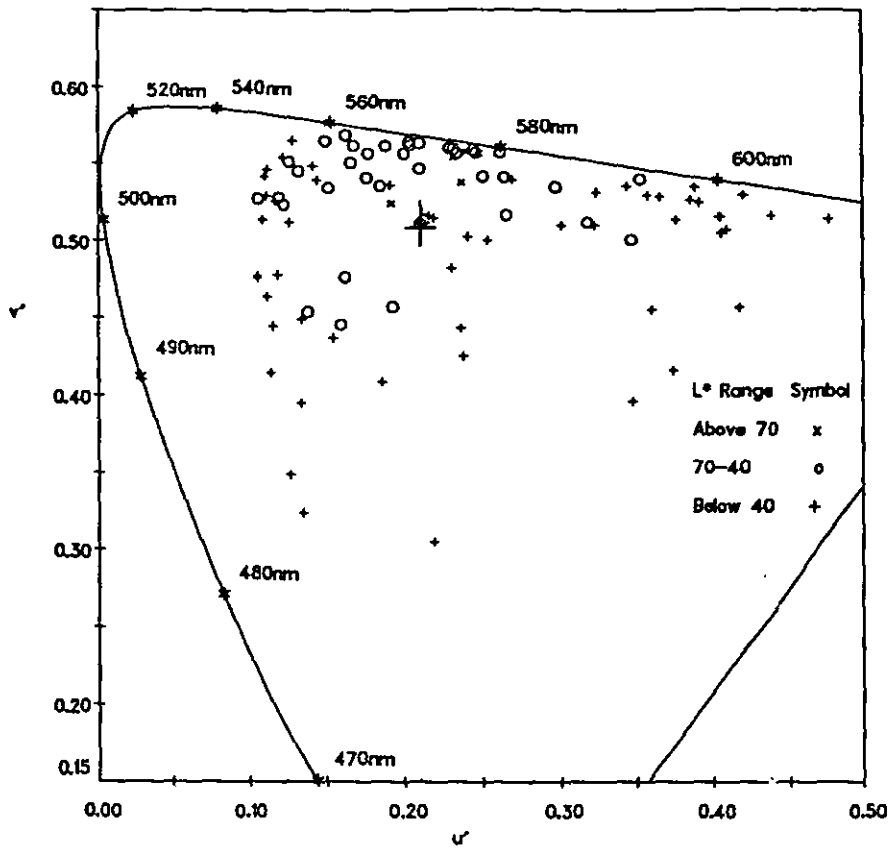


Figure 3.8 Chromaticity coordinates of 98 test stimuli plotted on the CIE $u'v'$ chromaticity diagram for phase 1 in Experiment 2. The larger plus symbol represents the reference white point.

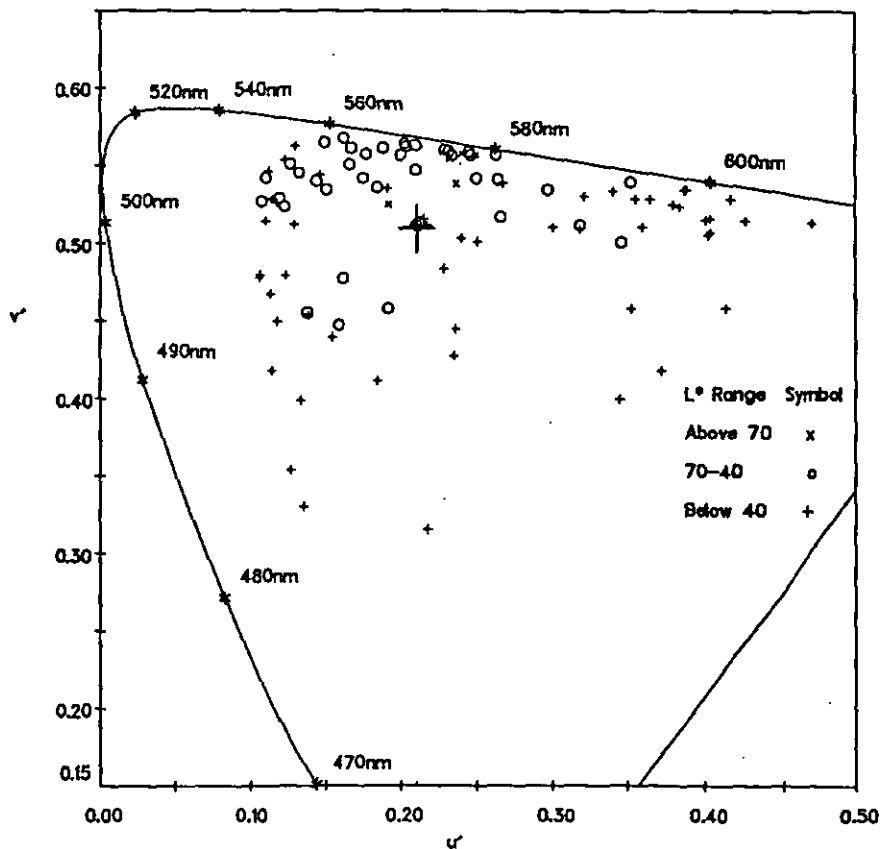


Figure 3.9 Chromaticity coordinates of 98 test stimuli plotted on the CIE $u'v'$ chromaticity diagram for phases 2 and 9 in Experiment 2. The larger plus symbol represents the reference white point.

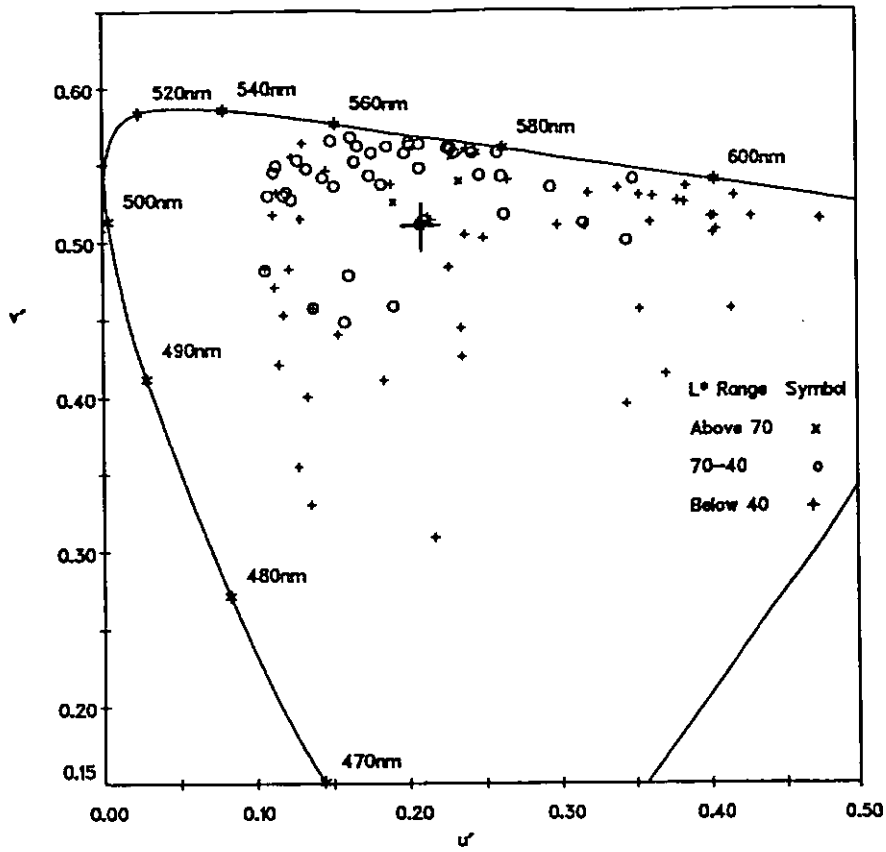


Figure 3.10 Chromaticity coordinates of 98 test stimuli plotted on the CIE $u'v'$ chromaticity diagram for phase 3 in Experiment 2. The larger plus symbol represents the reference white point.

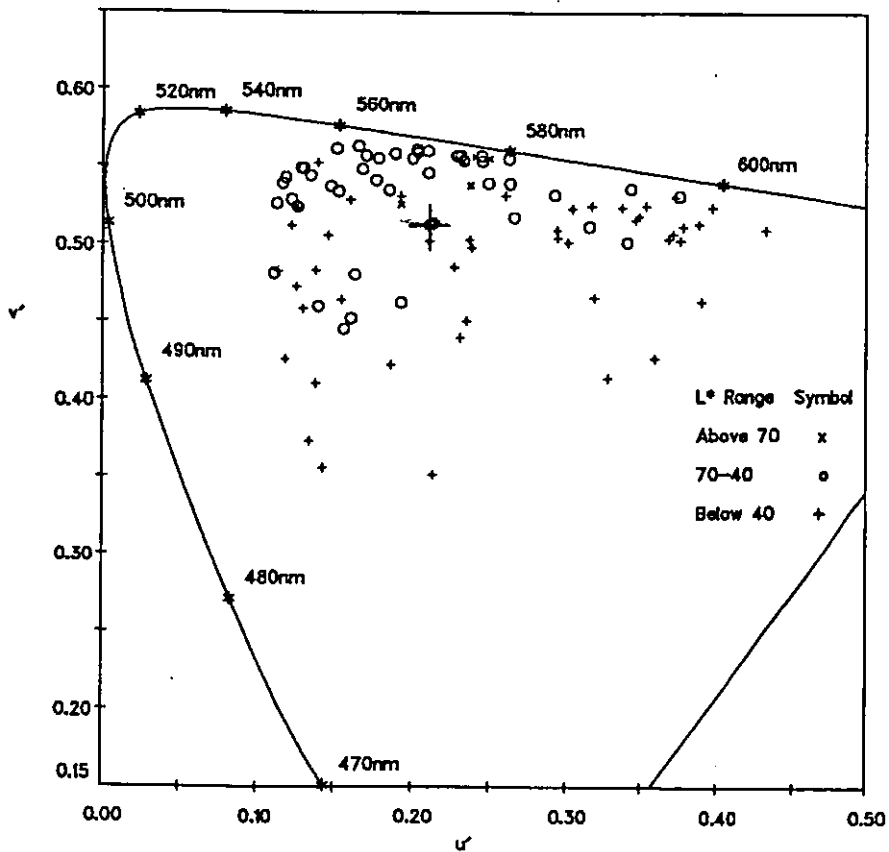


Figure 3.11 Chromaticity coordinates of 98 test stimuli plotted on the CIE $u'v'$ chromaticity diagram for phase 4 in Experiment 2. The larger plus symbol represents the reference white point.

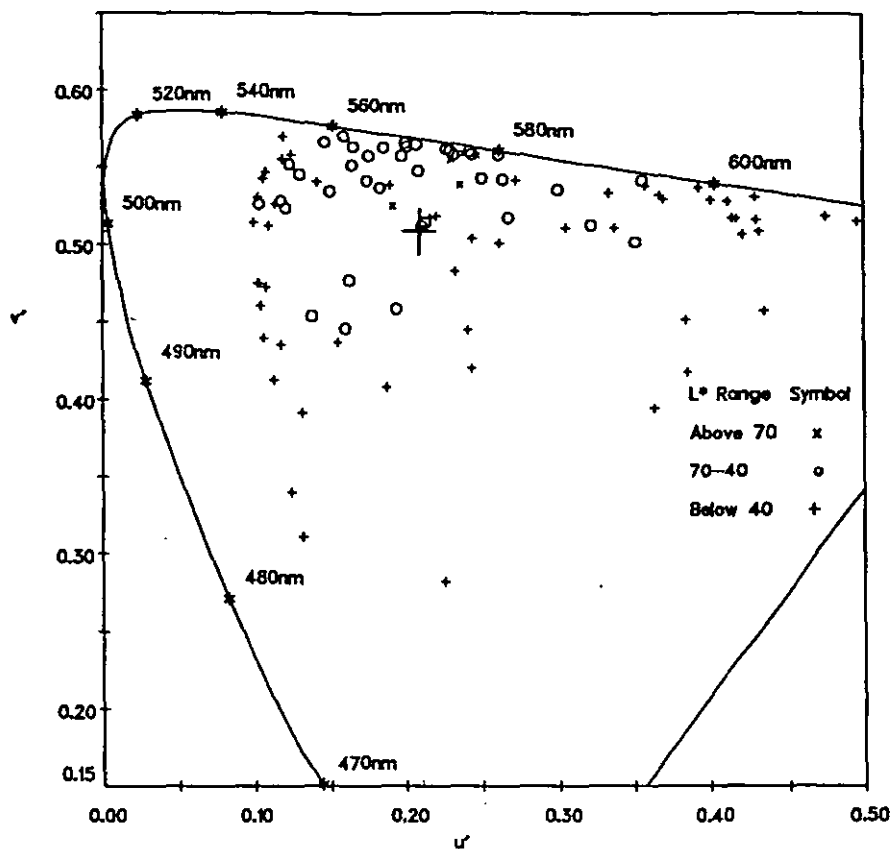


Figure 3.12 Chromaticity coordinates of 98 test stimuli plotted on the CIE $u'v'$ chromaticity diagram for phase 5 in Experiment 2. The larger plus symbol represents the reference white point.

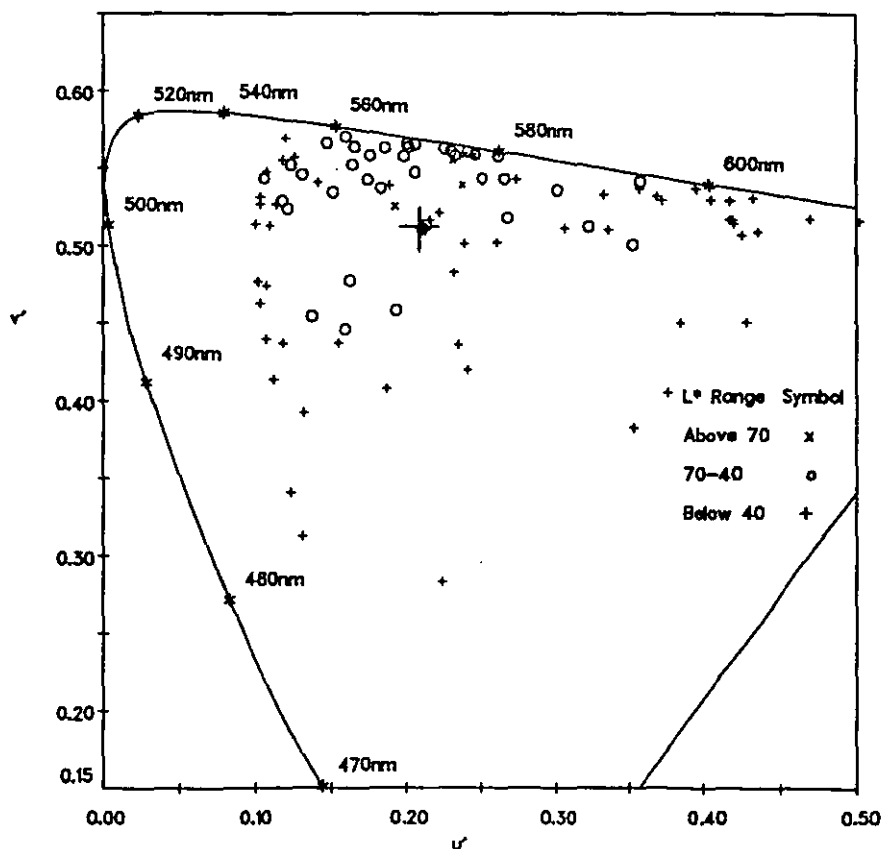


Figure 3.13 Chromaticity coordinates of 98 test stimuli plotted on the CIE $u'v'$ chromaticity diagram for phase 6 in Experiment 2. The larger plus symbol represents the reference white point.

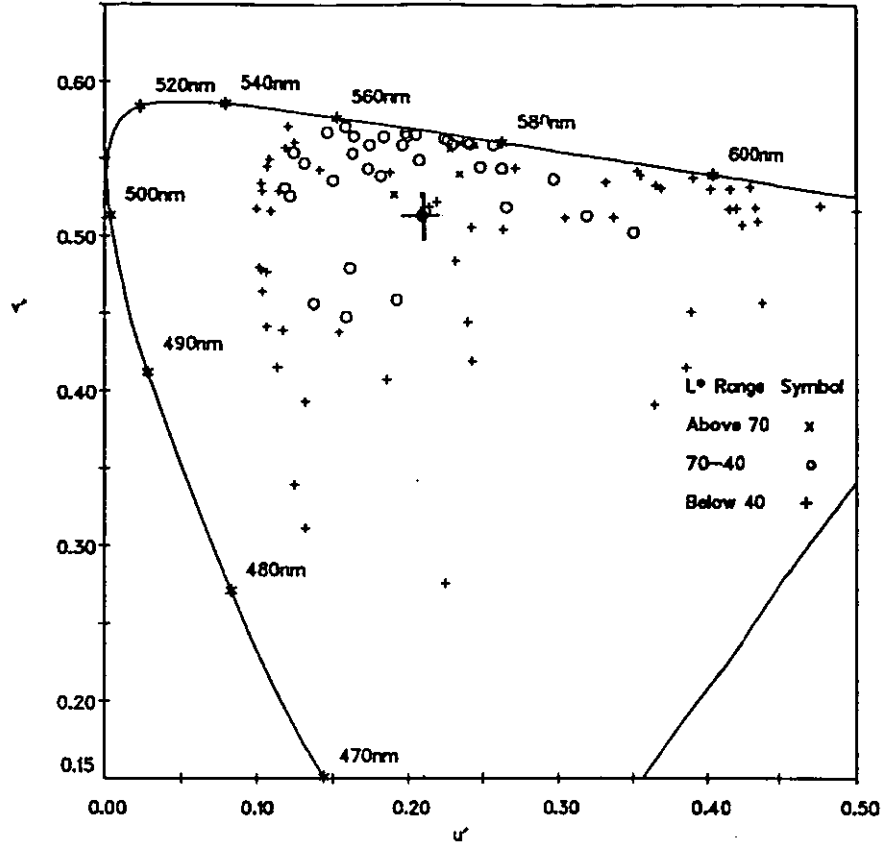


Figure 3.14 Chromaticity coordinates of 98 test stimuli plotted on the CIE $u'v'$ chromaticity diagram for phase 7 in Experiment 2. The larger plus symbol represents the reference white point.

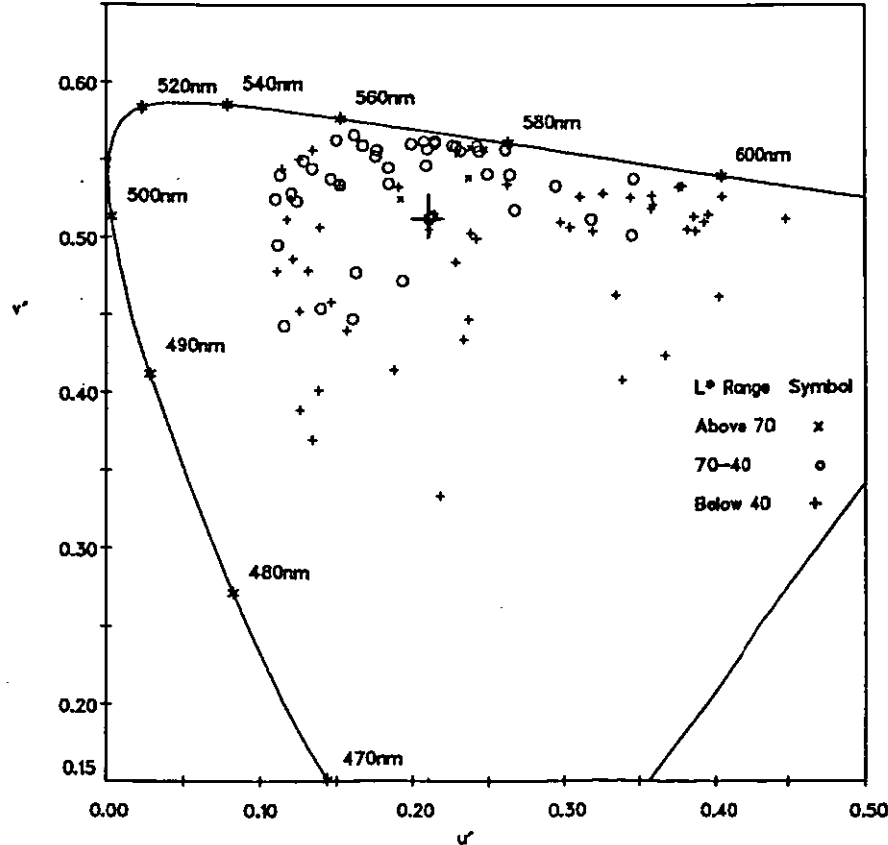


Figure 3.15 Chromaticity coordinates of 98 test stimuli plotted on the CIE $u'v'$ chromaticity diagram for phase 8 in Experiment 2. The larger plus symbol represents the reference white point.

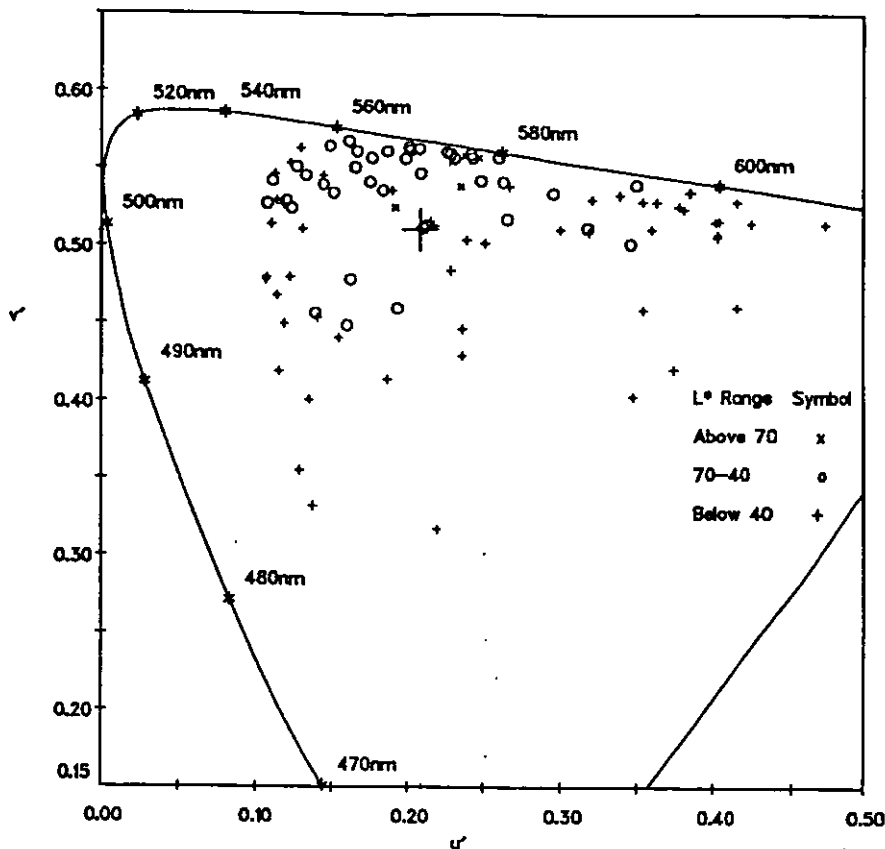


Figure 3.16 Chromaticity coordinates of 98 test stimuli plotted on the CIE $u'v'$ chromaticity diagram for phase 10 in Experiment 2. The larger plus symbol represents the reference white point.

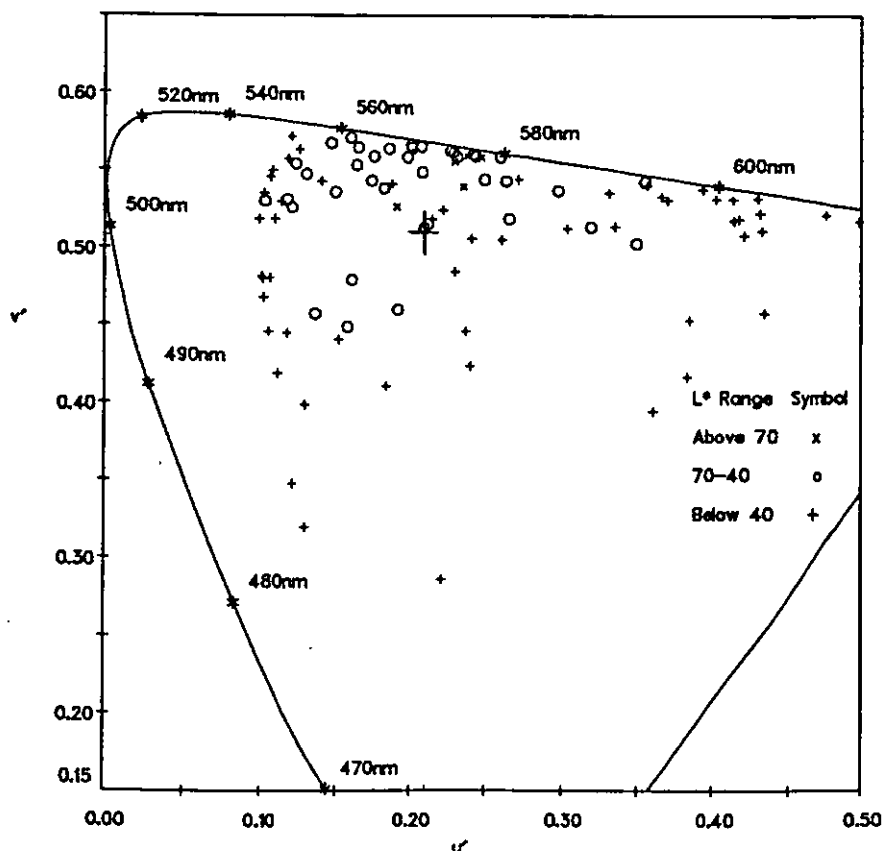


Figure 3.17 Chromaticity coordinates of 98 test stimuli plotted on the CIE $u'v'$ chromaticity diagram for phase 11 in Experiment 2. The larger plus symbol represents the reference white point.

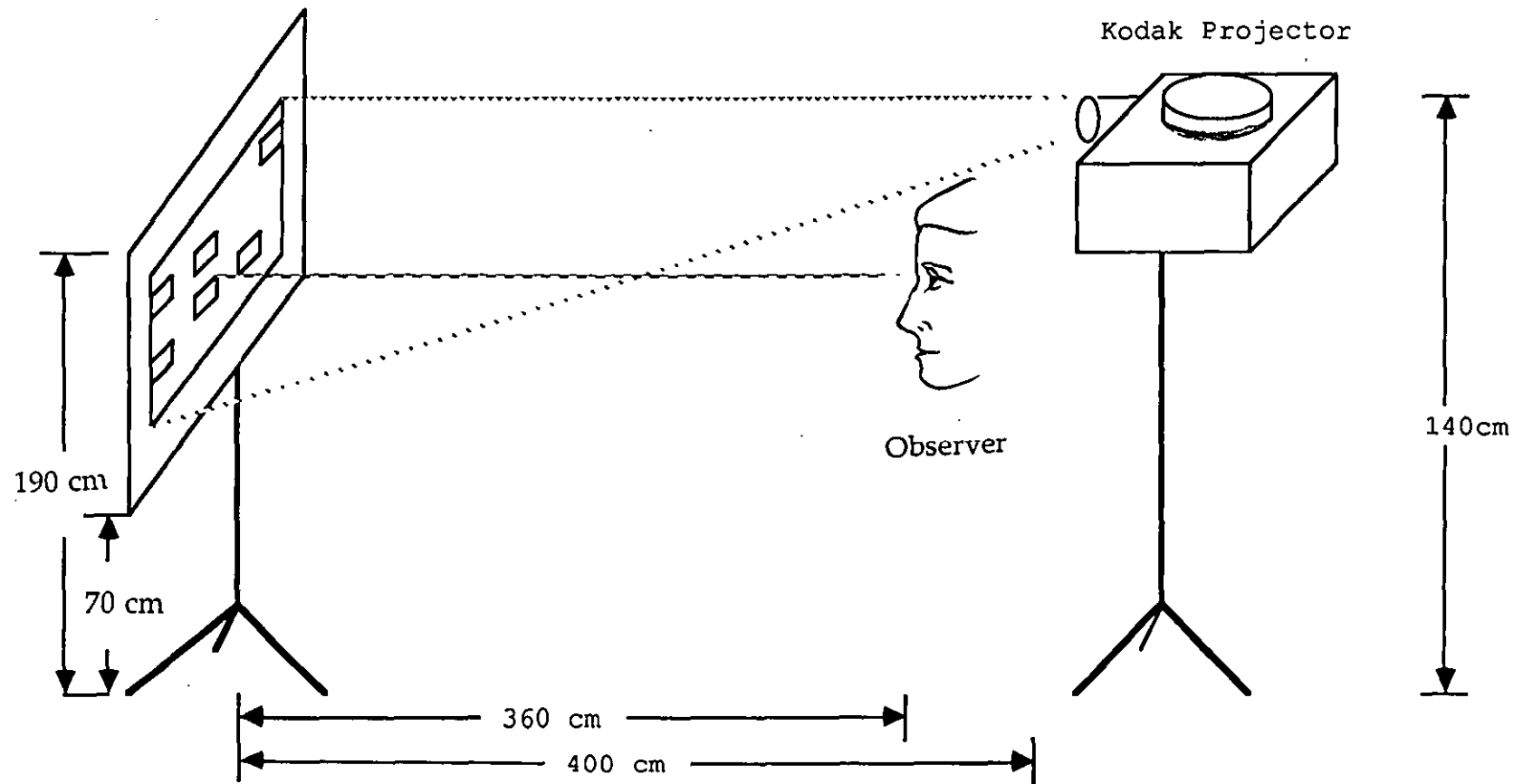


Figure 3.18 Diagram of the set-up of 35 mm slide experiment

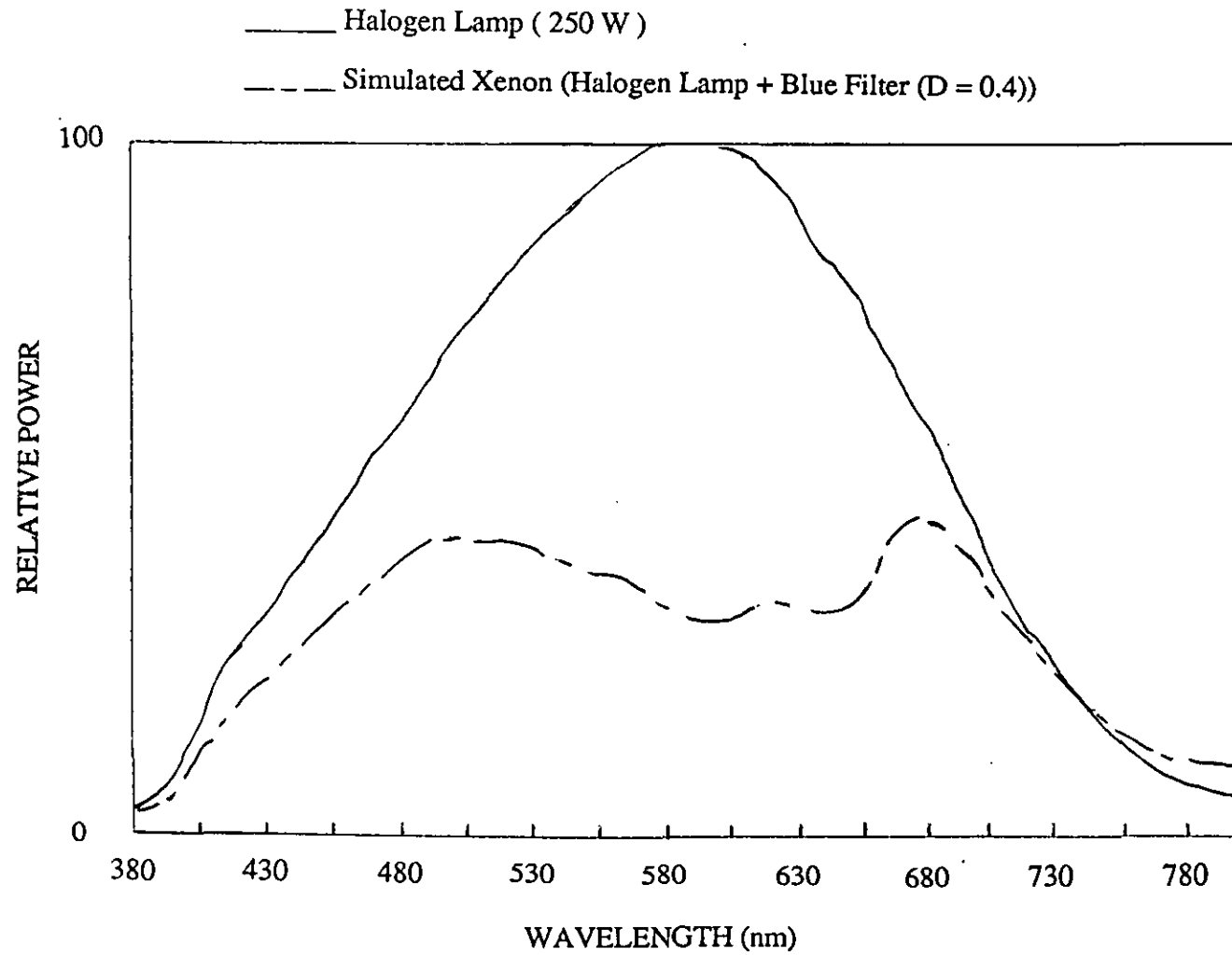


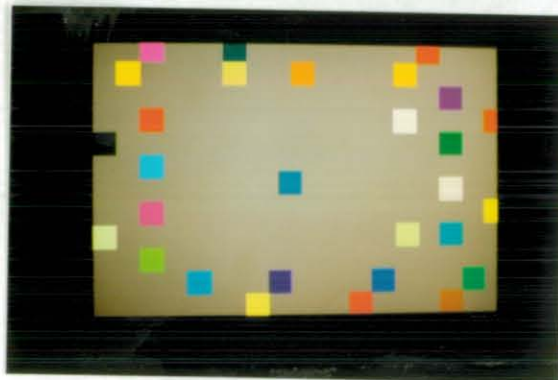
Figure 3.19 Spectral power distribution of Halogen high level light and simulated Xenon low level light

Figure 3.20 The image of 35 slide projected on a white screen

(a) The reference lightness, reference colourfulness and test samples are placed together



(b) The reference lightness, reference colourfulness and test samples are placed apart



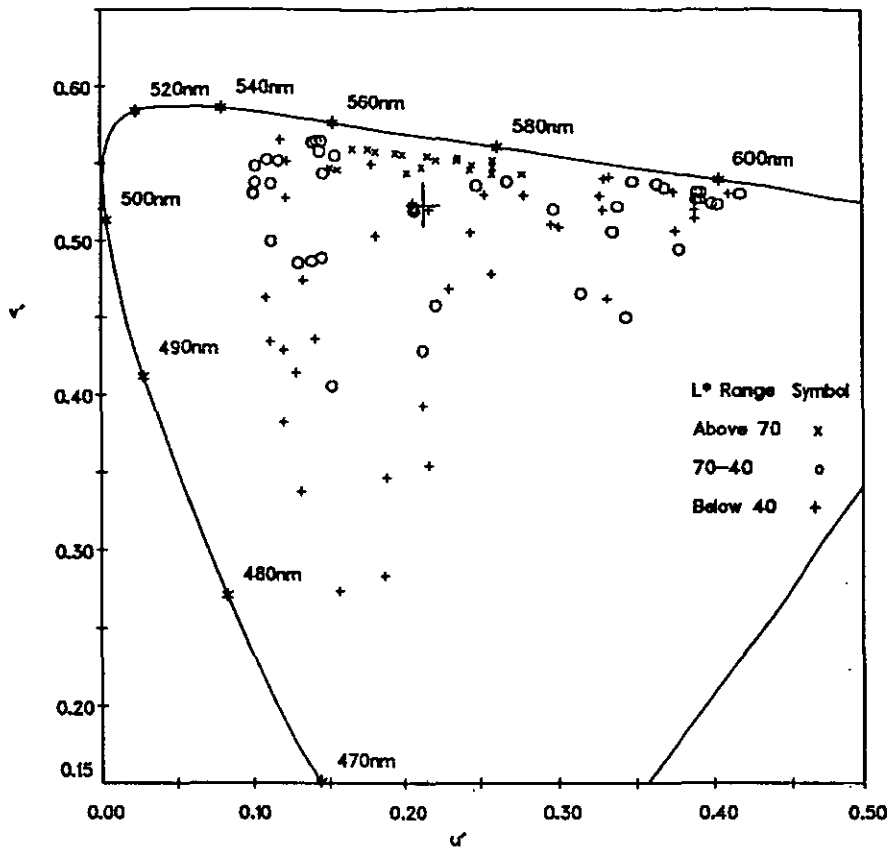


Figure 3.21 Chromaticity coordinates of 95 slide samples plotted on the CIE $u'v'$ diagram for phases 1 and 4 in Experiment 3. The larger plus symbol represents the reference white point.

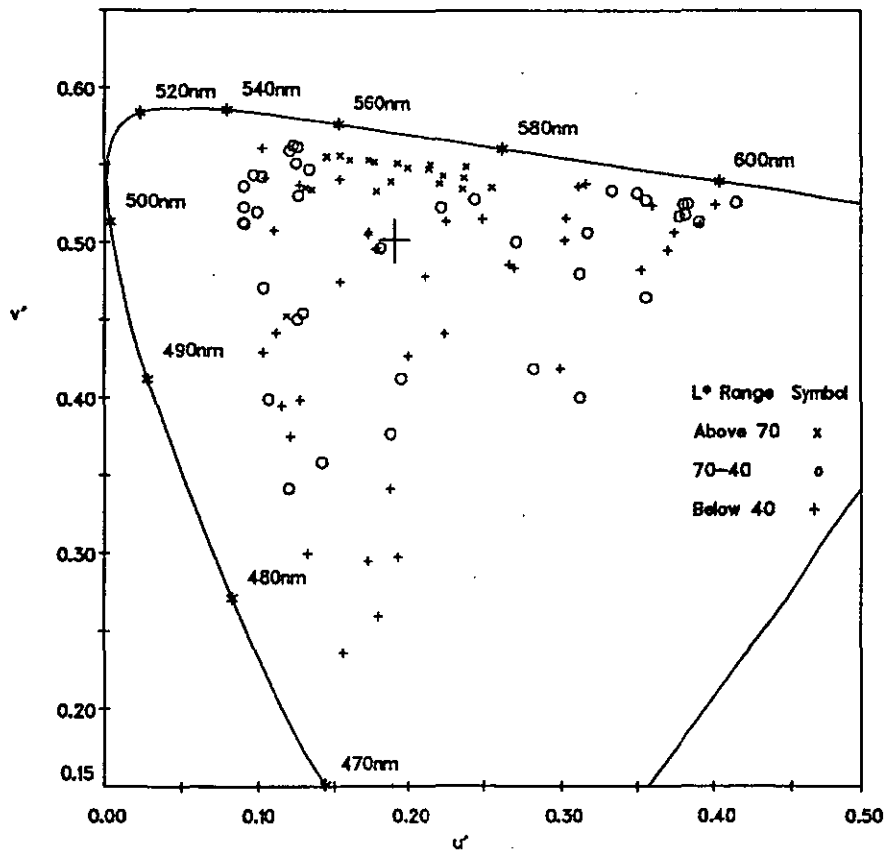


Figure 3.22 Chromaticity coordinates of 95 slide samples plotted on the CIE $u'v'$ diagram for phase 2 in Experiment 3. The larger plus symbol represents the reference white point.

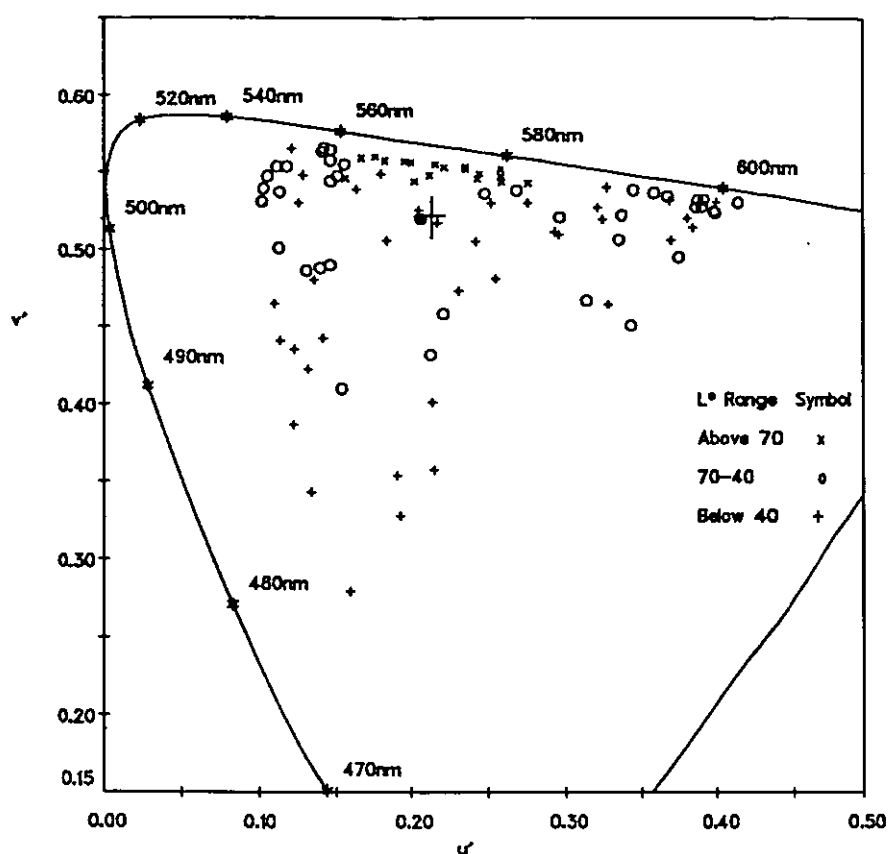


Figure 3.23 Chromaticity coordinates of 95 slide samples plotted on the CIE $u'v'$ diagram for phase 3 in Experiment 3. The larger plus symbol represents the reference white point.

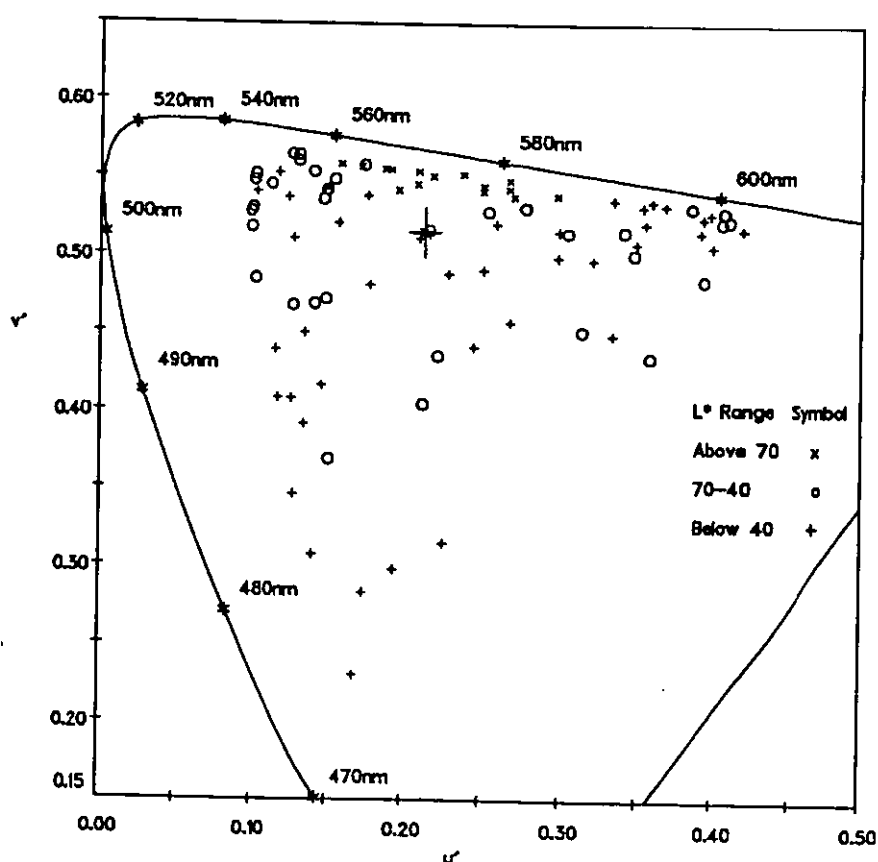


Figure 3.24 Chromaticity coordinates of 95 slide samples plotted on the CIE $u'v'$ diagram for phase 5 in Experiment 3. The larger plus symbol represents the reference white point.

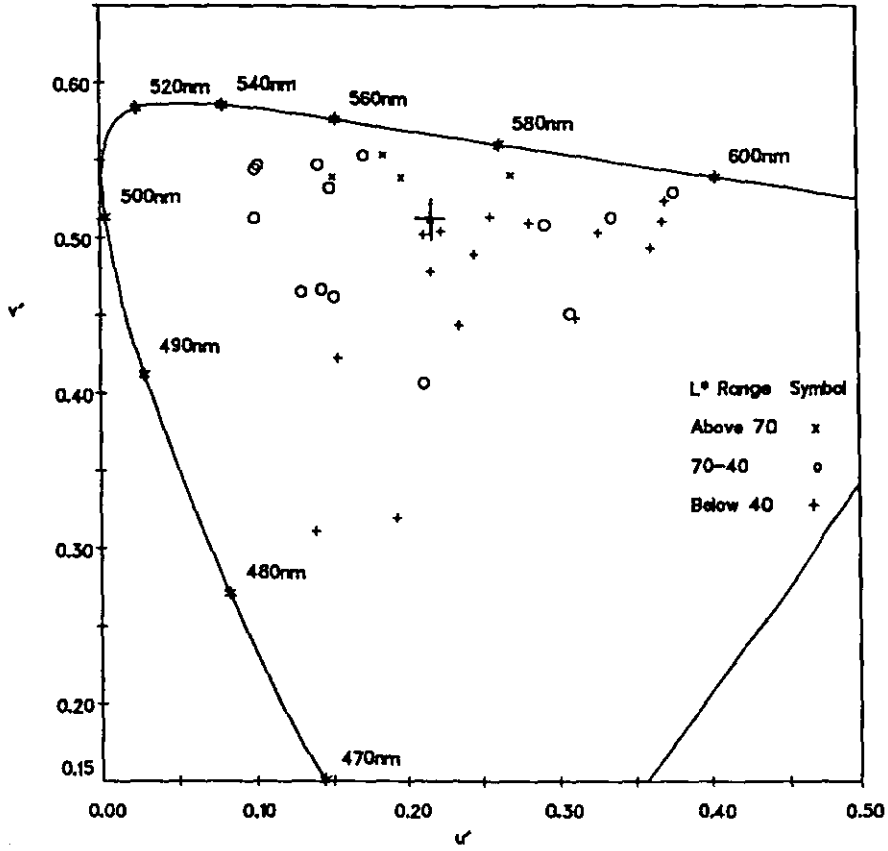


Figure 3.25 Chromaticity coordinates of 36 slide samples plotted on the CIE $u'v'$ diagram for phase 6 in Experiment 3. The larger plus symbol represents the reference white point.

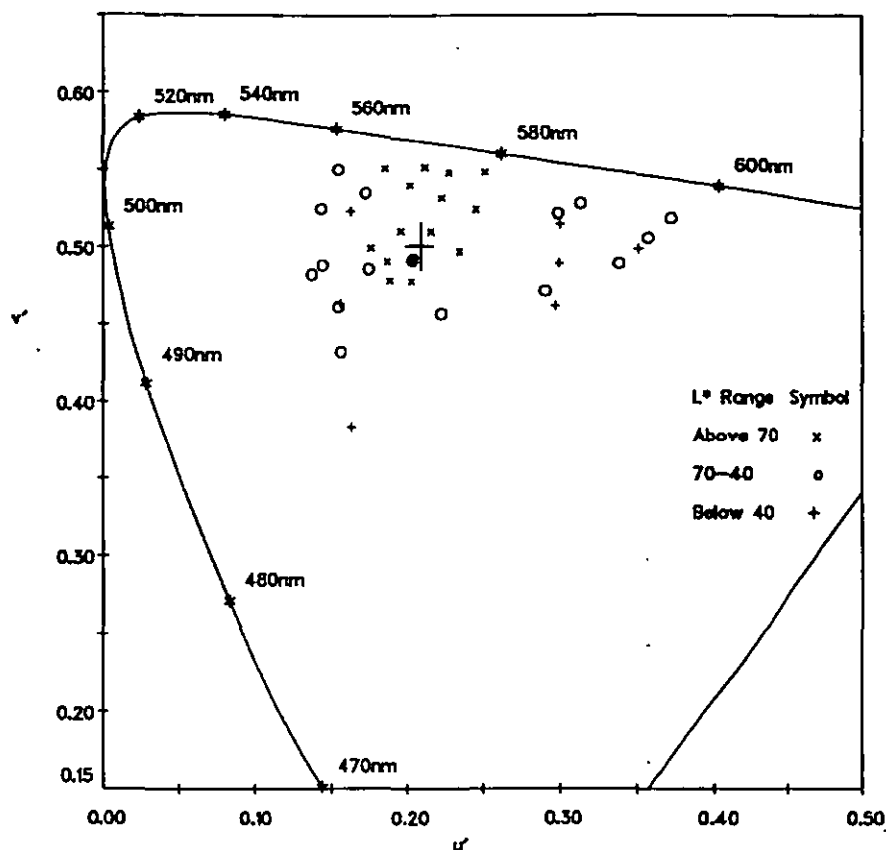


Figure 3.26 Chromaticity coordinates of 40 reflection paint samples plotted on the CIE $u'v'$ diagram under the viewing conditions of phases 1 and 7 in Experiment 4. The larger plus symbol represents the reference white point.

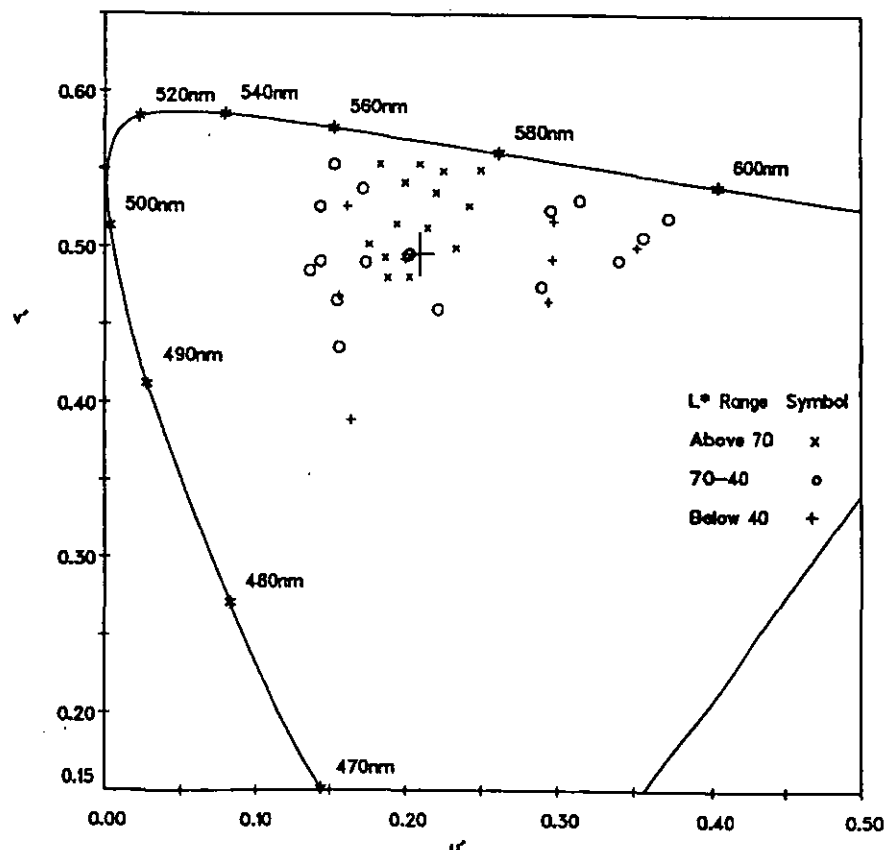


Figure 3.27 Chromaticity coordinates of 40 reflection paint samples plotted on the CIE $u'v'$ diagram under the viewing conditions of phases 2 and 8 in Experiment 4. The larger plus symbol represents the reference white point.

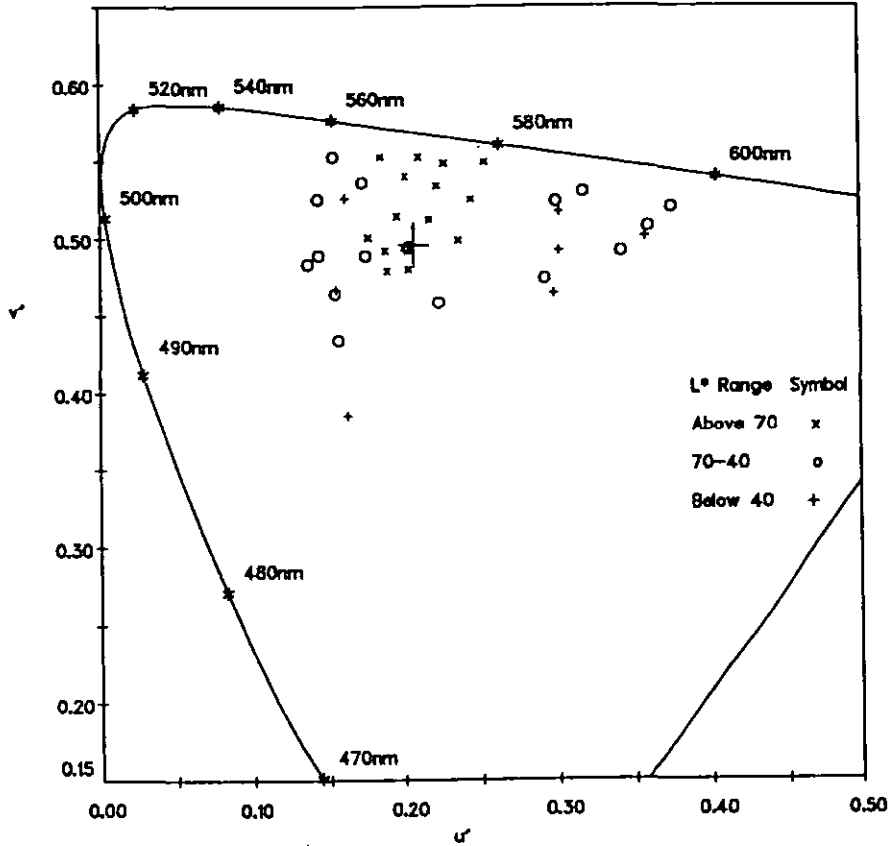


Figure 3.28 Chromaticity coordinates of 40 reflection paint samples plotted on the CIE $u'v'$ diagram under the viewing conditions of phases 3 and 9 in Experiment 4. The larger plus symbol represents the reference white point.

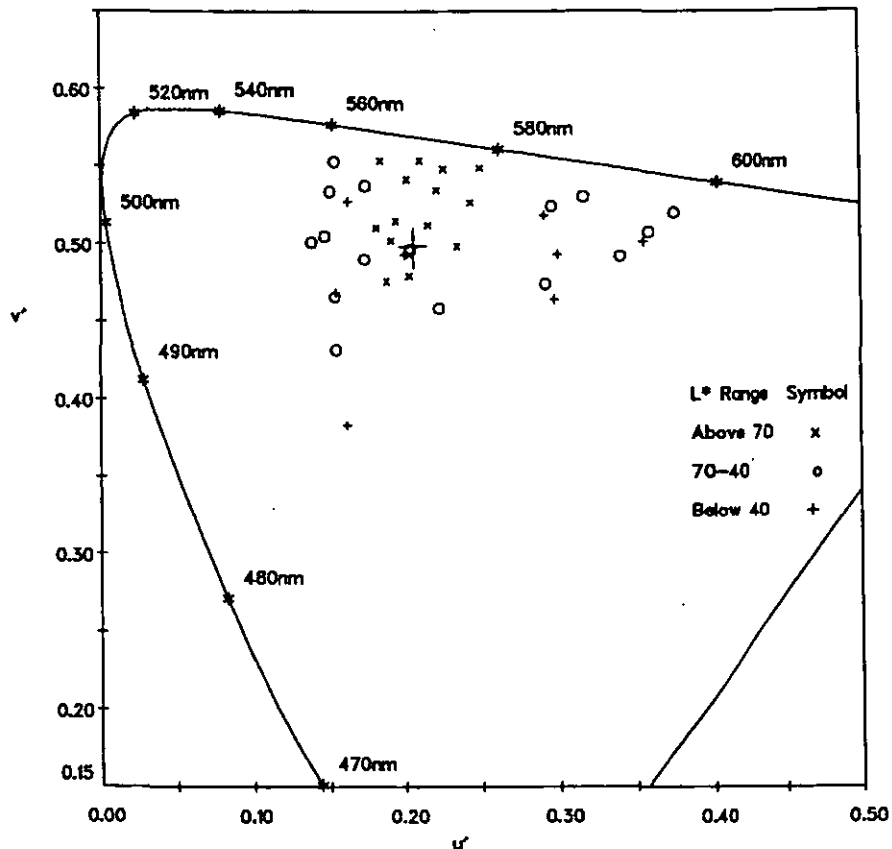


Figure 3.29 Chromaticity coordinates of 40 reflection paint samples plotted on the CIE $u'v'$ diagram under the viewing conditions of phases 4 and 10 in Experiment 4. The larger plus symbol represents the reference white point.

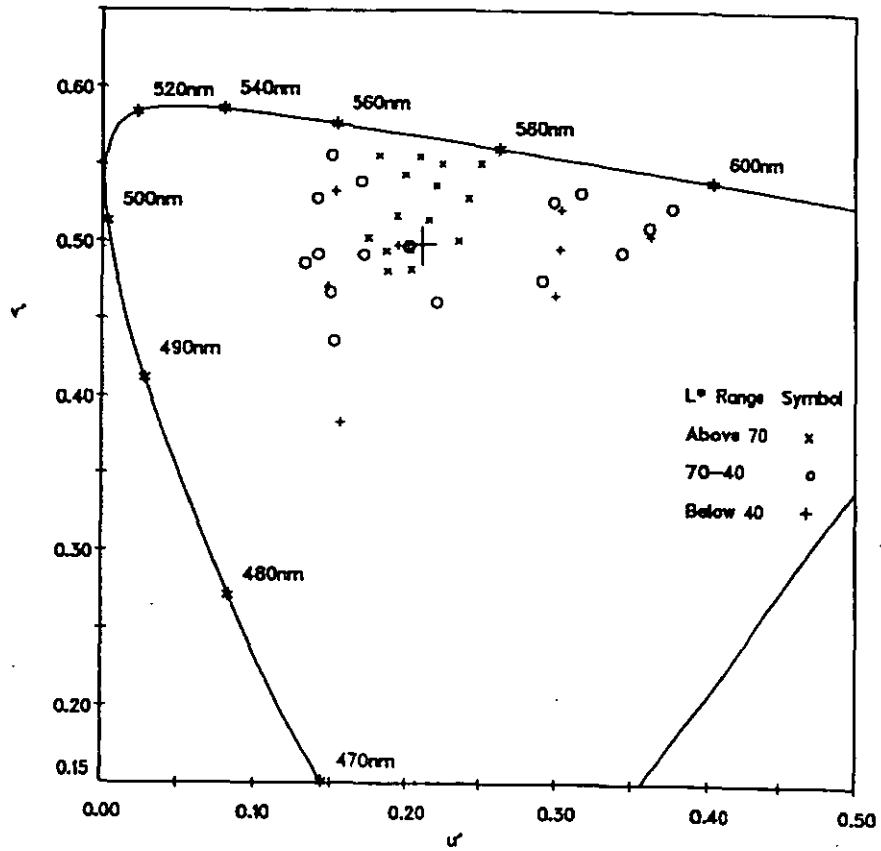


Figure 3.30 Chromaticity coordinates of 40 reflection paint samples plotted on the CIE $u'v'$ diagram under the viewing conditions of phases 5 and 11 in Experiment 4. The larger plus symbol represents the reference white point.

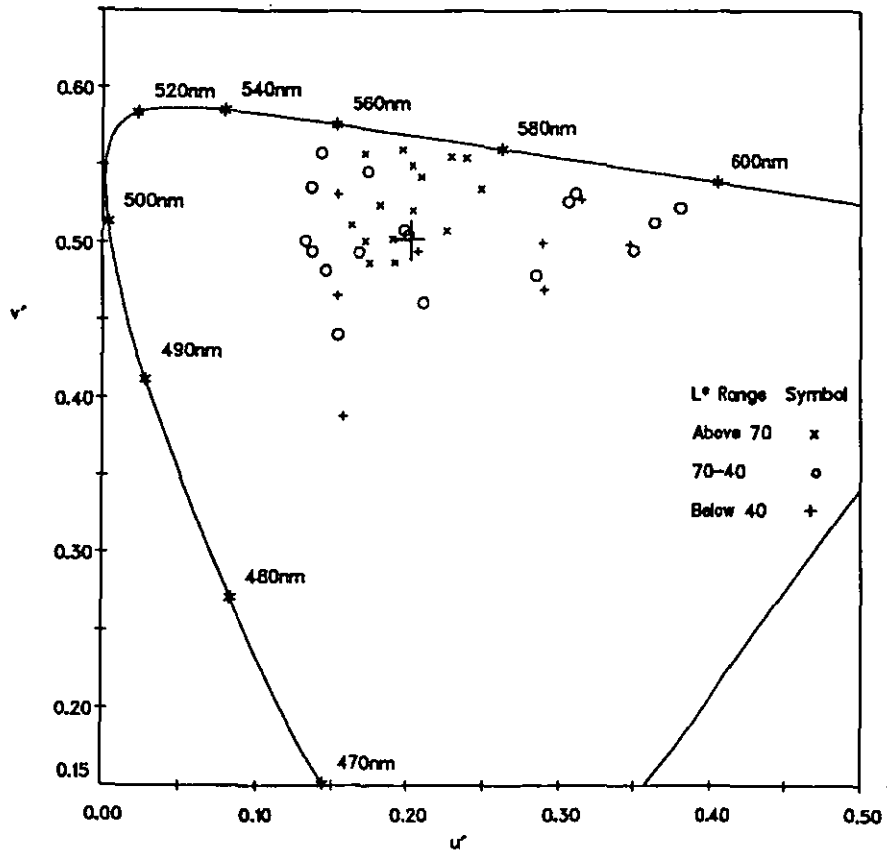


Figure 3.31 Chromaticity coordinates of 40 reflection paint samples plotted on the CIE $u'v'$ diagram under the viewing conditions of phases 6 and 12 in Experiment 4. The larger plus symbol represents the reference white point.

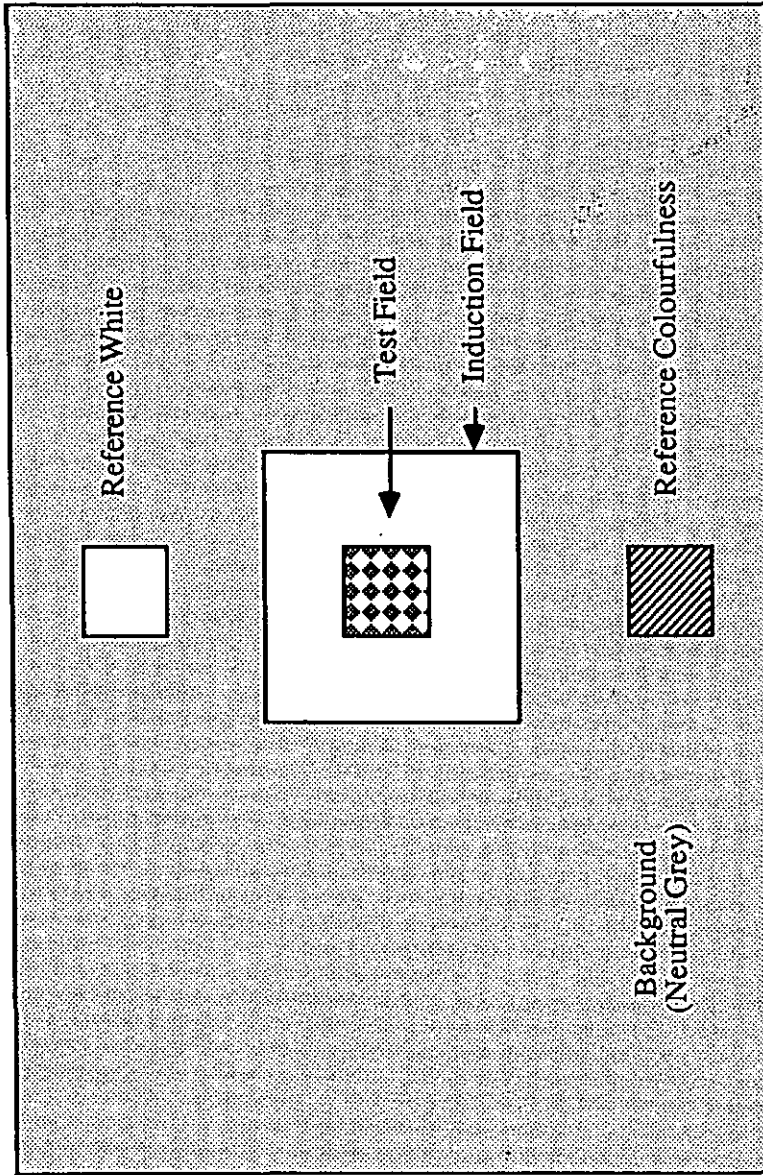


Figure 3.32 Display layout for Experiment 5

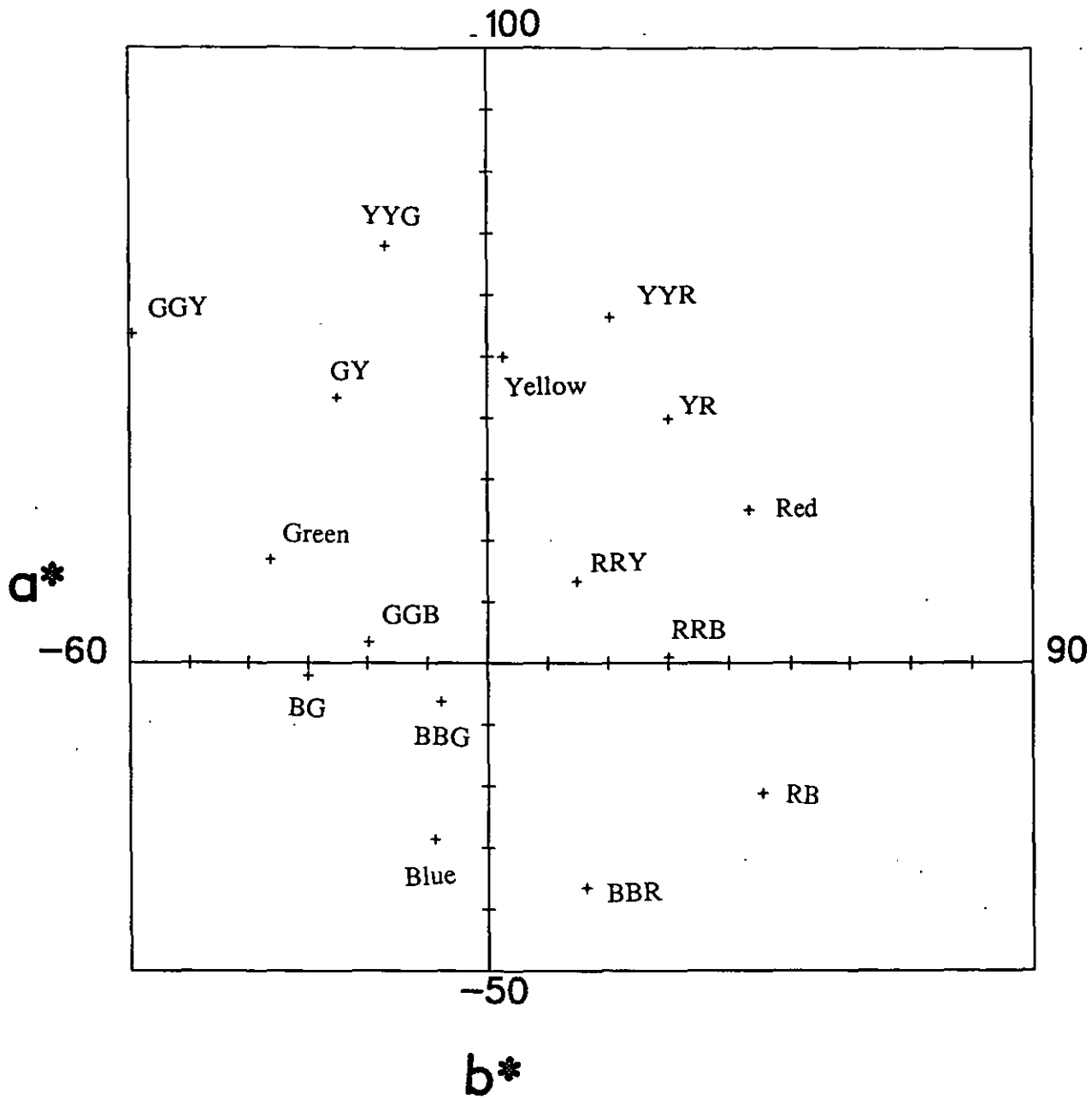


Figure 3.33 16 test field colours plotted on the CIE $L^*a^*b^*$ diagram for Experiment 5. Colours of YR, GY, BG and RB were used in the early studies^[102]

Figure 4.1 Comparison of visual response in Experiment 2 between high and low luminance levels: lightness (top), colourfulness (middle) and hue (bottom).

Left: phase 1 (y axis) vs phase 2 (x axis) with lighter background
Right: phase 6 (y axis) vs phase 7 (x axis) with darker background

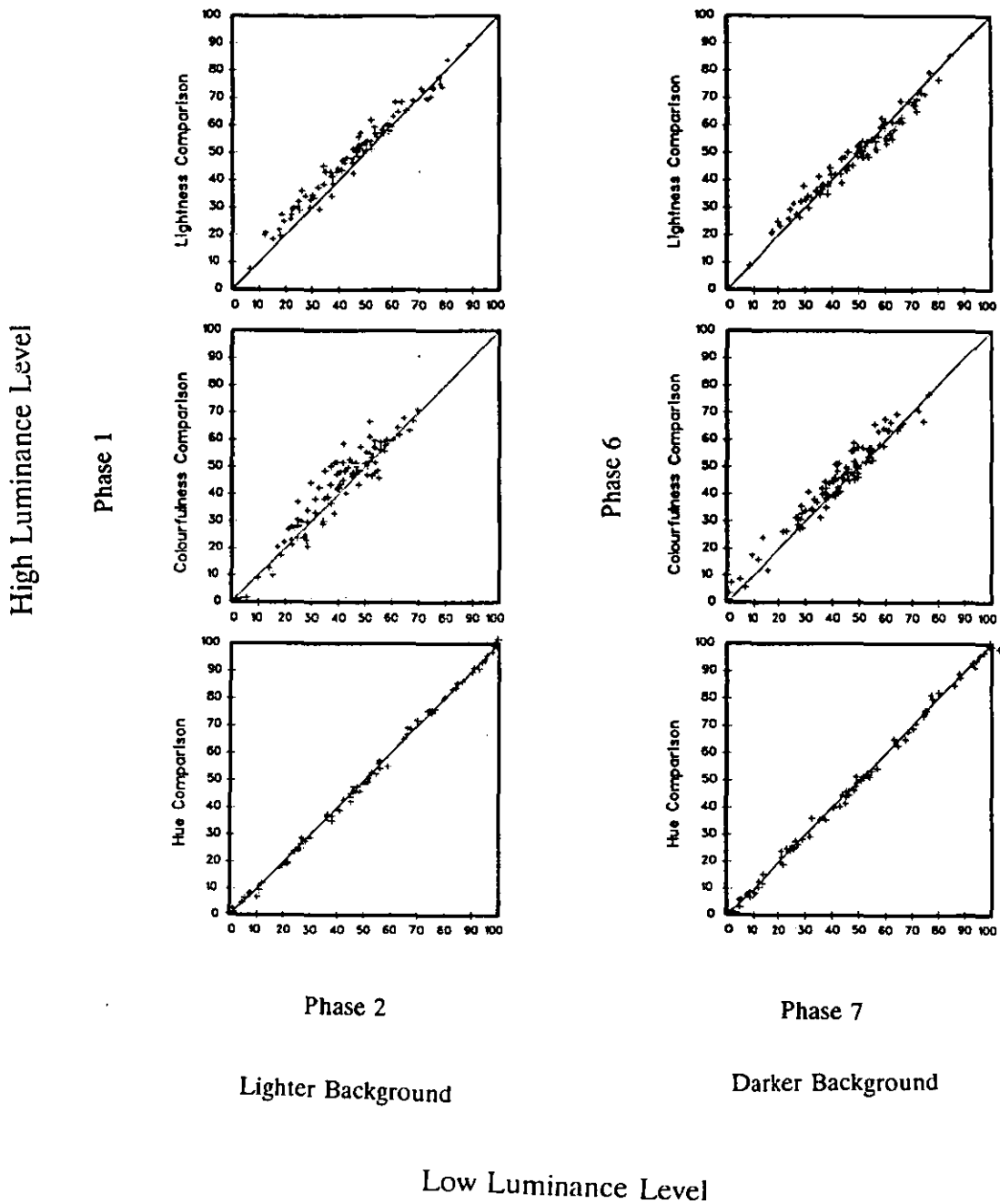


Figure 4.2 Comparison of visual response in Experiment 3 between high (phase 1, y axis) and low (phase 3, x axis) luminance levels: lightness (top), colourfulness (middle) and hue (bottom).

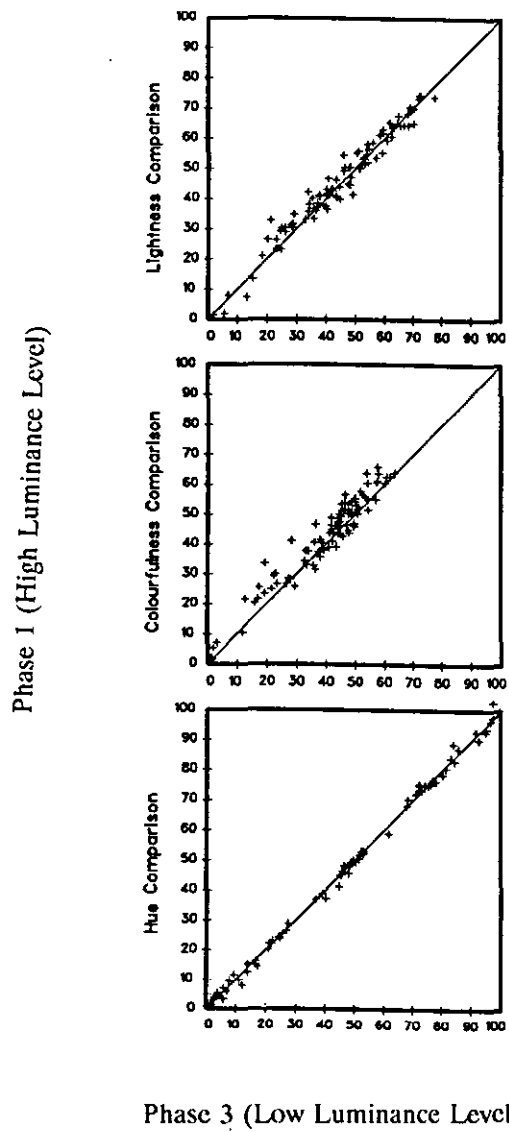


Figure 4.3 Comparison of visual response in Experiment 2 between phase 4 (y axis) with flare light and phase 2 (x axis): lightness (top), colourfulness (middle) and hue (bottom)

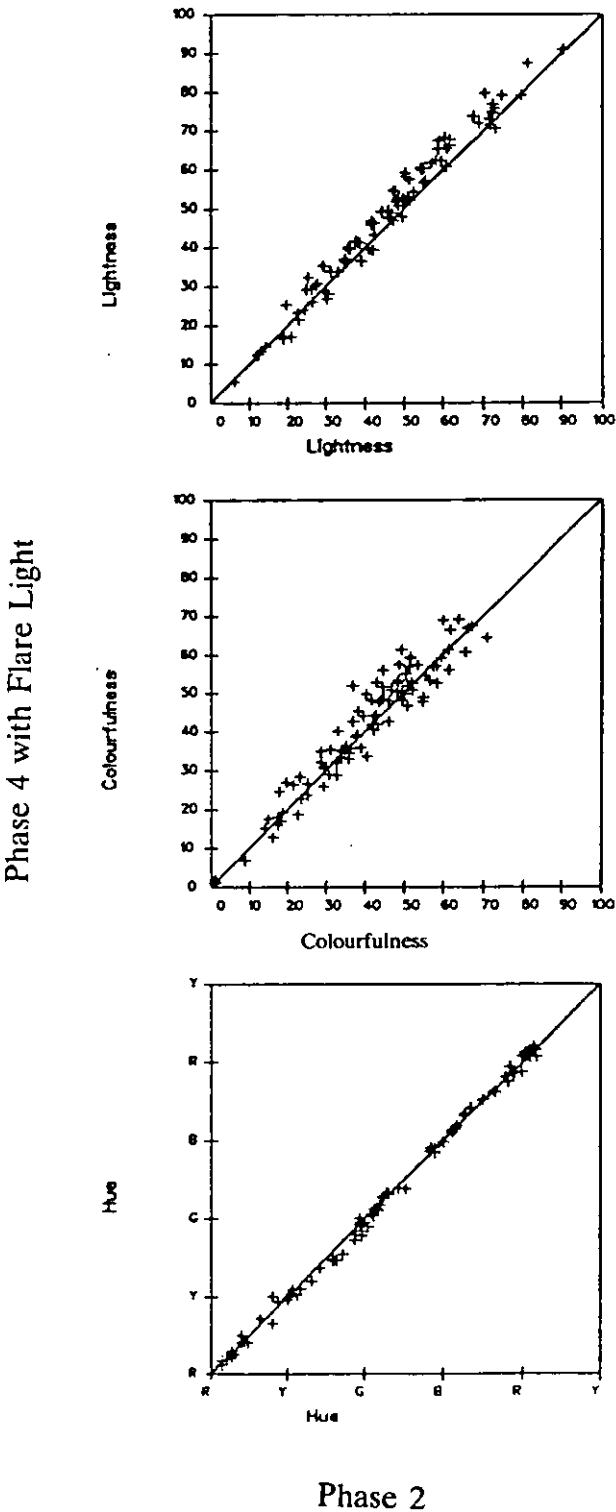


Figure 4.4 Comparison of visual response in Experiment 2 between darker and lighter grey backgrounds: lightness (top), colourfulness (middle) and hue (bottom)
 Left: phase 10 (y axis) vs phase 2 with white border
 Right: phase 6 (y axis) vs phase 11 with black border

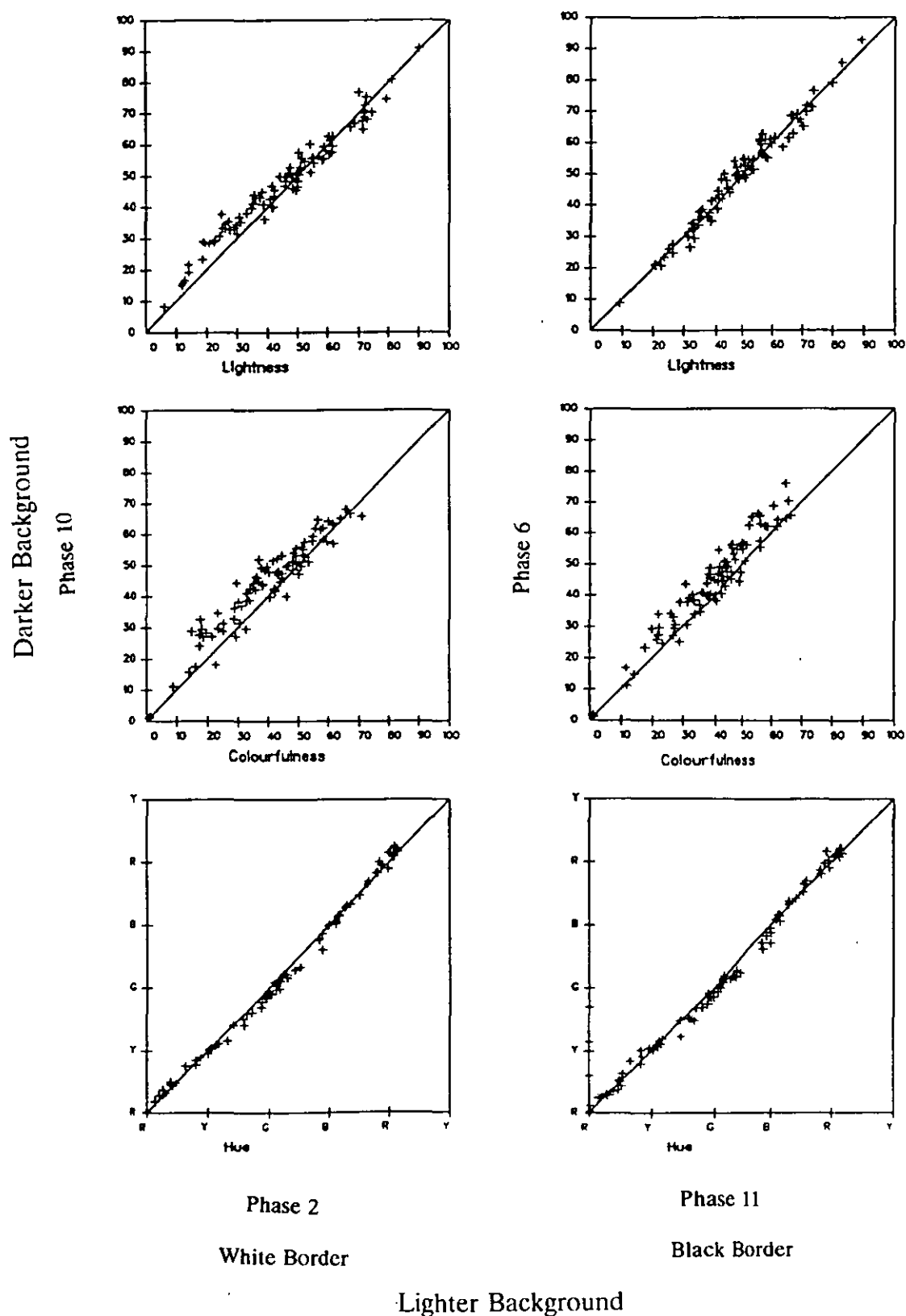


Figure 4.5 Comparison of visual response between black and white borders: lightness (top), colourfulness (middle) and hue (bottom) in Experiment 2

Left: phase 11 (y axis) vs phase 2 against lighter background

Right: phase 6 (y axis) vs phase 10 against darker background

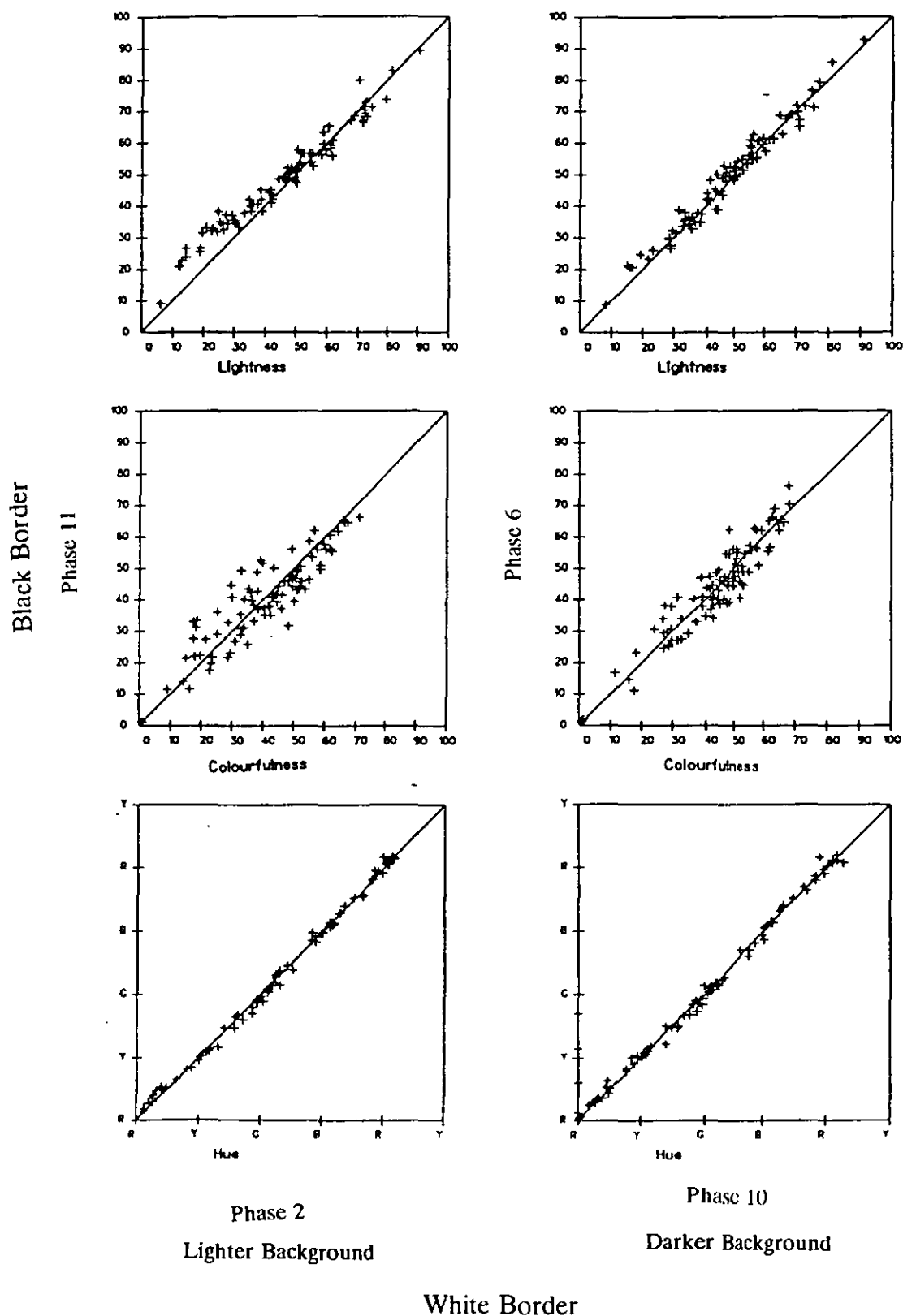


Figure 4.6 Response diagram plotted using phase 3 (4000K represented by "o") and phase 2 (5600K represented by "*"") data in Experiment 3

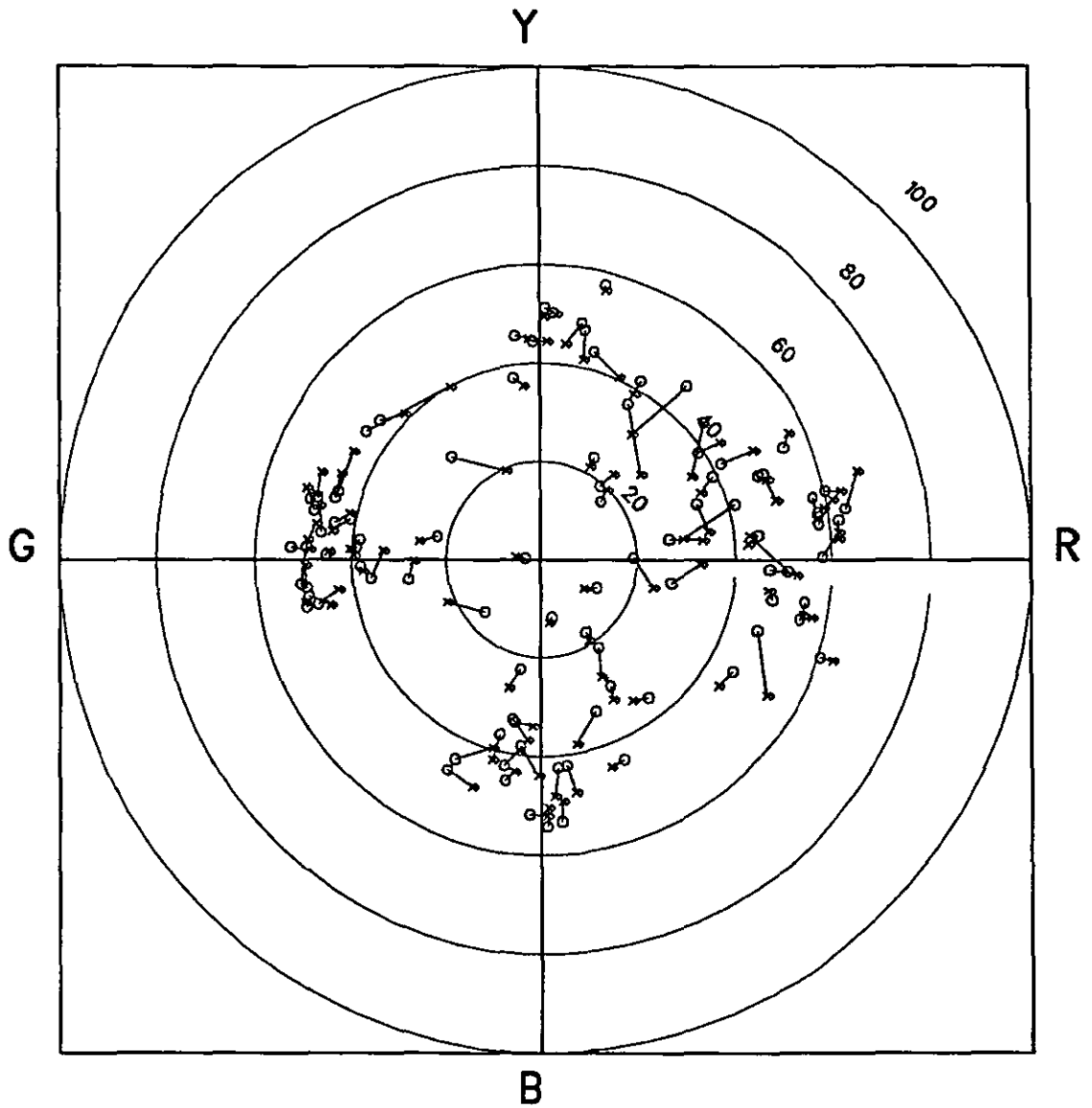


Figure 4.7 Comparison of lightness visual data obtained from phases 1 (top) and 5 (bottom) in Experiment 2 with those predicted by CMC (1:1), CIE, Nayatani and Hunt91 lightness scales

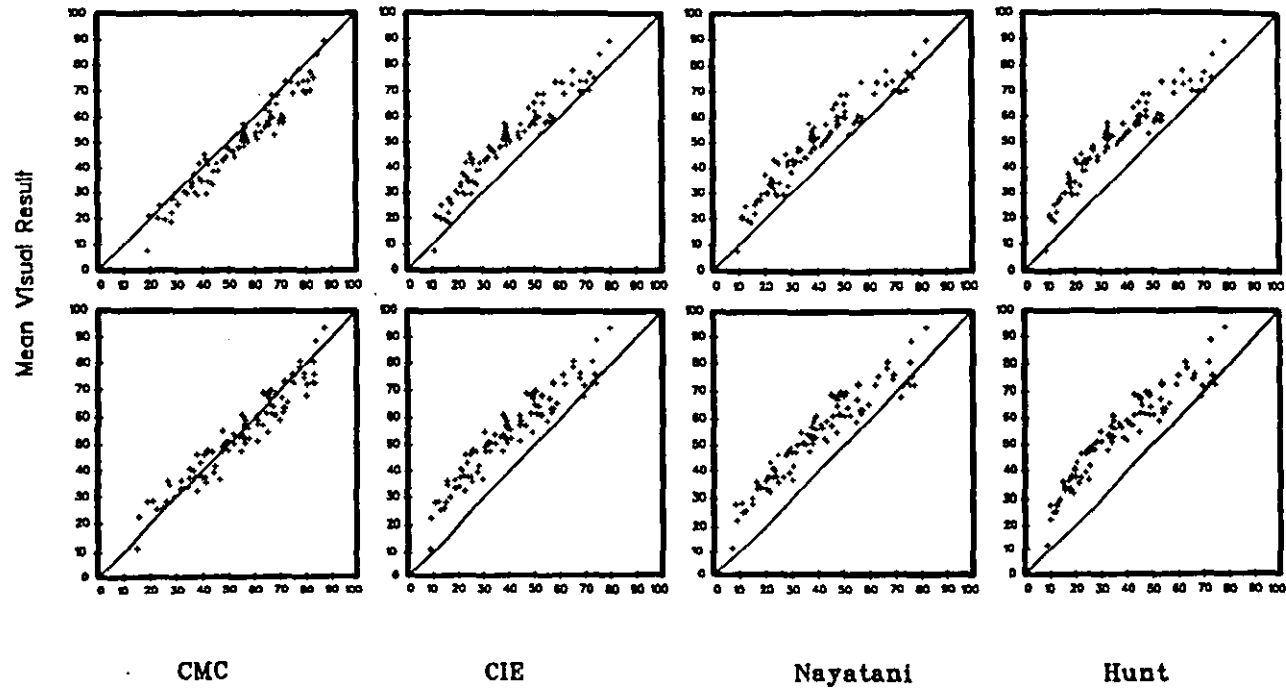


Figure 4.8 Comparison of lightness visual data obtained from phases 1 (top) and 2 (bottom) in Experiment 3 with those predicted by CMC (1:1), CIE, Nayatani and Hunt91 lightness scales

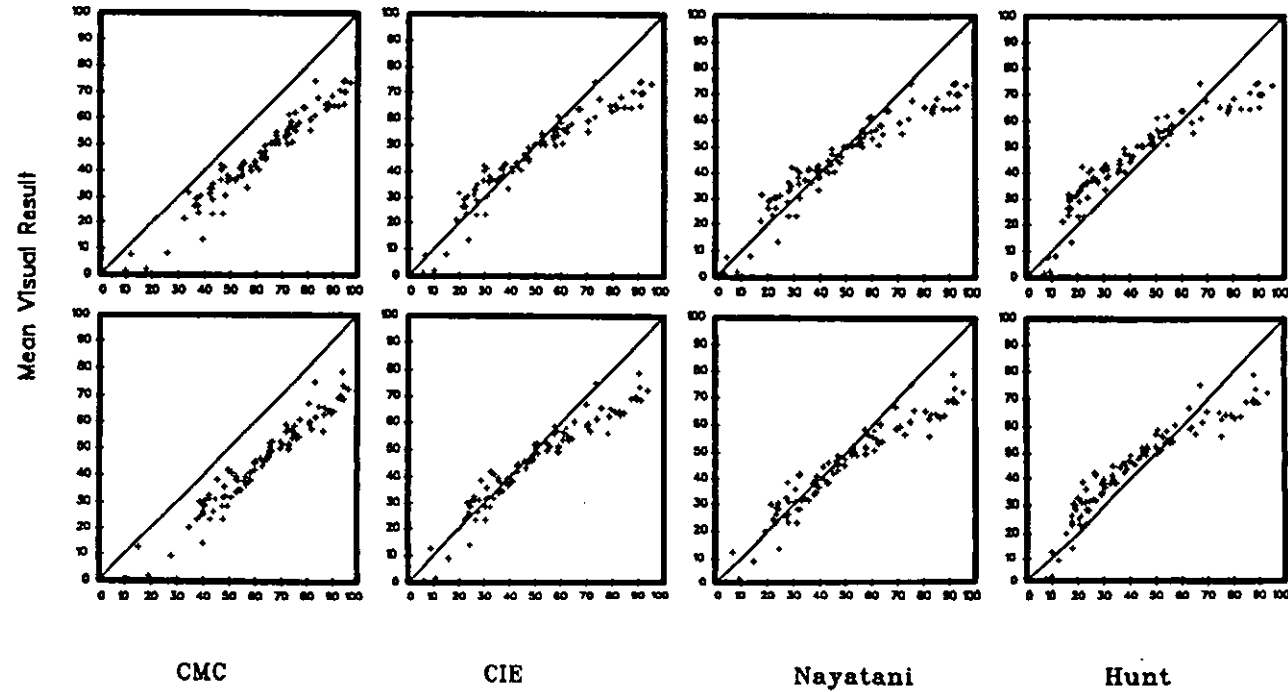


Figure 4.9 Comparison of lightness visual data obtained from phases 5 (top) and 6 (bottom) in Experiment 3 against those predicted by CMC (1:1), CIE, Nayatani and Hunt91 lightness scales

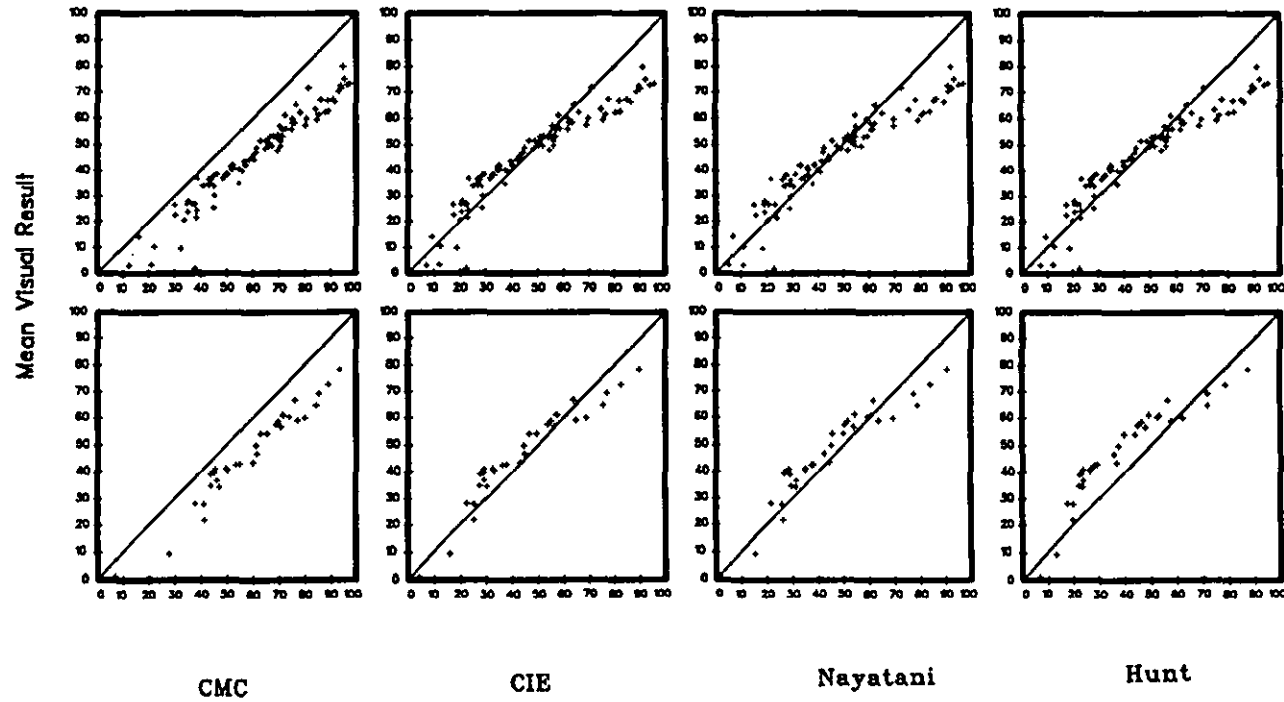


Figure 4.10 Comparison of colourfulness visual data obtained from phase 1 in Experiment 2 with those predicted by CMC (1:1), CIE $L^*a^*b^*$, CIE $L^*u^*v^*$, Nayatani and Hunt91 chroma scales

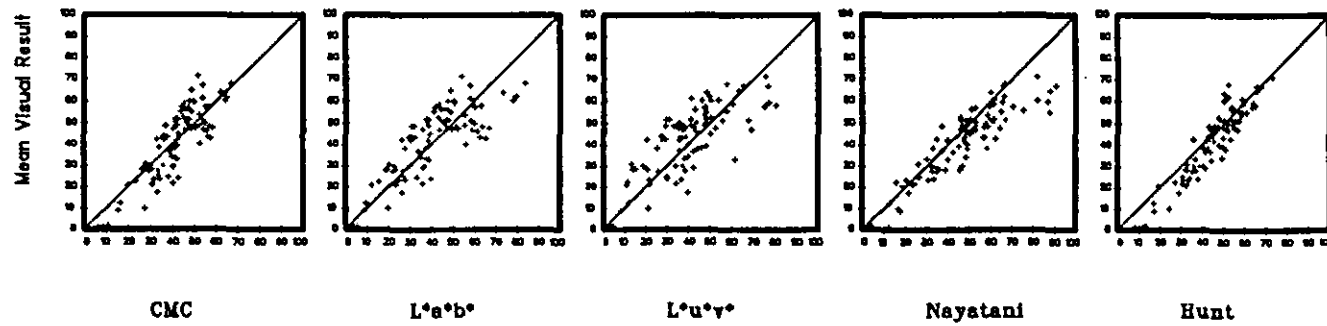


Figure 4.11 Comparison of colourfulness visual data obtained from phases 1 (top) and 2 in Experiment 3 with those predicted by CMC (1:1), CIE $L^*a^*b^*$, CIE $L^*u^*v^*$, Nayatani and Hunt91 chroma scales

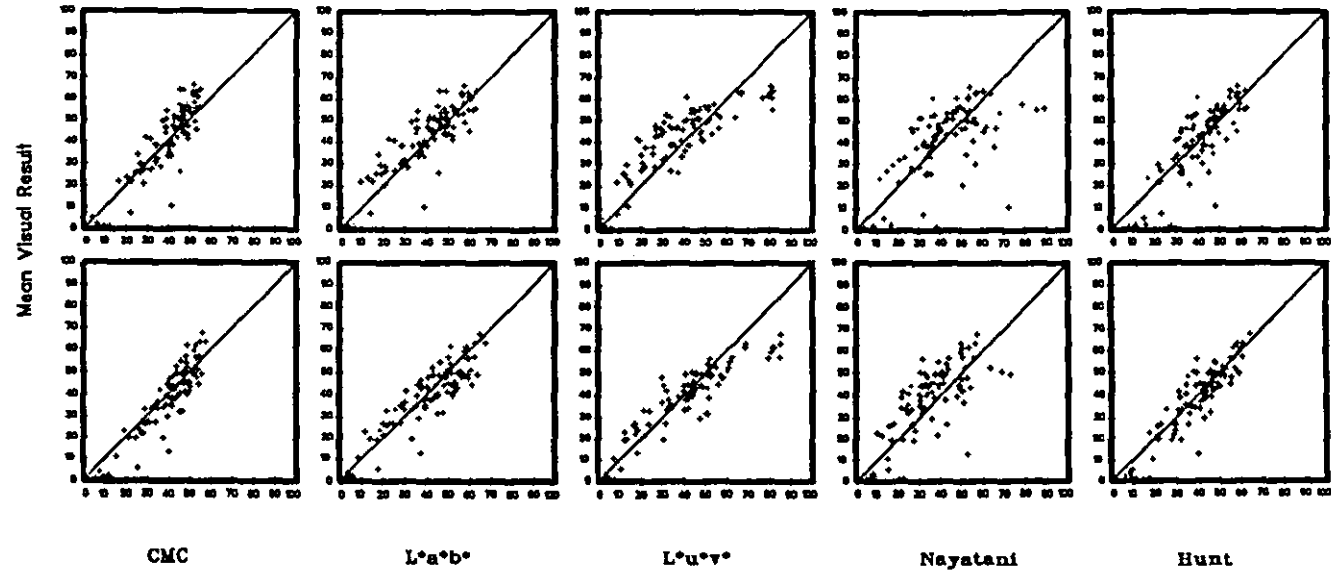


Figure 4.12 Comparison of hue visual data obtained from phases 1 (left) and 5 (right) in Experiment 2 with those predicted by Nayatani (top) and Hunt91 (bottom) hue scales

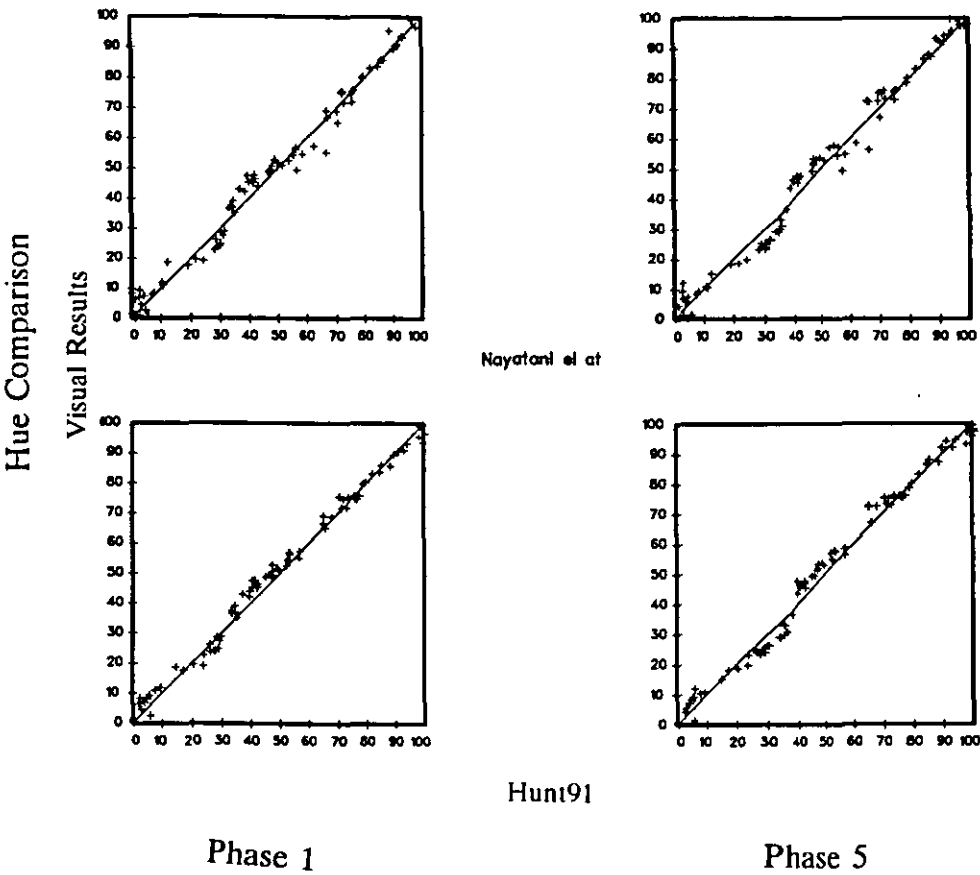


Figure 4.13 Comparison of hue visual data obtained from phases 1 (left) and 2 (right) in Experiment 3 with those predicted by Nayatani (top) and Hunt91 (bottom) hue scales

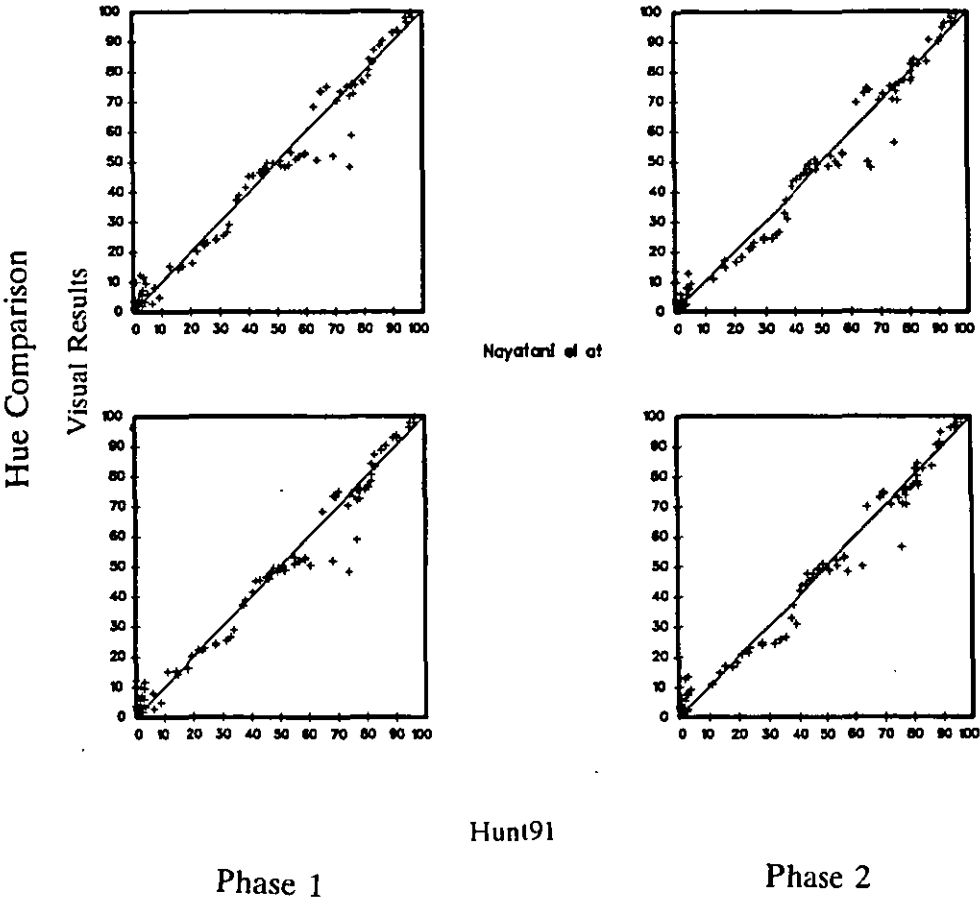


Figure 4.14 Comparison of lightness visual data obtained from phases 1 (top) and 5 (bottom) in Experiment 2 with those predicted by the modified Hunt91 lightness scales ($N_b=25$ together with z values of 1 and 0.85 for phases 1 and 5 respectively)

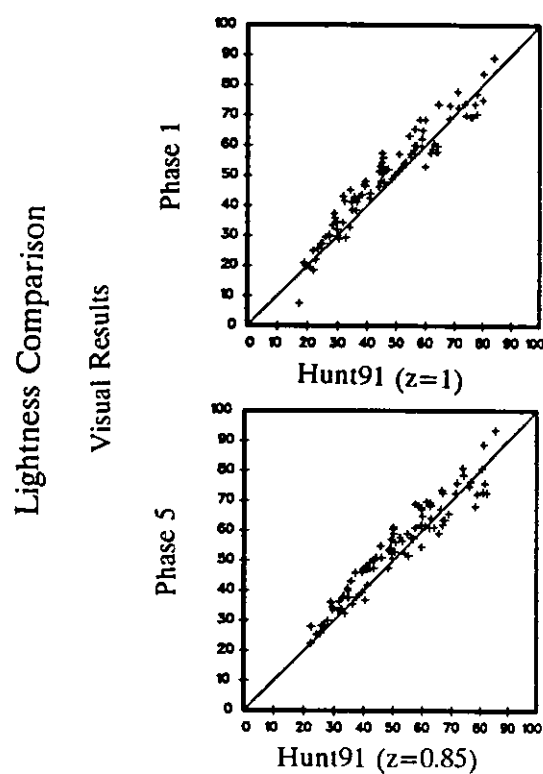


Figure 4.15 Comparison of lightness visual data obtained from phases 1 (top) and 2 (bottom) in Experiment 3 with those predicted by the modified Hunt91 lightness scale (J_{new})

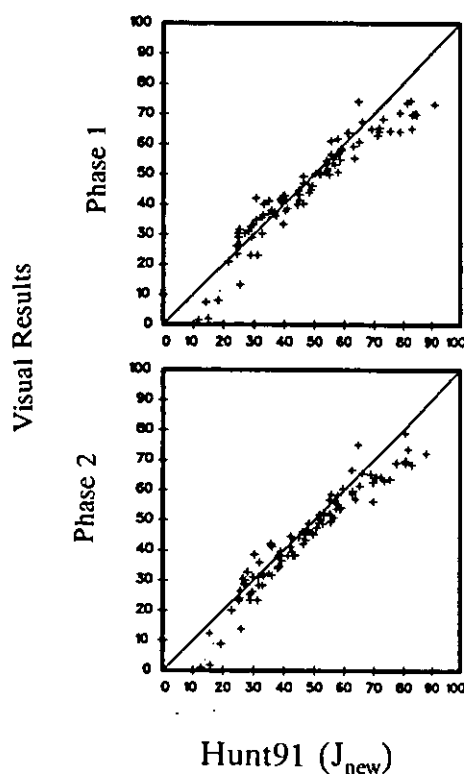


Figure 4.16 Comparison of colourfulness (top) and hue (bottom) visual data obtained from phases 1 (left) and 2 (right) in Experiment 3 with those predicted by the modified Hunt91 chroma and hue scales (at $\rho_D=\gamma_D=\beta_D=0$)

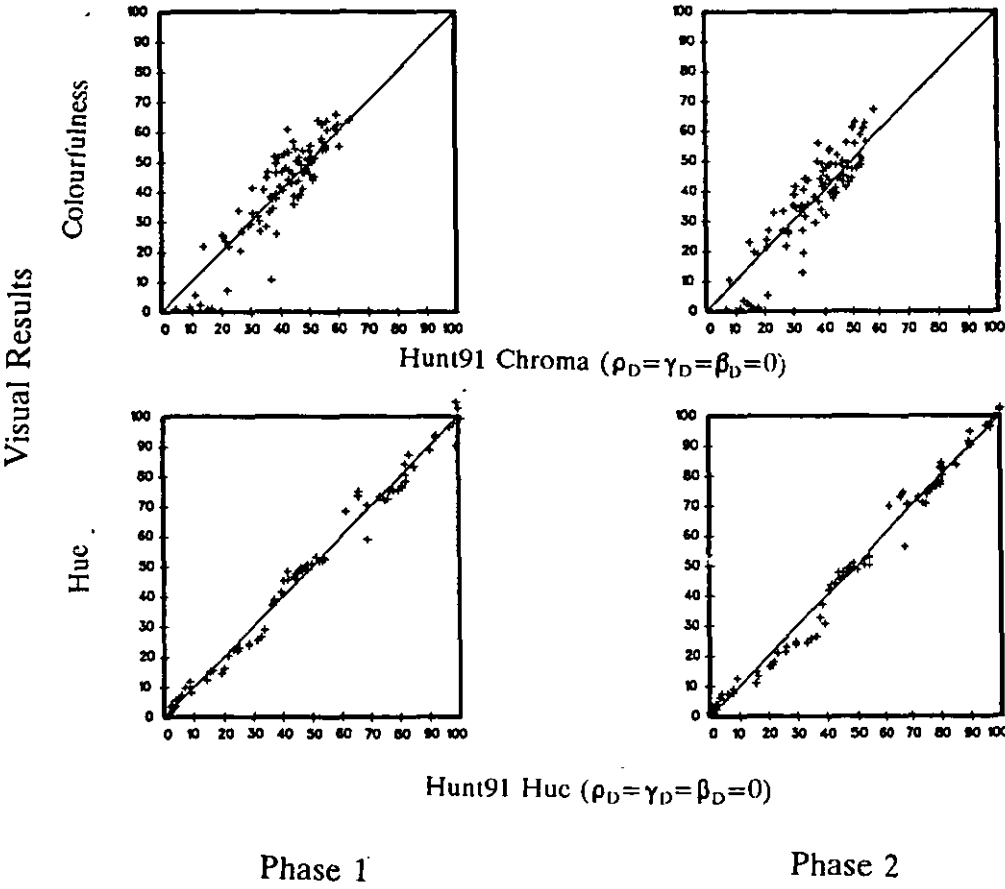


Figure 4.17 Comparison of visual data obtained in Experiment 4 between combined phase 1 (y axis) and the other phases. The lightness, brightness, colourfulness and hue are shown from left to right. The comparisons of combined phases cp1 and cps2 to 4 are shown from top to bottom.

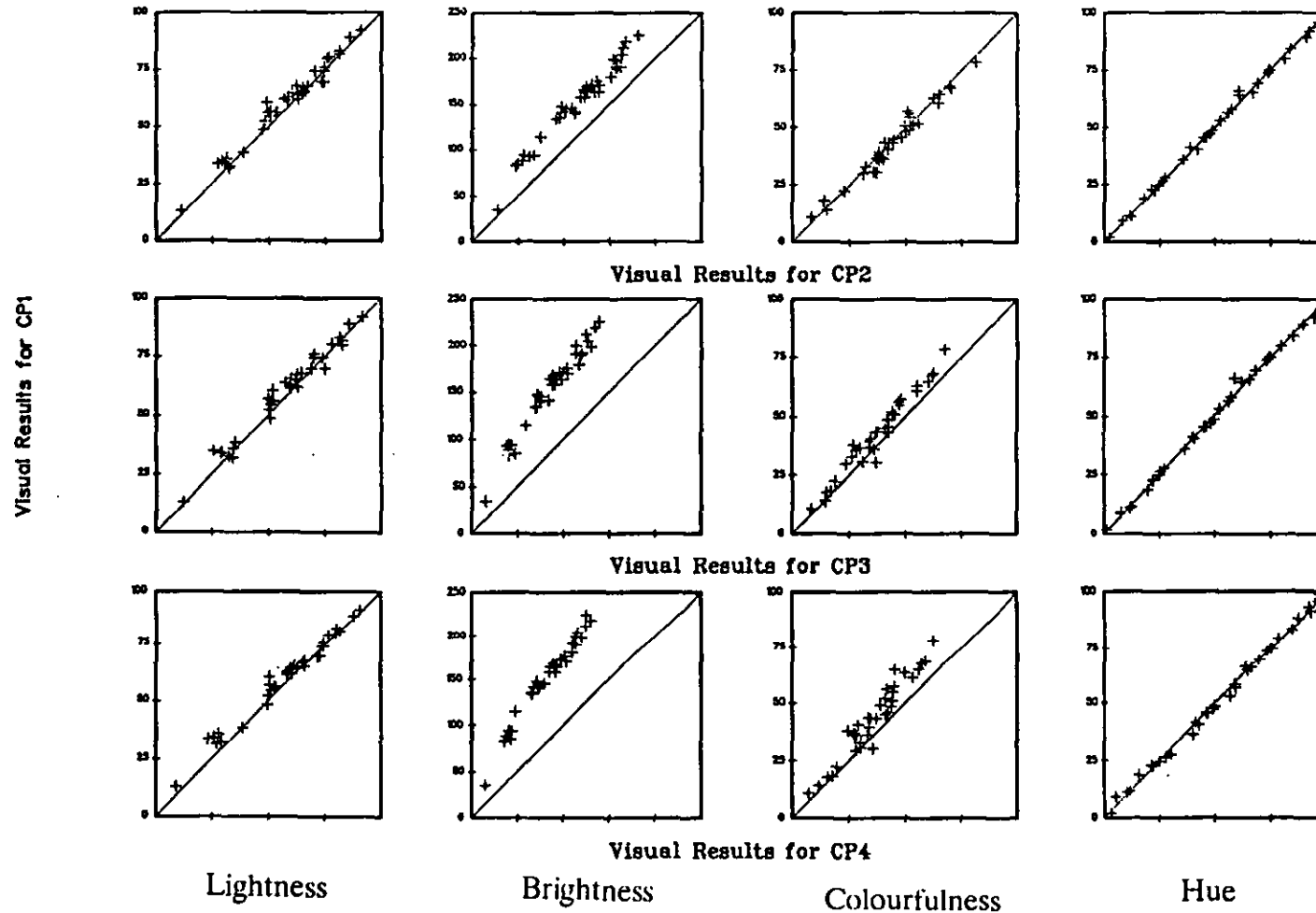


Figure 4.18 Comparison of visual data obtained in Experiment 4 between combined phase 1 (y axis) and the other phases. The lightness, brightness, colourfulness and hue are shown from left to right. The comparisons of combined phases cp1 and cps5 and 6 are shown from top to bottom.

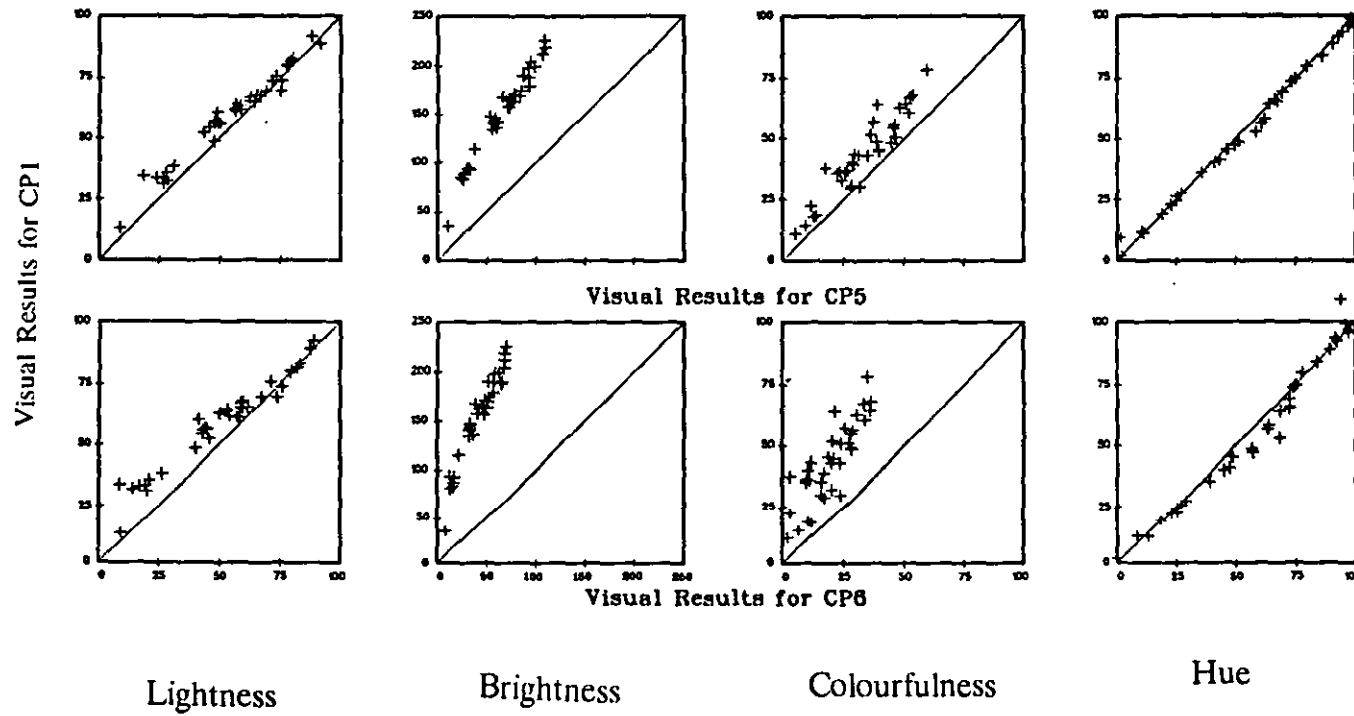
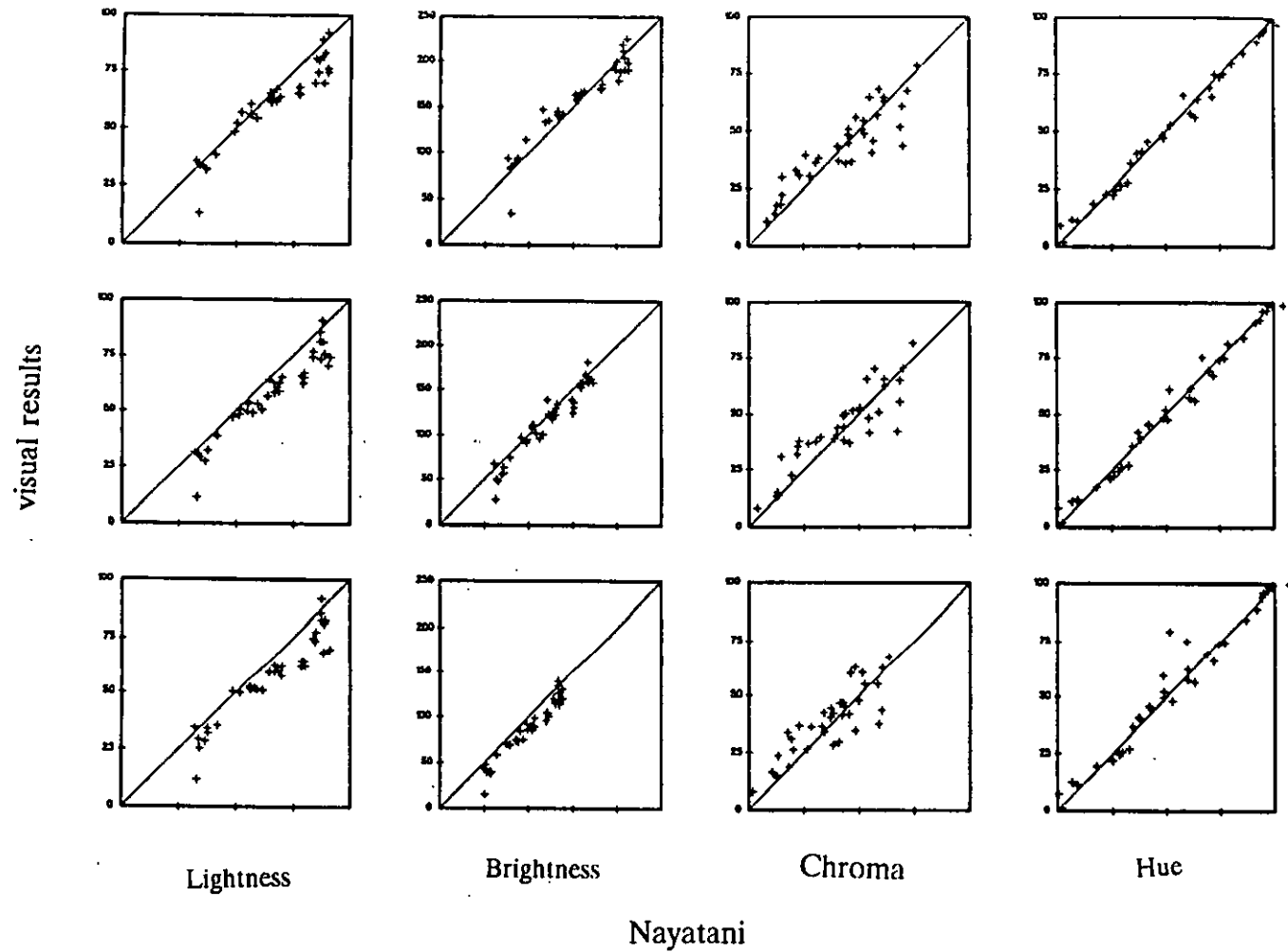


Figure 4.19 (a) Comparison between visual data (y axis) from combined phases cp1 (top) to cp3 (bottom) in Experiment 4 and those predicted by Nayatani model for lightness (left), brightness, chroma and hue (right)



(b) Comparison between visual data (y axis) from combined phases cp4 (top) to cp6 (bottom) in Experiment 4 and those predicted by Nayatani model for lightness (left), brightness, chroma and hue (right)

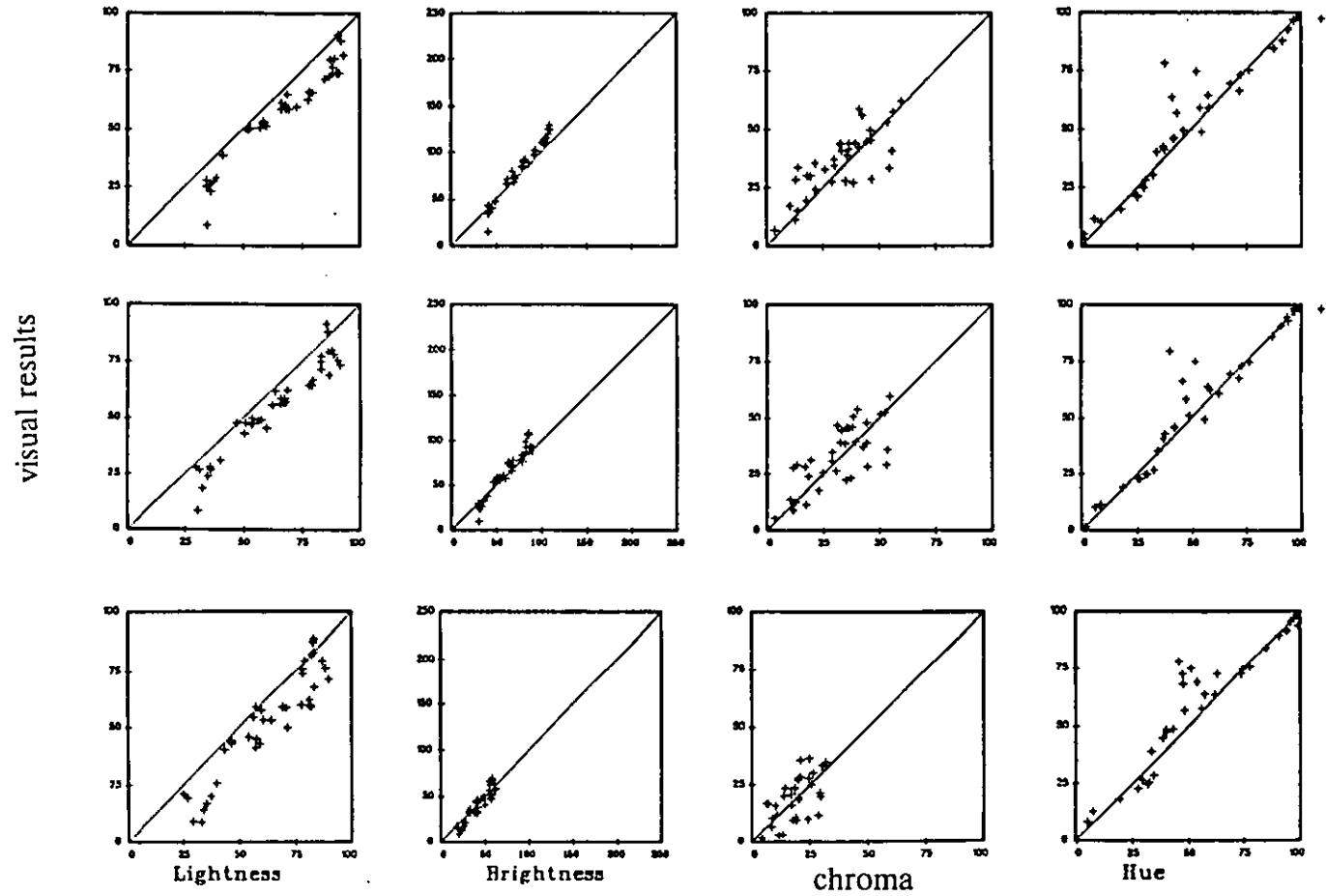
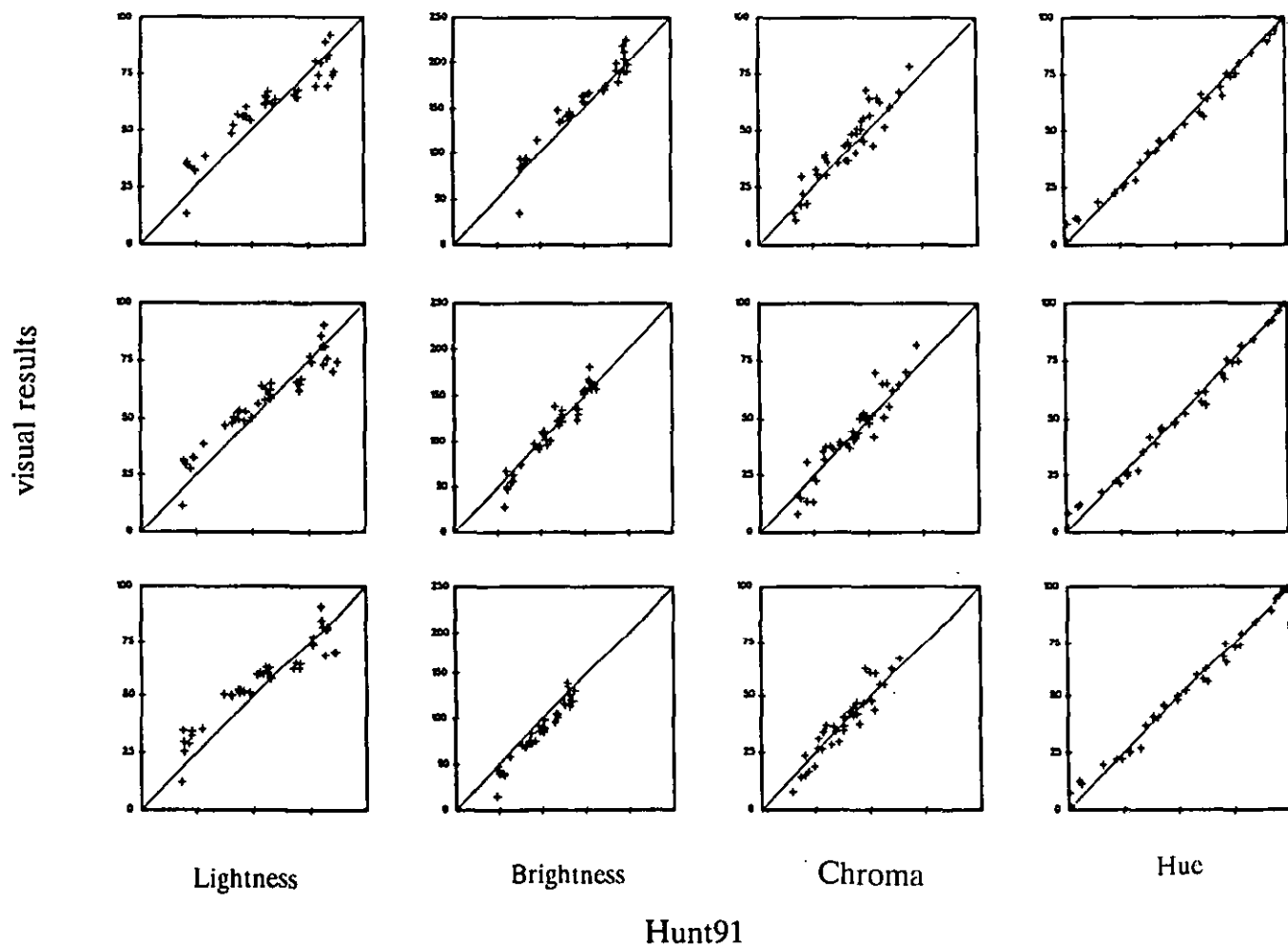


Figure 4.20 (a) Comparison between visual data (y axis) from combined phases cp1 (top) to cp3 (bottom) in Experiment 4 and those predicted by Hunt91 model for lightness (left), brightness, chroma and hue (right)



(b) Comparison between visual data (y axis) from combined phases cp4 (top) to cp6 (bottom) in Experiment 4 and those predicted by Hunt91 model for lightness (left), brightness, chroma and hue (right)

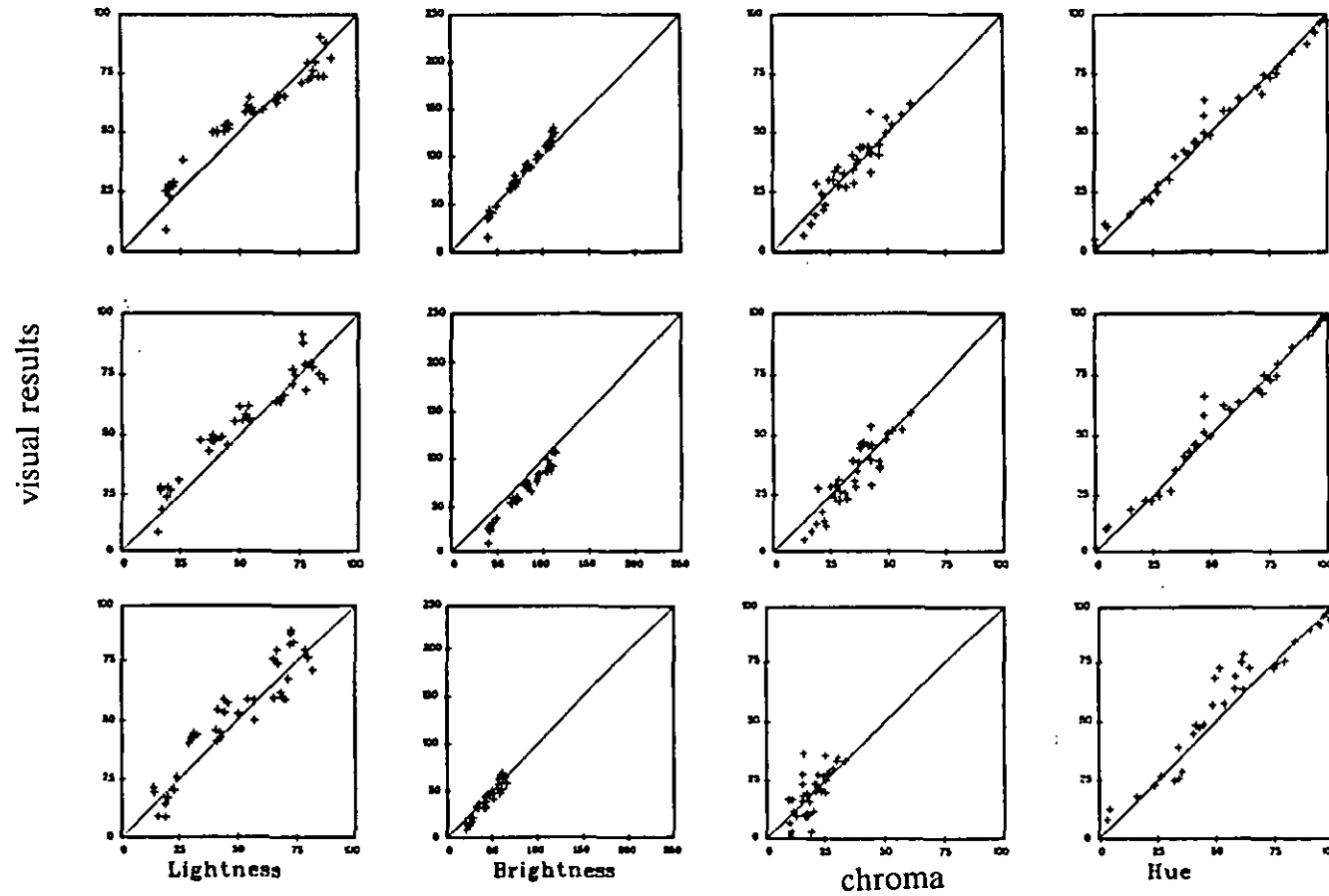


Figure 4.21 The lightness difference plotted against CIEL* of induction fields for test colours Red, RRY, YYR and Yellows in Experiment 5. The five circles refer to the test patch surrounded by five achromatic induction fields.

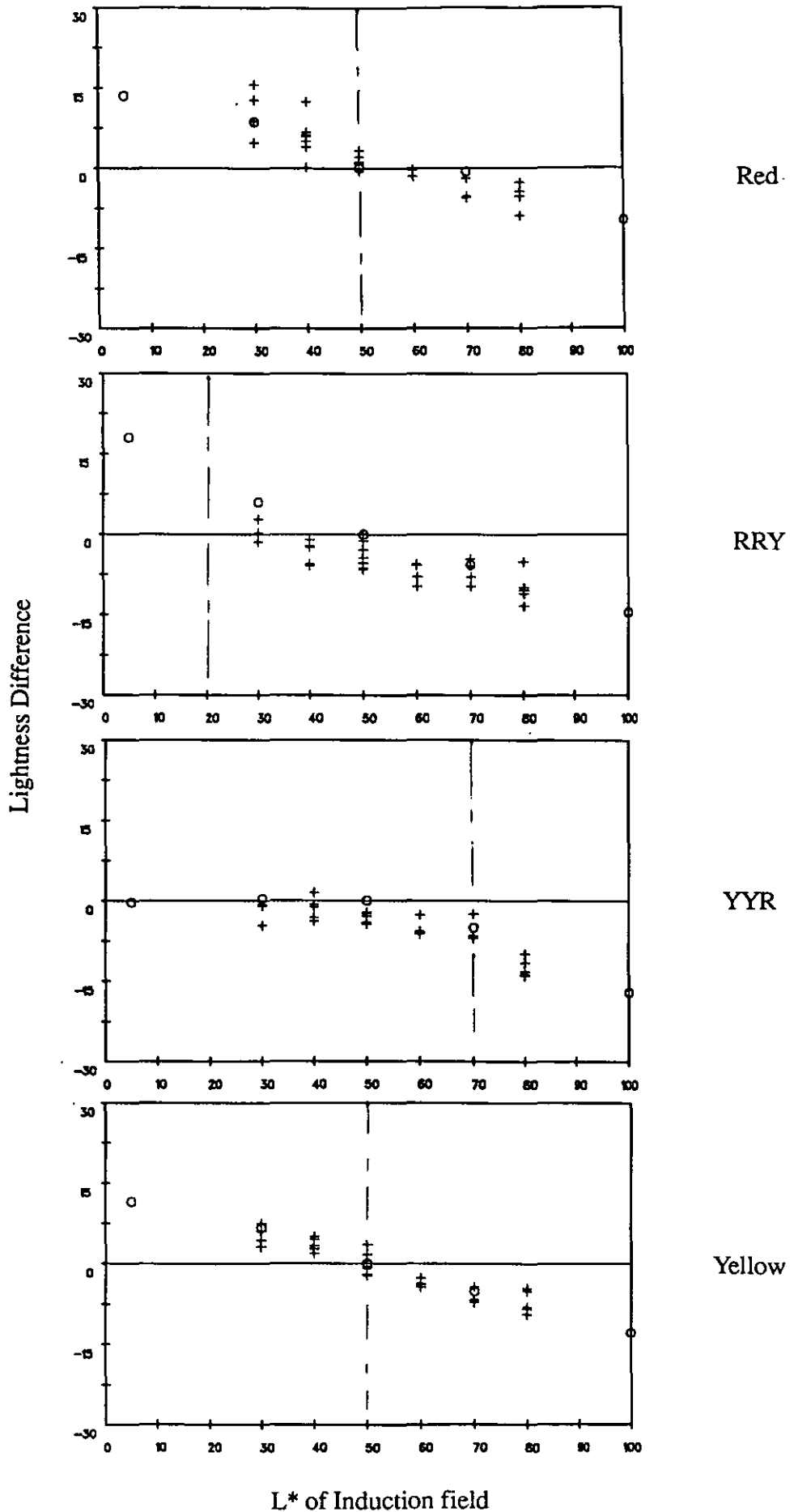


Figure 4.22 The lightness difference plotted against CIEL* of induction fields for test colours YYG, GGY, Green and GGB in Experiment 5. The five circles refer to the test patch surrounded by five achromatic induction fields.

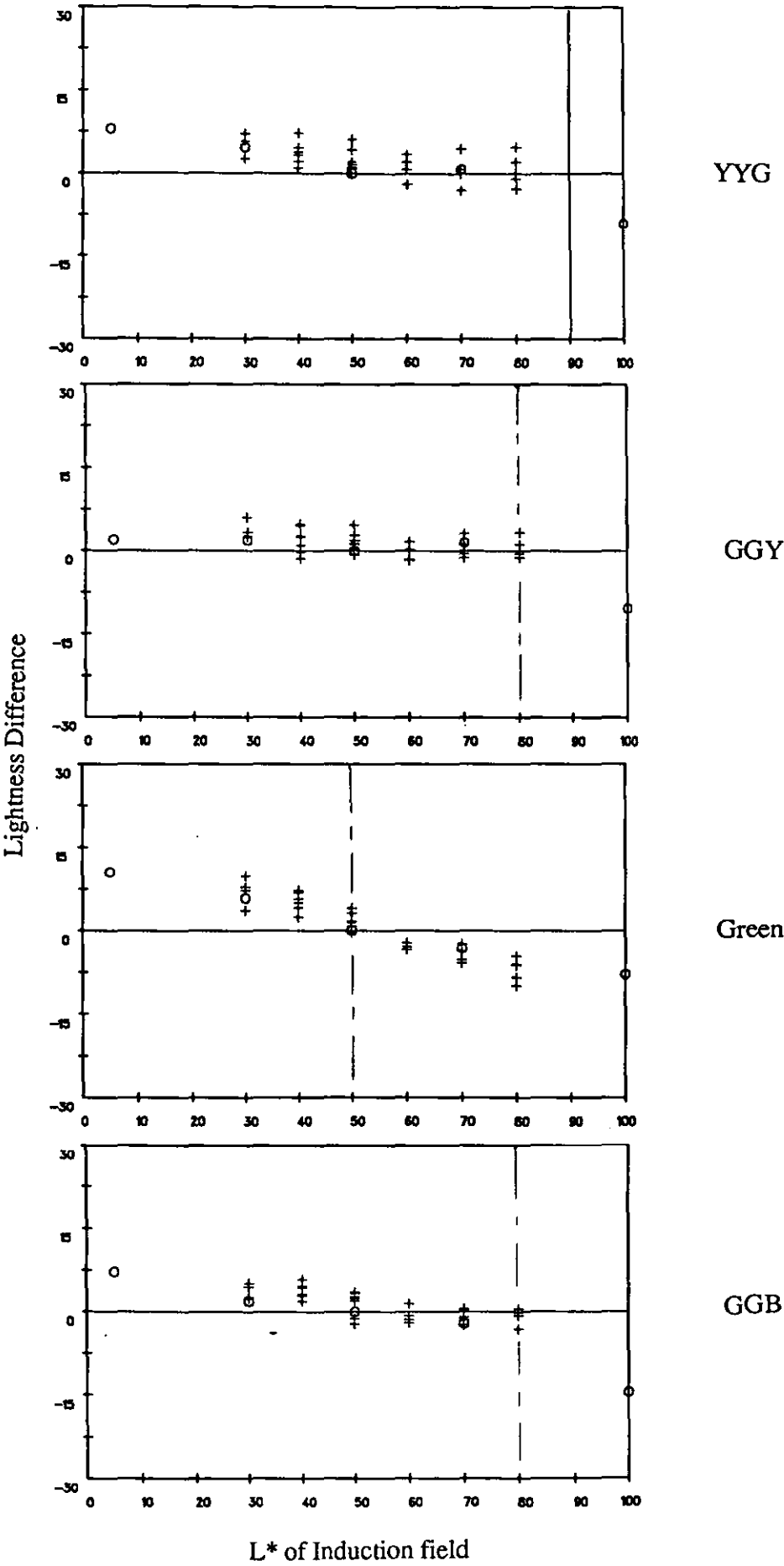


Figure 4.23 The lightness difference plotted against CIEL* of induction fields for test colours Blue, BBG, BBR, RRB and Grey in Experiment 5. The five circles refer to the test patch surrounded by five achromatic induction fields.

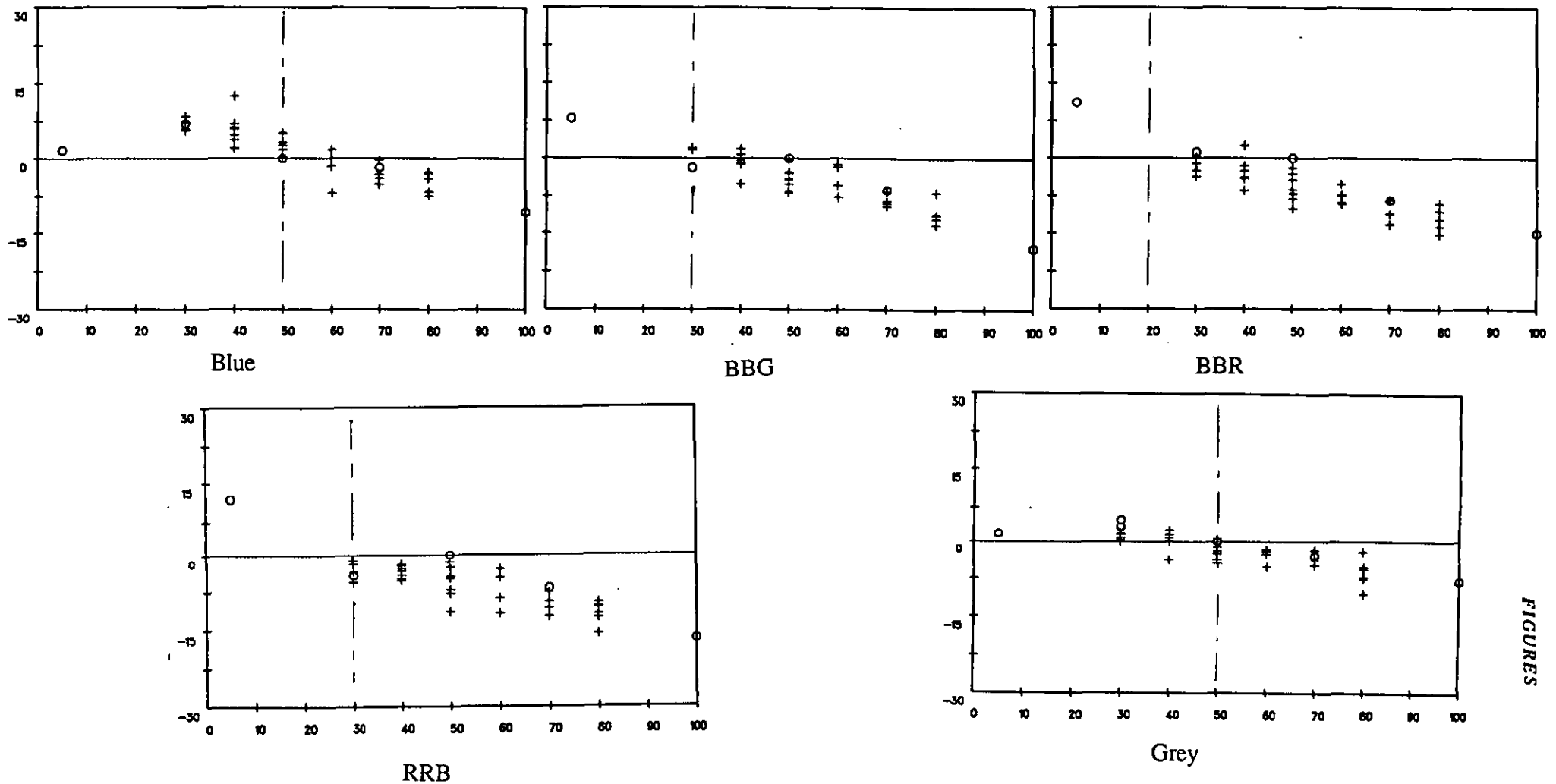


Figure 4.24 The lightness difference plotted against CIELAB hue angles of induction fields for test colours Red, Yellow, Green and Blue in Experiment 5. The five circles refer to the test patch surrounded by five achromatic induction fields, while the smaller plus symbols represent the lighter induction fields for each hue.

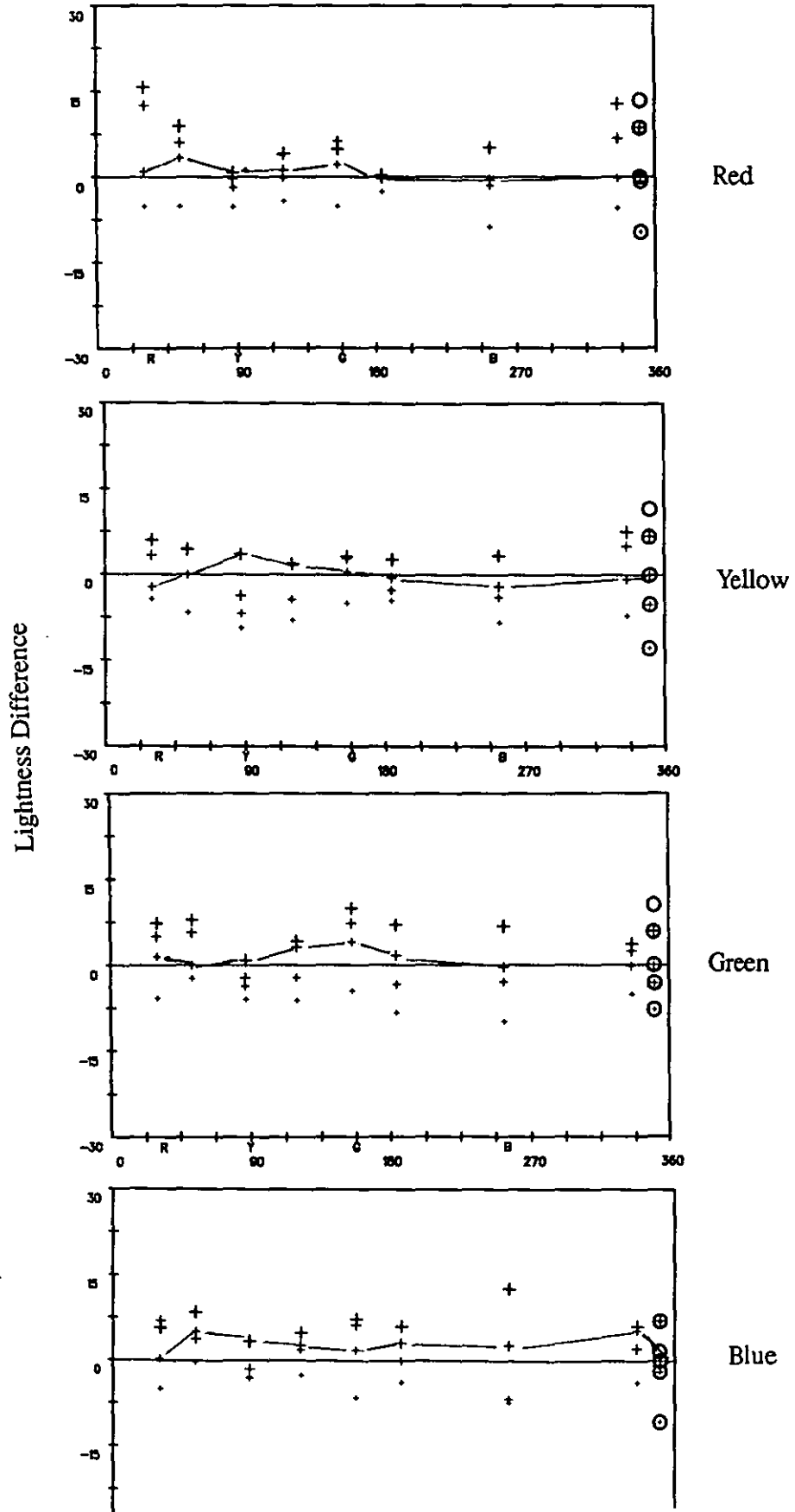


Figure 4.25 Difference in lightness between small ($2 \times 2 \text{ cm}^2$) and large ($6 \times 6 \text{ cm}^2$) sizes for each test colour used in Experiment 5 (top) and the other studies (bottom)^[102] plotted against its hue name

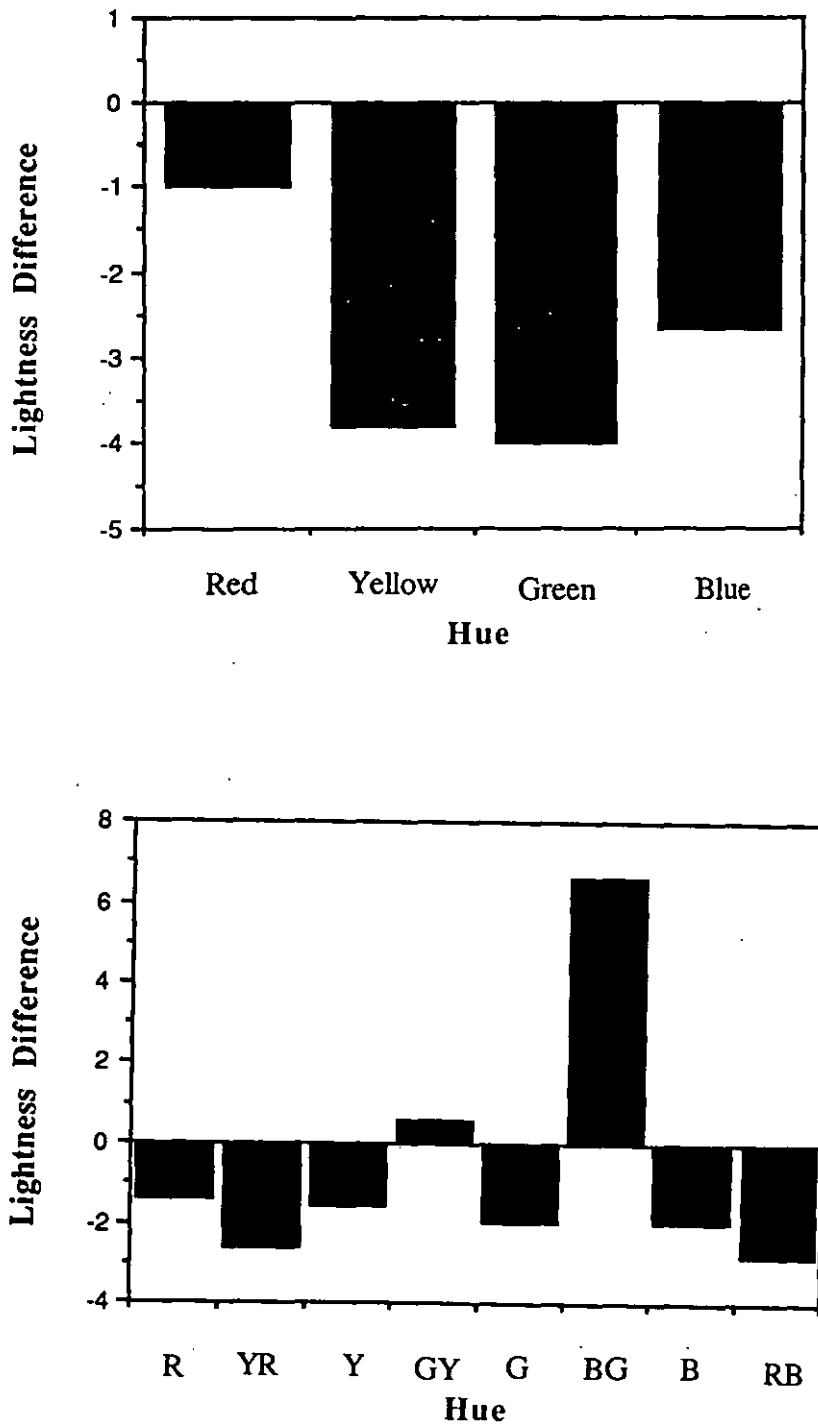


Figure 4.26 The colourfulness difference plotted against CIELAB hue angles of induction fields for test colours Red, RRY and YRR in Experiment 5. The five circles refer to the test patch surrounded by five achromatic induction fields while the smaller plus symbols represent the lighter induction fields for each hue.

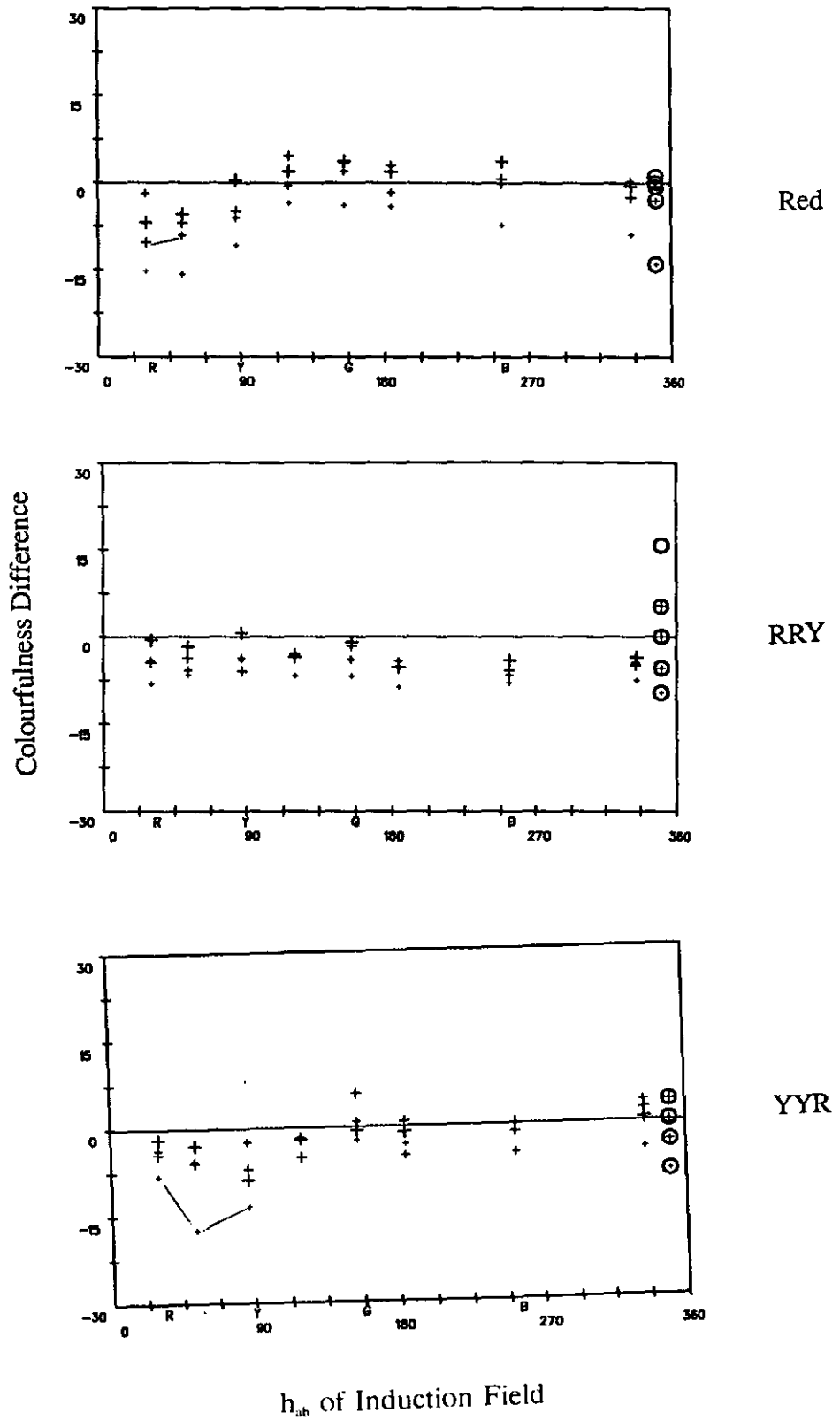


Figure 4.27 The colourfulness difference plotted against CIELAB hue angles of induction fields for test colours Yellow, YYG and GGY in Experiment 5. The five circles refer to the test patch surrounded by five achromatic induction fields while the smaller plus symbols represent the lighter induction fields for each hue.

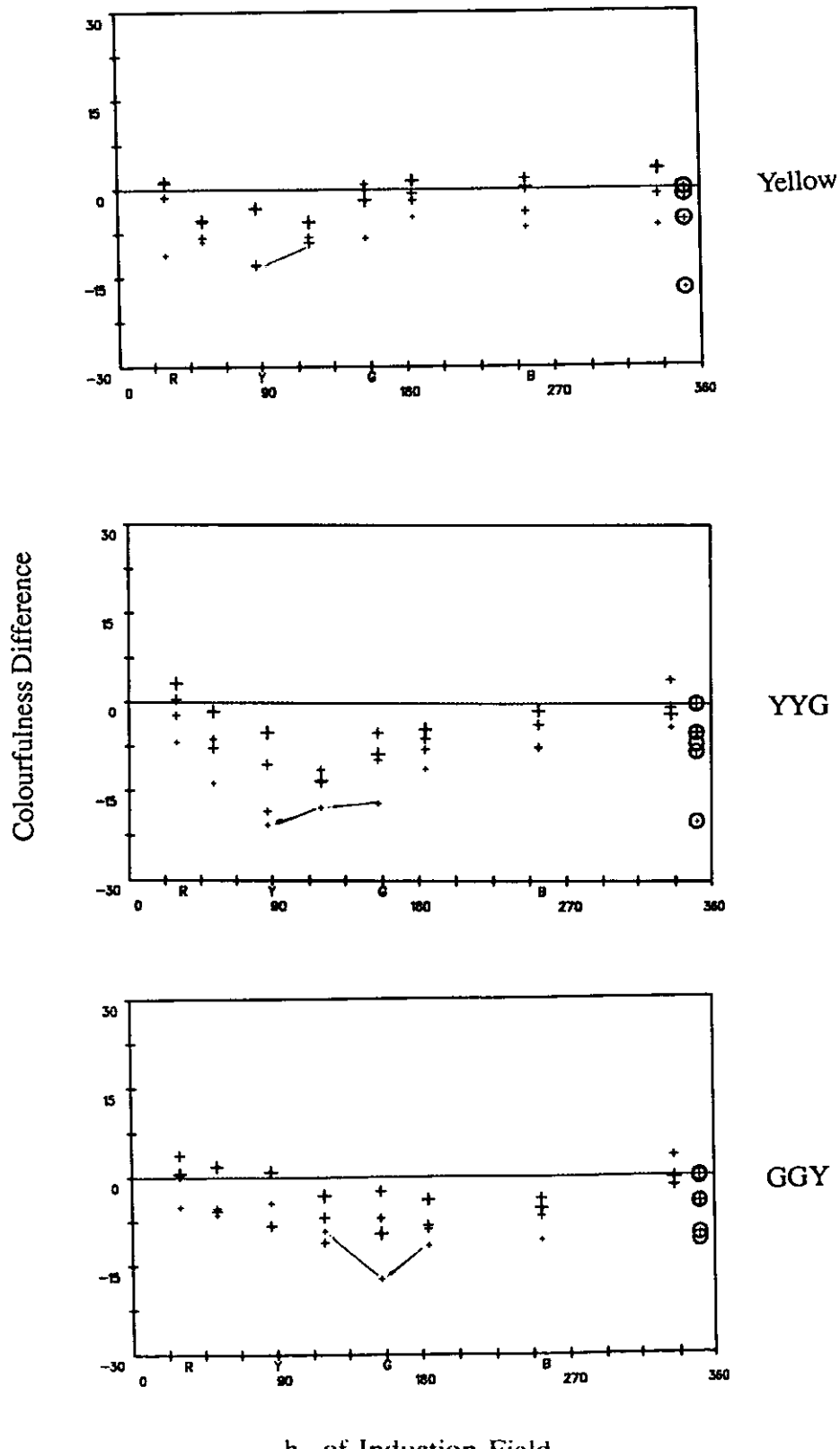


Figure 4.28 The colourfulness difference plotted against CIELAB hue angles of induction fields for test colours Green, GGB and BBG in Experiment 5. The five circles refer to the test patch surrounded by five achromatic induction fields while the smaller plus symbols represent the lighter induction fields for each hue.

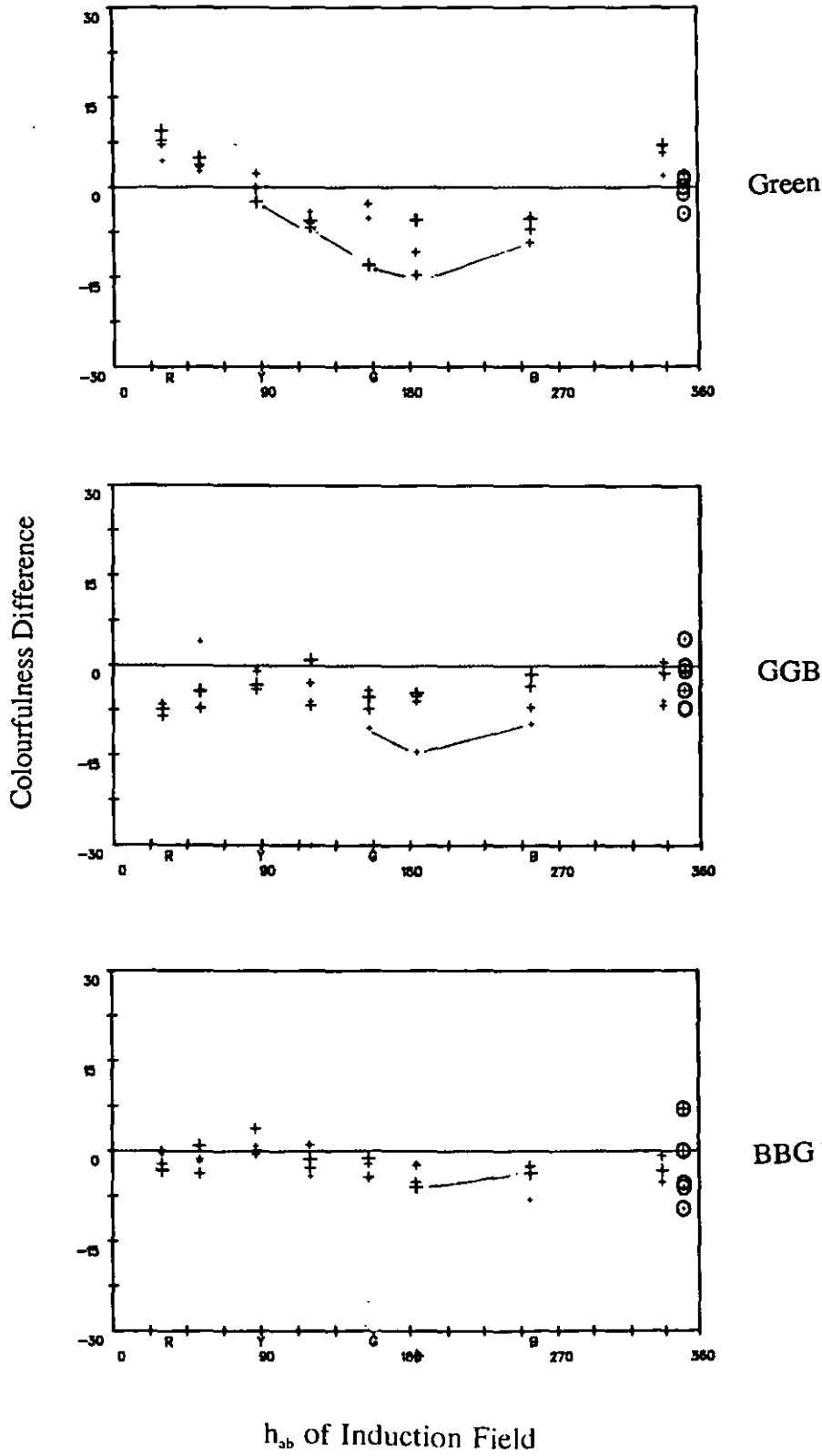


Figure 4.29 The colourfulness difference plotted against CIELAB hue angles of induction fields for test colours Blue, BBR and RRB in Experiment 5. The five circles refer to the test patch surrounded by five achromatic induction fields while the smaller plus symbols represent the lighter induction fields for each hue.

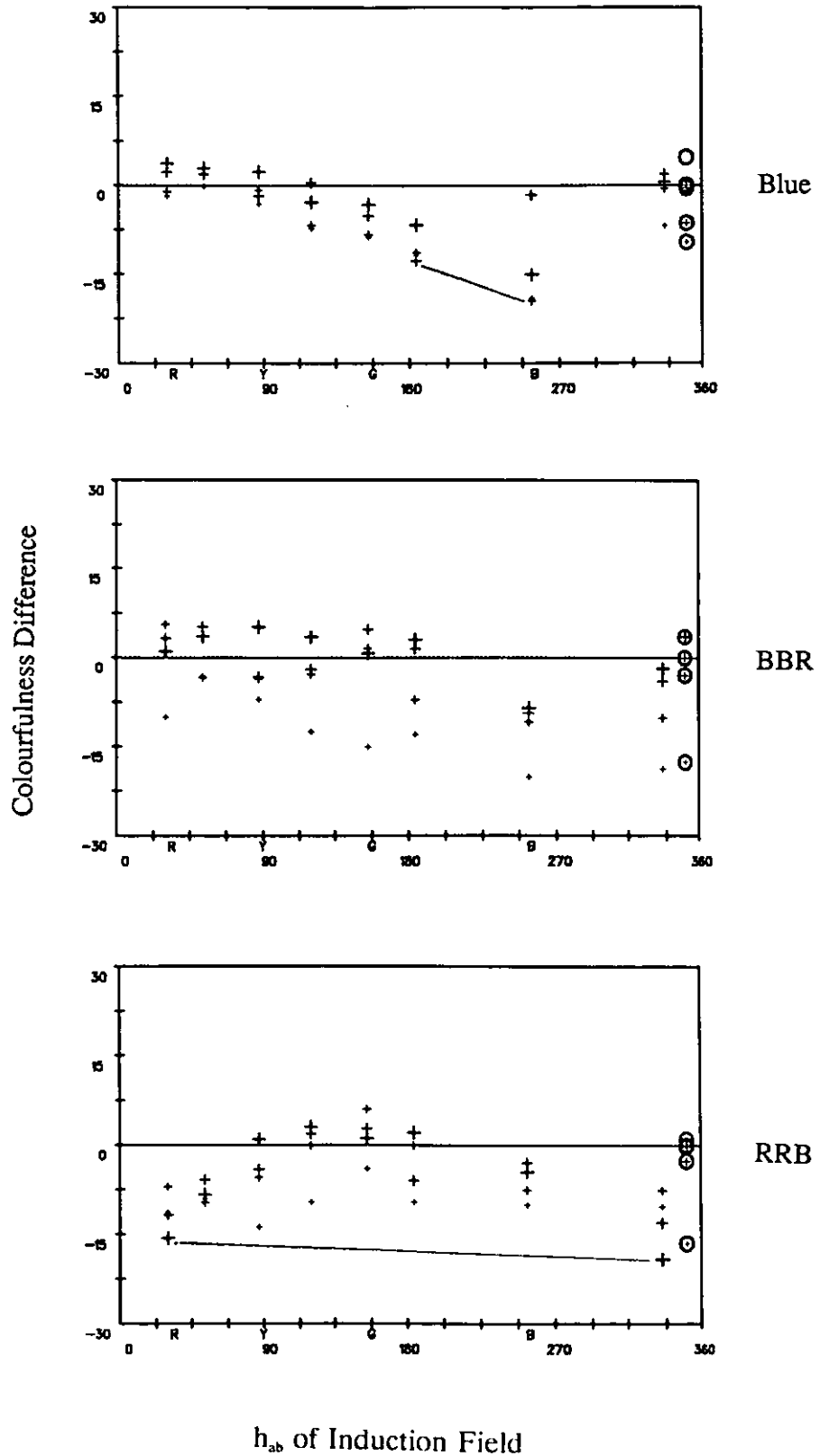


Figure 4.30 The colourfulness difference between small ($2 \times 2 \text{ cm}^2$) and large ($6 \times 6 \text{ cm}^2$) sizes for each test colour used in Experiment 5 (top) and the other studies (bottom)^[102] plotted against its hue name

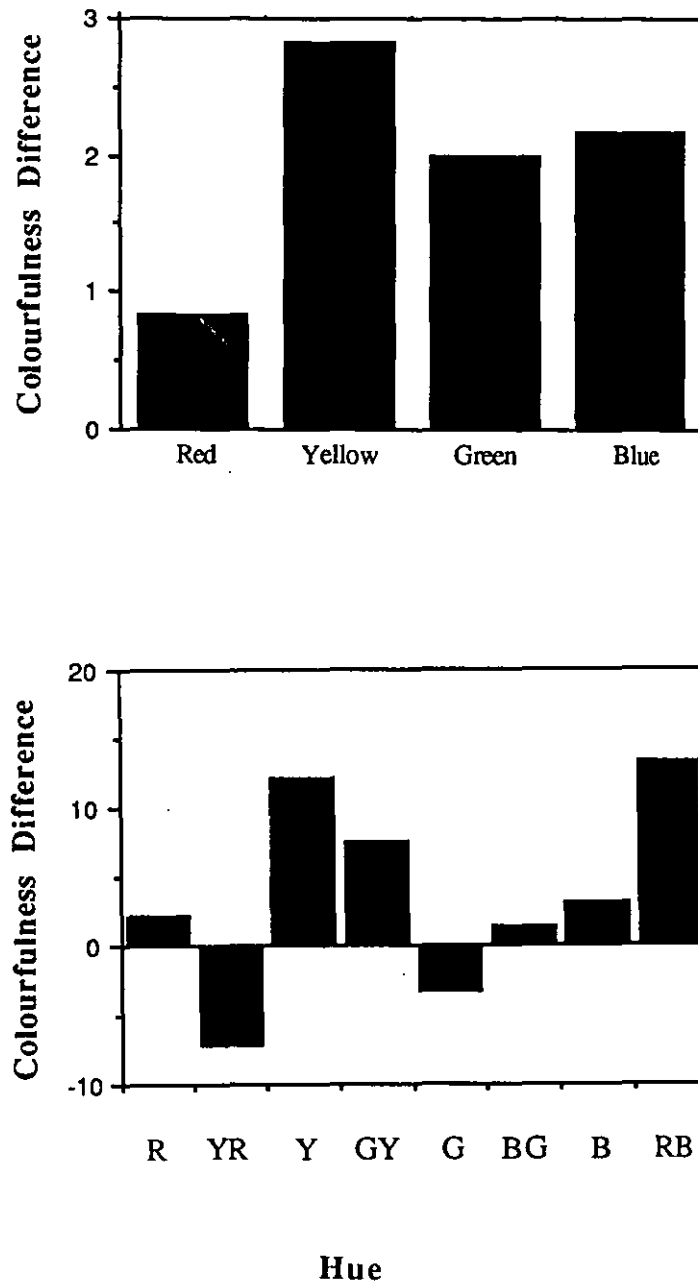
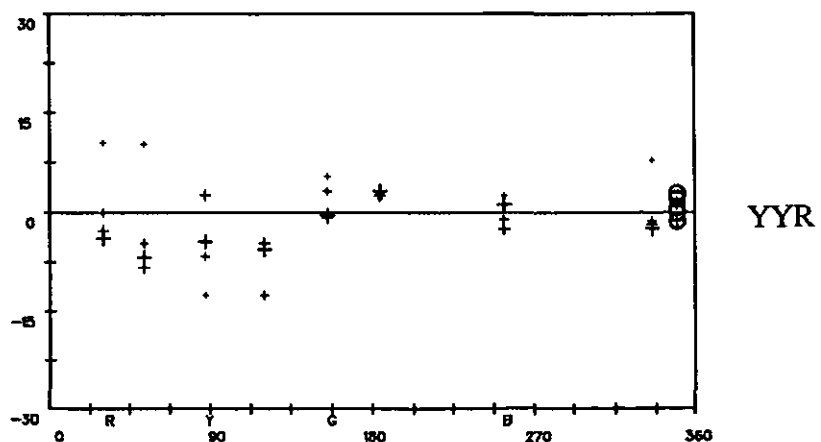
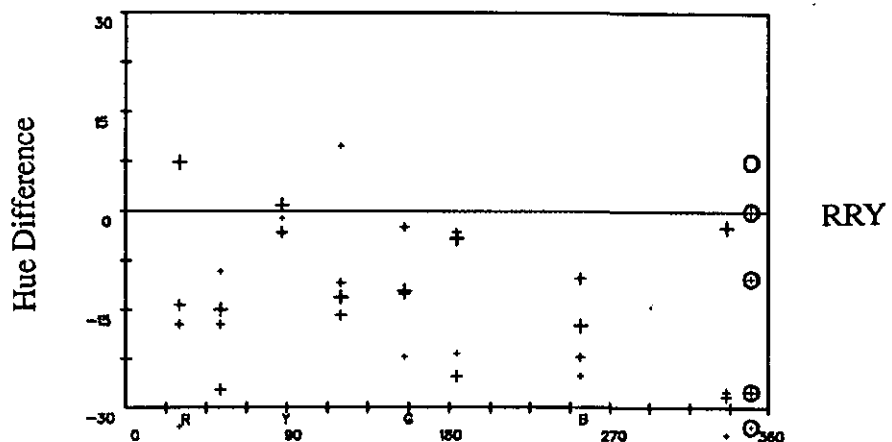
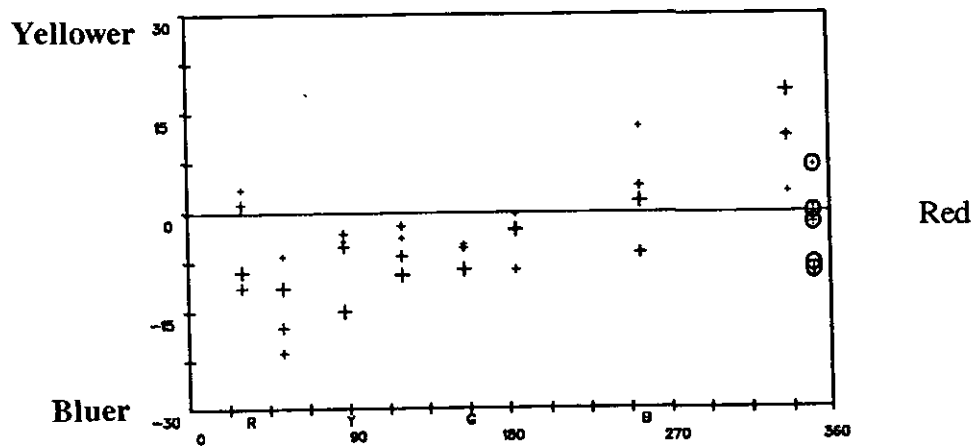


Figure 4.31 The hue difference plotted against CIELAB hue angles of induction fields for test colours Red, RRY and YYR in Experiment 5. The smaller plus symbols represent lighter induction fields for each hue, while the empty circle represents the darkest achromatic induction field.



h_{ab} of Induction Field

Figure 4.32 The hue difference plotted against CIELAB hue angles of induction fields for test colours Yellow, YYG and GGY in Experiment 5. The smaller plus symbols represent lighter induction fields for each hue, while the empty circle represents the darkest achromatic induction field.

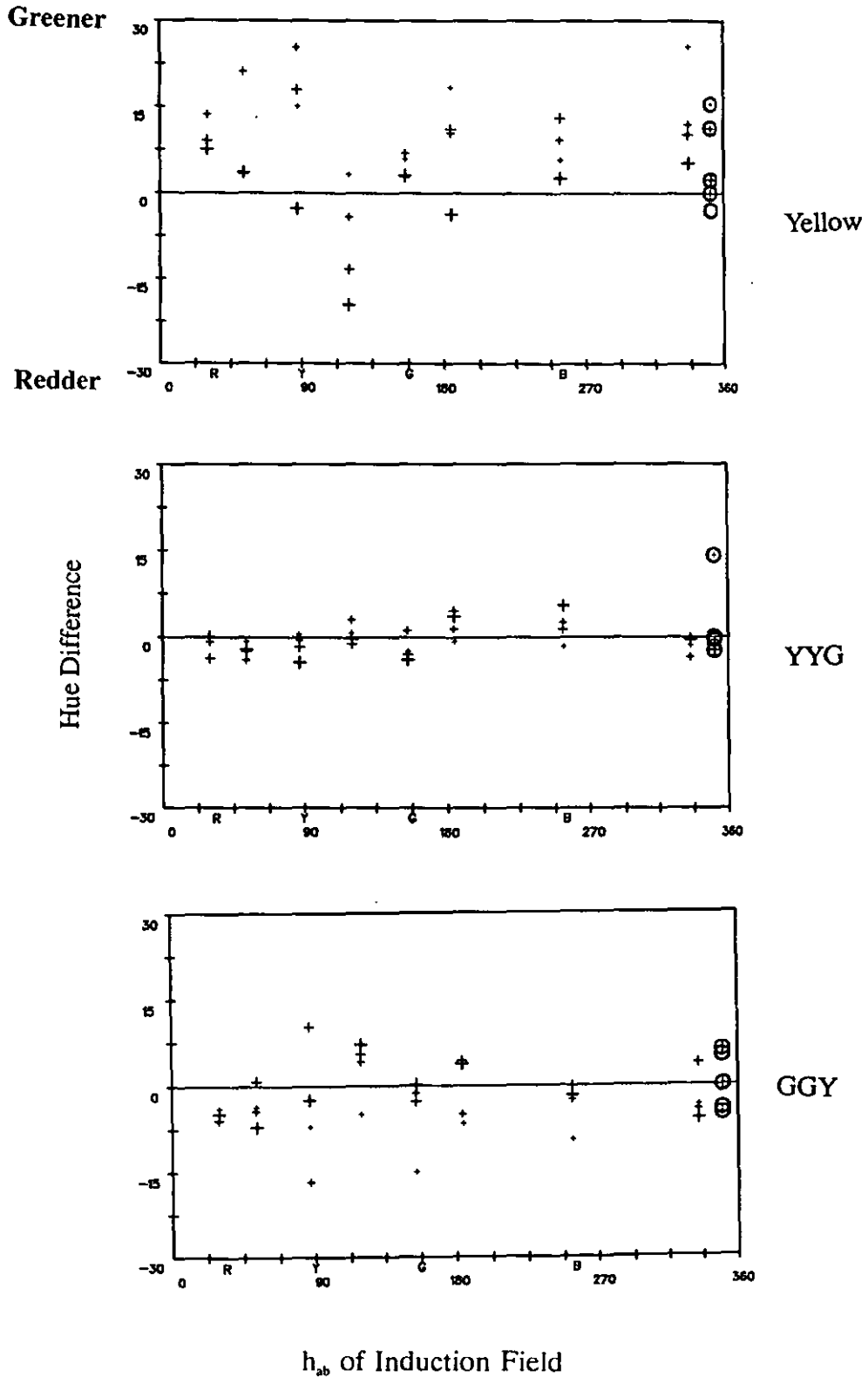


Figure 4.33 The hue difference plotted against CIELAB hue angles of induction fields for test colours Blue, BBR and RRB in Experiment 5. The smaller plus symbols represent lighter induction fields for each hue, while the empty circle represents the darkest achromatic induction field.

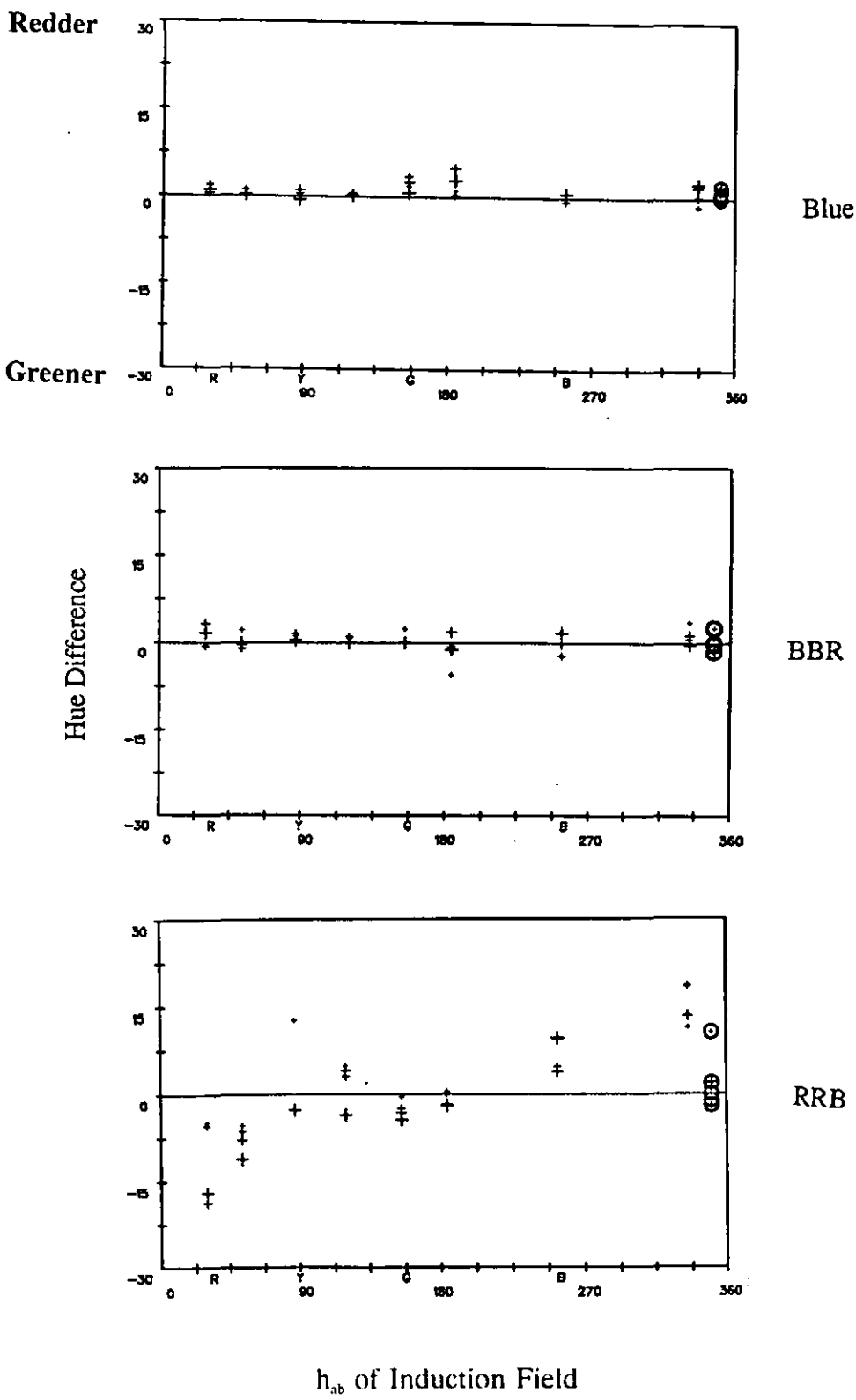


Figure 4.34 The hue difference plotted against CIELAB hue angles of induction fields for test colours Green, GGB and BBG in Experiment 5. The smaller plus symbols represent lighter induction fields for each hue, while the empty circle represents the darkest achromatic induction field.

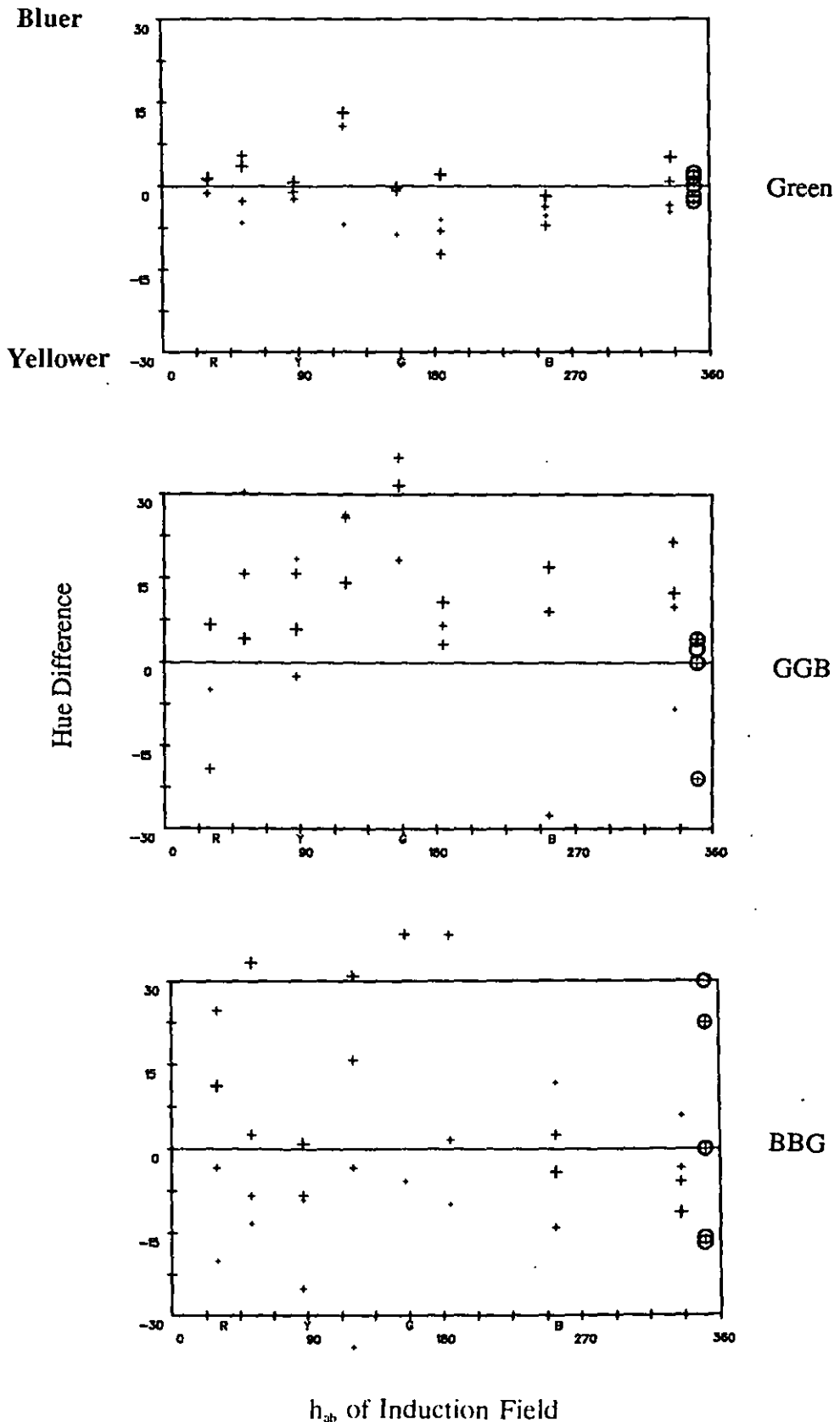


Figure 4.35 Constant - hue loci of NCS system (-----) and those predicted by the modified Hunt91 model (____) plotted on the CIE $u'v'$ chromaticity diagram.

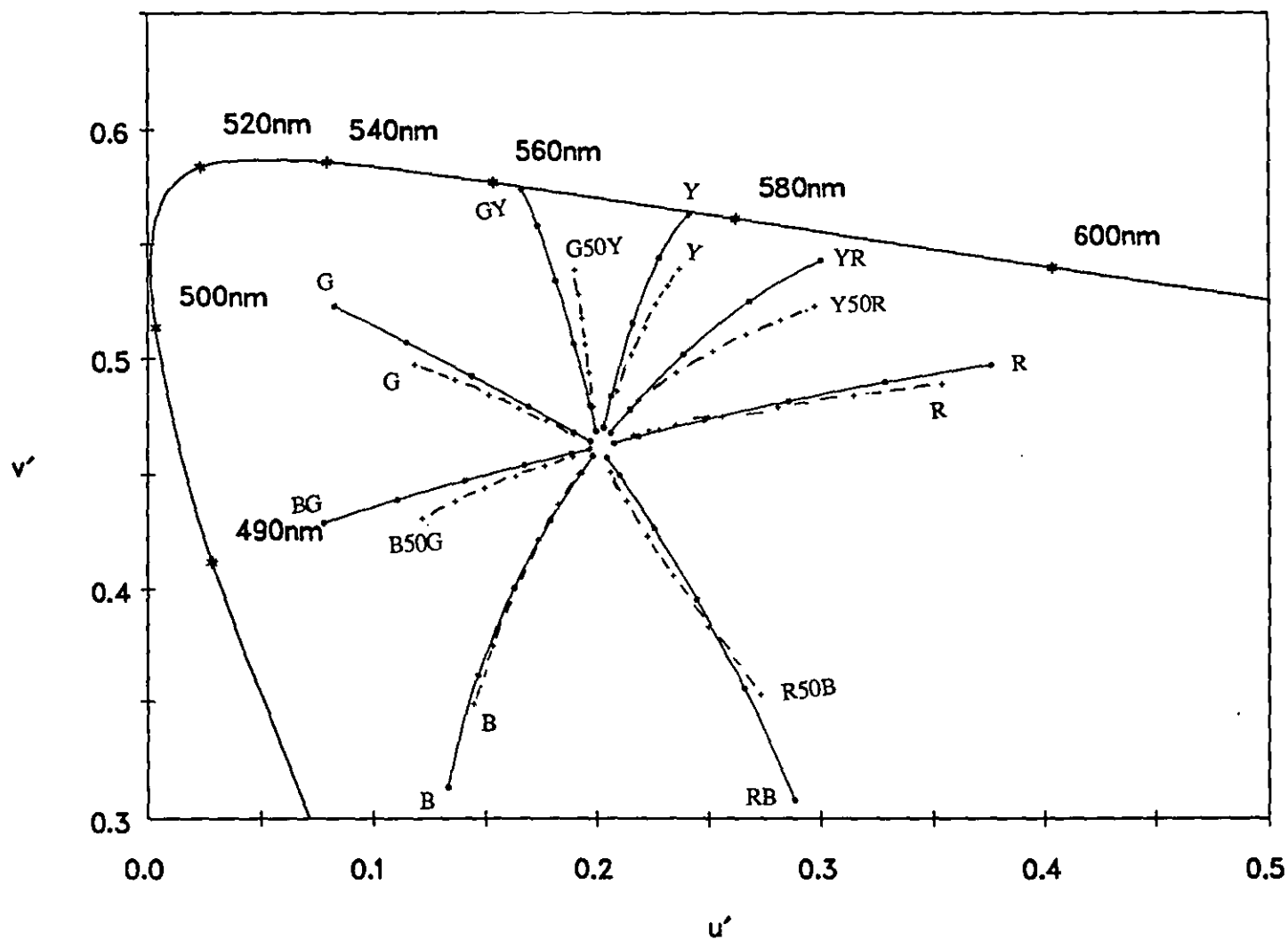


Figure 4.36 Constant - hue loci of Munsell system (----) and those predicted by the modified Hunt91 model (___) plotted on the CIE $u'v'$ chromaticity diagram.

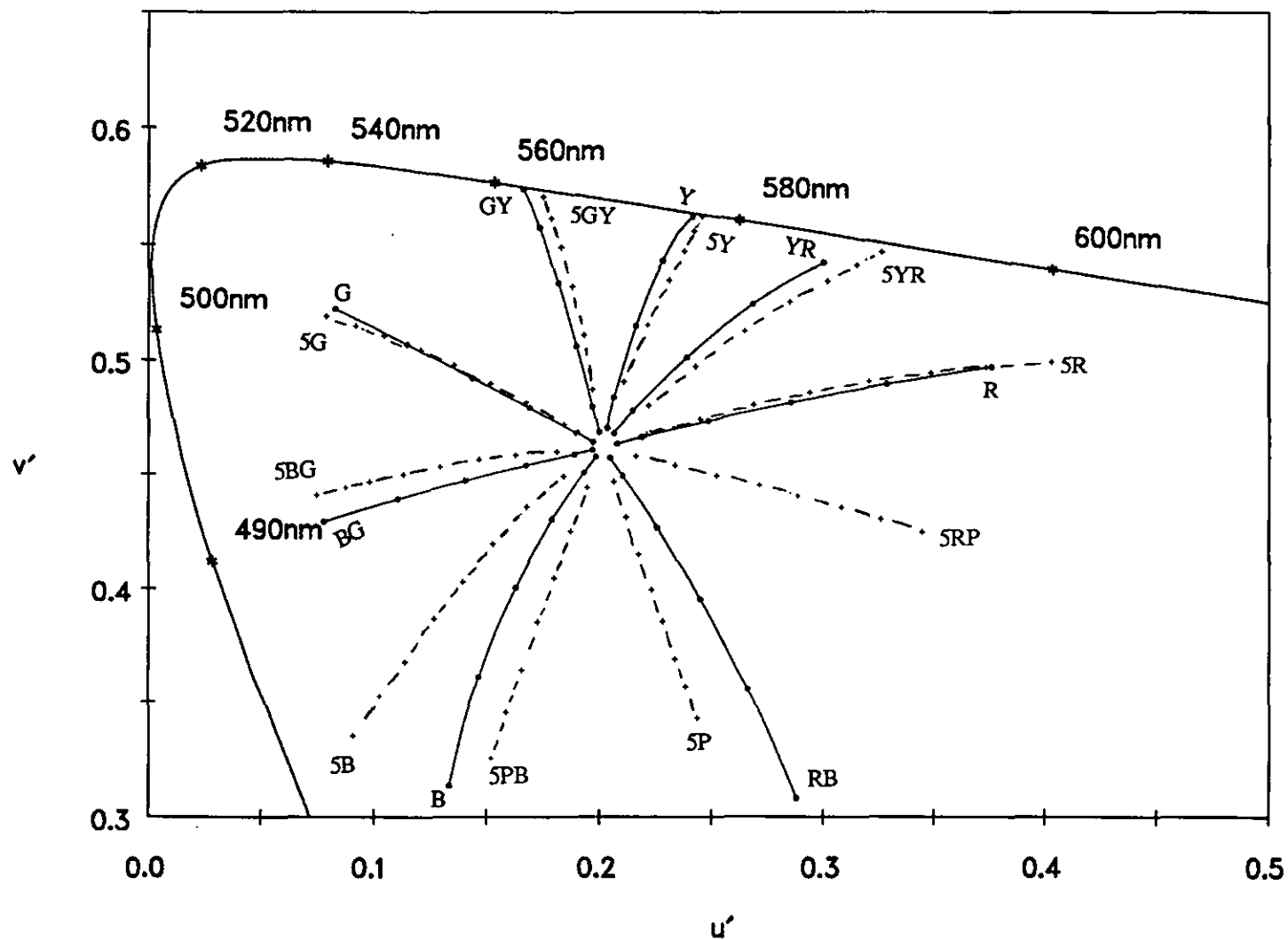


Figure 4.37 Constant - hue loci of Munsell system (----) and those predicted by the modified Hunt91 model (___) plotted on the CIE $u'v'$ chromaticity diagram. The chroma contours represent 2, 4, 6, 8, 10 and 12 Munsell chromas (---), and 20, 40, 60, 80, 100 and 120, chroma values in the modified Hunt91 model (___)

